

2-19-2020

Isotope-Based Methods for Evaluating Fish Trophic Geographies

Julie L. Vecchio
University of South Florida

Follow this and additional works at: <https://digitalcommons.usf.edu/etd>



Part of the [Biology Commons](#), [Ecology and Evolutionary Biology Commons](#), and the [Natural Resources Management and Policy Commons](#)

Scholar Commons Citation

Vecchio, Julie L., "Isotope-Based Methods for Evaluating Fish Trophic Geographies" (2020). *USF Tampa Graduate Theses and Dissertations*.
<https://digitalcommons.usf.edu/etd/8306>

This Dissertation is brought to you for free and open access by the USF Graduate Theses and Dissertations at Digital Commons @ University of South Florida. It has been accepted for inclusion in USF Tampa Graduate Theses and Dissertations by an authorized administrator of Digital Commons @ University of South Florida. For more information, please contact digitalcommons@usf.edu.

Isotope-Based Methods for Evaluating Fish Trophic Geographies

by

Julie L. Vecchio

A dissertation submitted in partial fulfillment
of the requirements for the degree of
Doctor of Philosophy
with a concentration in Marine Resource Assessment
College of Marine Science
University of South Florida

Major Professor: Ernst Peebles, Ph.D.
Steve Murawski, Ph.D.
Linda Lombardi-Carlson, Ph.D.
Chris Stallings, Ph.D.
Brad Rosenheim, Ph.D.

Date of Approval:
March 31, 2020

Keywords: Fish eye-lenses, carbon isotopes, nitrogen isotopes, fish movement, fish diets

Copyright © 2020, Julie L. Vecchio

DEDICATION

This work is first and foremost dedicated to my family. Chris has been my rock for many years. He always supports every crazy idea that I have. He's always up for adventure and I love him for that. Joseph has been as patient as he can be with his mom being a student his entire life. He is still afraid of fish, but I hope to help him get over that fear. My mom was incredulous when I said I wanted to go back to school for a PhD after nine years in the workforce, but she and my dad have both been incredibly supportive throughout the whole process. My sister, Lindsay, showed me that a Vecchio can complete a Ph.D. and has been a sympathetic ear when I feel like walking away. Additional contributors to my mental health throughout this process include the students who have accepted me into their ranks, specifically Kelly Vasbinder, Ryan Venturelli, Imogen Browne, Alex Illich and members of the 2015 cohort. Dr. Mya Breitbart, Dr. Amelia Shevenell, and Sami Francis were extremely supportive and helped me navigate completing my degree. Community contributors to my mental health include Tanks-a-Lot dive charters (Ryan Nelson, owner-operator), my close friends Larry and Lori Smith, who let me crash at their place whenever I need to escape, St. Petersburg Yoga, coffee, and Pass-a-Grill beach.

ACKNOWLEDGEMENTS

The science contained herein required a huge team effort. My major advisor Dr. Ernst Peebles spent countless hours talking through theory and interpretations with me over the past five years and gave helpful feedback on all drafts and presentations. He was instrumental in collecting the first specimens for this project, volunteering his boat, his time and his local knowledge of YOY Red Grouper. Each of my committee members was also instrumental in various facets of the project. Dr. Chris Stallings contributed ideas, data, and writing expertise for several chapters. Dr. Steve Murawski provided all Tilefish and many of the Red Grouper samples. He also was a consistent, calm presence while I was in the throes of writing. Dr. Linda Lombardi was instrumental in the collection of the Red Snapper for the project, is the world's leading expert on Tilefish and Red Grouper life history and was incredibly supportive throughout the entire dissertation process. Dr. Brad Rosenheim jumped onboard in the middle of my dissertation and brought a true isotope perspective to an otherwise fish-heavy group. His notes and conversation about isotopic process and terminology used in a variety of fields has been invaluable.

Members of the Peebles lab assisted me in a variety of ways. Amy Wallace taught me the finer points of eye-lens peeling and IRMS preparation. Jen Granneman invented the submersion method for peeling eye-lenses without them flying away. Briana Michaud, Vi Nguyen, and Jeremy Browning assisted with many fish dissections. Kaitlyn Rivers was a rock star intern who helped weigh otoliths, package IRSM samples, and do general lab work. Catherine Bruger was a fantastic technician who assisted in all lab tasks for several months.

FWRI's fisheries groups, under the guidance of Dr. Luiz Barbieri, provided a number of invaluable services. Luiz suggested that I become a FWRI volunteer and was a great help to my dissertation process. The Fisheries Independent Monitoring (FIM) Program provided many of the fish for this study. I put in a request and they delivered in a big way. FIM also provided the stomach contents data used in chapter 5. FWRI's age and growth lab provided otolith preparation, aging and measuring facilities. Jessica, Alison, Kristen and Kristen all provided invaluable assistance in otolith preparation and aging. Mike Schram aged and measured the increments on most of the fish otoliths except for the Tilefish, which were aged by Greta Helmueller.

NOAA Fisheries laboratory in Panama City contributed fish collected from routine reef fish monitoring. I specifically thank Chris Gardner for keeping track of the fish I needed and getting them to St. Pete. Tilefish were collected on the Mud and Blood cruises aboard the R/V *Weatherbird II* and processed by Jenny Ostroff. All stable isotope values were produced by Ethan Goddard in the Paleoceanography lab at the College of Marine Science, USF.

I also thank the avid fishers and fishing guides who contributed time, fish, and livelihood to this project. Andrew Herzog of Big Bully Outdoors, Larry Smith of BucketList Charters, and Charles Sobczak, volunteer captain from Sanibel Island all contributed time and vessels. Fishing guides on the east coast of Florida kept Red Grouper after Hurricane Irma and donated them to the project. Tom Herzhouser, the owner of the Tavern at Bayboro, always gave me Red Grouper carcasses once he was done filleting fish. These fish provided my practice eyes for learning the peeling technique.

Funding has come in various forms over the past four and a half years. I have been supported by the NOAA/NMFS Marine Resource Assessment fellowship program, the

Roche/ARCS fellowship program for college scientists, the Florida Sea Grant Guy Harvey fellowship, the Jack and Katherine Ann Lake fellowship, the Gulf Oceanographic Charitable Trust Fellowship, and the Spawning Habitat and Early Life Linkages (SHELF) project.

TABLE OF CONTENTS

List of Tables	v
List of Figures	vii
Abstract	ix
Chapter 1: Introduction and Background.....	1
Stable isotope ecology: general background.....	1
Geographic and isotopic setting.....	3
Muscle and liver $\delta^{15}\text{N}$ differential	6
Fish eye lenses as records of diet and movement over the lifetime.....	7
Chapter summaries.....	8
Chapter 2: Offset between muscle and liver $\delta^{15}\text{N}$ for short-term site fidelity	9
Chapter 3: Eye-lens cores as records of geographic location in fish postlarvae	10
Chapter 4: Eye-lens profiles as indicators of movement and diet shifts.....	10
Chapter 5: Integrating eye-lens isotope data with traditional fisheries data.....	12
Objectives	13
Literature Cited	13
Figures.....	19
Chapter 2: The $\delta^{15}\text{N}$ values in muscle and liver of marine Teleosts differ predictably and can be used as an indicator of site fidelity	21
Abstract	21
Introduction.....	22
Isotopic offsets between body tissues	22
Isotopic and geographic setting for wild fish in study	23
Objectives	25
Materials and Methods.....	25
Survey of diet-switch studies	25
Survey of wild-caught reef fish	27
Results.....	29
Survey of diet-switch studies	29
Values of $\Delta\delta^{15}\text{N}_{\text{M-L}}$ in wild-caught reef fishes as compared to $\text{CPO}_{\text{M-L}}$	30
Discussion	31
Conclusions and future applications	35
Literature Cited	36
Tables.....	41
Figures.....	45

Chapter 3: Distinguishing environmental from trophic influences in postlarval fish survival: a historical approach using stable isotopes	51
Abstract	51
Introduction	52
Interpreting bulk isotopes in fish tissue	53
Fish eye lenses can be used as an archival tissue.....	54
West Florida Shelf isoscape and species of interest	55
Statistical analysis of complex isotopic datasets	57
Objectives	57
Materials and Methods.....	58
Specimen collection	58
Eye lens preparation and sample analysis.....	58
Data analysis methods.....	60
Results.....	62
Correlations between isotopic values and internal or external parameters.....	62
Comparisons of species in isotopic space.....	63
General interpretation of postlarval location and movement.....	64
Discussion	65
Construction and use of interpretation rules	65
Gag spawning origin and postlarval movement.....	67
Black Seabass spawning origin and postlarval movement	68
Red Grouper spawning origin and postlarval movement	68
Red Snapper spawning origin and postlarval movement.....	69
Species-specific results suggest differences in spawning locations and movements	70
Conclusions and future directions.....	71
Literature Cited	72
Tables	80
Figures.....	84
 Chapter 4: Characterizing lifetime-scale movement in marine fishes: Tilefish are models of a sedentary life, Red Grouper are models of cryptic movement	88
Abstract	88
Introduction.....	89
Trophic position and basal resource dependence using $\delta^{15}\text{N}$ and $\delta^{13}\text{C}$	89
Fish eye-lenses as an archival tissue: physiology and isotopic conservation	90
Stable isotopes and detection of movement.....	91
Tilefish and Red Grouper: demersal predators with contrasting life histories	92
Potential as a model species.....	94
Objectives	95
Materials and Methods.....	95
Material collection and preparation	95
Isotope analysis.....	96
Eye-lens isotope data analysis	97
Isotope interpretations: movement or trophic increase.....	98
Tilefish simulation: model species approach.....	99

Results	100
Isotopic profiles and lifetime isotopic trends.....	100
Correlations between isotopes	101
Interpreting isotopic profiles as trophic growth and movement	102
Tilefish simulation: model species approach.....	102
Discussion.....	103
Development of an interpretation matrix.....	104
Geographic differences and trends in $\delta^{15}\text{N}$	105
Red Grouper move throughout the lifetime	106
Tilefish move little across isotopic gradients and are models of a sedentary life	107
Literature Cited	110
Tables.....	117
Figures.....	122
 Chapter 5: Ontogenetic movement and diet shifts in juvenile Red Grouper	 130
Abstract.....	130
Introduction.....	131
Fish eye lenses as archival tissue.....	131
Interpretation of $\delta^{13}\text{C}$ and $\delta^{15}\text{N}$ profiles in fish eye lenses	132
Red Grouper life history	133
Objectives	134
Materials and Methods.....	135
Fish collection and eye lens preparation.....	135
Isotope analysis.....	136
Eye-lens isotope data analysis	137
Eye-lens core isotope data analysis.....	137
Lifetime eye-lens profiles	138
Carbon bump: $\delta^{13}\text{C}$ maximum during the first year of life	138
Stomach-content collection, prey identification, and data analysis.....	139
Results.....	140
Analyzed Red Grouper	140
Eye-lens core isotopes.....	141
Lifetime eye-lens profiles: juveniles.....	142
Lifetime eye-lens profiles: WFS adults	143
Lifetime eye-lens profiles: non-WFS Red Grouper.....	143
Carbon bump.....	144
Basal resource dependence	145
Stomach contents	146
Discussion.....	147
WFS Spawning locations and postlarval habits.....	148
WFS lifetime isotopic profiles: trophic growth, diet, shifts, and basal-resource dependence.....	149
A bump in the $\delta^{13}\text{C}$ profiles of WFS Red Grouper.....	151
Non-WFS spawning locations	152
Non-WFS lifetime isotopic profiles: trophic growth and	

basal-resource dependence	153
Conclusions and future directions.....	154
Literature Cited	155
Tables.....	162
Figures.....	170
Chapter 6: Summary and Conclusions.....	179
Chapter Summaries.....	180
Chapter two: Isotopic differences between muscle and liver in captive and wild fishes	180
Chapter three: Using eye-lens cores to assess postlarval locations	183
Chapter four: Contrasting isotopic profiles in two benthic-modifying fish species	187
Chapter five: Red Grouper lifetime isotopes and the carbon bump.....	199
Conclusions and Future Directions.....	192
Literature Cited	195
Appendix A: Permission to retain fish and IACUC approval.....	200
Appendix B: Example Field and Lab Datasheets	202
Appendix C: Sample Preparation Protocols	204
Appendix D: Preliminary isotope tests using fish eye lenses	211

LIST OF TABLES

Table 2.1:	Parameters associated with studies used in the literature survey.....	41
Table 2.2:	Results of linear regressions between $\Delta\delta^{15}\text{N}_{\text{M-L}}$ and fish total length	42
Table 2.3:	Correlations between $\delta^{15}\text{N}_{\text{M-L}}$ and intrinsic or extrinsic parameters associated with marine teleost fishes in Table 2.2.....	42
Table 2.4:	Summary statistics for $\Delta\delta^{15}\text{N}_{\text{M-L}}$ from wild-caught specimens and specimens in diet-switch studies.....	43
Table 2.5:	Results of all Games-Howel pairwise comparisons.....	44
Table 3.1:	Expected isotopic outcomes (increase, decrease, or no change) of all possible combinations of three effects: geographic distribution of spawning (geographic origin), changes in trophic position (trophic growth), and movement along an isotopic gradient	80
Table 3.2:	Rules of interpretation for all isotopic outcomes based on known isotopic trends in fish tissue and WFS isoscape	81
Table 3.3:	Capture information and regression parameters used to convert eye-lens diameters to fish length.....	82
Table 3.4:	Number of samples, minimum, maximum, range, mean, and standard error for both $\delta^{15}\text{N}$ and $\delta^{13}\text{C}$ values recorded for eye-lens cores from the four species.....	82
Table 3.5:	Spearman rank correlations between $\delta^{15}\text{N}$ and ELD or collection latitude and between $\delta^{13}\text{C}$ and ELD or collection longitude by species.....	83
Table 3.6:	Pairwise SEAc proportion overlap and PERMANOVA comparisons	83
Table 4.1:	General interpretations of bulk isotopic trends within fish eye-lenses	117
Table 4.2:	General interpretations for all correlation outcomes within the eye-lens isotopic profiles of individual fishes as well as capture location as a function of length for the species.....	118

Table 4.3:	Statistics for non-linear least-squares regression for isotopic values ($\delta^{15}\text{N}$ and $\delta^{13}\text{C}$) as a function of eye lens diameter (ELD) in both Tilefish and Red Grouper	119
Table 4.4:	Individual Tilefish information ordered by capture fork length (FL).....	120
Table 4.5:	Individual Red Grouper information ordered by capture fork length (FL)	121
Table 5.1:	Basic biological parameters for all Red Grouper with eye-lenses analyzed.....	162
Table 5.2:	Isotopic values of Red Grouper eye-lens cores (inner-most eye-lens layer, collected from the West Florida Shelf (WFS), Campeche Bank (Mexico), and the North Atlantic Ocean off the coast of southeast Florida (SE-FL).....	162
Table 5.3:	Spearman rank correlations between stable isotope values ($\delta^{15}\text{N}$ or $\delta^{13}\text{C}$) and eye-lens diameter (ELD) or collection location (Collection Lat & Collection Lon) in Red Grouper eye-lens	163
Table 5.4:	Biological, statistical, and interpretation information for individual juvenile Red Grouper ordered by capture standard length (SL).....	164
Table 5.5:	Biological, statistical, and interpretation information for individual adult Red Grouper ordered by capture standard length (SL).....	165
Table 5.6:	Height and diametric location within the eye-lens of first transition from quickly increasing $\delta^{13}\text{C}$ to quickly decreasing $\delta^{13}\text{C}$ in eye-lens profiles (Carbon Bump)	166
Table 5.7:	Mean (\pm SE), min, and max proportion of the lifespan utilizing each available basal resource	166
Table 5.8:	Percent by volume of diets consumed by 521 Red Grouper collected from the WFS 2007-2015	167

LIST OF FIGURES

Figure 1.1:	General $\delta^{13}\text{C}$ and $\delta^{15}\text{N}$ trends within the three geographic study regions discussed in this dissertation.....	19
Figure 1.2:	General $\delta^{13}\text{C}$ and $\delta^{15}\text{N}$ trends on the WFS in fish muscle tissue after Radabaugh and Peebles (2014).....	20
Figure 2.1:	Catch locations for all wild-caught reef fish by species	45
Figure 2.2:	Mean values $\delta^{15}\text{N}_{\text{M-L}}$ measured in captive, diet-switch studies	46
Figure 2.3:	Linear regression between $\delta^{15}\text{N}_{\text{muscle}}$ and $\delta^{15}\text{N}_{\text{liver}}$ measured in 12 captive, diet-switch studies.....	47
Figure 2.4:	Mean values of $\Delta\delta^{15}\text{N}_{\text{M-L}}$ (\pm 95% CI) by species for wild specimens collected July-September in Florida waters	48
Figure 2.5:	Means and 95% CI for $\Delta\delta^{15}\text{N}_{\text{M-L}}$ by reproductive category for White Grunt captured on the WFS.....	49
Figure 2.6:	Means and CI for $\Delta\delta^{15}\text{N}_{\text{M-L}}$ by season for two species of reef fish collected on the WFS: a. Red Grouper, b. Black Seabass.....	50
Figure 3.1:	Capture locations by species	84
Figure 3.2:	Mean (\pm SE) eye-lens core $\delta^{13}\text{C}$ and $\delta^{15}\text{N}$ values by species	85
Figure 3.3:	Eye-lens core $\delta^{13}\text{C}$ and $\delta^{15}\text{N}$ values by species	86
Figure 3.4:	Schematic of spawning locations and profiles for each species based on the interpretations in Table 3.5, with differences in relative spawning locations indicated by Figure 3.2	87
Figure 4.1:	Collection locations for all individuals within the Gulf of Mexico	122
Figure 4.2:	Isotopic distribution for all Red Grouper and Tilefish eye-lens layers.....	123
Figure 4.3:	Non-linear regression of isotopic values $\delta^{15}\text{N}$ and $\delta^{13}\text{C}$ as a function of eye-lens diameter (ELD) for both Tilefish and Red Grouper	124

Figure 4.4:	Spearman rank correlations (<i>Rho</i>) representing correlation between $\delta^{15}\text{N}$ and $\delta^{13}\text{C}$ for simulated population of 1,000 Tilefish	125
Figure 4.5:	Lifetime profiles of $\delta^{13}\text{C}$ and $\delta^{15}\text{N}$ in Tilefish eye-lenses ordered by fork length at capture	126
Figure 4.6:	Lifetime profiles of $\delta^{13}\text{C}$ and $\delta^{15}\text{N}$ in Red Grouper eye-lenses ordered by fork length at capture	127
Figure 4.7:	Tilefish lifetime correlations between $\delta^{15}\text{N}$ and $\delta^{13}\text{C}$	128
Figure 4.8:	Red Grouper lifetime correlations between $\delta^{15}\text{N}$ and $\delta^{13}\text{C}$	129
Figure 5.1:	Collection locations and collection depths for all Red Grouper organized by standard length (SL) at capture	170
Figure 5.2:	Eye-lens core isotopic values for all Red Grouper analyzed. Points are coded by catch location and maturity	171
Figure 5.3:	Profiles of $\delta^{13}\text{C}$ and $\delta^{15}\text{N}$ as a function of eye-lens diameter for individual juvenile Red Grouper from the West Florida Shelf (WFS) ordered by standard length (SL)	172
Figure 5.4:	Profiles of $\delta^{13}\text{C}$ and $\delta^{15}\text{N}$ as a function of eye-lens diameter for individual adult Red Grouper from the West Florida Shelf (WFS) ordered by standard length (SL)	174
Figure 5.5:	Profiles of $\delta^{13}\text{C}$ and $\delta^{15}\text{N}$ as a function of eye-lens diameter for individual adult Red Grouper	175
Figure 5.6:	Profiles of $\delta^{13}\text{C}$ as a function of eye-lens diameter for all West Florida Shelf (WFS) Red Grouper identified as having a “carbon bump”	176
Figure 5.7:	Proportion of total lifespan utilizing each available basal resource	177
Figure 5.8:	Proportion by volume of diets consumed by 521 Red Grouper collected from the WFS 2007-2015	178

ABSTRACT

Data on the movement and diets of fish during a variety of life stages are important inputs to fisheries stock assessments and marine ecosystem models. Stable isotopes may provide previously inaccessible information on movement and diet of a variety of managed and forage fish species. Here I used several novel means of interpretation for stable isotope data to infer diets and movements of several important fisheries species over both short (weeks to months) and long (lifetime) timescales. Prior captive diet switch studies of marine teleosts converge on a constant partitioning offset (CPO_{M-L}) whereby $\delta^{15}N_{\text{muscle}}$ is uniformly higher than $\delta^{15}N_{\text{liver}}$. Mean ($\pm SE$) difference across all studies was $\delta^{15}N_{M-L} = 1.67 \pm 0.14\%$. I then compared the $\delta^{15}N_{M-L}$ values from 575 marine fishes representing eight species from continental shelf waters of Florida, USA to this CPO_{M-L} . I found that mean values of $\delta^{15}N_{M-L}$ for five of the eight species did not differ significantly from CPO_{M-L} , but mean values for three species were lower than CPO_{M-L} . These results suggest that the species at CPO_{M-L} were both stationary and consuming a diet of stationary prey. The species with $\delta^{15}N_{M-L}$ values far from CPO_{M-L} were either moving or consuming prey that was actively migrating through the area.

For lifetime-scale studies, I used the $\delta^{13}C$ and $\delta^{15}N$ values in the fish eye-lenses. I used the isotopic values in the eye-lens core (inner-most lamina) to estimate geographic location and habitat use of postlarvae from four species common to the northern West Florida Shelf (WFS). I found that isotopic values differed among the four species, suggesting different habitat by the postlarvae of each species. Relative isotopic values corresponded with relative geographies assessed through traditional fisheries demographic studies. In addition, correlation between eye-

lens core isotope values and the parameters of eye-lens diameter or catch location each indicated that while some species move inshore during the postlarval period, others move little or move alongshore during this period.

I compared the eye-lens isotopic ($\delta^{13}\text{C}$ and $\delta^{15}\text{N}$) profiles of two benthic-modifying species from the WFS to assess degree of habitat and diet stability in each species. Traditional fisheries data suggests that Tilefish (*Lopholatilus chamaeleonticeps*) shows high site fidelity and diet stability over the lifetime. Values of $\delta^{13}\text{C}$ and $\delta^{15}\text{N}$ in sequential eye-lens laminae were strongly correlated across the lifetime with increases in both profiles over time. These results suggest that Tilefish are highly stationary throughout the lifetime. Red Grouper (*Epinephelus morio*) are known for a sedentary lifestyle during the adult phase. However, as larvae and juveniles there is evidence that the species crosses the WFS to shallow water, and back to deeper areas. Eye-lens isotope profiles for adults showed low values of correlation between $\delta^{13}\text{C}$ and $\delta^{15}\text{N}$. While $\delta^{15}\text{N}$ increased steadily over the lifetime, $\delta^{13}\text{C}$ did not. These results suggest much lower rates of both site fidelity and diet stability for Red Grouper than for Tilefish.

I used eye-lens stable isotope profiles combined with catch data and stomach content analysis to construct an in-depth depiction of Red Grouper diet and movement histories over the lifetime. I found that fish spawned on the WFS had isotopically distinct eye-lens cores from fish spawned in other regions. However, eye-lens core values were relatively consistent between juveniles and adults, suggesting a consistent region of postlarval habitat within the WFS system. Finally, I found that 60 to 66% of Red Grouper from WFS displayed a unique feature of the $\delta^{13}\text{C}$ profile, whereby values peaked then decreased, completing the cycle before the end of the first year. Despite similarities in diet for individuals from the Florida Reef Tract and Campeche Bank, few had similar $\delta^{13}\text{C}$ profiles. Combined with catch data and stomach content data, these isotopic

data suggest ontogenetic cross-shelf movement along with a continually shifting diet over the first year of life.

The tools developed and tested here can provide additional data for interpreting movement and diets of important fisheries species for current single-species stock assessments. Using the difference between $\delta^{15}\text{N}$ in the muscle and liver tissue of a single fish can provide information about the movement of fish over the preceding few months. Analyzing the $\delta^{13}\text{C}$ and $\delta^{15}\text{N}$ values in the eye-lens cores of individual fishes can indicate movement and diet during the earliest weeks of life using a historical approach. The whole eye-lens isotope profiles of $\delta^{13}\text{C}$ and $\delta^{15}\text{N}$ can suggest lifetime movement and combining the isotope profile data with traditional fisheries data may provide additional insight into the movement and diet of a species. These isotopic and statistical techniques will be invaluable as fisheries stock assessment continues to move to a more ecosystem-based approach.

CHAPTER 1: INTRODUCTION AND BACKGROUND

Single-species fisheries management is being supplanted by ecosystem-based fisheries management (O'Farrell et al. 2017), and this trend is expected to continue as computational power and ecosystem model sophistication increases (Marshall et al. 2019). Current methods of fisheries management and decision-making rely on understanding the biological and physical needs of target species, especially during life-stages that precede targeted fisheries. As Maunder and Piner (2015) discuss, knowledge of growth, natural mortality, and recruitment are all essential inputs to successful stock assessments. Additional data including diet and trophic dependencies, episodic events such as red tides, and habitat needs have begun to be incorporated into recent fisheries stock assessments as well (SEDAR 2018; SEADAR 2019). With this increased focus on a holistic approach to the management of ecosystems, additional life history, trophic, and habitat data will be necessary for most species. One field poised to provide high-value, low investment data is stable isotope analysis. Over the past several years, the foundations have been laid for using bulk stable-isotope values (especially $\delta^{13}\text{C}$ and $\delta^{15}\text{N}$) in various fish tissues, including muscle, liver, and eye lenses, as indicators of movement and diet. These methods are especially well-developed in regions such as the West Florida Shelf (WFS), where detailed isoscapes are available (Radabaugh and Peebles 2014).

STABLE ISOTOPE ECOLOGY: GENERAL BACKGROUND

In marine organisms, the bulk isotopic values of $\delta^{13}\text{C}$ and $\delta^{15}\text{N}$ can be used as proxies for trophic position, basal resource dependence, and location. Observed $\delta^{15}\text{N}$ values are not affected

by lipid content in tissues, but may be affected by chemical treatments (Skinner et al. 2016). The observed $\delta^{13}\text{C}$ values may be influenced by lipid content in tissues with high percentages of fat, requiring mathematical or chemical lipid corrections (Skinner et al. 2016). Tissues with C:N ratios above 3.5 are generally considered high in lipid, requiring mathematical or chemical manipulation. To circumvent uncertainties associated with lipid correction and normalization, I selected tissues and isotopes for the current project that did not require mathematical or chemical manipulation.

Relative trophic position of organisms within an ecosystem is assessed using $\delta^{15}\text{N}$ (Chikaraishi et al. 2007; Hunsicker et al. 2010; Bradley et al. 2015). Trophic position is ordinarily estimated by using simple addition from the $\delta^{15}\text{N}$ baseline values of primary producers with an average increase of 3.4‰ per trophic level (Fry 2006). Recently, Hussey et al. (2014) showed mathematically that this average difference among trophic levels may ignore important variability within the system, under-estimating low trophic position differences in $\delta^{15}\text{N}$ values while over-estimating high trophic position $\delta^{15}\text{N}$ differences. As a consequence, trophic position may be under-estimated in many top predators, with modeled food chain length potentially shorter than reality. Nevertheless, tissue $\delta^{15}\text{N}$ value remains an important and powerful proxy when considering trophic position in many ecologically relevant contexts.

In most species of fish, the trophic position of the individual increases as the fish grows, taking advantage of larger, higher trophic position prey, and resulting in increased values of $\delta^{15}\text{N}$ in all tissues. The trend has been demonstrated using $\delta^{15}\text{N}$ isotope values in muscle tissue from several species including Summer Flounder (*Paralichthys dentatus*) and Yellowfin Tuna (*Thunnus albacares*) (Graham et al. 2007; Buchheister and Latour 2011). A similar observation has been made using eye-lens profiles for individual fishes, with lowest observed values

corresponding to the initiation of external feeding and increasing values of $\delta^{15}\text{N}$ as the fish continues to grow over the lifetime (Wallace et al. 2014; Quaeck-Davies et al. 2018; Simpson et al. 2019).

In contrast, $\delta^{13}\text{C}$ is primarily used to assess trophic dependence (Grippo et al. 2011) and can be interpreted as geographic position of predators due to predictable spatial variability in $\delta^{13}\text{C}$ in many marine systems (Barnes et al. 2009; Radabaugh and Peebles 2014; Trueman et al. 2017; Brault et al. 2018). This difference can be more useful than the small and variable isotopic increase with increasing trophic position ($\sim 0.5\text{-}1.5\text{‰}$ per trophic level) due to more consistent differences with less variability (Fry 2006). Phytoplankton fractionate carbon isotopes during photosynthesis at higher rates than benthic primary producers such as benthic microalgae, macroalgae, and vascular plants (Fry and Wainright 1991; Keough et al. 1998; Burkhardt et al. 1999; Radabaugh et al. 2014; Puigcorbe et al. 2015). In general, values of $\delta^{13}\text{C}$ in phytoplankton are near -24‰ (Fry 2006), whereas those of benthic algae are closer to -19‰ (Radabaugh et al. 2014). Difference in $\delta^{13}\text{C}$ fractionation between planktonic and benthic photosynthetic organisms has been attributed to boundary layer effects (France et al. 1995) and to light availability for individual cells (Radabaugh et al. 2014). At higher trophic positions, $\delta^{13}\text{C}$ values can be interpreted to represent the basal resource most responsible for maintaining the food web for a particular region (Elliot Smith et al. 2018; Paar et al. 2019) or the basal resource dependence of a species of interest (Duke et al. 2018).

GEOGRAPHIC AND ISOTOPIC SETTING

The work in this dissertation is geographically centered on the West Florida Shelf (WFS), a wide continental margin bordering the western edge of the state of Florida, U.S.A. The WFS

consists of drowned limestone reef covered in a thin sand veneer in most areas (Balsam and Beeson 2003; Hine and Locker 2011). In limited locations, the limestone of the prehistoric reef projects above the soft sediment, providing habitat for sessile organisms (Wall and Stallings 2018). These exposed rocky reefs covered in attached fauna function as aggregation sites for varied nekton and larger motile benthic organisms (Ainsworth et al. 2015). These densely populated areas provide habitat and food for many commercially and recreationally important fisheries species such as snappers (Lutjanidae) and groupers (Serranidae) (Gledhill and David 2004).

Previous work has established isotopic background patterns in both $\delta^{13}\text{C}$ and $\delta^{15}\text{N}$ on the WFS (Figure 1.1, 1.2). In short, $\delta^{13}\text{C}$ of fish muscle tissue decreases with water column depth/distance from shore (Radabaugh and Peebles 2014). Benthic microalgae dominate primary production in shallow water (Doi et al. 2010), whereas phytoplankton are the only source of primary productivity in deeper water (Popp et al. 1998; Burkhardt et al. 1999) due to a lack of adequate photosynthetically active radiation (PAR) reaching the bottom. Due to the higher rates of fractionation discussed above, $\delta^{13}\text{C}$ in phytoplankton is typically lower than in benthic producers (Radabaugh et al. 2014). This pattern is carried through the system and reflected in fish tissue. Higher values of $\delta^{13}\text{C}$ are generally observed in muscle tissue of fish living in shallow water and lower values are found in fish collected in deeper water within the same species (Radabaugh et al. 2013). The pattern of high background values of $\delta^{13}\text{C}$ in shallow water on the WFS has been shown to hold over seasons (Radabaugh et al. 2013) and among years (Huelster 2015).

In contrast, $\delta^{15}\text{N}$ of fish tissue in the Gulf of Mexico varies with distance to major sources of nutrient run-off from animal husbandry and treated municipal wastewater (Howarth et al.

1996; Burkart and James 1999). The $\delta^{15}\text{N}$ entering the system reflects the trophic position of farm animals and humans, resulting in elevated background levels near the mouth of major rivers such as the Mississippi (Kendall et al. 2001; Duan et al. 2014; Walker et al. 2017). Water along the southern WFS has little riverine input, leaving diazotrophs such as *Trichodesmium* sp. as a primary source of $\delta^{15}\text{N}$ into the system (McClelland et al. 2003; Holl et al. 2007). These cells utilize atmospheric N_2 for amino acid synthesis during cell growth, resulting in an ecosystem with relatively low levels of background $\delta^{15}\text{N}$ (Holl et al. 2007). In practical terms, this means that $\delta^{15}\text{N}$ is highest close to the mouth of the Mississippi River (at the northwest edge of the WFS) and declines southeastward toward the Florida Keys (Radabaugh and Peebles 2014; Peebles and Hollander 2020). Patterns are carried through to fish tissue, with higher values of $\delta^{15}\text{N}$ in fish farther north on the WFS and lower values of $\delta^{15}\text{N}$ from fish closer to the Florida Keys (Radabaugh and Peebles 2014; Peebles and Hollander 2020; Figure 1.1, 1.2).

Some specimens were collected from Campeche Bank north of the Yucatan peninsula. Like the WFS, this area consists of a wide, shallow continental shelf extending offshore from a major landmass. The bank projects northward from the shore into the southern Gulf of Mexico covering approximately 125 miles (Kormmcker et al. 1959). Much of the area is covered in rock with a large reef complex, Alacran Reef, occupying much of the area. Unconsolidated sediment consists primarily of carbonate sand in the region (Kormmcker et al. 1959). A modeled $\delta^{13}\text{C}$ isoscape has not been published for the region; however, shallower areas seem to have higher levels of background $\delta^{13}\text{C}$ due to clear water and the availability of light to the bottom for the proliferation of benthic microalgae (Michaud, unpublished data). Deeper waters have more negative values of $\delta^{13}\text{C}$ due to light limitations of benthic photosynthetic organisms (Michaud, unpublished data). A modeled $\delta^{15}\text{N}$ isoscape has been published for the region with relatively

uniform, low values of background $\delta^{15}\text{N}$ (Peebles and Hollander 2020), consistent with low levels of river run-off (Kormmcker et al. 1959) bringing little organic nitrogen from human activities into the region (Figure 1.1). Uncertainty remains for both the $\delta^{13}\text{C}$ and $\delta^{15}\text{N}$ isoscapes in this region due to low sample density, and an improved isoscape would increase interpretive power for fish and mobile organisms collected from the Campeche Bank.

Finally, some samples were collected from near the southeast coast of Florida. This region does not have modeled isoscapes for $\delta^{13}\text{C}$ or $\delta^{15}\text{N}$. However, a geographically limited study in Biscayne National Park, a small section of the Florida Reef Tract, suggests trends in the background values of both $\delta^{13}\text{C}$ and $\delta^{15}\text{N}$ isotopes in fish tissue (Figure 1.1). The park extends from the northern edge of the Florida Keys to just south of the city of Miami, Florida. It includes continuous reef along the outer edge and numerous patch reefs in shallow water (Brock et al. 2004). Similar to patterns observed on WFS, $\delta^{13}\text{C}$ values decreased with depth, indicative of decreases in benthic production (Curtis 2016). The researchers also found that $\delta^{15}\text{N}$ increased with latitude, similar to observations on the WFS (Curtis 2016). It is unknown whether $\delta^{15}\text{N}$ would continue to increase to the north of the heavily populated region of southeast Florida or if the $\delta^{15}\text{N}$ maximum for the region occurs near Miami.

MUSCLE AND LIVER $\delta^{15}\text{N}$ DIFFERENTIAL

Historically, researchers have interpreted the $\delta^{13}\text{C}$ and $\delta^{15}\text{N}$ values of individual tissues or whole organism, depending upon the size of the organism under study (McClelland and Montoya 2002; Elsdon et al. 2010). However, one limitation to this approach is the temporal limitation of the turnover time of each individual tissue. For example, muscle tissue integrates one to two months of growth into the isotopic values (Mohan et al. 2016). In contrast, liver tissue turns over more quickly, representing only one to two weeks with turnover driven by metabolism (Barreto-

Curiel et al. 2017). Isotopic values within each tissue represent not only the diet and location over the preceding weeks to months, but may be influenced by nutritional state, species, sex, or even time of year (Awkerman et al. 2007; Hussey et al. 2010; Poupin et al. 2014; Mohan et al. 2016). This aspect of interpretation should continue to be investigated in the future.

Individual species (Popp et al. 2007; Olin et al. 2013; Mohan et al. 2016) or small groups of similar species (Hussey et al. 2010) have been investigated for their unique isotopic fractionations with diet. However, no study has investigated whether a consistent offset exists between the values in various tissues within individual fish living in a stable physical and trophic environment. Many of the previous studies that have investigated isotopic values in body tissues have used both liver and muscle as these tissues are easily accessible and vary in turnover time. Investigating this constant partitioning offset between two tissues in many species across the globe is a novel approach and has the advantage of applicability across taxa regardless background isoscape.

FISH EYE LENSES AS RECORDS OF DIET AND MOVEMENT OVER THE LIFETIME

Whereas tissue isotopic differentials are one effective tool for broadening the scope of body tissue isotope analysis, tissue turnover limits timescales to the preceding few months. In contrast, fish eye lenses serve as a permanent record of stable isotopes over the lifetime of the individual (Wallace et al. 2014). Using the isotopic data within the eye lens has the potential to increase knowledge of both habitat and food utilization for important fisheries species, especially during life stages that are not susceptible to standard fisheries or sampling gears.

Because eye-lens protein does not turn over throughout the life of an individual (Lynnerup et al. 2008), this tissue can be used as a record of both trophic and geographic history.

Eye lenses of vertebrates and some invertebrates (i.e., squids) are composed primarily of proteins called crystallins (Mahler et al. 2013). Research using radiocarbon dating on human eye lenses has revealed that crystallins are not re-worked (Lynnerup et al. 2008). Thus, the isotope values found therein represent a permanent, historical record. Recent work on Greenland sharks (*Somniosus microcephalus*) confirms this idea in fish (Nielsen et al. 2016). The eye lens is an ideal candidate for studying the $\delta^{13}\text{C}$ and $\delta^{15}\text{N}$ stable isotopic histories throughout the lifetime of the individual because they are high in both carbon and nitrogen. Recent research into several fish species on the West Florida Shelf (WFS) has shown that the $\delta^{13}\text{C}$ and $\delta^{15}\text{N}$ values in the eye lens can reveal trophic and movement histories for individual fish in areas where background isoscapes exist (Wallace et al. 2014; Kurth et al. 2019; Meath et al. 2019). Full integration of environmental isotopic values within an eye-lens lamina requires approximately 54 days in juvenile, hatchery-reared Red Drum (Granneman 2018). Because additional material is added to the eye lens as the fish grows, resolution of the isotopic record seems to be highest during the first year of life, and lower as growth slows with age. Sampling of eye-lens laminae is accomplished via manual delamination (peeling), resulting in a signal resolution of approximately three to four months (Wallace et al. 2014).

CHAPTER SUMMARIES

The following are short summaries of each data chapter and how they fit together into a coherent document. I wrote each chapter as stand-alone research articles to be published in the literature with co-authors. The individuals who contributed data or ideas to each of the chapters are specifically mentioned in the acknowledgements section of this document.

Chapter 2: Offset between muscle and liver $\delta^{15}\text{N}$ for short-term site fidelity

In chapter two I take advantage of the differential turnover times between liver and muscle tissue within an individual fish. I used literature review to investigate whether a single value (constant partitioning offset, CPO) exists for the difference between $\delta^{15}\text{N}$ of muscle and liver in teleost fishes consuming a consistent diet. I then compared the calculated average to the differences observed in wild fish. If wild fish differentials were constrained within the bounds of $\text{CPO}_{\text{M-L}}$, then I concluded that the fish and its prey did not move along the $\delta^{15}\text{N}$ gradient over the preceding two to three months. If these values were not within the bounds of $\text{CPO}_{\text{M-L}}$, then I concluded that the fish or prey did move along the $\delta^{15}\text{N}$ during the preceding few months. Distances were not assessed, but larger isotopic differences from the captive mean suggest longer distances moved.

This approach is not only applicable to a wide array of teleost fish, but is also easily accessible as a screening technique. Both muscle and liver are easy to obtain and preserve from fish collected for other purposes. These tissues require minimal training to extract properly and are easily collected. They are easy to preserve using ice and a cooler, and show no isotopic degradation during freezing (Stallings et al. 2015). I used only $\delta^{15}\text{N}$ values for this study because $\delta^{13}\text{C}$ values can be impacted by lipid content. Liver tissue is high in lipid storage molecules, rendering $\delta^{13}\text{C}$ unreliable or requiring additional chemical or mathematical manipulation to be useful (Buchheister and Latour 2010; Chen et al. 2012). If applied to other species in other regions, this technique can efficiently distinguish between fish that are healthy, stationary, and eating a consistent diet from those that should be investigated for physiological stress, movement, or diet changes.

Chapter 3: Eye-lens cores as records of geographic location in fish postlarvae

In chapter three, I explore the utility of the isotope values preserved in the eye-lens core as a record of postlarval (post-flection larvae) and early juvenile (post-settlement) location. Using a fish-length to eye-lens diameter regression equation unique to each species, I calculate that the center of the eye lens (core) represents the earliest weeks of life. During this time, postlarvae from all investigated species consume the same foods (zooplankton) (Nunn et al. 2012; Umezawa et al. 2018), with a trophic position of approximately 3.0 (McCutchan et al. 2003). Therefore, values of $\delta^{13}\text{C}$ and $\delta^{15}\text{N}$ differentiate individuals that are living and feeding in different locations. This simplification of the data allows comparison of locations and movements of several species that use broadly similar habitats on the WFS. These geographic locations further constrain habitat needs for each of the four species, Red Grouper (*Epinephelus morio*), Gag (*Mycteroperca microlepis*), Red Snapper (*Lutjanus campechanus*), and Black Seabass (*Centropristis striata*). I find that each utilizes a unique set of geographic locations with differing habitat characteristics. Each also employs a unique set of movements during the first few weeks of life within the context of the northern WFS.

Chapter 4: Eye-lens profiles as indicators of movement and diet shifts

In chapter four, I investigate the $\delta^{13}\text{C}$ and $\delta^{15}\text{N}$ across the lifetime of individual fish, comparing two species with broadly similar adult life histories. With no movement along the $\delta^{15}\text{N}$ gradient for the region, the value for $\delta^{15}\text{N}$ within an individual eye-lens profile would be expected to increase steadily throughout the lifetime of the fish (Graham et al. 2007; Bradley et al. 2015). Similarly, a lack of movement in the $\delta^{13}\text{C}$ isoscape direction results in steadily increasing values of $\delta^{13}\text{C}$ within the eye lens. Movement in either direction would be expected to obscure these patterns and result in low correlation between the profiles of $\delta^{13}\text{C}$ and $\delta^{15}\text{N}$.

Decades of biological sampling suggests that Tilefish (*Lopholatilus chamaeleonticeps*) spend their life in burrows near the shelf edge (Fisher et al. 2014) and do not change location over time. Throughout the lifespan, these fish feed on benthic invertebrates (Wenner and Barans 2001). I observe that Tilefish profiles of both $\delta^{13}\text{C}$ and $\delta^{15}\text{N}$ increase steadily over the lifetime. This species may be considered a model of isotopic consistency in both $\delta^{13}\text{C}$ and $\delta^{15}\text{N}$, reflecting consistency in both diet and location over the lifetime. Despite the expected ratio of isotopic increase between $\delta^{13}\text{C}$ and $\delta^{15}\text{N}$ of 1:3, I find that the rate of increase for $\delta^{13}\text{C}$ is almost as high as the rate of increase for $\delta^{15}\text{N}$ in Tilefish, suggesting that $\delta^{13}\text{C}$ fractionation with growth in fish may be higher than traditionally thought.

Adult Red Grouper also remain stationary. Many individuals excavate sandy sediment (Coleman et al. 2010; Wall et al. 2011), revealing small limestone outcroppings. Individuals as small as 340 mm TL have been documented engaging in this activity (Ellis 2015); the fish use these excavations as their home territory. Conventional tagging studies have shown that Red Grouper are frequently recaptured at or near their original tagging location (Coleman et al. 2011), suggesting movement is limited in many adults. However, limited data is available for Red Grouper less than ~2 years of age as long-term sampling programs rarely encounter individuals smaller than ~300 mm TL. This makes the use of eye lens $\delta^{13}\text{C}$ and $\delta^{15}\text{N}$ profiles a unique and important proxy for tracking Red Grouper throughout the lifetime. Isotopic eye-lens profiles are poorly correlated in the species. These results suggest that the species is much less stationary in early life than would have been thought from tagging studies alone, prompting further investigations into the movements and diets of the species.

Chapter 5: Integrating eye-lens isotope data with traditional fisheries data

The most recent Southeast Data Assessment and Review (SEDAR) stock assessment for Gulf of Mexico Red Grouper declared the species not overfished or undergoing overfishing (SEADAR 2019). Despite population models in the SEDAR report indicating the stock to be of sufficient size, the SEDAR panel cautioned that several areas of uncertainty for the species, including locations and habits of young juveniles (SEADAR 2019), could affect these estimates. Therefore, understanding the habitat needs, movement patterns, and trophic characteristics of Red Grouper in detail throughout the entire WFS system and beyond will be of utmost importance for future stock assessments.

In chapter five, I utilize the tools developed in chapters three and four, combined with traditional fisheries data such as stomach content analysis and capture location, to create a clearer picture of Red Grouper diet and habitat needs over the lifespan. The highest isotopic resolution is available in the first year of life, the time period with the highest growth rate. I find high degree of isotopic similarity among eye-lens cores of fish from WFS regardless of capture year or age. I also find isotopically distinct eye-lens core values from Campeche Bank and southeast Florida. I find that although many Red Grouper use a mixed benthic and planktonic basal resource, major diet components shift throughout the juvenile period. Finally, I find an isotopic feature in the $\delta^{13}\text{C}$ eye-lens profile of many individuals whereby the $\delta^{13}\text{C}$ value peaks before the end of the first year of life. Catch records indicate that most individuals captured during the first year of life were captured in shallow seagrass beds. Although seagrass captures cannot represent the entire population during early life, it seems likely that the peak in $\delta^{13}\text{C}$ is a result of Red Grouper using shallow habitats with primarily benthic basal resources during this period.

OBJECTIVES

The objective of this dissertation is to create and test novel methods of generating lifetime-scale biological data for ecosystem models and fisheries management. Using first principles, background isoscapes, and standardized statistics I show that it is possible to create robust movement and diet interpretations of fish isotope data. I use the CPO between muscle and liver tissue within the same individual to assess movement and diet on timescales of weeks to months. I also present three unique studies that develop methods of interpretation for bulk eye-lens $\delta^{13}\text{C}$ and $\delta^{15}\text{N}$ values. I use the isotope values in the eye-lens core to represent the diet and locations of postlarvae during the earliest weeks of free-swimming life. I use the lifetime isotopic profiles of two benthic-associated fish species to investigate the degree of lifetime movement and diet variability. Finally, I use the lifetime isotopic values combined with traditional fisheries data (capture location and stomach content analysis) to create an in-depth account of the lifetime trophic and movement history of a single species. Rules developed here are generally applicable to many fish species, providing life-history data for forage fish, small reef fishes, and other species which have been poorly studied in the past. These four isotopic studies demonstrate the utility of bulk isotope values for fisheries research, providing data for improvements to ecosystem modeling, fisheries stock assessment and, ultimately, fisheries management.

LITERATURE CITED

- Ainsworth, C. H., M. J. Schirripa, and H. N. M. Luna. 2015. An ATLANTIS ecosystem model for the Gulf of Mexico supporting integrated ecosystem assessment, p. 161. *In* U. D. o. Commerce [ed.].
- Awkerman, J. A., K. A. Hobson, and D. J. Anderson. 2007. Isotopic ($\delta^{15}\text{N}$ and $\delta^{13}\text{C}$) evidence for intersexual foraging differences and temporal variation in habitat use in waved albatrosses. *Canadian Journal of Zoology* **85**: 273-279.

- Balsam, W. L., and J. P. Beeson. 2003. Sea-floor sediment distribution in the Gulf of Mexico. *Deep-Sea Research Part I-Oceanographic Research Papers* **50**: 1421-1444.
- Barnes, C., S. Jennings, and J. T. Barry. 2009. Environmental correlates of large-scale spatial variation in the delta C-13 of marine animals. *Estuarine Coastal and Shelf Science* **81**: 368-374.
- Barreto-Curiel, F., U. Focken, L. R. D'Abramo, and M. T. Viana. 2017. Metabolism of *Seriola lalandi* during starvation as revealed by fatty acid analysis and compound-specific analysis of stable isotopes within amino acids. *Plos One* **12**: 17.
- Bradley, C. J., N. J. Wallsgrave, C. A. Choy, J. C. Drazen, E. D. Hetherington, D. K. Hoen, and B. N. Popp. 2015. Trophic position estimates of marine teleosts using amino acid compound specific isotopic analysis. *Limnology and Oceanography-Methods* **13**: 476-493.
- Brault, E. K., P. L. Koch, K. W. McMahon, K. H. Broach, A. P. Rosenfield, W. Sauthoff, V. J. Loeb, K. R. Arrigo, and W. O. Smith. 2018. Carbon and nitrogen zooplankton isoscapes in West Antarctica reflect oceanographic transitions. *Marine Ecology Progress Series* **593**: 29-45.
- Brock, J. C., C. W. Wright, T. D. Clayton, and A. Nayegandhi. 2004. LIDAR optical rugosity of coral reefs in Biscayne National Park, Florida. *Coral Reefs* **23**: 48-59.
- Buchheister, A., and R. J. Latour. 2010. Turnover and fractionation of carbon and nitrogen stable isotopes in tissues of a migratory coastal predator, summer flounder (*Paralichthys dentatus*). *Canadian Journal of Fisheries and Aquatic Sciences* **67**: 445-461.
- . 2011. Trophic ecology of Summer Flounder in lower Chesapeake Bay inferred from stomach content and stable isotope analyses. *Transactions of the American Fisheries Society* **140**: 1240-1254.
- Burkart, M. R., and D. E. James. 1999. Agricultural-nitrogen contributions to hypoxia in the Gulf of Mexico. *Journal of Environmental Quality* **28**: 850-859.
- Burkhardt, S., U. Riebesell, and I. Zondervan. 1999. Effects of growth rate, CO₂ concentration, and cell size on the stable carbon isotope fractionation in marine phytoplankton. *Geochimica Et Cosmochimica Acta* **63**: 3729-3741.
- Chen, G., H. Zhou, D. Ji, and B. Gu. 2012. Stable isotope enrichment in muscle, liver, and whole fish tissues of brown-marbled groupers (*Epinephelus fuscoguttatus*). *Ecological Processes* **1**: 1-5.
- Chikaraishi, Y., Y. Kashiyamal, N. O. Ogawa, H. Kitazato, and N. Ohkouchi. 2007. Metabolic control of nitrogen isotope composition of amino acids in macroalgae and gastropods: implications for aquatic food web studies. *Marine Ecology Progress Series* **342**: 85-90.
- Coleman, F. C., C. C. Koenig, K. M. Scanlon, S. Heppell, S. Heppell, and M. W. Miller. 2010. Benthic habitat modification through excavation by red grouper, *Epinephelus morio*, in the northeastern Gulf of Mexico. *Open Fish Science Journal* **3**: 1-15.
- Coleman, F. C., K. M. Scanlon, and C. C. Koenig. 2011. Groupers on the edge: shelf edge spawning habitat in and around marine reserves of the northeastern Gulf of Mexico. *Professional Geographer* **63**: 456-474.
- Curtis, J. S. 2016. Resource use overlap in a native grouper and invasive lionfish. University of South Florida.
- Doi, H., E. Kikuchi, S. Shikano, and S. Takagi. 2010. Differences in nitrogen and carbon stable isotopes between planktonic and benthic microalgae. *Limnology* **11**: 185-192.

- Duan, S., M. A. Allison, T. S. Bianchi, B. A. McKee, A. M. Shiller, L. Guo, and B. E. Rosenheim. 2014. Sediment, organic carbon, nutrients, and trace elements: sources, transport, and biogeochemical cycles in the lowermost Mississippi River. *Biogeochemical Dynamics at Major River-Coastal Interfaces: Linkages with Global Change*: 397-420.
- Duke, E. M., A. E. Harada, and R. S. Burton. 2018. Large interannual variation in spawning in San Diego marine protected areas captured by molecular identification of fish eggs. *Marine Ecology Progress Series* **604**: 199-210.
- Elliot Smith, E. A., C. Harrod, and S. D. Newsome. 2018. The importance of kelp to an intertidal ecosystem varies by trophic level: insights from amino acid $\delta^{13}\text{C}$ analysis. *Ecosphere* **9**.
- Ellis, R. D. 2015. Ecological Effects of Red Grouper (*Epinephelus morio*) in Florida Bay. PhD dissertation. The Florida State University.
- Elsdon, T. S., S. Ayvazian, K. W. McMahon, and S. R. Thorrold. 2010. Experimental evaluation of stable isotope fractionation in fish muscle and otoliths. *Marine Ecology Progress Series* **408**: 195-205.
- Fisher, J. A. D., K. T. Frank, B. Petrie, and W. C. Leggett. 2014. Life on the edge: environmental determinants of tilefish (*Lopholatilus chamaeleonticeps*) abundance since its virtual extinction in 1882. *Ices Journal of Marine Science* **71**: 2371-2378.
- France, R., J. Holmquist, M. Chandler, and A. Cattaneo. 1995. $\delta^{15}\text{N}$ evidence for nitrogen fixation associated with macroalgae from a seagrass - mangrove - coral reef system. *Marine Ecology Progress Series* **167**: 197-199.
- Fry, B. 2006. Stable isotope ecology. Springer Science+Business Media.
- Fry, B., and S. C. Wainright. 1991. Diatom sources of C-13 rich carbon in marine food webs. *Marine Ecology Progress Series* **76**: 149-157.
- Gledhill, C., and A. David. 2004. Survey of fish assemblages and habitat within two marine protected areas on the West Florida shelf, p. 614-625. *In* R. L. Creswell [ed.], *Proceedings of the Fifty-Fifth Annual Gulf and Caribbean Fisheries Institute*.
- Graham, B. S., D. Grubbs, K. Holland, and B. N. Popp. 2007. A rapid ontogenetic shift in the diet of juvenile Yellowfin Tuna from Hawaii. *Marine Biology* **150**: 647-658.
- Granneman, J. E. 2018. Evaluation of trace-metal and isotopic records as techniques for tracking lifetime movement patterns in fishes. University of South Florida.
- Grippo, M. A., J. W. Fleeger, S. F. Dubois, and R. Condrey. 2011. Spatial variation in basal resources supporting benthic food webs revealed for the inner continental shelf. *Limnology and Oceanography* **56**: 841-856.
- Hine, A. C., and S. D. Locker. 2011. The Florida Gulf of Mexico continental shelf—great contrasts and significant transitions. *The Gulf of Mexico: Origin, Waters, and Marine Life*.
- Holl, C. M., T. A. Villareal, C. D. Payne, T. D. Clayton, C. Hart, and J. P. Montoya. 2007. *Trichodesmium* in the western Gulf of Mexico: N-15(2)-fixation and natural abundance stable isotope evidence. *Limnology and Oceanography* **52**: 2249-2259.
- Howarth, R. W., G. Billen, D. Swaney, A. Townsend, N. Jaworski, K. Lajtha, J. A. Downing, R. Elmgren, N. Caraco, T. Jordan, F. Berendse, J. Freney, V. Kudeyarov, P. Murdoch, and Z. L. Zhu. 1996. Regional nitrogen budgets and riverine N&P fluxes for the drainages to the North Atlantic Ocean: Natural and human influences. *Biogeochemistry* **35**: 75-139.
- Huelster, S. 2015. Comparison of isotope-based biomass pathways with groundfish community structure in the eastern Gulf of Mexico. Masters. University of South Florida.

- Hunsicker, M. E., T. E. Essington, K. Y. Aydin, and B. Ishida. 2010. Predatory role of the commander squid *Beryteuthis magister* in the eastern Bering Sea: insights from stable isotopes and food habits. *Marine Ecology Progress Series* **415**: 91-108.
- Hussey, N. E., J. Brush, I. D. McCarthy, and A. T. Fisk. 2010. δ N-15 and δ C-13 diet-tissue discrimination factors for large sharks under semi-controlled conditions. *Comparative Biochemistry and Physiology a-Molecular & Integrative Physiology* **155**: 445-453.
- Hussey, N. E., M. A. MacNeil, B. C. McMeans, J. A. Olin, S. F. J. Dudley, G. Cliff, S. P. Wintner, S. T. Fennessy, and A. T. Fisk. 2014. Rescaling the trophic structure of marine food webs. *Ecology Letters* **17**: 239-250.
- Kendall, C., S. R. Silva, and V. J. Kelly. 2001. Carbon and nitrogen isotopic compositions of particulate organic matter in four large river systems across the United States. *Hydrological Processes* **15**: 1301-1346.
- Keough, J. R., C. A. Hagley, E. Ruzycski, and M. Sierszen. 1998. δ C-13 composition of primary producers and role of detritus in a freshwater coastal ecosystem. *Limnology and Oceanography* **43**: 734-740.
- Kormicker, L. S., F. Bonet, R. Cann, and C. Hoskin. 1959. Alacran Reef, Campeche Bank, Mexico. *Institute of marine science* **6**: 1-22.
- Kurth, B. N., E. Peebles, and C. D. Stallings. 2019. Atlantic Tarpon (*Megalops atlanticus*) exhibit upper estuarine habitat dependence followed by foraging system fidelity after ontogenetic habitat shifts. *Estuarine Coastal and Shelf Science*.
- Lynnerup, N., H. Kjeldsen, S. Heegaard, C. Jacobsen, and J. Heinemeier. 2008. Radiocarbon Dating of the Human Eye Lens Crystallines Reveal Proteins without Carbon Turnover throughout Life. *Plos One* **3**.
- Mahler, B., Y. W. Chen, J. Ford, C. Thiel, G. Wistow, and Z. R. Wu. 2013. Structure and dynamics of the fish eye lens protein, gamma M7-Crystallin. *Biochemistry* **52**: 3579-3587.
- Marshall, K. N., L. E. Koehn, P. S. Levin, T. E. Essington, and O. P. Jensen. 2019. Inclusion of ecosystem information in US fish stock assessments suggests progress toward ecosystem-based fisheries management. *Ices Journal of Marine Science* **76**: 1-9.
- Maunder, M. N., and K. R. Piner. 2015. Contemporary fisheries stock assessment: many issues still remain. *Ices Journal of Marine Science* **72**: 7-18.
- McClelland, J. W., C. M. Holl, and J. P. Montoya. 2003. Relating low δ N-15 values of zooplankton to N-2-fixation in the tropical North Atlantic: insights provided by stable isotope ratios of amino acids. *Deep-Sea Research Part I-Oceanographic Research Papers* **50**: 849-861.
- McClelland, J. W., and J. P. Montoya. 2002. Trophic relationships and the nitrogen isotopic composition of amino acids in plankton. *Ecology* **83**: 2173-2180.
- McCutchan, J. H., W. M. Lewis, C. Kendall, and C. C. McGrath. 2003. Variation in trophic shift for stable isotope ratios of carbon, nitrogen, and sulfur. *Oikos* **102**: 378-390.
- Meath, B., E. B. Peebles, B. A. Seibel, and H. Judkins. 2019. Stable isotopes in the eye lenses of *Doryteuthis plei* (Blainville 1823): exploring natal origins and migratory patterns in the eastern Gulf of Mexico. *Continental Shelf Research*.
- Mohan, J. A., S. D. Smith, T. L. Connelly, E. T. Attwood, J. W. McClelland, S. Z. Herzka, and B. D. Walther. 2016. Tissue-specific isotope turnover and discrimination factors are

- affected by diet quality and lipid content in an omnivorous consumer. *Journal of Experimental Marine Biology and Ecology* **479**: 35-45.
- Nielsen, J., R. B. Hedeholm, J. Heinemeier, P. G. Bushnell, J. S. Christiansen, C. B. Ramsey, R. W. Brill, M. Simon, K. F. Steffensen, and J. F. Steffensen. 2016. Eye lens radiocarbon reveals centuries of longevity in the Greenland shark (*Somniosus microcephalus*). *Science* **353**: 702-704.
- Nunn, A. D., L. H. Tewson, and I. G. Cowx. 2012. The foraging ecology of larval and juvenile fishes. *Reviews in Fish Biology and Fisheries* **22**: 377-408.
- O'Farrell, H., A. Gruss, S. R. Sagarese, E. A. Babcock, and K. A. Rose. 2017. Ecosystem modeling in the Gulf of Mexico: current status and future needs to address ecosystem-based fisheries management and restoration activities. *Reviews in Fish Biology and Fisheries* **27**: 587-614.
- Olin, J. A., N. E. Hussey, A. Grgicak-Mannion, M. W. Fritts, S. P. Wintner, and A. T. Fisk. 2013. Variable delta N-15 diet-tissue discrimination factors among sharks: Implications for trophic position, diet and food web models. *Plos One* **8**.
- Paar, M., B. Lebreton, M. Graeve, M. Greenacre, R. Asmus, and H. Asmus. 2019. Food sources of macrozoobenthos in an Arctic kelp belt: trophic relationships revealed by stable isotope and fatty acid analyses. *Marine Ecology Progress Series* **615**: 31-49.
- Peebles, E. B., and D. J. Hollander. 2020. Combining Isoscapes with Tissue-Specific Isotope Records to Recreate the Geographic Histories of Fish, p. 203-218. *In* S. A. Murawski et al. [eds.], *Scenarios and Responses to Future Deep Oil Spills*. Springer, Cham.
- Popp, B. N., B. S. Graham, R. J. Olson, C. C. S. Hannides, M. J. Lott, G. A. Lopez-Ibarra, F. Galvan-Magana, and B. Fry. 2007. Insight into the Trophic Ecology of Yellowfin Tuna, *Thunnus albacares*, from Compound-Specific Nitrogen Isotope Analysis of Proteinaceous Amino Acids.
- Popp, B. N., E. A. Laws, R. R. Bidigare, J. E. Dore, K. L. Hanson, and S. G. Wakeham. 1998. Effect of phytoplankton cell geometry on carbon isotopic fractionation. *Geochimica Et Cosmochimica Acta* **62**: 69-77.
- Poupin, N., F. Mariotti, J. F. Huneau, D. Hermier, and H. Fouillet. 2014. Natural isotopic signatures of variations in body nitrogen fluxes: A compartmental model analysis. *Plos Computational Biology* **10**.
- Puigcorbe, V., C. R. Benitez-Nelson, P. Masque, E. Verdeny, A. E. White, B. N. Popp, F. G. Prahl, and P. J. Lam. 2015. Small phytoplankton drive high summertime carbon and nutrient export in the Gulf of California and Eastern Tropical North Pacific. *Global Biogeochemical Cycles* **29**: 1309-1332.
- Quaek-Davies, K., V. A. Bendall, K. M. MacKenzie, S. Hetherington, J. Newton, and C. N. Trueman. 2018. Teleost and elasmobranch eye lenses as a target for life-history stable isotope analyses. *PeerJ* **6**: 26.
- Radabaugh, K. R., D. J. Hollander, and E. B. Peebles. 2013. Seasonal delta C-13 and delta N-15 isoscapes of fish populations along a continental shelf trophic gradient. *Continental Shelf Research* **68**: 112-122.
- Radabaugh, K. R., E. M. Malkin, D. J. Hollander, and E. B. Peebles. 2014. Evidence for light-environment control of carbon isotope fractionation by benthic microalgal communities. *Marine Ecology Progress Series* **495**: 77-90.
- Radabaugh, K. R., and E. B. Peebles. 2014. Multiple regression models of $\delta^{13}\text{C}$ and $\delta^{15}\text{N}$ for fish populations in the eastern Gulf of Mexico. *Continental Shelf Research* **84**: 158-168.

- SEADAR. 2019. SEDAR 61 Stock assessment report: Gulf of Mexico Red Grouper, p. 285. SEDAR.
- SEADAR. 2018. SEDAR 52: Gulf of Mexico Red Snapper, p. 434. SEDAR. NOAA.
- Simpson, S., D. Sims, and C. N. Trueman. 2019. Ontogenetic trends in resource partitioning and trophic geography of sympatric skates (Rajidae) inferred from stable isotope composition across eye lenses. *Marine Ecology Progress Series* **624**: 103-116.
- Skinner, M. M., A. A. Martin, and B. C. Moore. 2016. Is lipid correction necessary in the stable isotope analysis of fish tissues? *Rapid Communications in Mass Spectrometry* **30**: 881-889.
- Stallings, C. D., J. A. Nelson, K. L. Rozar, C. S. Adams, K. R. Wall, T. S. Switzer, B. L. Winner, and D. J. Hollander. 2015. Effects of preservation methods of muscle tissue from upper-trophic level reef fishes on stable isotope values (δ C-13 and δ N-15). *PeerJ* **3**.
- Trueman, C. N., K. M. MacKenzie, and K. S. Glew. 2017. Stable isotope-based location in a shelf sea setting: accuracy and precision are comparable to light-based location methods. *Methods in Ecology and Evolution* **8**: 232-240.
- Umezawa, Y., A. Tamaki, T. Suzuki, S. Takeuchi, C. Yoshimizu, and I. Tayasu. 2018. Phytoplankton as a principal diet for callinassid shrimp larvae in coastal waters, estimated from laboratory rearing and stable isotope analysis. *Marine Ecology Progress Series* **592**: 141-158.
- Walker, B. D., E. R. M. Druffel, J. Kolasinski, B. J. Roberts, X. Xu, and B. E. Rosenheim. 2017. Stable and radiocarbon isotopic composition of dissolved organic matter in the Gulf of Mexico. *Geophysical Research Letters* **44**: 8424-8434.
- Wall, C. C., B. T. Donahue, D. F. Naar, and D. A. Mann. 2011. Spatial and temporal variability of red grouper holes within Steamboat Lumps Marine Reserve, Gulf of Mexico. *Marine Ecology Progress Series* **431**: 243-254.
- Wall, K. R., and C. D. Stallings. 2018. Subtropical epibenthos varies with location, reef type, and grazing intensity. *Journal of Experimental Marine Biology and Ecology* **509**: 54-65.
- Wallace, A. A., D. J. Hollander, and E. B. Peebles. 2014. Stable isotopes in fish eye lenses as potential recorders of trophic and geographic history. *Plos One* **9**.
- Wenner, E. L., and C. A. Barans. 2001. Benthic habitats and associated fauna of the upper- and middle-continental slope near the Charleston Bump, p. 161-175. *In* G. R. Sedberry [ed.], *Island in the Stream: Oceanography and Fisheries of the Charleston Bump*. American Fisheries Society Symposium.

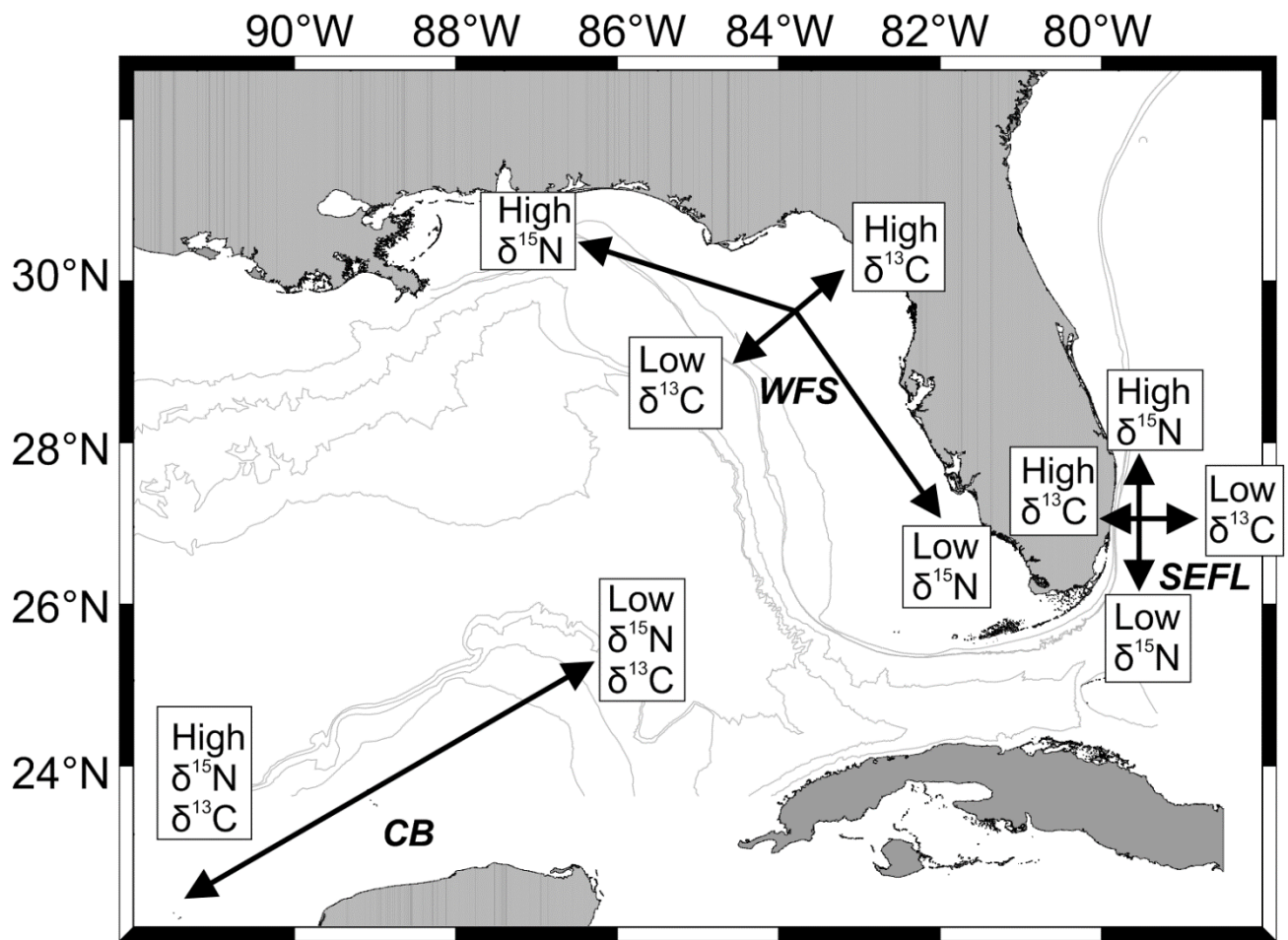


Figure 1.1 General $\delta^{13}\text{C}$ and $\delta^{15}\text{N}$ trends within the three geographic study regions discussed in this dissertation. West Florida Shelf (WFS) isotope trends after Radabaugh and Peebles (2014). Campeche Bank (CB) isotope trends after Peebles and Hollander (2020) and B. Michaud (unpublished data). Southeast Florida (SEFL) trends after Curtis (2016).

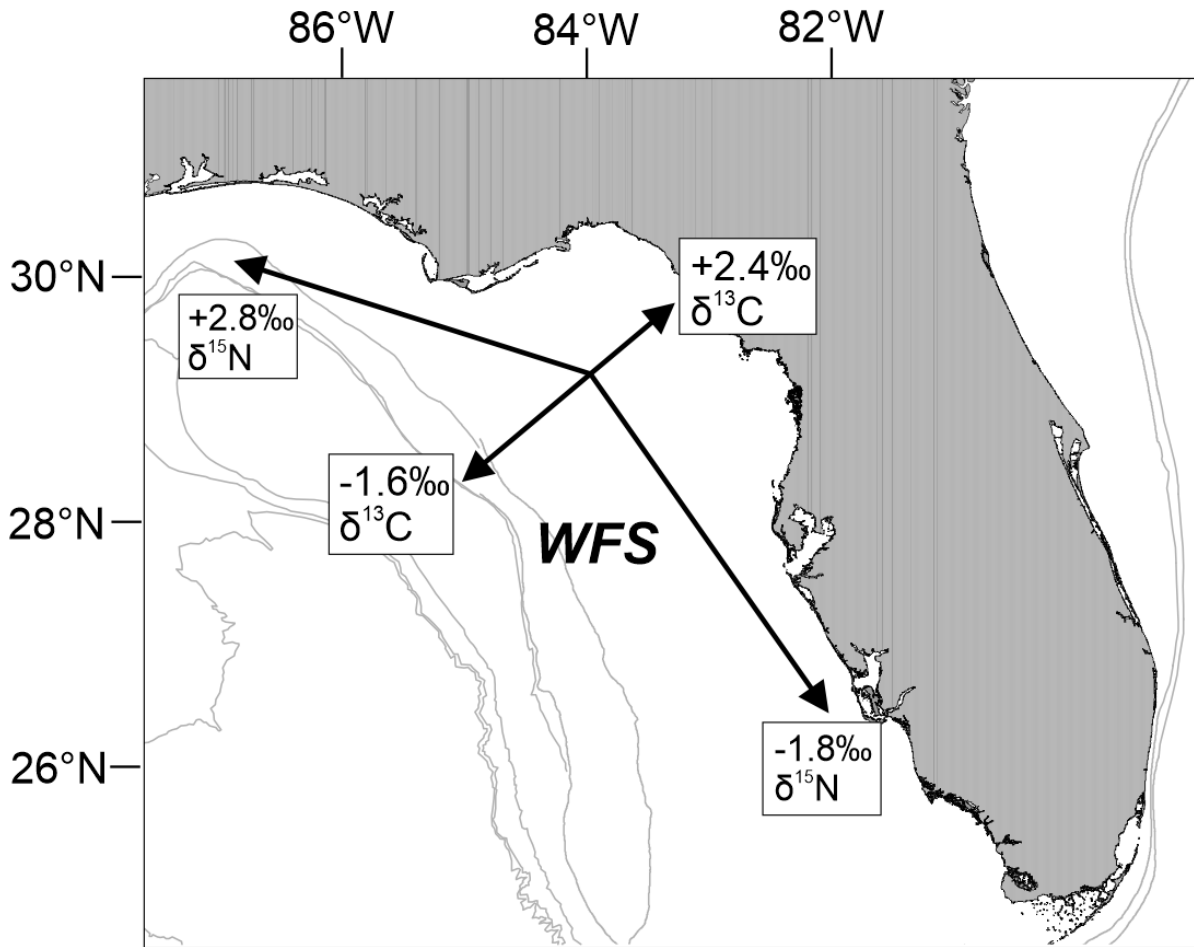


Figure 1.2. General $\delta^{13}\text{C}$ and $\delta^{15}\text{N}$ trends on the WFS in fish muscle tissue after Radabaugh and Peebles (2014). Values derived from variance from mean values for each isotope based on multiple regression models.

CHAPTER 2: THE $\delta^{15}\text{N}$ VALUES IN MUSCLE AND LIVER OF MARINE TELEOSTS
DIFFER PREDICTABLY AND CAN BE USED AS AN INDICATOR OF SITE FIDELITY

ABSTRACT

We investigated the $\delta^{15}\text{N}$ offset between two tissue types, skeletal muscle (relatively slow turnover rate) and liver (relatively fast turnover rate; $\delta^{15}\text{N}_{\text{M-L}}$), as an indicator of marine fish site fidelity at a timescale of weeks-to-months. We calculated $\delta^{15}\text{N}_{\text{M-L}}$ from twelve published studies of captive marine teleost species that consumed isotopically consistent diets. The constant partitioning offset (difference between $\delta^{15}\text{N}$ in muscle and liver tissue of the same individual [$\text{CPO}_{\text{M-L}}$]: $\Delta\delta^{15}\text{N}_{\text{M-L}}$) was $1.67 \pm 0.30\text{‰}$ (mean \pm CI). Variation around the mean partitioning offset was not correlated with size, trophic position, tail aspect ratio, or water temperature. We used the 95% confidence interval for $\text{CPO}_{\text{M-L}}$ as a baseline for comparing the $\Delta\delta^{15}\text{N}_{\text{M-L}}$ values from eight wild-caught fish species captured from Florida, USA continental-shelf waters. The $\Delta\delta^{15}\text{N}_{\text{M-L}}$ values from five species were not different from $\text{CPO}_{\text{M-L}}$, reflecting a lack of isoscape-scale movements by these predatory species and their prey during recent months, consistent with the literature. The mean $\Delta\delta^{15}\text{N}_{\text{M-L}}$ values for three species were lower than $\text{CPO}_{\text{M-L}}$, suggesting that these predatory species or their prey had recently moved along the $\delta^{15}\text{N}$ gradient. All species with $\Delta\delta^{15}\text{N}_{\text{M-L}}$ values lower than $\text{CPO}_{\text{M-L}}$ are generalist predators that consume mixed diets of migratory forage fishes and benthic invertebrates. As a method, $\Delta\delta^{15}\text{N}_{\text{M-L}}$ appears to be useful for identifying short-term movements of marine teleosts or their prey and has the potential for widespread application.

INTRODUCTION

Seasonal diet and habitat use information are essential inputs to fisheries stock assessments and ecosystem models. However, these parameters may be difficult to obtain due to the difficulty and cost associated with field experiments. By utilizing the internal chemistry of individual organisms, researchers can broaden access to short-term movement information for many additional species for which the incorporation of movement data was impractical. Ratios of the two nitrogen stable isotopes ($^{15}\text{N}:^{14}\text{N}$, expressed as $\delta^{15}\text{N}$) have been measured for a multitude of terrestrial and aquatic animal species (Pinnegar and Polunin 1999; Fry et al. 2003; Ellis et al. 2014; Tzadik et al. 2017). Values of $\delta^{15}\text{N}$ have served as proxies for trophic position (Dalerum and Angerbjorn 2005; Bradley et al. 2015), food-web structure (Post 2002; Chikaraishi et al. 2009), habitat use (Fry et al. 2002; Brame et al. 2014), organic nutrient subsidies (Nelson et al. 2012; Larson et al. 2013), inorganic nutrient source (Gaston and Suthers 2004), and tissue turnover rate (Downs et al. 2014; Vander Zanden et al. 2015). Studies of $\delta^{15}\text{N}$ -based tissue turnover rate in bony fishes have consistently reported that liver tissue turns over at a faster rate than muscle tissue (Logan et al. 2006; Ankjaero et al. 2012; Mohan et al. 2016). Liver tissue requires days to weeks to equilibrate and is generally controlled by metabolic rate (Matley et al. 2016). Muscle requires weeks to months to equilibrate and is typically controlled by growth (Varela et al. 2012; Davis et al. 2015; Mohan et al. 2016).

Isotopic offsets between body tissues

Even under constant isotopic conditions, muscle and liver tissues may not reach identical values within the same individual due to physiological differences between tissue types

(Michaud et al. 2013; Sturrock et al. 2014). Authors have noted that $\delta^{15}\text{N}_{\text{muscle}}$ values are higher than $\delta^{15}\text{N}_{\text{liver}}$ values in several marine teleost field studies (Haas et al. 2009; Michaud et al. 2013; Davis et al. 2015). Haas et al. (2009) used $\delta^{15}\text{N}_{\text{muscle}}$ and $\delta^{15}\text{N}_{\text{liver}}$ to examine movements of Mummichogs (*Fundulus heteroclitus*) within an estuary, but noted that $\delta^{15}\text{N}_{\text{muscle}}$ values were always higher than $\delta^{15}\text{N}_{\text{liver}}$, even for fish caged in place. Davis et al. (2015) found $\delta^{15}\text{N}_{\text{muscle}}$ averaged 1.5‰ higher than $\delta^{15}\text{N}_{\text{liver}}$ in four of five reef-fish species. Likewise, Michaud et al. (2013) found that $\delta^{15}\text{N}_{\text{muscle}}$ in Arctic Charr (*Salvelinus alpinus*) was approximately 1‰ higher than $\delta^{15}\text{N}_{\text{liver}}$ with small differences based on sex, maturity state, or feeding status. The results of several other stable isotope studies using wild, marine teleosts have included higher values of $\delta^{15}\text{N}_{\text{muscle}}$ than $\delta^{15}\text{N}_{\text{liver}}$ (e.g. Graham et al. 2007; Chouvelon et al. 2015; Logan et al. 2015).

An offset between $\delta^{15}\text{N}$ values for muscle and liver in fish fed a consistent diet has never been investigated on a broad scale. The final $\delta^{15}\text{N}$ muscle and liver values from diet-switch experiments (Suzuki et al. 2005; Buchheister and Latour 2010; Mohan et al. 2016) can be expected to remain constant after sufficient time to complete turnover of the tissues under study. Thus, the difference between $\delta^{15}\text{N}$ values of muscle and liver recorded at the end of long-duration experiments can be used to calculate an offset between $\delta^{15}\text{N}_{\text{muscle}}$ and $\delta^{15}\text{N}_{\text{liver}}$ in captive fishes. This constant partitioning offset ($\text{CPO}_{\text{M-L}}$: $\Delta\delta^{15}\text{N}_{\text{M-L}}$) can be used to infer movement and diet changes in wild fish in regions with known geographic trends in background isoscapes.

Isotopic and geographic setting for wild fish in study

The continental shelf around Florida, USA, includes a clearly defined $\delta^{15}\text{N}$ gradient observed in both basal resources and fish muscle (Radabaugh et al. 2013; Radabaugh and Peebles 2014). The region includes diverse soft- and hard-bottom habitats. Scleractinian coral

reefs of the Florida reef tract extend northward along the southeast coast of the Florida peninsula, including Biscayne National Park (Ogden et al. 1994; Harlem et al. 2012). On the western side of the peninsula, the expansive West Florida Shelf (WFS) is composed of a mosaic of soft- and hard-bottom habitats (Locker et al. 2010; Hine and Locker 2011; Wall and Stallings 2018). A fine-scale isoscape has been established for the WFS (Radabaugh et al. 2013; Radabaugh and Peebles 2014) with higher $\delta^{15}\text{N}$ values in the north and lower values in the south. This established isoscape can serve as the backdrop against which to examine the differences between slow- and fast-turnover tissues in a range of wild-caught fish species, inferring levels of site fidelities for predators and their prey. Previous work has taken advantage of the large differences in background $\delta^{15}\text{N}$ between estuaries and coastal systems of the Gulf of Mexico. Studies of both blue crabs (*Callinectes sapidus*) (Gelpi et al. 2013) and brown shrimp (*Farfantepenaeus aztecus*) (Fry et al. 2003) compared slow- and fast-turnover tissues to examine movement into or out of Louisiana estuaries for settlement and spawning.

Some teleosts species in the region, such as Golden Tilefish (*Lopholatilus chamaeleonticeps*) exhibit high site fidelity and consume consistent, benthos-derived diets (Grimes et al. 1986; Grimes and Turner 1999). In contrast, the short-term movements and diets of species such as Red Grouper (*Epinephelus morio*) may be less consistent. While most tagged individuals are re-captured only short distances from their original tagging location, re-capture studies can present bias toward stationary individuals (Burns, 2009). In addition, stomach-content studies indicate that the species diet tends to include both benthic prey and migratory forage fishes in the water column (Bullock and Smith 1991; Brule and Canche 1993).

Objectives

We conducted a literature survey of captive diet-switch studies that reported tissue-specific $\delta^{15}\text{N}$ values for marine teleosts. We used the published results of these experiments to calculate $\text{CPO}_{\text{M-L}}$. We hypothesized that (1) $\text{CPO}_{\text{M-L}} = 0$ after the fish had been fed an isotopically consistent diet for sufficient time to complete turn-over of both tissues. If $\text{CPO}_{\text{M-L}} \neq 0$ we hypothesized that (2) factors such as water temperature, body size, or metabolic rate would correlate with this difference. We then compared $\text{CPO}_{\text{M-L}}$ with the observed $\Delta\delta^{15}\text{N}_{\text{M-L}}$ of eight reef-associated fish species caught on Florida's continental shelf to investigate the relative amount of short-term movement in these predatory fishes or their prey. We hypothesized that (3) species with little movement and local diets would have $\Delta\delta^{15}\text{N}_{\text{M-L}}$ values no different from $\text{CPO}_{\text{M-L}}$ while species which migrated or consumed migrating prey would have $\Delta\delta^{15}\text{N}_{\text{M-L}}$ significantly different from $\text{CPO}_{\text{M-L}}$. The method can be applied to less-well studied populations to quickly evaluate relative site fidelities of fish species within a region.

MATERIALS AND METHODS

Survey of diet-switch studies

We compiled 14 $\delta^{15}\text{N}_{\text{muscle}}$ and $\delta^{15}\text{N}_{\text{liver}}$ measurements from 12 previous studies in marine teleosts where the qualifications were that the study must investigate captive fish in diet-switch experiments that measured bulk $\delta^{15}\text{N}_{\text{muscle}}$ and $\delta^{15}\text{N}_{\text{liver}}$ values. We limited the results to the final $\delta^{15}\text{N}_{\text{muscle}}$ and $\delta^{15}\text{N}_{\text{liver}}$ values from experiments for which a minimum of three months elapsed post diet-change or $\delta^{15}\text{N}$ values remained consistent for two consecutive sampling events. A minimum duration of 90 days has been shown to be sufficient to allow both muscle and liver tissues time to stabilize after an isotopic shift (Trueman et al. 2006; Mohan et al. 2016). In the

case of studies investigating the effect of feed quality or starvation on tissue isotope values, we included only isotope values from the control group or those fed a “high” quality diet. Fish in the starvation group or consuming “low” quality feed were excluded. Research subjects in each of the studies (1) were fed a starting diet until tissue isotope values stabilized, (2) were subjected to a change in feed, and (3) were fed the second diet for a minimum of three months or until measured values of $\delta^{15}\text{N}$ were stable in both tissues. Diets consisted of either commercial fish feeds (fish feed in Table 2.1) or wild-caught prey items (each wild type identified in Table 2.1). In the case of wild-caught prey, the feed was either collected or bought in a single batch for the duration of the study to ensure isotopic consistency.

Together, the experiments analyzed included 101 captive fish representing 12 marine species in 11 families (Table 2.1). The studies were conducted on four continents and used fish specimens from three ocean basins, with water temperatures ranging from 8 to 28°C. The smallest, most sedentary species was the Sand Goby (*Pomatoschistus minutus*). The largest, most mobile species was the Pacific Bluefin Tuna (*Thunnus orientalis*). Total mass and length ranged over several orders of magnitude (Table 2.1).

For each of the 12 studies, we recorded diet type (commercial fish feed or a type of wild feed) and the number of days since diet change. Most studies also provided information on length, weight, and water temperature. However, if fish length or weight was missing, we estimated the missing parameter based on information provided by the study combined with published length-weight relationships. For example, if length was reported but not total weight, we calculated total weight using the combined species-specific, weight-at-length regressions provided by FishBase (<http://www.fishbase.org/search.php>). We also collected information on estimated trophic position and tail aspect ratio, a proxy for swimming speed and overall

metabolic rate, reported by FishBase (Froese and Pauly 2018). To test hypothesis (1) we calculated the parameter $\Delta\delta^{15}\text{N}_{\text{M-L}}$ by subtracting mean $\delta^{15}\text{N}_{\text{liver}}$ from mean $\delta^{15}\text{N}_{\text{muscle}}$ within each study. To test hypothesis (2) we used a correlation matrix (Pearson's r) to evaluate all possible pairings of variables ($\Delta\delta^{15}\text{N}_{\text{M-L}}$, $\delta^{15}\text{N}_{\text{muscle}}$, $\delta^{15}\text{N}_{\text{liver}}$, mean length, mean weight, water temperature, trophic level, tail aspect ratio) and visually examined scatterplots of each pairing to qualitatively assess nonlinear relationships. We used linear regression to relate $\delta^{15}\text{N}_{\text{muscle}}$ to $\delta^{15}\text{N}_{\text{liver}}$, which produced an intercept and slope describing the average partitioning offset ($\Delta\delta^{15}\text{N}_{\text{M-L}}$).

Survey of wild-caught reef fishes

Between 2011 and 2017, we collected reef fishes using a variety of vessels and gear types (longline, hook-and-line, pole spear) from continental shelf waters around Florida, USA. From the WFS, we collected White Grunt (*Haemulon plumierii*; $n = 141$), Gray Snapper (*Lutjanus griseus*; $n = 77$), Red Snapper (*Lutjanus campechanus*; $n = 9$), Black Seabass (*Centropristis striata*; $n = 10$), Golden Tilefish ($n = 36$), and Red Grouper ($n = 45$). We collected Graysby (*Cephalopholis cruentata*; $n = 69$) and lionfishes (*Pterois miles/P. volitans*; $n = 64$) from coral reefs in Biscayne National Park off the coast of southeastern Florida (Figure 2.1). We collected all species during the months of July, August, and September. Additional Red Grouper and Black Seabass were collected seasonally (Table 2.4). Because all specimens were collected as a part of other field sampling efforts, total numbers and the availability of ancillary data, such as gonad mass, differed among species.

We recorded length, weight, sex, and maturity state in the field for all specimens. We also recorded gonad mass for White Grunt, as these specimens were collected for a reproduction study (Stallings et al. 2016). For isotope analysis, we removed a 3–5 g sample of both muscle

from the dorsal musculature above the lateral line and liver tissue from each specimen, wrapped each sample in aluminum foil, and stored each at -20°C until analysis. Freezing has been found to impart no isotopic preservation effect on the tissues (Stallings et al. 2015).

Prior to isotope analysis, we thawed and dried samples at 55°C for a minimum of 48 h. Once dried, we homogenized the samples into a powder using a stainless-steel ball mill (Wig-L-Bug™). We then packaged sub-samples of 500–750 µg into 3.3 x 5 mm tin capsules for stable-isotope analysis performed in duplicate. Isotope analysis was performed using a Carlo-Erba NA2500 Series II elemental analyzer coupled to a continuous-flow Thermo-Finnigan Delta+ XL isotope ratio mass spectrometer at the University of South Florida College of Marine Science in St. Petersburg, Florida. Calibration standards were NIST 8573 and NIST 8574 L-glutamic acid standard reference materials. Analytical precision was measured using NIST 1577b bovine liver. Results are presented in standard notation (δ notation, in ‰) relative to the international standard of air using the equation:

$$\delta^{15}\text{N} = R_{\text{sample}}/R_{\text{standard}} - 1$$

We calculated mean and standard error of $\Delta\delta^{15}\text{N}_{\text{M-L}}$ for each wild-caught species collected during the July to September period. Using power analysis, we determined that the minimum sample size required to compare data to $\text{CPO}_{\text{M-L}}$ was seven. All wild-caught species included at least nine individuals. We performed regressions between total length and $\Delta\delta^{15}\text{N}_{\text{M-L}}$ for each species. Despite two significant correlations between fish total length and $\Delta\delta^{15}\text{N}_{\text{M-L}}$ (Red Snapper: $p = 0.02$, $R^2 = 0.58$; White Grunt: $p = 0.03$, $R^2 = 0.03$), slopes were uniformly shallow (range: -0.003-0.000) and R^2 values were low, suggesting a weak relationship between $\Delta\delta^{15}\text{N}_{\text{M-L}}$ and fish size in wild species (Table 2.2). We, therefore, combined all specimens by species. We also combined values of $\Delta\delta^{15}\text{N}_{\text{M-L}}$ for all capture locations for each species.

Shapiro-Wilkes tests suggested $\Delta\delta^{15}\text{N}_{\text{M-L}}$ data could not be distinguished from a normal distribution ($W = 0.94$, $p = 0.29$). To test hypothesis (3) we used the Kruskal-Wallis (K-W) rank-based ANOVA to compare the distributions of $\Delta\delta^{15}\text{N}_{\text{M-L}}$ values for each wild-caught species with the $\text{CPO}_{\text{M-L}}$ identified by the literature survey. We used the Games-Howell (G-H) post-hoc test to compare individual species with $\text{CPO}_{\text{M-L}}$. We selected these tests due their robust treatment of the study's unbalanced design and observed heterogeneity of variance (Olejnik and Lee 1990; Sokal and Rohlf 1994).

To investigate the influence of gonad mass on White Grunt $\Delta\delta^{15}\text{N}_{\text{M-L}}$, we performed linear regression of $\Delta\delta^{15}\text{N}_{\text{M-L}}$ as a function of gonad mass for each recorded sex category: mature females, mature males, and immature individuals. Linear regressions of $\Delta\delta^{15}\text{N}_{\text{M-L}}$ against gonad mass resulted in $R^2 < 0.05$ for each group, and slopes were not different from zero at $p = 0.05$. Therefore, we combined all specimens from each group (regardless of gonad mass) for the K-W and G-H tests of sex and maturity in relation to $\text{CPO}_{\text{M-L}}$. We collected both Red Grouper and Black Seabass throughout the year. Within each species, we compared each of four seasons to the $\text{CPO}_{\text{M-L}}$ distribution using K-W and G-H tests. All statistical analyses were conducted using Statgraphics Centurion 18 (The Plains, Virginia, USA).

RESULTS

Survey of diet-switch studies

The mean $\text{CPO}_{\text{M-L}}$ value ($\Delta\delta^{15}\text{N}_{\text{M-L}}$) was 1.67‰ and the standard error was 0.14‰. The minimum value was 0.5‰ in Yellowtail Amberjack (*Seriola lalandi*) while the maximum value was 2.42‰ in Summer Flounder (*Paralichthys dentatus*) which made the total range 1.92‰. The 95% confidence interval (CI) for the mean was 1.37–1.98‰. A one-tailed t-test indicated the true

value of $\delta^{15}\text{N}_{\text{M-L}}$ was significantly larger than zero ($t = 12.02, p < 0.001$). Thus, we rejected hypothesis (1) that $\text{CPO}_{\text{M-L}} = 0$.

$\text{CPO}_{\text{M-L}}$ was not correlated with length, weight, trophic position, tail aspect ratio, or values of $\delta^{15}\text{N}_{\text{muscle}}$ or $\delta^{15}\text{N}_{\text{liver}}$ (Table 2.3), nor did they group by temperature (Figure 2.2). However, values for $\delta^{15}\text{N}_{\text{muscle}}$ and $\delta^{15}\text{N}_{\text{liver}}$ were strongly correlated with one another (Pearson product-moment $r = 0.98, p < 0.001$). These results led us to reject hypothesis (2) that intrinsic or extrinsic factors would correlate with $\Delta\delta^{15}\text{N}_{\text{M-L}}$.

Linear regression indicated a significant relationship between $\delta^{15}\text{N}_{\text{muscle}}$ and $\delta^{15}\text{N}_{\text{liver}}$ with evenly distributed residuals (Figure 2.3). The equation was:

$$\delta^{15}\text{N}_{\text{liver}} = \delta^{15}\text{N}_{\text{muscle}} - 1.61\text{‰}$$

($n = 14, R^2 = 0.96, \text{intercept } p < 0.05, \text{slope } p < 0.05$)

Whereas the slope of this relationship was one, the negative intercept demonstrated that muscle contained consistently heavier nitrogen than liver. For the remainder of the analyses, we compared all $\Delta\delta^{15}\text{N}_{\text{M-L}}$ values from wild-caught fish to the 95% confidence range for $\text{CPO}_{\text{M-L}}$ ($1.67 \pm 0.30\text{‰}$).

Values of $\Delta\delta^{15}\text{N}_{\text{M-L}}$ in wild-caught reef fishes as compared to $\text{CPO}_{\text{M-L}}$

When we calculated $\Delta\delta^{15}\text{N}_{\text{M-L}}$ for 575 wild-caught reef fish, we found a difference among $\Delta\delta^{15}\text{N}_{\text{M-L}}$ values across the eight species and $\text{CPO}_{\text{M-L}}$ ($H = 228.86, \text{df} = 8, p < 0.001$; Figure 2.4). Post-hoc pairwise comparisons indicated Red Grouper ($t = 7.50, p < 0.001$), Graysby ($t = 5.64, p < 0.01$), and Gray Snapper ($t = 4.86, p < 0.01$) differed from $\text{CPO}_{\text{M-L}}$, while Black Seabass, Red Snapper, Golden Tilefish, lionfishes, and White Grunt did not (Table 2.5). In White Grunt, K-W indicated differences among the sex and maturity states ($H = 33.14, \text{df} = 3, p < 0.001$; Table 2.4;

Figure 2.5). Post-hoc tests indicated that only mature females differed from CPO_{M-L} ($t = 3.03$, $p < 0.05$, Figure 2.5).

Seasonal values of $\Delta\delta^{15}N_{M-L}$ were significantly lower than CPO_{M-L} in both Red Grouper ($H = 39.79$, $df = 4$, $p < 0.001$) and Black Seabass ($H = 24.01$, $df = 4$, $p < 0.001$; Table 2.5). Red Grouper with the highest value of $\Delta\delta^{15}N_{M-L}$ were collected in fall and those with the lowest values were collected in spring (Table 2.4; Figure 2.6a). For Black Seabass, fish captured in all seasons had lower values of $\Delta\delta^{15}N_{M-L}$ than CPO_{M-L} . Individuals with the highest values were collected in summer. Those with the lowest values were collected in winter (Table 2.5; Figure 2.6b).

DISCUSSION

Knowing the expected partitioning offset between body tissues within an individual is one means of utilizing stable isotopes to investigate movement within marine fish species. We found a constant partitioning offset (CPO_{M-L}) value of $\Delta\delta^{15}N_{M-L}$ across captive fishes in isotopically stable environments with varying phylogenetic, biological, and ecological characteristics. Although our inference is limited to the species examined, the consistency of CPO_{M-L} suggests that it may be typical in marine teleosts. Using this literature-based CPO_{M-L} , we showed that $\Delta\delta^{15}N_{M-L}$ values for eight species of wild-caught fishes ranged from slightly above to far below CPO_{M-L} , suggesting short-term (i.e., during the three months preceding capture) variation in diet and site fidelities of species which seem ecologically similar upon first inspection.

Given that consistent trophic fractionation is expected under experimental conditions (Bradley et al. 2015; Vander Zanden et al. 2015), we were not surprised to observe values for

$\delta^{15}\text{N}_{\text{muscle}}$ and $\delta^{15}\text{N}_{\text{liver}}$ that differed among species (Table 2.1). We were surprised, however, to observe a consistent difference between $\delta^{15}\text{N}_{\text{muscle}}$ and $\delta^{15}\text{N}_{\text{liver}}$ regardless of size, trophic position, or swimming speed (metabolic rate) of the test subjects (Table 2.2; Figures 2a and b). We observed that $\delta^{15}\text{N}_{\text{muscle}}$ values were uniformly higher than $\delta^{15}\text{N}_{\text{liver}}$. Therefore, we rejected hypothesis (1) that $\text{CPO}_{\text{M-L}} = 0$ and hypothesis (2) that intrinsic or extrinsic factors would correlate with the value of $\Delta\delta^{15}\text{N}_{\text{M-L}}$ when fish are fed an isotopically consistent diet. We propose that a consistent partitioning offset exists between $\delta^{15}\text{N}_{\text{muscle}}$ and $\delta^{15}\text{N}_{\text{liver}}$. However, additional studies would further examine the cellular processes leading to this relationship. Including compound-specific evaluations may help clarify the physiology behind the observed $\text{CPO}_{\text{M-L}}$ value. We further propose the use the 95% confidence interval for $\text{CPO}_{\text{M-L}}$ (1.37–2.97‰) as a range against which researchers can evaluate wild-caught fishes to assess the extent of recent (within the preceding months) movement or diet changes within the context of a known isoscape. Future investigations of $\text{CPO}_{\text{M-L}}$ have the potential to decrease the size of CI if our findings are corroborated. Wild-caught fish would be expected to have $\Delta\delta^{15}\text{N}_{\text{M-L}}$ values overlapping with $\text{CPO}_{\text{M-L}}$ range if they were both stationary and eating a consistent, locally derived diet during the preceding weeks. Wild-caught fish with $\Delta\delta^{15}\text{N}_{\text{M-L}}$ outside $\text{CPO}_{\text{M-L}}$ range may be candidates for further investigation into some combination of movement along the regional $\delta^{15}\text{N}$ gradient and a recent diet change, including feeding on migratory prey moving across the isoscape.

The observation of lower $\delta^{15}\text{N}_{\text{liver}}$ as compared to $\delta^{15}\text{N}_{\text{muscle}}$ is common among captive and wild marine teleost species, closer to the $\delta^{15}\text{N}$ values of the various food sources they consume (e.g. Mohan et al. 2016, Buchheister and Latour 2011). This trend contrasts with other vertebrate taxa such as mammals and birds (Vanderklift and Ponsard 2003). One explanation for

observed lower $\delta^{15}\text{N}_{\text{liver}}$ values of marine teleosts is that the liver incorporates a higher proportion of source amino acids than muscle (Pinnegar and Polunin 1999; Downs et al. 2014). A lower $\delta^{15}\text{N}$ value may indicate less reconfiguration or transamination of the amino acids within the liver than within the muscle (Braun et al. 2014). Fractionation often occurs with growth, protein synthesis, and amino acid intracellular metabolism (Poupin et al. 2014). Shorter amino acid residence times within liver tissue (Michaud et al. 2013; Barreto-Curiel et al. 2017) may result in smaller overall fractionation in marine fishes. The physiological reason for $\text{CPO}_{\text{M-L}}$ merits further investigation and may lead to an improvement to $\text{CPO}_{\text{M-L}}$ estimates.

Wild-caught reef fish displayed $\Delta\delta^{15}\text{N}_{\text{M-L}}$ values consistent with values reported for each tissue in other species (e.g. Serrano et al. 2007; Madigan et al. 2012; Matley et al. 2016). The range of measured $\Delta\delta^{15}\text{N}_{\text{M-L}}$ values was also consistent with hypothesis (3) that species with little movement and locally derived diets have $\Delta\delta^{15}\text{N}_{\text{M-L}}$ values no different from $\text{CPO}_{\text{M-L}}$, while species that migrate across an isoscape, or eat migratory prey, have $\Delta\delta^{15}\text{N}_{\text{M-L}}$ values different from $\text{CPO}_{\text{M-L}}$. Among the eight wild-caught species examined, $\Delta\delta^{15}\text{N}_{\text{M-L}}$ could not be distinguished from $\text{CPO}_{\text{M-L}}$ in five species, including White Grunt, lionfishes, and Golden Tilefish. These species associate closely with the benthos and consistently consume benthic or near-benthic prey (Grossman et al. 1985; Albins 2015; Pereira et al. 2015; Hixon et al. 2016). It is reasonable to suspect that these species had both high site fidelity and locally derived food during the weeks to months prior to capture.

Values of $\Delta\delta^{15}\text{N}_{\text{M-L}}$ for Red Snapper and Black Seabass were no different from $\text{CPO}_{\text{M-L}}$. However, both species were represented by small sample sizes and mean values were near the lower edge of the $\text{CPO}_{\text{M-L}}$ range. We suggest collecting additional specimens to help clarify these species' relationships to $\text{CPO}_{\text{M-L}}$. An isotopically derived understanding of the diets and

movements of Red Snapper on the WFS would be especially useful since the fishery for this species is both valuable and contentious (Burns 2009; Hollenbeck et al. 2015; O'Farrell et al. 2017).

The $\Delta\delta^{15}\text{N}_{\text{M-L}}$ values of three species, Gray Snapper, Graysby, and Red Grouper, were significantly lower than $\text{CPO}_{\text{M-L}}$. These generalist predators consume mixed diets of small, migratory fishes and benthic invertebrates (Bullock and Smith 1991; Brule and Canche 1993; Yeager et al. 2014; Curtis et al. 2017). Individuals that rely on mobile food sources, such as migratory forage fishes, are likely consuming nitrogen with a different isotopic composition from local values (Graham et al. 2010; Lorrain et al. 2015). Mixed schools of small, migratory fishes are known to travel north and south along the WFS as water temperature changes throughout the year (Sutherland and Fable Jr. 1980; Anderson and Torres 2016). These schools often move across the nitrogen isoscape; therefore, their whole-body $\delta^{15}\text{N}$ values may not align with the isotopic background where they were consumed. Highly mobile prey species would be expected to impart $\Delta\delta^{15}\text{N}_{\text{M-L}}$ values in their predators that also differ from $\text{CPO}_{\text{M-L}}$.

We were able to examine the potential effects of reproductive biology and capture season on tissue isotopic offsets for three species. We found that $\Delta\delta^{15}\text{N}_{\text{M-L}}$ of mature female White Grunt differed from $\text{CPO}_{\text{M-L}}$, potentially due to high metabolic investment in gonadal tissue (Hendry et al. 1999). Strikingly, mature female White Grunt were the only wild-caught fish examined for which $\Delta\delta^{15}\text{N}_{\text{M-L}}$ was larger than $\text{CPO}_{\text{M-L}}$. Immature and mature male White Grunt $\Delta\delta^{15}\text{N}_{\text{M-L}}$ values were not different from $\text{CPO}_{\text{M-L}}$ (Table 2.5; Figure 2.5). Similarly, Michaud et al. (2013) found higher values of $\Delta\delta^{15}\text{N}_{\text{M-L}}$ in reproductive females than in male Arctic Charr. The reorganization of lipid and protein in the liver to form oocytes could be responsible for the observed differences between tissues (Martin et al. 1993). The potential relationship between

reproductive state and $\Delta\delta^{15}\text{N}_{\text{M-L}}$ should be investigated further during future studies of $\Delta\delta^{15}\text{N}_{\text{M-L}}$ in wild-caught marine teleosts.

Values of $\Delta\delta^{15}\text{N}_{\text{M-L}}$ were lower than $\text{CPO}_{\text{M-L}}$ for both Red Grouper and Black Seabass throughout the year (Table 2.5; Figure 2.6), suggesting continuous movement of either the fish themselves or their prey. Values for Red Grouper $\Delta\delta^{15}\text{N}_{\text{M-L}}$ observed during spring were the lowest of all seasons, consistent with a diet including migratory forage fishes moving northward along WFS (Sutherland and Fable Jr. 1980; Anderson and Torres 2016), provided these prey had incorporated the $\delta^{15}\text{N}$ from areas to the south of the sampling location (Radabaugh and Peebles 2014). Low values of $\Delta\delta^{15}\text{N}_{\text{M-L}}$ in Black Seabass during winter may reflect seasonal movement of either the Black Seabass or their prey. Both seasonal differences and inter-species differences may be further clarified by investigating the $\Delta\delta^{15}\text{N}_{\text{M-L}}$ and whole-body $\delta^{15}\text{N}$ values of small, migratory forage fishes on the WFS.

Conclusions and future applications

A consistent, non-zero $\text{CPO}_{\text{M-L}}$ value suggests that a true offset may exist between the nitrogen isotopes in liver and muscle of marine teleosts under ideal conditions. However, future studies on a broad taxonomic range of species should be conducted to continue to clarify this relationship. We suggest that the relationship between $\Delta\delta^{15}\text{N}_{\text{M-L}}$ and $\text{CPO}_{\text{M-L}}$ in wild-caught fish provides insight into geographic movement and diet differences among species. While $\Delta\delta^{15}\text{N}_{\text{M-L}}$ values in wild-caught fish may reflect either movement by the individuals themselves or their prey, this parameter presents a novel and useful indicator of site fidelity. The $\text{CPO}_{\text{M-L}}$ value and $\Delta\delta^{15}\text{N}_{\text{M-L}}$ in wild fish have the potential for worldwide application to a wide variety of ecological inquiries, with spatial resolution that is dependent on the slope of local isotopic gradients.

LITERATURE CITED

- Albins, M. A. 2015. Invasive Pacific lionfish *Pterois volitans* reduce abundance and species richness of native Bahamian coral-reef fishes. *Mar. Ecol. Prog. Ser.* **522**: 231-243.
- Anderson, J. D., and A. D. Torres. 2016. Genetic variability and population structure of Gulf Menhaden compared with Yellowfin Menhaden. *Marine and Coastal Fisheries* **8**: 425-435.
- Ankjaero, T., J. T. Christensen, and P. Gronkjaer. 2012. Tissue-specific turnover rates and trophic enrichment of stable N and C isotopes in juvenile Atlantic Cod *Gadus morhua* fed three different diets. *Mar. Ecol. Prog. Ser.* **461**: 197-209.
- Barreto-Curiel, F., U. Focken, L. R. D'Abramo, and M. T. Viana. 2017. Metabolism of *Seriola lalandi* during starvation as revealed by fatty acid analysis and compound-specific analysis of stable isotopes within amino acids. *Plos One* **12**: 17.
- Bradley, C. J., N. J. Wallsgrove, C. A. Choy, J. C. Drazen, E. D. Hetherington, D. K. Hoen, and B. N. Popp. 2015. Trophic position estimates of marine teleosts using amino acid compound specific isotopic analysis. *Limnology and Oceanography-Methods* **13**: 476-493.
- Brame, A. B., C. C. McIvor, E. B. Peebles, and D. J. Hollander. 2014. Site fidelity and condition metrics suggest sequential habitat use by juvenile common snook. *Mar. Ecol. Prog. Ser.* **509**: 255-269.
- Braun, A., A. Vikari, W. Windisch, and K. Auerswald. 2014. Transamination Governs Nitrogen Isotope Heterogeneity of Amino Acids in Rats. *Journal of Agricultural and Food Chemistry* **62**: 8008-8013.
- Brule, T., and L. G. R. Canche. 1993. Food habits of juvenile red groupers, *Epinephelus morio* (Valenciennes, 1828) from Campeche bank, Yucatan, Mexico. *Bulletin of Marine Science* **52**: 772-779.
- Buchheister, A., and R. J. Latour. 2010. Turnover and fractionation of carbon and nitrogen stable isotopes in tissues of a migratory coastal predator, summer flounder (*Paralichthys dentatus*). *Canadian Journal of Fisheries and Aquatic Sciences* **67**: 445-461.
- . 2011. Trophic ecology of Summer Flounder in lower Chesapeake Bay inferred from stomach content and stable isotope analyses. *Transactions of the American Fisheries Society* **140**: 1240-1254.
- Bullock, L. H., and G. B. Smith. 1991. Seabasses (Pisces: Serranidae). *Memoirs of the Hourglass Cruises* **8**: 1-243.
- Burns, K. 2009. Evaluation of the efficacy of the minimum size rule in the Red Grouper and Red Snapper fisheries with respect to J and circle hook mortality and barotrauma and the consequences for survival and movement. University of South Florida.
- Chikaraishi, Y., Y. Kashiyamal, N. O. Ogawa, H. Kitazato, and N. Ohkouchi. 2007. Metabolic control of nitrogen isotope composition of amino acids in macroalgae and gastropods: implications for aquatic food web studies. *Mar. Ecol. Prog. Ser.* **342**: 85-90.
- Chikaraishi, Y., N. O. Ogawa, Y. Kashiyama and others 2009. Determination of aquatic food-web structure based on compound-specific nitrogen isotopic composition of amino acids. *Limnology and Oceanography-Methods* **7**: 740-750.
- Curtis, J. S., K. R. Wall, M. A. Albins, and C. D. Stallings. 2017. Diet shifts in a native mesopredator across a range of invasive lionfish biomass. *Mar. Ecol. Prog. Ser.* **573**: 215-228.

- Dalerum, F., and A. Angerbjorn. 2005. Resolving temporal variation in vertebrate diets using naturally occurring stable isotopes. *Oecologia* **144**: 647-658.
- Davis, J. P., K. A. Pitt, B. Fry, and R. M. Connolly. 2015. Stable isotopes as tracers of residency for fish on inshore coral reefs. *Estuarine Coastal and Shelf Science* **167**: 368-376.
- Downs, E. E., B. N. Popp, and C. M. Holl. 2014. Nitrogen isotope fractionation and amino acid turnover rates in the Pacific white shrimp, *Litopenaeus vannamei*. *Mar. Ecol. Prog. Ser.* **516**: 239-250.
- Ellis, G. S., G. Herbert, and D. J. Hollander. 2014. Reconstructing carbon sources in a dynamic estuarine ecosystem using oyster amino acid delta C-13 values from shell and tissue. *Journal of Shellfish Research* **33**: 217-225.
- Froese, R., and D. Pauly. 2018. FishBase. In R. Froese and D. Pauly [eds.], Fishbase.org.
- Fry, B., D. M. Baltz, M. C. Benfield, J. W. Fleeger, A. Gace, H. L. Haas, and Z. J. Quinones-Rivera. 2003. Stable isotope indicators of movement and residency for brown shrimp (*Farfantepenaeus aztecus*) in coastal Louisiana marshscapes. *Estuaries* **26**: 82-97.
- Fry, B., S. R. Silva, C. Kendall, and R. K. Anderson. 2002. Oxygen isotope corrections for online delta S-34 analysis. *Rapid Communications in Mass Spectrometry* **16**: 854-858.
- Gaston, T. F., and I. M. Suthers. 2004. Spatial variation in delta C-13 and delta N-15 of liver, muscle and bone in a rocky reef planktivorous fish: the relative contribution of sewage. *Journal of Experimental Marine Biology and Ecology* **304**: 17-33.
- Gelpi, C. G., B. Fry, R. E. Condrey, J. W. Fleeger, and S. F. Dubois. 2013. Using delta C-13 and delta N-15 to determine the migratory history of offshore Louisiana blue crab spawning stocks. *Mar. Ecol. Prog. Ser.* **494**: 205-218.
- Graham, B. S., P. L. Koch, S. D. Newsome, K. W. McMahon, and D. Aurioles. 2010. Using Isoscapes to Trace the Movements and Foraging Behavior of Top Predators in Oceanic Ecosystems, p. 299-318. In J. B. West, G. J. Bowen, T. E. Dawson and K. P. Tu [eds.], *Isoscapes: Understanding Movement, Pattern, and Process on Earth through Isotope Mapping*.
- Grimes, C. B., K. W. Able, and R. S. Jones. 1986. Tilefish, *Lopholatilus chamaeleonticeps*, habitat, behavior and community structure in mid-Atlantic and Southern New England waters. *Environmental Biology of Fishes* **15**: 273-292.
- Grimes, C. B., and S. C. Turner. 1999. The complex life history of tilefish *Lopholatilus chamaeleonticeps* and vulnerability to exploitation. *Life in the Slow Lane: Ecology and Conservation of Long-Lived Marine Animals* **23**: 17-26.
- Grossman, G. D., M. J. Harris, and J. E. Hightower. 1985. The relationship between tilefish, *Lopholatilus chamaleleonticeps*, abundance and sediment composition off Georgia. *Fishery Bulletin* **83**: 443-447.
- Guelinckx, J., J. Maes, P. Van Den Driessche, B. Geysen, F. Dehairs, and F. Ollevier. 2007. Changes in delta C-13 and delta N-15 in different tissues of juvenile Sand Goby *Pomatoschistus minutus*: a laboratory diet-switch experiment. *Mar. Ecol. Prog. Ser.* **341**: 205-215.
- Haas, H. L., C. J. Freeman, J. M. Logan, L. Deegan, and E. F. Gaines. 2009. Examining mummichog growth and movement: Are some individuals making intra-season migrations to optimize growth? *Journal of Experimental Marine Biology and Ecology* **369**: 8-16.

- Harlem, P. W., J. Boyer, H. O. Briceño, J. W. Fourqurean, P. O. Gardinali, R. Jaffé, J. F. Meeder, and M. S. Ross. 2012. Assessment of natural resource conditions in and adjacent to Biscayne National Park. Natural Resource Report.
- Hendry, A. P., O. K. Berg, and T. P. Quinn. 1999. Condition dependence and adaptation-by-time: breeding date, life history, and energy allocation within a population of salmon. *Oikos* **85**: 499-514.
- Hine, A. C., and S. D. Locker. 2011. The Florida Gulf of Mexico continental shelf—great contrasts and significant transitions. *The Gulf of Mexico: Origin, Waters, and Marine Life*.
- Hixon, M. A., S. J. Green, M. A. Albins, J. L. Akins, and J. A. Morris. 2016. Lionfish: a major marine invasion. *Mar. Ecol. Prog. Ser.* **558**: 161-165.
- Hollenbeck, C. M., D. S. Portnoy, E. Saillant, and J. R. Gold. 2015. Population structure of red snapper (*Lutjanus campechanus*) in US waters of the western Atlantic Ocean and the northeastern Gulf of Mexico. *Fisheries Research* **172**: 17-25.
- Larson, J. H., W. B. Richardson, J. M. Vallazza, and J. C. Nelson. 2013. Rivermouth Alteration of Agricultural Impacts on Consumer Tissue delta N-15. *Plos One* **8**.
- Locker, S. D., R. A. Armstrong, T. A. Battista, J. J. Rooney, C. Sherman, and D. G. Zawada. 2010. Geomorphology of mesophotic coral ecosystems: current perspectives on morphology, distribution, and mapping strategies. *Coral Reefs* **29**: 329-345.
- Logan, J., H. Haas, L. Deegan, and E. Gaines. 2006. Turnover rates of nitrogen stable isotopes in the salt marsh mummichog, *Fundulus heteroclitus*, following a laboratory diet switch. *Oecologia* **147**: 391-395.
- Logan, J. M., W. J. Golet, and M. E. Lutcavage. 2015. Diet and condition of Atlantic bluefin tuna (*Thunnus thynnus*) in the Gulf of Maine, 2004-2008. *Environmental Biology of Fishes* **98**: 1411-1430.
- Lorrain, A., B. S. Graham, B. N. Popp and others 2015. Nitrogen isotopic baselines and implications for estimating foraging habitat and trophic position of yellowfin tuna in the Indian and Pacific Oceans. *Deep-Sea Research Part II-Topical Studies in Oceanography* **113**: 188-198.
- Madigan, D. J., S. Y. Litvin, B. N. Popp, A. B. Carlisle, C. J. Farwell, and B. A. Block. 2012. Tissue Turnover Rates and Isotopic Trophic Discrimination Factors in the Endothermic Teleost, Pacific Bluefin Tuna (*Thunnus orientalis*). *Plos One* **7**.
- Martin, N. B., D. F. Houlihan, C. Talbot, and R. M. Palmer. 1993. Protein-metabolism during sexual maturation in female Atlantic salmon (*Salmo salar* L). *Fish Physiology and Biochemistry* **12**: 131-141.
- Matley, J. K., A. T. Fisk, A. J. Tobin, M. R. Heupel, and C. A. Simpfendorfer. 2016. Diet-tissue discrimination factors and turnover of carbon and nitrogen stable isotopes in tissues of an adult predatory coral reef fish, *Plectropomus leopardus*. *Rapid Communications in Mass Spectrometry* **30**: 29-44.
- Michaud, W. K., J. B. Dempson, J. D. Reist, and M. Power. 2013. Ecological influences on the difference in delta N-15 and delta C-13 values between fish tissues: implications for studies of temporal diet variation. *Ecology of Freshwater Fish* **22**: 520-529.
- Miller, T. W. 2006. Tissue-specific response of delta N-15 in adult Pacific herring (*Clupea pallasii*) following an isotopic shift in diet. *Environmental Biology of Fishes* **76**: 177-189.
- Mohan, J. A., S. D. Smith, T. L. Connelly, E. T. Attwood, J. W. McClelland, S. Z. Herzka, and B. D. Walther. 2016. Tissue-specific isotope turnover and discrimination factors are

- affected by diet quality and lipid content in an omnivorous consumer. *Journal of Experimental Marine Biology and Ecology* **479**: 35-45.
- Nelson, J., R. Wilson, F. Coleman, C. Koenig, D. DeVries, C. Gardner, and J. Chanton. 2012. Flux by fin: fish-mediated carbon and nutrient flux in the northeastern Gulf of Mexico. *Mar. Biol.* **159**: 365-372.
- Nuche-Pascual, M. T., J. P. Lazo, R. I. Ruiz-Cooley, and S. Z. Herzka. 2018. Amino acid-specific N-15 trophic enrichment factors in fish fed with formulated diets varying in protein quantity and quality. *Ecology and Evolution* **8**: 9192-9217.
- O'Connell, T. C. 2017. 'Trophic' and 'source' amino acids in trophic estimation: a likely metabolic explanation. *Oecologia* **184**: 317-326.
- O'Farrell, S., J. N. Sanchirico, I. Chollett and others 2017. Improving detection of short-duration fishing behaviour in vessel tracks by feature engineering of training data. *Ices Journal of Marine Science* **74**: 1428-1436.
- Ogden, J. C., J. W. Porter, N. P. Smith, A. M. Szmant, W. C. Jaap, and D. Forcucci. 1994. A long-term interdisciplinary study of the Florida-keys seascape. *Bulletin of Marine Science* **54**: 1059-1071.
- Olejnik, S., and J. Lee. 1990. Multiple comparison procedures when population variances differ. Annual meeting of the American educational research association.
- Olsen, S. A., P. K. Hansen, H. Givskud, A. Ervik, and O. B. Samuelsen. 2015. Changes in fatty acid composition and stable isotope signature of Atlantic cod (*Gadus morhua*) in response to laboratory dietary shifts. *Aquaculture* **435**: 277-285.
- Pereira, P. H. C., B. Barros, R. Zemoi, and B. P. Ferreira. 2015. Ontogenetic diet changes and food partitioning of *Haemulon* spp. coral reef fishes, with a review of the genus diet. *Reviews in Fish Biology and Fisheries* **25**: 245-260.
- Pinnegar, J. K., and N. V. C. Polunin. 1999. Differential fractionation of delta C-13 and delta N-15 among fish tissues: implications for the study of trophic interactions. *Functional Ecology* **13**: 225-231.
- Post, D. M. 2002. Using stable isotopes to estimate trophic position: Models, methods, and assumptions. *Ecology* **83**: 703-718.
- Poupin, N., F. Mariotti, J. F. Huneau, D. Hermier, and H. Fouillet. 2014. Natural Isotopic Signatures of Variations in Body Nitrogen Fluxes: A Compartmental Model Analysis. *Plos Computational Biology* **10**.
- Radabaugh, K. R., D. J. Hollander, and E. B. Peebles. 2013. Seasonal delta C-13 and delta N-15 isoscapes of fish populations along a continental shelf trophic gradient. *Continental Shelf Research* **68**: 112-122.
- Radabaugh, K. R., and E. B. Peebles. 2014. Multiple regression models of $\delta^{13}\text{C}$ and $\delta^{15}\text{N}$ for fish populations in the eastern Gulf of Mexico. *Continental Shelf Research* **84**: 158-168.
- Serrano, R., M. A. Blanes, and L. Orero. 2007. Stable isotope determination in wild and farmed gilthead sea bream (*Sparus aurata*) tissues from the western Mediterranean. *Chemosphere* **69**: 1075-1080.
- Sokal, R. R., and F. J. Rohlf. 1994. *Biometry: The Principles and Practices of Statistics in Biological Research* Third (3rd) Edition.
- Stallings, C. D., J. A. Nelson, K. L. Rozar, C. S. Adams, K. R. Wall, T. S. Switzer, B. L. Winner, and D. J. Hollander. 2015. Effects of preservation methods of muscle tissue from upper-trophic level reef fishes on stable isotope values (delta C-13 and delta N-15). *Peerj* **3**.

- Stallings, C. D., E. B. Peebles, O. Ayala, J. S. Curtis, and K. R. Wall. 2016. Lunar periodicity in spawning of white grunt, *Haemulon plumieri*. *Bulletin of Marine Science* **92**: 545-550.
- Sturrock, A. M., C. N. Trueman, J. A. Milton, C. P. Waring, M. J. Cooper, and E. Hunter. 2014. Physiological influences can outweigh environmental signals in otolith microchemistry research. *Mar. Ecol. Prog. Ser.* **500**: 245-264.
- Sutherland, D. F., and W. A. Fable Jr. 1980. Results of a King Mackerel (*Scomberomorus cavalla*) and Atlantic Spanish Mackerel (*Scomberomorus maculatus*) migration study., p. 25. National Oceanic and Atmospheric Administration.
- Suzuki, K. W., A. Kasai, K. Nakayama, and M. Tanaka. 2005. Differential isotopic enrichment and half-life among tissues in Japanese temperate bass (*Lateolabrax japonicus*) juveniles: implications for analyzing migration. *Canadian Journal of Fisheries and Aquatic Sciences* **62**: 671-678.
- Sweeting, C. J., J. Barry, C. Barnes, N. V. C. Polunin, and S. Jennings. 2007. Effects of body size and environment on diet-tissue delta N-15 fractionation in fishes. *Journal of Experimental Marine Biology and Ecology* **340**: 1-10.
- Trueman, C. N., R. A. R. McGill, and P. H. Guyard. 2006. The effect of growth rate on tissue-diet isotopic spacing in rapidly growing animals. An experimental study with Atlantic salmon (*Salmo salar*). *Rapid Communications in Mass Spectrometry* **20**: 2634-2634.
- Tzadik, O. E., J. S. Curtis, J. E. Granneman and others 2017. Chemical archives in fishes beyond otoliths: A review on the use of other body parts as chronological recorders of microchemical constituents for expanding interpretations of environmental, ecological, and life-history changes. *Limnology and Oceanography-Methods* **15**: 238-263.
- Vander Zanden, M. J., M. K. Clayton, E. K. Moody, C. T. Solomon, and B. C. Weidel. 2015. Stable Isotope Turnover and Half-Life in Animal Tissues: A Literature Synthesis. *Plos One* **10**.
- Vanderklift, M. A., and S. Ponsard. 2003. Sources of variation in consumer-diet delta(15)N enrichment: a meta-analysis. *Oecologia* **136**: 169-182.
- Varela, J. L., F. de la Gandara, A. Ortega, and A. Medina. 2012. C-13 and N-15 analysis in muscle and liver of wild and reared young-of-the-year (YOY) Atlantic bluefin tuna. *Aquaculture* **354**: 17-21.
- Wall, K. R., and C. D. Stallings. 2018. Subtropical epibenthos varies with location, reef type, and grazing intensity. *Journal of Experimental Marine Biology and Ecology* **509**: 54-65.
- Yeager, L. A., C. A. Layman, and C. M. Hammerschlag-Peyer. 2014. Diet variation of a generalist fish predator, grey snapper *Lutjanus griseus*, across an estuarine gradient: trade-offs of quantity for quality? *Journal of Fish Biology* **85**: 264-277.

Table 2.1. Parameters associated with studies used in the literature survey. TAR is tail aspect ratio, TP is trophic position, Mean T is mean study temperature, MTL is mean total length, MM is mean mass, and Sampling Day is either the beginning or end of the diet-switch study. $\delta^{15}\text{N}_{\text{muscle}}$ and $\delta^{15}\text{N}_{\text{liver}}$ are presented with standard errors and are expressed in standard per-mille (‰) notation. $\Delta\delta^{15}\text{N}_{\text{M-L}}$ is calculated for each experiment. Bold values were derived from FishBase (<http://www.fishbase.org/search.php>).

Authors	Year	Species	TAR	TP	Mean T (°C)	n	MTL (mm)	MM (g)	Sampling Day	Diet	$\delta^{15}\text{N}_{\text{muscle}}$	$\delta^{15}\text{N}_{\text{liver}}$	$\Delta\delta^{15}\text{N}_{\text{M-L}}$
Guelinckx et al.	2008	<i>Pomatoschistus minutus</i> Sand Goby	1.07	3.2	17	12	42.8	1	90	fish feed	12.88±0.10	10.51±0.03	2.37
Sweeting et al.	2007	<i>Dicentrarchus labrax</i> European Seabass	1.22	3.5	8.5	3	150	41	150	eel	17.83±0.39	16.05±0.40	1.78
"	"	"	"	"	"	3	150	41	150	dab	17.48±0.40	15.45±0.49	2.03
Mohan et al.	2016	<i>Micropogonias undulatus</i> Atlantic Croaker	1.26	4	28	12	110	17	104	fish feed	13.04±0.04	11.50±0.13	1.54
Suzuki et al.	2005	<i>Lateolabrax japonicus</i> Japanese Seabass	1.29	3.4	23	13	110	20	100	fish feed	16.17±0.05	14.35±0.09	1.82
Olsen et al.	2015	<i>Gadus morhua</i> Atlantic Cod	1.3	4.1	9	6	300	304	121	fish feed	12.79±0.03	10.78±0.08	2.01
Barreto-Curiel et al.	2017	<i>Totoaba macdonaldi</i> Totoaba	1.4	4.1	26	3	33	28	60	fish feed	12.20±0.06	10.10±0.06	2.10
Buchheister & Latour	2010	<i>Paralichthys dentatus</i> Summer Flounder	1.4	4.5	20.4	10	300	375	180	squid	15.55±0.18	14.51±0.07	1.04
"	"	"	"	"	"	10	300	375	180	krill	12.01±0.05	9.59±0.11	2.42
Matley et al.	2016	<i>Plectropomus leopardus</i> Leopard Coral Grouper	1.54	4.4	29	5	449	1634	196	bream	11.90±0.18	10.60±0.18	1.30
Trueman et al.	2006	<i>Salmo salar</i> Atlantic Salmon	2.05	4.5	8	6	325	314.7	315	fish feed	10.20±0.12	8.70±0.12	1.50
Miller	2006	<i>Clupea pallasii</i> Pacific Herring	2.32	3.2	10.6	5	169	47	302	fish feed	12.50±0.22	11.00±0.31	1.50
Nuche-Pascual et al.	2018	<i>Seriola lalandi</i> Yellowtail Amberjack	3.49	4.2	18	3	180	75	98	fish feed	12.88±0.10	12.38±0.12	0.50
Madigan et al.	2012	<i>Thunnus orientalis</i> Pacific Bluefin Tuna	6.39	4.5	20	10	2470	1.70x10 ⁵	2000	squid, sardines	16.10±0.09	14.60±0.09	1.50

Table 2.2. Results of linear regressions between $\Delta\delta^{15}\text{N}_{\text{M-L}}$ and fish total length. Bold values indicate statistically significant relationships.

Species	N	Intercept	Slope	F	<i>p</i>	R ²
All	451	1.57	-0.001	23.16	<<0.001	0.048
Black Seabass	10	0.87	0.000	0.01	0.917	0.001
Graysby	69	1.15	-0.002	1.91	0.170	0.027
Gray Snapper	77	0.29	0.002	2.41	0.124	0.031
Golden Tilefish	36	2.41	-0.001	2.78	0.104	0.077
lionfishes	64	1.85	-0.001	3.51	0.065	0.053
Red Grouper	45	-0.09	0.001	3.67	0.062	0.076
Red Snapper	9	2.81	-0.003	9.82	0.016	0.584
White Grunt	141	2.48	-0.003	4.87	0.029	0.033

Table 2.3. Correlations between $\delta^{15}\text{N}_{\text{M-L}}$ and intrinsic or extrinsic parameters associated with marine teleost fishes in Table 2.1. Correlations are calculated as Pearson's product moment (*r*). Variables are tail aspect ratio (TAR), trophic position (TP), mean temperature (T), mean total length (MTL), mean mass (MM), mean values of $\delta^{15}\text{N}_{\text{muscle}}$ and $\delta^{15}\text{N}_{\text{liver}}$ from each study.

	$\Delta\delta^{15}\text{N}_{\text{M-L}}$	p-value
TAR	-0.42	0.13
TP	-0.34	0.24
T (°C)	-0.20	0.48
MTL	-0.16	0.58
MM	-0.10	0.74
$\delta^{15}\text{N}_{\text{muscle}}$	0.02	0.94
$\delta^{15}\text{N}_{\text{liver}}$	-0.20	0.50

Table 2.4. Summary statistics for $\Delta\delta^{15}\text{N}_{\text{M-L}}$ from wild-caught specimens and specimens in diet-switch studies. Season is season of capture and SE is standard error of the mean. Rows in bold font include mean values significantly different from constant partitioning offset (CPO).

Species	Season	Sex	<i>n</i>	$\Delta\delta^{15}\text{N}_{\text{M-L}}$			
				Min	Max	Range	Mean \pm SE
*Red Grouper	Summer	All	45	-1.41	1.87	3.28	0.44\pm0.09
“	Winter	All	13	-0.14	1.15	1.29	0.26\pm0.11
“	Spring	All	61	-1.14	1.29	2.43	0.19\pm0.06
“	Fall	All	25	-0.34	1.58	1.92	0.48\pm0.10
*Graysby	Summer	All	69	-0.26	1.67	1.94	0.85\pm0.04
*Gray Snapper	Summer	All	77	-0.83	2.40	3.23	0.90\pm0.08
*Black Seabass	Summer	All	10	0.28	1.88	1.59	1.01\pm0.14
“	Winter	All	8	0.12	0.84	0.72	0.43\pm0.10
“	Spring	All	8	0.38	1.48	1.10	0.87\pm0.16
“	Fall	All	9	0.09	1.51	1.41	0.73\pm0.19
Red Snapper	Summer	All	9	0.55	1.78	1.22	1.20 \pm 0.15
Lionfishes	Summer	All	64	-0.02	2.32	2.35	1.45 \pm 0.07
Golden Tilefish	Summer	All	36	-0.33	2.61	2.94	1.39 \pm 0.12
White Grunt	Summer	All	141	0.11	3.44	3.33	1.96 \pm 0.05
“	Summer	Female	66	0.76	3.44	2.68	2.13 \pm 0.06
“	Summer	Male	37	0.62	2.77	2.15	1.57 \pm 0.07
“	Summer	Immature	38	0.11	3.11	3.00	2.05 \pm 0.10
Constant Partitioning offset			14	0.5	2.42	1.92	1.67\pm0.14

Table 2.5. Results of all Games-Howell pairwise comparisons. “Lit” is the constant partitioning offset (CPO) derived from captive studies. Black Seabass (SB), Graysby (GB), Gray Snapper (GS), Golden Tilefish (GT), lionfishes (LF), Red Grouper (RG), White Grunt (WG). Rows in bold font signify significant difference. Levels of significance are indicated: * < 0.05, ** < 0.01, *** < 0.001

Species	<i>t</i>	<i>p</i>	Season	<i>t</i>	<i>p</i>	Sex	<i>t</i>	<i>p</i>
Lit-SB	3.35	0.06	Lit-RG Fall	7.07	***	Lit-Female	3.03	*
Lit-GB	5.64	***	Lit-RG Spring	9.73	***	Lit-Immature	2.19	0.15
Lit-GS	4.86	**	Lit-RG Summer	7.41	***	Lit-Male	0.67	0.91
Lit-GT	1.53	0.83	Lit-RG Winter	7.89	***	Immature-Female	0.66	0.91
Lit-LF	1.46	0.86	RGSpring-RG	2.58	0.09	Immature-Male	3.83	**
Lit-RG	7.5	***	RGSummer-RG	0.31	0.99	Male-Female	5.97	***
Lit-RS	2.22	0.44	RGSummer-RG	2.29	0.16			
Lit-WG	1.97	0.58	RGWinter-RG	1.51	0.56			
GB-SB	1.17	0.95	RGWinter-RG	0.55	0.98			
GS-GB	0.57	1	RGWinter-RG	1.25	0.72			
GS-SP	0.75	0.99	Lit-SB Fall	3.95	**			
GT-GB	4.38	**	Lit-SB Spring	3.87	**			
GT-GS	3.55	*	Lit-SB Summer	3.35	*			
GT-SB	4.38	0.5	Lit-SB Winter	7.25	***			
LF-GB	7.45	***	SBSpring-SB	0.56	0.98			
LF-GS	5.37	***	SBSummer-SB	1.21	0.75			
LF-GT	0.39	1	SBSummer-SB	0.72	0.95			
LF-SB	2.81	0.2	SBWinter-SB	1.39	0.65			
RG-GB	4.19	**	SBWinter-SB	2.39	0.18			
RG-GS	4.01	**	SBWinter-SB Summer	3.46	*			
RG-GT	6.56	***						
RG-LF	8.92	***						
RG-SB	3.65	*						
RS-GB	2.22	0.46						
RS-GS	1.78	0.69						
RS-GT	0.95	0.99						
RS-LF	1.4	0.88						
RS-RG	4.39	*						
RS-SB	0.92	0.99						
WG-GB	17.01	***						
WG-GS	11.69	***						
WG-GT	4.49	**						
WG-LF	6.25	***						
WG-RG	14.54	***						
WG-RS	4.61	*						
WG-SB	6.48	**						

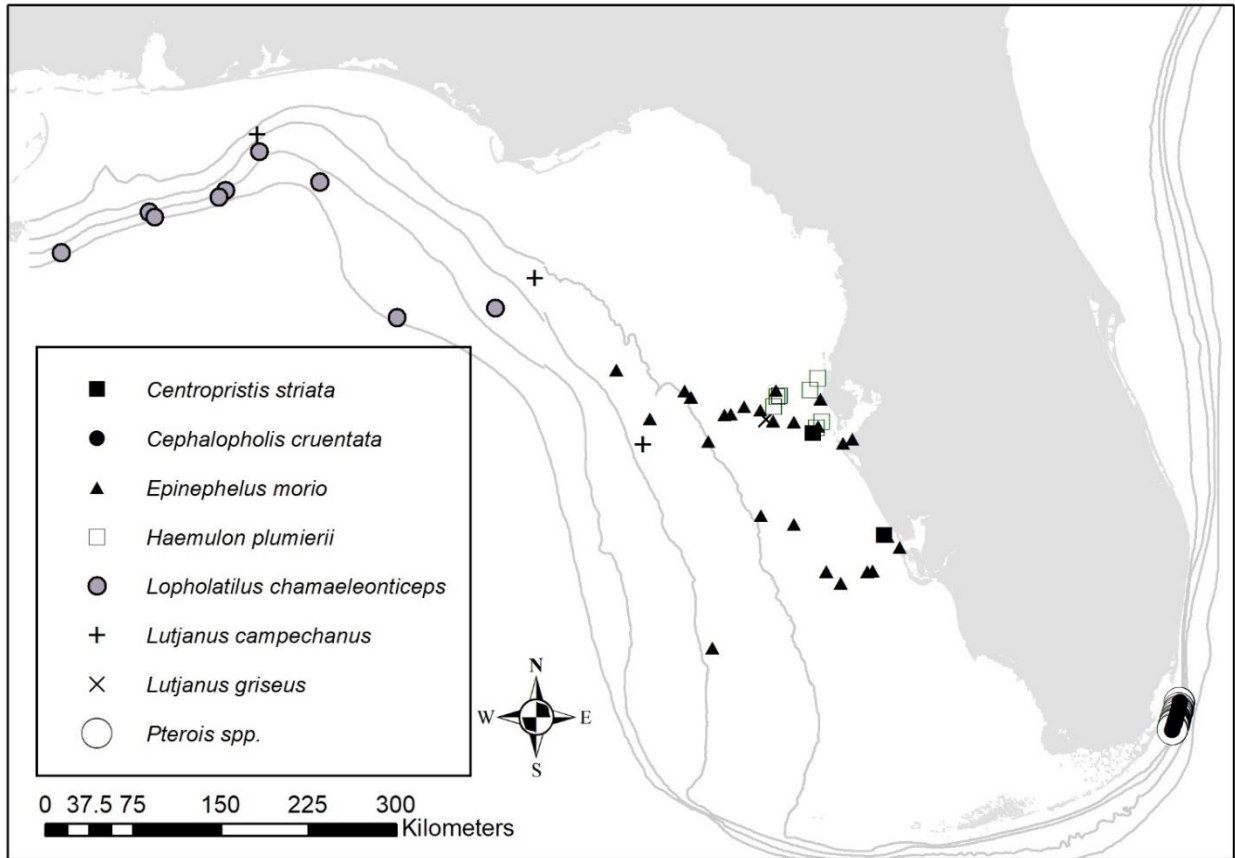


Figure 2.1. Catch locations for all wild-caught reef fish by species. Graysby (*Cephalopholis cruentata*) and lionfishes (*Pterois spp.*) were collected in Biscayne National Park (southeast Florida). All other species, Black Seabass (*Centropristis striata*), Red Grouper (*Epinephelus morio*), White Grunt (*Haemulon plumierii*), Golden Tilefish (*Lopholatilus chamaeleonticeps*), Red Snapper (*Lutjanus campechanus*), and Gray Snapper (*Lutjanus griseus*) were collected on the West Florida Shelf (WFS) off the west coast of Florida.

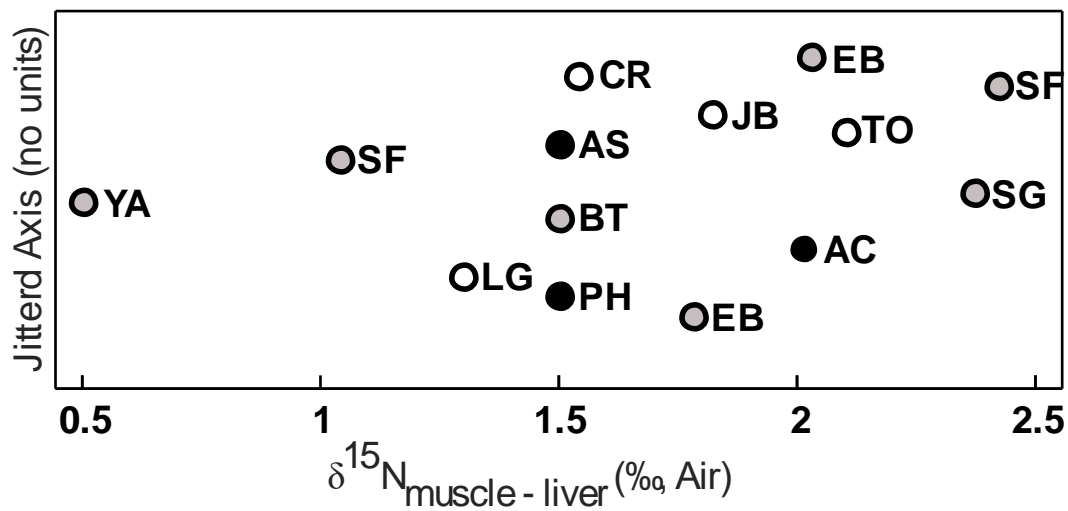


Figure 2.2. Mean values $\delta^{15}\text{N}_{\text{M-L}}$ measured in captive, diet-switch studies. Global mean (\pm SE): $\delta^{15}\text{N}_{\text{M-L}} = 1.67 \pm 0.14$. Black circles are studies conducted in cold water [8–10 °C; Atlantic Cod (AC), Atlantic Salmon (AS), and Pacific Herring (PH)]. Gray circles are studies conducted at intermediate temperatures [19–24 °C; European Seabass (EB), Pacific Bluefin Tuna (BT), Yellowtail Amberjack (YA), Sand Goby (SG), and Summer Flounder (SF)]. White circles are studies conducted in warm water [26–29 °C; Atlantic Croaker (CR), Japanese Temperate Bass (JB), Leopard Coral Grouper (LG), and Totoaba (TO)]. No trends were observed with respect to size, temperature, trophic level, or swimming speed.

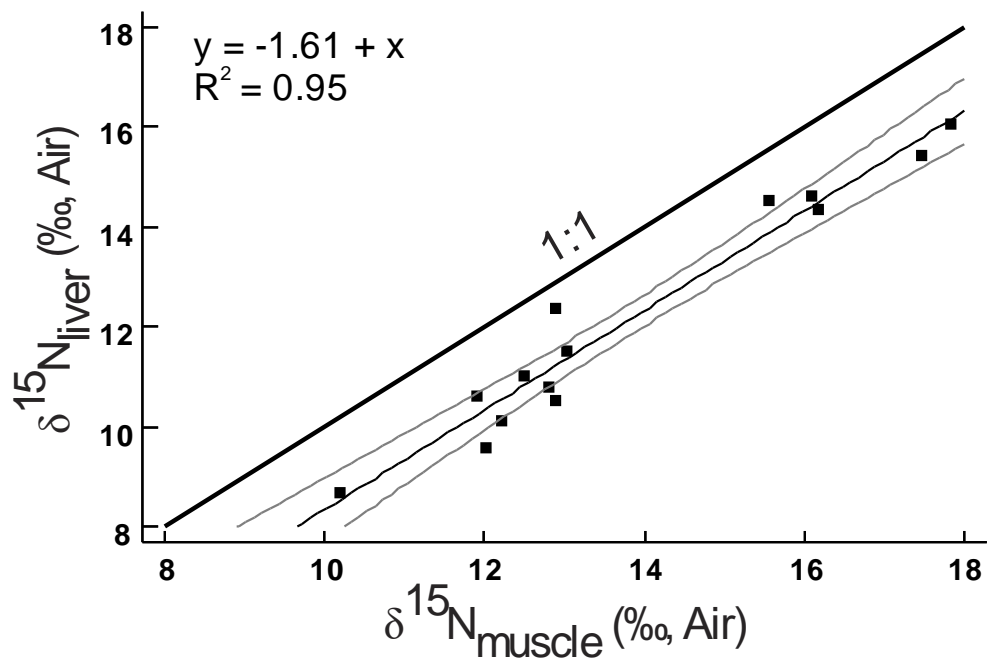


Figure 2.3. Linear regression between $\delta^{15}\text{N}_{\text{muscle}}$ and $\delta^{15}\text{N}_{\text{liver}}$ measured in 12 captive, diet-switch studies. Gray lines are 95% confidence intervals. Upper line shows theoretical 1:1 relationship.

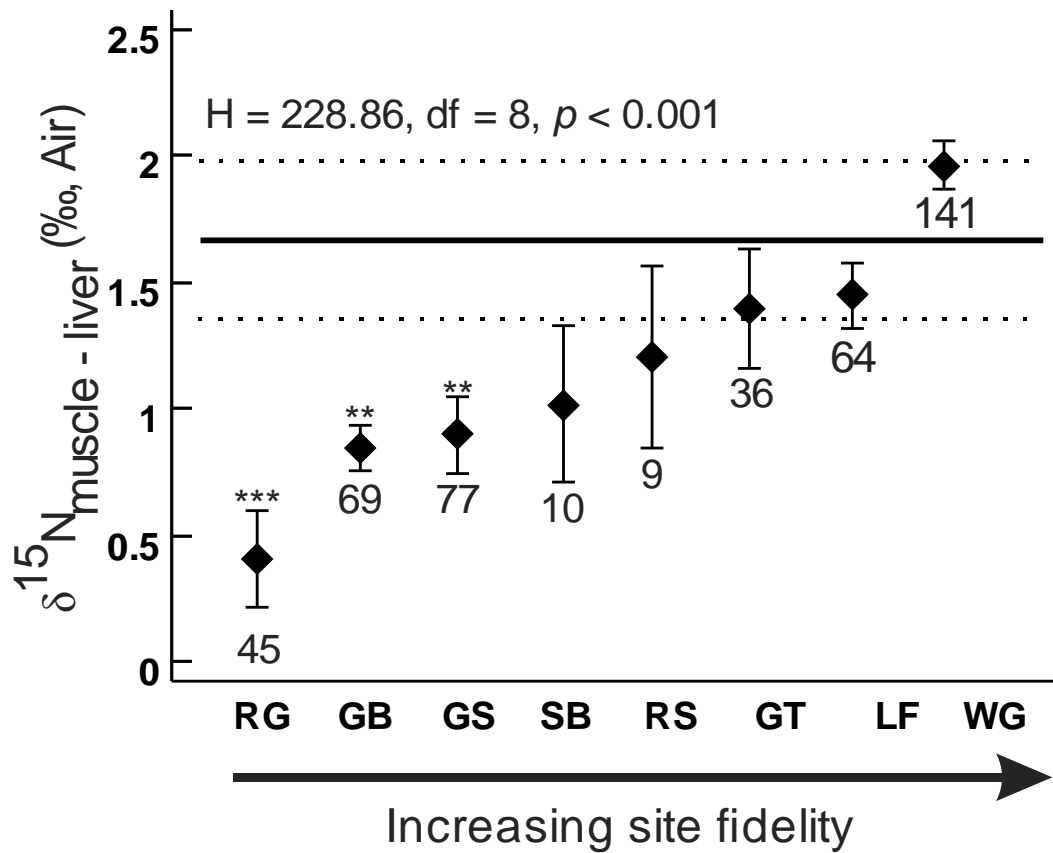


Figure 2.4. Mean values of $\Delta\delta^{15}\text{N}_{\text{M-L}}$ (\pm 95% CI) by species for wild specimens collected July-September in Florida waters. Red Grouper (RG), Graysby (GB), Gray Snapper (GS), Black Seabass (SB), Red Snapper (RS), Golden Tilefish (GT), lionfishes (LF), and White Grunt (WG). Mean constant partitioning offset (CPO) \pm CI is represented by horizontal solid and dashed lines. Numbers below each column are sample sizes. Species different from captive, diet-switch studies based on Games-Howell post-hoc test are indicated by level of significance: * < 0.05, ** < 0.01, *** < 0.001

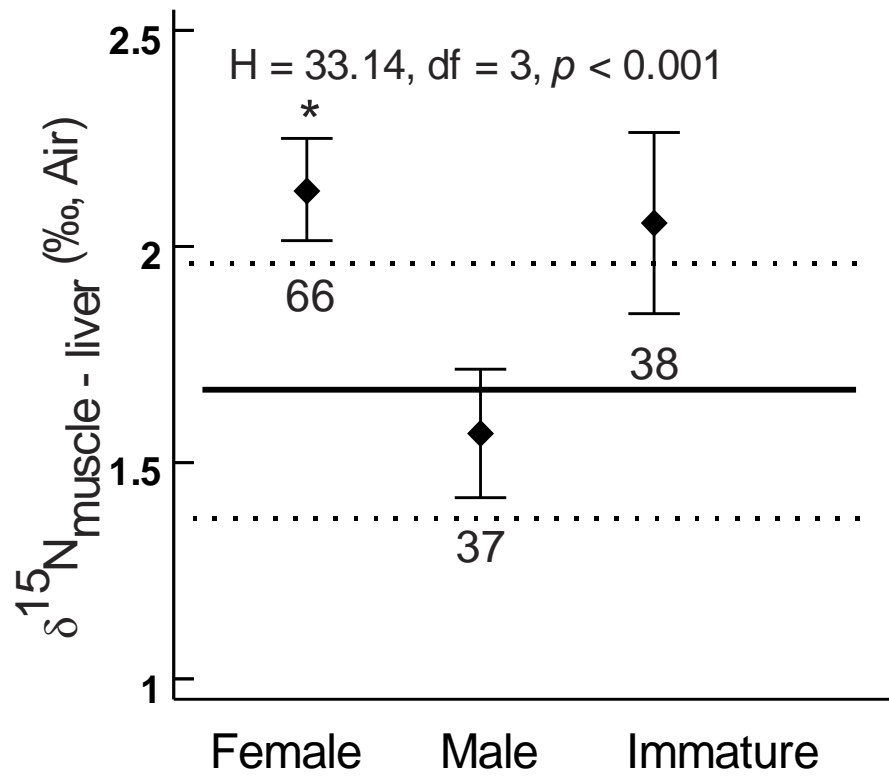


Figure 2.5. Means and 95% CI for $\Delta\delta^{15}\text{N}_{\text{M-L}}$ by reproductive category for White Grunt captured on the WFS (see Fig. 2.4 for explanation of data presentation).

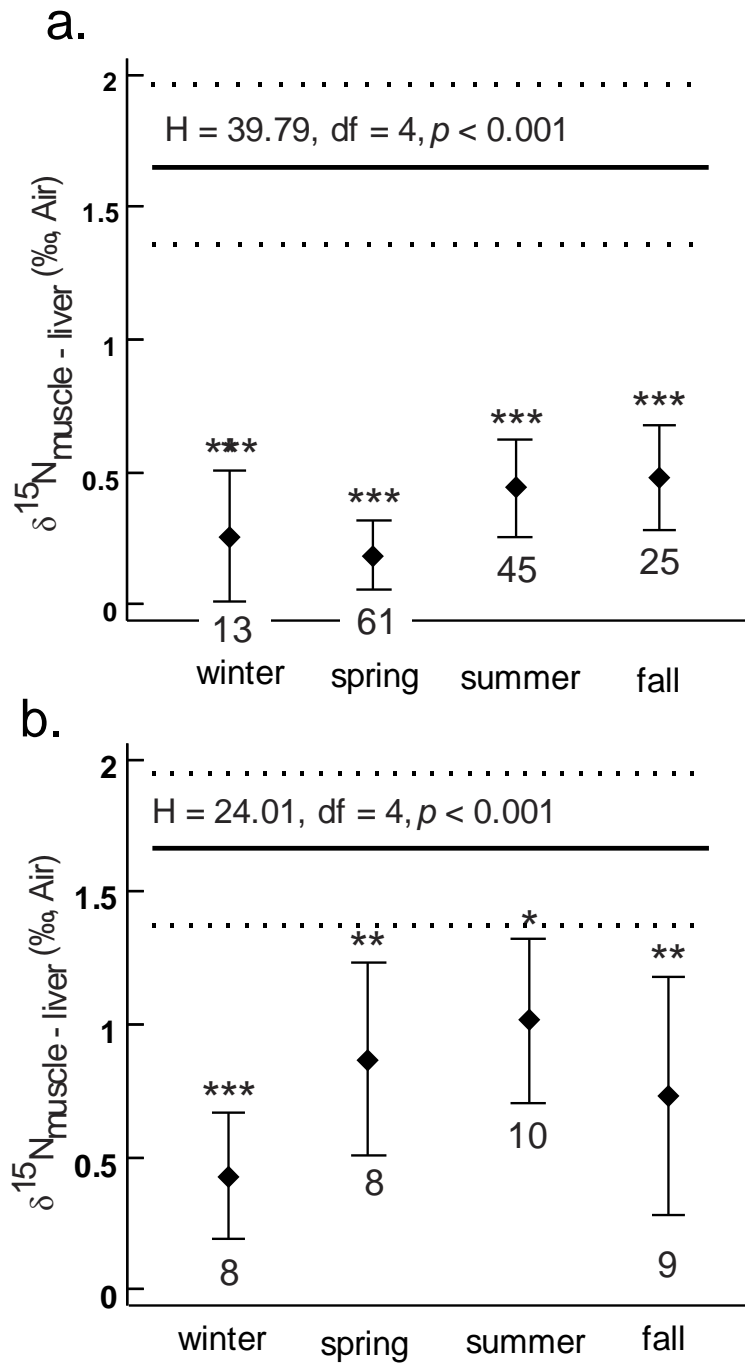


Figure 2.6. Means and CI for $\Delta\delta^{15}\text{N}_{\text{M-L}}$ by season for two species of reef fish collected on WFS: a. Red Grouper, b. Black Seabass (see Figure 2.4 for explanation of data presentation).

CHAPTER 3: DISTINGUISHING ENVIRONMENTAL FROM TROPHIC INFLUENCES IN POSTLARVAL FISH SURVIVAL: A HISTORICAL APPROACH USING STABLE ISOTOPES

ABSTRACT

Survival of marine teleosts through the larval stage can depend on a variety of physical and biological factors. A historical approach using the central region (core) of fish eye-lenses may provide insight into common geographic locations or movement patterns of individuals that survive to the juvenile and adult phases. Teleost eye lenses preserve isotopic values for the entire lifespan. Here, we present a readily accessible method of disentangling multiple influences on bulk isotope values using the eye-lens cores from four reef-fish species in the eastern Gulf of Mexico. By correlating $\delta^{13}\text{C}$ and $\delta^{15}\text{N}$ values of the eye-lens core with juvenile capture location and with core size (growth over the first few weeks of life), we were able to distinguish movement from geographic origin. While postlarval locations of Black Seabass and Red Snapper had wide isotopic distributions, central Gag and Red Grouper geographies were more confined. Gag isotopes showed evidence of movement inshore during the postlarval and early juvenile period. Red Grouper showed trophic-position increase or movement north, while Black Seabass showed evidence of southward movement with increasing length. In short, the $\delta^{13}\text{C}$ and $\delta^{15}\text{N}$ isotope values in the cores of fish eye lenses describe the geographic patterns of individuals that have successfully survived the larval stage.

INTRODUCTION

Fisheries scientists have suggested that egg and larval-stage survival is one key to variation in year-class strength of exploited marine fish populations for over 100 years (Hjort 1914). Whereas millions of eggs can be released and fertilized during a single spawning event (Winemiller and Rose 1993, Rogers et al. 2009), only a miniscule percentage survive to harvestable or reproductive size. An array of trophodynamic processes and physical conditions interact over the pre-recruitment lifespan, leading to recruitment variability (Houde 2009). Common intrinsic or extrinsic characteristics of the postlarval and juvenile periods such as location or available food resources may provide clues to the best oceanographic conditions or locations for larval and early juvenile survival within a population (Robertson et al. 1999, Houde 2009).

By definition the postlarval stage in a bony fish's life includes the period of first feeding until settlement to the juvenile habitat. At this stage, the larvae have control over their buoyancy. However, they still considered planktonic because they lack the strength to swim against prevailing currents (Powell and Tucker 1992, Burghart et al. 2014). The postlarval and early juvenile stages have been some of the most difficult to study in wild marine fish populations. Larval fish can be difficult to identify, with many related species looking almost identical, even to the trained eye (Drass et al. 2000, Vandersea et al. 2008, Marancik et al. 2012). Historically, researchers have used ichthyoplankton surveys to directly sample the egg and larval stages of marine fish species (e.g., SEAMAP program in southeastern US; Eldridge 1988). During the planktonic period, which can last weeks to months (Cowen 1991, Pepin and Myers 1991), individual larvae can move far from their spawning origin (Colin 2012, Burghart et al. 2014), decoupling larval collection location from either spawning or settlement habitat.

Previous research has demonstrated that larval survival can be linked to several intrinsic and extrinsic factors (Leis and Carson-Ewart 1999, Houde 2009, Lim and Mukai 2014) and may be location-specific (Beets 1997, Edwards et al. 2008, Marancik et al. 2012). Only larvae that survive to maturity will contribute to the future of the population. Therefore, using a historical record collected from fish that do survive to the late juvenile or adult stage may be better suited to investigating the habits and location of successful larvae than direct larval collections.

Otolith microchemistry has been the preferred forensic method for geographic interpretation of fish origin. This method can be useful in detecting the chemical fingerprints of natal rivers in anadromous species (Chang and Geffen 2013) and movements of freshwater (Clarke et al. 2015) and marine species (Jones et al. 2013, Cook et al. 2014, Tzadik et al. 2017b). However, investigators have identified several difficulties when relying exclusively on this technique for historical reconstruction. First, physiology may interfere with the incorporation of measurable elements into the otolith structure (Sturrock et al. 2014). Second, the distribution of elements useful in microchemistry studies may change significantly year-to-year in open systems, requiring annual resampling of the background (Jones et al. 2013) and absolute knowledge of specimen age. Third, spatial scale or distribution of easily sampled elements can heavily influence results (Sturrock et al. 2014, Tzadik et al. 2017a).

Interpreting bulk isotopes in fish tissues

Bulk stable isotope values within animal tissues result from the combined isotopes of all amino acids within the tissue. Each amino acid undergoes a unique isotopic fractionation upon incorporation into the tissue; therefore, the bulk value represents a mass-balanced average of the fractionation among all amino acids present (Whiteman et al. 2019). Bulk stable isotope values may result from a combination of inputs, including geographic location (Seminoff et al. 2012,

Trueman et al. 2017), movement across isoscapes (McMahon et al. 2011, MacKenzie et al. 2012), and trophic position (Post 2002, Guinan et al. 2015, Dalponti et al. 2018), which may be difficult to tease apart. Despite these difficulties, some common patterns have been observed among species. Values of bulk $\delta^{15}\text{N}$ are generally considered to represent the trophic position of an organism, with consumer tissue becoming enriched in relation to its food source (McCutchan et al. 2003). In ecological studies, the average increase in $\delta^{15}\text{N}$ is 3.4‰ per trophic level (Vanderklift and Ponsard 2003, Fry 2006). Bulk $\delta^{15}\text{N}$ values can also provide insight into nutrient sources, with a consistent difference between eutrophic and oligotrophic waters (Hansson et al. 1997). Bulk $\delta^{13}\text{C}$ values are often used to infer the dominant primary-producer type (basal resource) that supports food webs or individual taxa [e.g., planktonic vs. benthic; Fry and Wainright (1991); Kendall et al. (2001)]. Along continental shelves, $\delta^{13}\text{C}$ gradients often exist in which consumer values are highest in clear, shallow waters and lowest in deep or turbid waters, due to greater influence of benthic production in the shallower areas. Benthic algae $\delta^{13}\text{C}$ is generally enriched by approximately 5‰ as compared to phytoplankton due to light limitations at depth (Fry and Wainright 1991, Radabaugh et al. 2014).

Fish eye lenses can be used as an archival tissue

Fish eye lenses grow throughout the lifespan, adding a thin layer of cells along the outer surface of the existing lens (Nicol 1989, Vihtelic 2008). The cells then lose all organelles in the process of attenuated apoptosis (Wride 2011), leaving primarily crystallin proteins behind (Mahler et al. 2013). Protein movement within the embryonic eye lens appears to be isotropic, but research has found little movement of protein during the post-embryo stage (Shi et al. 2009). Small amounts of protein turnover does occur in the metabolically active outer lamina (Stewart et al. 2013); however, this turnover is limited. Because the cells become metabolically inert, the

proteins in each eye-lens lamina reflect the chemical composition within the body at the time of formation, resulting in the ability to age individuals based on radiocarbon within the eye-lens nucleus (Lynnerup et al. 2008, Nielsen et al. 2016).

Recent investigations have indicated fish and squid eye lenses also preserve a record of $\delta^{13}\text{C}$ and $\delta^{15}\text{N}$ over the lifetime (Wallace et al. 2014, Quaeck-Davies et al. 2018, Kurth et al. 2019, Meath et al. 2019). Controlled feeding experiments have shown that stable-isotope integration into fish eye lenses begins within two weeks of a diet-switch, and is 100% by 54 days post-switch (Granneman 2018). Therefore, the $\delta^{13}\text{C}$ and $\delta^{15}\text{N}$ within the inner-most eye-lens layer (hereafter: core) should represent the geographic location and diet (trophic position and basal-resource dependence) during the earliest weeks of life for an individual fish. These core isotope values can provide a historical perspective on the postlarval and early juvenile period of those fish captured during the late juvenile and adult phases (Meath et al. 2019).

West Florida Shelf isoscape and species of interest

The West Florida Shelf (WFS) is a continental shelf area located on the eastern side of the Gulf of Mexico. The area includes an expansive mosaic of soft- and hard-bottom habitats (Locker et al. 2010, Hine and Locker 2011, Wall and Stallings 2018) that extend over 600 km from north to south and over 200 km west from Florida, USA. An isoscape constructed using fish muscle tissue has been established for the WFS with patterns of both $\delta^{15}\text{N}$ and $\delta^{13}\text{C}$ consistent among seasons and years (Radabaugh et al. 2013, Huelster 2015). Across species, $\delta^{15}\text{N}$ values are highest in the northwest, due to wastewater and animal husbandry inputs introduced via the Mississippi River and other rivers in the area (Radabaugh and Peebles 2014, Peebles and Hollander 2020). Values of $\delta^{15}\text{N}$ are lowest in the southeast, which is consistent with little freshwater inflow and low nutrient availability, leaving diazotrophs such as *Trichodesmium*

spp., which directly incorporate atmospheric nitrogen, as the main providers of organic nitrogen to the marine system (Holl et al. 2007). Values of $\delta^{13}\text{C}$ are highest in shallow, nearshore waters and decreased in an offshore direction, which is consistent with shallow-water communities relying heavily on benthic production and deep-water communities exclusively utilizing planktonic algae as a basal resource (Fry and Wainright 1991, Radabaugh et al. 2014). See Figure 1.1 for general trends in both $\delta^{13}\text{C}$ and $\delta^{15}\text{N}$ isotopes on the WFS.

For the current study, we investigated four commercially and recreationally important reef-fish species common on the WFS for which the life cycles are relatively well known. Black Seabass (*Centropristis striata*) juveniles and adults are concentrated in low-relief hard-bottom areas of the northeastern WFS (Hood et al. 1994, Weaver 1996). Red Grouper (*Epinephelus morio*) also inhabit low-relief, hard-bottom areas of the WFS, but juveniles and adults tend to inhabit deeper waters than Black Seabass (Moe 1969, Johnson and Collins 1994, Lombardi-Carlson 2014), with the center of abundance being south and west of Black Seabass. The species has been observed spawning in small groups distributed across the low-relief WFS (Coleman et al. 1996, Coleman et al. 2010). High concentrations of spawning occurs near the 70 m depth contour (Wall et al. 2011, Grasty et al. 2019) and juveniles are generally found in shallower waters. Gag (*Mycteroperca microlepis*) utilize many parts of the WFS during their life cycle. Spawning occurs on the shelf edge in large aggregations (Fitzhugh et al. 2005, Ellis and Powers 2012), whereas juveniles inhabit the polyhaline regions of estuaries for a year or more (Stallings et al. 2010, Switzer et al. 2012). Older juveniles and non-spawning adults use high-relief habitats (Bullock and Smith 1991). Red Snapper (*Lutjanus campechanus*) were scarce on the WFS for decades but have re-expanded their range from the north-central Gulf of Mexico (Hollenbeck et al. 2015). To date, a small number of Red Snapper eggs has been genetically identified and

females with hydrated oocytes have been captured on the WFS (Burrows et al. 2018, Nguyen & Peebles, unpublished data) indicating spawning does occur in the region. However, the distribution of spawning locations, eggs, and larvae are unknown.

Statistical analysis of complex isotopic datasets

Simultaneous or sequential correlations have been used in a wide variety of fields to aid in data interpretation (Du et al. 2003, Zhang et al. 2006, Mahmoud and Sunarso 2018). In the case of isotopes, values may be simultaneously correlated to other known factors, thereby segregating the confounding interpretations for the bulk isotopic values (Meath et al. 2019). The range of possible interpretations may be limited, resulting in a single, most parsimonious, explanation of the eye-lens core isotopic data. By taking advantage of the isotopically conservative nature of eye-lens tissue combined with the established isotopic trends on the WFS, the spatial distributions and movements of reef-fish species during postlarval and early juvenile periods may be uncovered. An understanding of the geographic distribution of larvae that ultimately settle into juvenile habitats could lead to improved stock assessments and/or improved marine protected area management.

Objectives

Here we aimed to disentangle the multiple influences on bulk isotope values within the eye-lens cores of four reef-fish species in the eastern Gulf of Mexico. To accomplish this goal, we began by constructing a generalized matrix of interpretations to segregate the isotopic inputs to the eye-lens cores using statistical methods. This matrix could be used by any researcher doing similar work in any isotopic setting. We then used the constructed matrix to mathematically infer

the geographic extent and comparative movement of the four target reef fish species. We found that, despite broad similarities in habitat needs among the species, each displayed differences in larval central locations and movements.

MATERIALS AND METHODS

Specimen collection

During routine monitoring efforts in 2015-2017, Florida Fish and Wildlife Conservation Commission's Fisheries Independent Monitoring Program (FIM) and the National Oceanic and Atmospheric Administration Southeast Area Monitoring and Assessment Program (SEAMAP) groundfish trawl survey retained juveniles from each of four species, Black Seabass, Gag, Red Grouper, and Red Snapper from major estuaries on the west coast of Florida and the WFS (Figure 3.1). Each fish was measured for standard length (SL). Both eyes were extracted, wrapped in aluminum foil, and frozen at - 20°C until analysis (Stallings et al. 2015). Otoliths were extracted, dried, and cleaned of tissue. Aging was completed by counting annuli in whole otoliths using a dissecting stereomicroscope and transmitted light in Black Seabass, Gag, and Red Grouper (Casselmann 1990, Kimura and Lyons 1991). For Red Snapper, otoliths were thin sectioned using an IsoMet low speed saw and mounted on a slide before aging under transmitted light (White and Palmer 2004).

Eye lens preparation and sample analysis

We thawed one eye from each fish and removed the lens. Laminae were separated using two sets of fine-tipped forceps under a dissecting stereomicroscope. We generally followed Wallace et al. (2014), with the exception that the lens was immersed in deionized water for

delamination (Stewart et al. 2013), which has been shown to have no effect on isotopic values (Meath et al. 2019). Once a lamina was removed, we measured the diameter of the remaining tissue and changed the water in the dish. The hardened eye-lens core, the innermost sphere of tissue, was retained for this study. We measured the eye-lens core diameter (ELD) to the nearest 0.05 mm using a calibrated ocular micrometer.

In many cases, a single eye lens did not provide sufficient mass for reliable isotopic analysis. If this was the case, we delaminated the second eye lens of that individual. If the lens core diameters were identical, the two cores were combined for isotopic analysis (Wallace et al. 2014, Meath et al. 2019). If core diameters were not identical, the specimen was eliminated. Eye-lens cores were then placed in a drying oven at 55°C for 12 hours to ensure complete desiccation.

Eye-lens cores with a mass of 150-600 µg were packaged into 3.3 x 5 mm tin capsules for stable-isotope analysis performed using a Carlo-Erba NA2500 Series II elemental analyzer coupled to a continuous-flow Thermo-Finnigan Delta+ XL isotope ratio mass spectrometer (IRMS) at the University of South Florida College of Marine Science in St. Petersburg, Florida. Calibration standards were NIST 8573 and NIST 8574 L-glutamic acid standard reference materials. Analytical precision, obtained by replicate measurements of NIST 1577b bovine liver, was ± 0.20‰ for δ¹³C and ± 0.17‰ for δ¹⁵N.

Results are presented in standard notation (□□notation, ‰) relative to the international standard of air and Vienna Pee Dee Belemnite.

$$\delta X = \left(\frac{R_{sample}}{R_{standard}} - 1 \right) \times 1000$$

where X is the element (carbon or nitrogen) and R is the corresponding ratio ¹³C/¹²C or ¹⁵N/¹⁴N.

Data analysis methods

Prior to isotopic analysis, we devised a method for segregating the three potential sources of variability for bulk isotope values. In short, we listed all possible isotopic outcomes from each of the three inputs to the bulk isotope values in each species (geographic origin, change in trophic position, and postlarval/juvenile movement; Table 3.1). In this model, observed values were classed as “isotopic outcomes” and represented the incorporation of each of the three inputs. Consistency among the three inputs results in consistent outcomes (positive, negative, or zero; Table 3.1).

Working backward from observed values, we devised a general interpretation for each of the three outcomes of correlations between $\delta^{13}\text{C}$ or $\delta^{15}\text{N}$ eye-lens core values and internal or external parameters such as size at analysis or juvenile location (positive correlation, negative correlation, or no correlation; Table 3.2). We included a set of simplifying assumptions based on the known biology or life history of the species under study (Table 3.2).

Eye-lens cores were not precisely uniform in diameter for all specimens ($0.35 \leq \text{ELD} \leq 1.1$ mm) due to the relative imprecision of manual delamination. Using these variable ELDs, capture locations, and isotope values, we devised a method of segregating the isotopic effects of postlarval location from movement or trophic change (Table 3.1 & 3.2). We constructed regression equations for standard length (SL) as a function of ELD in each species (Table 3.3). We calculated SL for each specimen at the time of eye-lens core completion based on these regressions and compared these to SL at settlement based on published literature.

We recorded the eye-lens core $\delta^{13}\text{C}$ and $\delta^{15}\text{N}$ values for each specimen. For each species, we calculated mean, standard error, minimum, and maximum values of $\delta^{13}\text{C}$ and $\delta^{15}\text{N}$ of eye-lens cores. We used the total range of $\delta^{15}\text{N}$ values in eye-lens cores to infer the extent of

postlarval/early juvenile distribution in a north-south direction on the WFS, and total range of $\delta^{13}\text{C}$ values to infer distribution across depth (Radabaugh and Peebles 2014). We used Spearman rank correlation to compare $\delta^{13}\text{C}$ or $\delta^{15}\text{N}$ with ELD and with juvenile collection location (latitude or longitude) for each species. Using the interpretation rules presented in Tables 3.1 and 3.2, we then described differences in the postlarval locations and movements of the four species.

We compared the multivariate differences in stable isotope eye-lens core values among species using PERMANOVA [Package vegan; Adonis routine (Oksanen et al. 2019)] and multivariate pairwise comparisons [package EcolUtils; (Salazar 2019)]. We calculated the dispersion of $\delta^{13}\text{C}$ and $\delta^{15}\text{N}$ stable isotope values using stable isotope Bayesian ellipses in R (SIBER), which describes aspects of a population's isotopic dispersion by plotting and measuring the bivariate standard deviation, or standard ellipse area (SEAc), of isotope biplots (Jackson et al. 2011). The value used for comparisons of isotopic width was SEAc, or the mode of $n = 20,000$ standard ellipses generated via Bayesian permutation. We considered differences in SEAc significant between species if $\geq 95\%$ of posterior draws for one species was smaller than for the other. We also used SIBER to measure the degree of overlap between isotopic postlarval distributions for each species. Because there is no defined measure of overlap, we classified each pair using descriptive terminology from correlation (0.00-0.19 = very weak; 0.20-0.39 = weak; 0.40-0.59 = moderate; 0.60-0.79 = strong; 0.80-1.0 = very strong). All statistical analyses were completed in R (R Core Team 2018). All data are published in the Gulf of Mexico Research Initiative Information and Data Cooperative (GRIIDC) website (<https://data.gulfresearchinitiative.org/data/R1.x135.120:0012>).

RESULTS

For each of the four species, total numbers of specimens ranged from 38 to 52. Age at collection ranged from a under one year to over three years. The range of collection lengths was 37 to 325 mm SL (Table 3.3). ELD at collection ranged from 0.9 to 7.5 mm. Analyzed ELD ranged from 0.3 – 1.1 mm (Table 3.3). Each eye lens consisted of at least two laminae with only the innermost tissue used for analysis. Analyzed eye-lens core diameters translated to SL of 14 – 47 mm and represent the weeks just before and just after settlement to juvenile habitats (Table 3.3).

The total range of $\delta^{15}\text{N}$ values for all species combined was 7.02‰. The lowest value was a Red Snapper at 4.61‰ and the highest value was also Red Snapper at 11.24‰ (Table 3.4). The combined range of $\delta^{13}\text{C}$ values was 6.85‰ with the lowest value being -21.00‰ for Gag and the highest being -14.15‰ for Black Seabass (Table 3.4). Mean (\pm SE) $\delta^{15}\text{N}$ and $\delta^{13}\text{C}$ values were highest for Black Seabass and the species had the largest total range of $\delta^{13}\text{C}$ values. We found the largest range of $\delta^{15}\text{N}$ values (6.62‰) and the smallest range of $\delta^{13}\text{C}$ (4.07‰) in Red Snapper (Table 3.4; Figure 3.2).

Correlations between isotopic values and internal or external parameters

In Black Seabass, all correlations were weak but significant. ELD had a negative correlation with core $\delta^{15}\text{N}$ and a positive correlation with $\delta^{13}\text{C}$. Collection latitude had a positive correlation with $\delta^{15}\text{N}$, whereas collection longitude negatively correlated with $\delta^{13}\text{C}$. According to the interpretation rules (Table 3.2), these results indicate Black Seabass postlarvae moved south and offshore during the weeks represented by these data (Table 3.5).

In Gag, ELD had a moderate, positive correlation with $\delta^{13}\text{C}$, but no correlation with $\delta^{15}\text{N}$. Latitude and $\delta^{15}\text{N}$ had a weak correlation, but $\delta^{13}\text{C}$ and longitude did not correlate (Table 3.5). According to the interpretation rules, Gag moved inshore or switched from planktonic to benthic

dependence. However, they did not move in a north-south direction. In addition, larval locations were moderately distributed in a north-south direction but were constrained in an east-west direction (Table 3.5).

In Red Grouper, $\delta^{15}\text{N}$ had a moderate correlation with ELD and $\delta^{13}\text{C}$ had a weak correlation with ELD (Table 3.5). There was no correlation between $\delta^{15}\text{N}$ and collection latitude or between $\delta^{13}\text{C}$ and collection longitude. According to the interpretation rules, Red Grouper moved north or increased trophic position as they grew, while also moving slightly inshore or changing basal-resource dependence. In addition, postlarval area was quite constrained in both the north-south and east-west directions (Table 3.5).

For Red Snapper, neither $\delta^{13}\text{C}$ nor $\delta^{15}\text{N}$ values correlated with ELD. However, $\delta^{15}\text{N}$ did have a moderate correlation with collection latitude and $\delta^{13}\text{C}$ had a weak negative correlation with collection longitude (Table 3.5). The interpretation rules indicated that Red Snapper did not change basal-resource dependence or move substantially during the first weeks of life. However, their larval area was widely distributed in the north-south direction (Table 3.5).

Comparisons of species in isotopic space

We found significant multivariate differences among eye-lens core isotope values of the four species (PERMANOVA $F = 8.42$, $p < 0.001$). Pairwise comparison indicated that Black Seabass and Red Snapper were not significantly different nor were Red Grouper and Gag. However, each pair of species was significantly different from the other (Figure 3.3; Table 3.6). SEAc was largest for Black Seabass ($5.83 \pm 1.52\%{}^2$) and smallest for Red Grouper ($2.40 \pm 0.59\%{}^2$); Red Snapper ($4.13 \pm 1.27\%{}^2$) and Gag ($2.77 \pm 0.74\%{}^2$) were intermediate. Black Seabass SEAc size was significantly different from Gag and Red Grouper. SEAc extent was not

significantly different between any other pair of species (Figure 3.3). We observed moderate overlap between SEAc for Red Snapper and Black Seabass at 0.48. However, the major axis for the Red Snapper standard ellipse was in the $\delta^{15}\text{N}$ direction (north-south), but the major axis for Black Seabass standard ellipse was oblique to both axes (Table 3.6; Figure 3.3). SEAc overlap between Red Snapper and Gag and between Gag and Red Grouper were also moderate (43% and 49% respectively), with major axes for each ellipse being orthogonal to one another (Figure 3.3). We observed weak overlap in SEAc between Black Seabass and Gag (0.21), with major axes being oblique to one another. Both Gag and Red Grouper standard ellipses had major axes in the $\delta^{13}\text{C}$ direction. However, the Gag ellipse was offset in the positive $\delta^{15}\text{N}$ direction. Red Grouper and Red Snapper also had weak overlap (0.26) with major axes being orthogonal to one another. The lowest proportion of SEAc overlap was between Black Seabass and Red Grouper (0.08) with the Black Seabass ellipse positioned much higher in the $\delta^{15}\text{N}$ direction than Red Grouper (Figure 3.3; Table 3.6).

General interpretation of postlarval location and movement

By combining SEAc, and correlations between isotope values and size or location, we constructed a schematic diagram of postlarval/early juvenile distribution and movement for each of the four species (Figure 3.4). While the species use broadly similar habitats, subtle differences became apparent using these data. Black Seabass postlarvae were widely distributed, with little movement except for a subtle southward trend along the WFS. The central area for Red Grouper postlarvae was isotopically small with movement to the north and inshore. Gag postlarval distribution was also confined, with inshore movement during the postlarval period. Red Snapper

postlarval distribution was confined in the east-west direction but was diffuse in the north-south direction. No movement was detected over the postlarval period.

DISCUSSION

We devised a novel strategy for inferring postlarval distribution and movement of fish using the $\delta^{13}\text{C}$ and $\delta^{15}\text{N}$ values in cores of fish eye lenses. We tested the strategy using several reef-fish species common to the hard-bottom habitats of the WFS. Despite the classification of all four species as reef fishes, we found differences in distribution and movement, using a combination of three statistical methods: correlation, PERMANOVA, and SIBER. While one species was widely distributed and experienced little movement, others were more narrowly distributed and experienced significant movement during the first weeks of life. This novel analysis approach can be adapted for use in other geographic areas that have strong trends in background isotopic signatures and may serve as a method of identifying important larval habitats or geographic areas.

Construction and use of interpretation rules

Outer eye-lens isotopic values align closely with values observed in the muscle in many fish species (Quaeck 2017). The WFS isoscape was constructed using the isotope values in white muscle of several demersal species found throughout the region. Isotope values from eye-lens cores may be somewhat lower than those used to create the WFS isoscape due to the trophic position of postlarvae as opposed to adult fish (Bradley et al. 2015, McMahon et al. 2015, McMahon and McCarthy 2016). However, isotopic trends in the WFS isoscape have been shown to be robust and should be present in eye lenses as well. Gag eye-lens core values reported here

align closely with the muscle $\delta^{13}\text{C}$ and $\delta^{15}\text{N}$ values ($\sim -21\text{‰}$ and 8‰ respectively) of a few newly settled Gag in a previous study (Weisberg et al. 2014). With postlarvae of all four species consuming similar prey at close to the same trophic position (Powell and Tucker 1992, Berlinsky et al. 2000, Drass et al. 2000, Umezawa et al. 2018), differences in eye-lens core isotopes should be attributable to geographic variation and movement.

A study of *Epinephelus septemfasciatus* (Convict Grouper, a congener of Red Grouper) early life history found that the total eye diameter at the onset of exogenous feeding was 0.3 mm (Park et al. 2014), and fish eye-lens diameters are known to be approximately half of total eye diameter (Collery et al. 2014). The smallest ELD in our study was 0.3 mm, indicating analyzed material was derived from exogenous feeding. In addition, $\delta^{15}\text{N}$ values in the cores were uniformly the lowest in the eye-lens series (data not presented). In species with substantial maternal contribution to the early eye lens, exogenous feeding is indicated by a steep decline in $\delta^{15}\text{N}$ values (Simpson 2018).

Bulk $\delta^{13}\text{C}$ and $\delta^{15}\text{N}$ values are known to incorporate trophic position (McMahon and McCarthy 2016) and geographic location (Graham et al. 2010) into a single value. This combination of influences may present interpretation difficulties. While compound-specific isotope analysis is an effective tool for separating trophic from movement influences (Ellis 2012, McMahon et al. 2013, Bradley et al. 2015), the method remains expensive and time-consuming. Instead, our approach was to address these various influences statistically, using several independent analyses to segregate influences on bulk isotopic values. We considered three major influences on the bulk isotopic values within fish eye-lens cores: geographic origin (Trueman et al. 2017), trophic growth (Dalponti et al. 2018, McMeans et al. 2019), and movement along the isotopic gradient (Graham et al. 2010; Table 3.1). With isotopic eye-lens incorporation being

50% complete within 30 d (Granneman 2018), we expect relatively little change to occur; however, by correlating ELD with isotopic values, we were able to test that assumption.

Gag spawning origin and postlarval movement

Despite Gag collections occurring exclusively in estuaries (Figure 3.1) where shallow, nutrient-rich water can result in high isotopic values (Barnes et al. 2009, Radabaugh and Peebles 2014, Trueman et al. 2017), values of $\delta^{13}\text{C}$ and $\delta^{15}\text{N}$ were low, indicating an offshore, southern origin (Radabaugh and Peebles 2014). The species is known to spawn in high-relief areas near the outer WFS (Coleman et al. 1996, Coleman et al. 2011). Physical models suggest that larvae may take advantage of bottom currents to arrive at estuary mouths, often as much as 150 km away (Weisberg et al. 2014). Spearman rank correlation results are also consistent with this pattern, indicating young Gag move into areas with higher background $\delta^{13}\text{C}$ during the first several weeks of life, but do not increase in $\delta^{15}\text{N}$ over that same period, suggesting no increase in trophic position or movement north along the isotopic gradient (Table 3.5; Figure 3.4). Weisberg et al. (2014) also observed that muscle $\delta^{13}\text{C}$ and $\delta^{15}\text{N}$ values in newly settling larvae were substantially lower than juveniles that had been residing in seagrass beds for several months.

The standard ellipse size was quite small for Gag, with low mean values for both $\delta^{13}\text{C}$ and $\delta^{15}\text{N}$, suggesting most surviving juveniles originated from a confined spawning area near the southwestern extent of the study region. A weak positive correlation between $\delta^{15}\text{N}$ and collection latitude suggested that individuals spending their postlarval period farther to the north were later collected from estuaries farther north. In contrast, non-significant correlation between $\delta^{13}\text{C}$ and collection longitude suggests that longitudinal origin had no effect on later juvenile location. If the primary effect on $\delta^{13}\text{C}$ is due to seagrass residence (Weisberg et al. 2014) and spawning

grounds are confined by depth (Coleman et al. 2004), then this lack of correlation with juvenile location would be expected.

Black Seabass spawning origin and postlarval movement

High mean values of both $\delta^{13}\text{C}$ and $\delta^{15}\text{N}$ in Black Seabass (Table 3.4, Figure 2), suggest this species originated farthest north and farthest inshore. The large standard ellipse area suggests the widest postlarval distribution of the four species. Little is known about Black Seabass spawning habits in the Gulf of Mexico, but adults and juveniles are found most frequently in low-relief hard bottom habitats spread across the northeaster quadrant of the WFS (Weaver 1996). Significant correlations between $\delta^{15}\text{N}$ and collection latitude and between $\delta^{13}\text{C}$ and collection longitude indicate the postlarval distribution is quite wide in both the north-south and east-west directions. A significant negative correlation between $\delta^{15}\text{N}$ and ELD may suggest movement to the south, which corresponds to a common direction of wind-driven currents in the region throughout most of the year (Mayer et al. 2017). A lack of correlation between $\delta^{13}\text{C}$ and ELD indicates no movement inshore or offshore as the postlarvae grow, along with no major change in basal-resource dependence between 15 and 40 mm SL. These results are consistent with aspects of Black Seabass biology and circulation in the area (Weaver 1996, Mayer et al. 2017).

Red Grouper spawning origin and postlarval movement

Red Grouper are thought to spawn in small harems spread across low-relief areas of the WFS (Coleman et al. 2010, Coleman et al. 2011). Repeated studies inside a marine protected area indicated that depressions maintained for reproductive purposes were clustered near 70 m

depth (Wall et al. 2011, Grasty et al. 2019). While our isotopic observation of a wide total $\delta^{13}\text{C}$ and $\delta^{15}\text{N}$ distribution (Table 3.4; Figure 3.4) supports the idea of scattered reproductive areas, the small SEAc suggests a high concentration of spawning as reported in the literature (Figure 3.3). Taken together with the lack of correlation between $\delta^{15}\text{N}$ or $\delta^{13}\text{C}$ and capture location, these data suggest a large proportion of the individuals that survived to the juvenile stage originated from a confined geographic area. A significant correlation between $\delta^{15}\text{N}$ and ELD suggests that the species either increases tropic position quickly or moves northward throughout the postlarval and early juvenile period. Juveniles are often found in the Big Bend region and near the mouths of northern estuaries in the study region (Figure 3.1), whereas spawning seems to be most common south of 28°N (Wall et al. 2014, Grasty et al. 2019). A weak correlation between $\delta^{13}\text{C}$ and ELD suggests little movement inshore between 14 and 36 mm SL.

Red Snapper spawning origin and postlarval movement

Red Snapper were common on the WFS before the mid-twentieth century, but became rare as the result of heavy fishing pressure (Burns and Froeschke 2012, SEDAR 2018). Recent commercial and recreational catches have suggested a range expansion over the past several years with the species returning to the central WFS. Evidence of Red Snapper spawning on the WFS includes eggs collected directly west of Tampa Bay and identified via DNA barcoding (Burrows et al. 2018) and several females collected in spawning condition (hydrated oocytes) from multiple locations on the WFS (Nguyen & Peebles, unpublished data). In our study, the constrained range of $\delta^{13}\text{C}$ values and dispersed $\delta^{15}\text{N}$ values (Table 3.4; Figure 3.3), suggests a narrow depth range but an expansive along-shelf distribution of larvae. These interpretations are corroborated by a moderate correlation between $\delta^{15}\text{N}$ and capture latitude, coupled with a weak negative correlation between $\delta^{13}\text{C}$ and capture longitude (Table 3.5; Figure 3.4). These results

suggest Red Snapper did not move north or south when settling into juvenile habitats. In addition, a lack of significant correlations between $\delta^{13}\text{C}$ or $\delta^{15}\text{N}$ and ELD indicates no major geographic movement, no trophic growth, or no change in basal-resource dependence during the first weeks of life, which is similar to previous findings in the northern Gulf of Mexico (Wells et al. 2008).

Species-specific results suggest differences in spawning locations and movements

Mean (\pm SE) isotopic values for the four species indicated that the central location for each species was unique, with Black Seabass being concentrated farthest north and inshore, and Red Grouper being concentrated farthest south and offshore. Extent of north-south dispersion was highest in Red Snapper, whereas extent of east-west dispersion was highest in Black Seabass (Figure 2). Most importantly, these central locations agree with reported spawning locations for each of these species (Coleman et al. 1996, Weaver 1996, Saul et al. 2013).

Multivariate analyses suggested subtle, but potentially important, differences between fish eye-lens core $\delta^{13}\text{C}$ and $\delta^{15}\text{N}$ isotopic values of the four reef-fish species. The two complimentary methods (PERMANOVA and SIBER) identified similar trends and differences among the four species. A lack of difference and a high degree of overlap between Black Seabass and Red Snapper agrees with a shared northern latitude. Both species are known to be concentrated in the northern portion of the study area (Hood et al. 1994, Ainsworth et al. 2018), and the Red Snapper population has been expanding from the north toward the south. Red Snapper juvenile capture locations were in deeper water than Black Seabass (Figure 3.1), which corresponds with core $\delta^{13}\text{C}$ values being lower in Red Snapper.

A high degree of overlap and no significant difference between Gag and Red Grouper suggests shared locations and basal-resource dependences between these two species during the first few weeks of life. Both are known to spawn in 70-100 m of water near the shelf break, and evidence of spawning for both species has been observed in the same marine reserves (Wall et al. 2011, Ellis and Powers 2012, Grasty et al. 2019). This similarity in isotopic signatures presents the possibility that Red Grouper use a similar mechanism of postlarval transport across the WFS. While Gag eye-lens cores are isotopically similar to Red Grouper cores, and Red Snapper cores are isotopically similar to Black Seabass cores during the first weeks of life, the two pairs of species are distinctly different. Overall, the patterns observed here indicate subtle geographic and life-history differences among these reef-fishes during the first weeks of life.

Conclusions and future directions

Here we used bulk stable isotope analysis on the cores of eye lenses from juvenile fish as a chemical time-capsule to investigate the trophic and location history of individuals during the postlarval and early juvenile period. We explored a statistical technique to distinguish the isotopic influences on larvae that ultimately survive to the juvenile stage in four WFS reef-fish species. We showed that isotope data in eye-lens cores combined with catch location and ELD could be used to uncover subtle differences among species that use broadly similar geographic areas. We also showed that movement and trophic change could be inferred within each species over a time window of only a few weeks. Finally, we added evidence to suggest the range expansion in Red Snapper is multi-generational, not merely the result of juveniles or adults moving into the area with spawning occurring elsewhere.

While the use of eye-lens core stable isotopes as indicators of larval origin is quite promising, several additional developments could improve interpretation. First, technological

advances should enable future researchers to use even smaller eye-lens samples, potentially further subdividing the postlarval period. As compound-specific isotope analysis of eye lenses becomes more accessible, this technique should be investigated for corroboration of the current results. Isotopic techniques should also be paired with other emerging technologies such as egg and larval surveys which identify fish via DNA barcoding (Burrows et al. 2018) to better quantify the earliest larval period. Finally, additional species should be investigated, including pelagic and migratory species.

LITERATURE CITED

- Able, K. W., M. P. Fahay, and G. R. Shepherd. 1995. Early life history of Black Seabass, *Centropristis striata*, in the mid-Atlantic bight and New Jersey estuary. *Fishery Bulletin* **93**:429-445.
- Ainsworth, C. H., C. B. Paris, N. Perlin, L. N. Dornberger, W. F. Patterson, E. Chancellor, S. Murawski, D. Hollander, K. Daly, I. C. Romero, F. Coleman, and H. Perryman. 2018. Impacts of the Deepwater Horizon oil spill evaluated using an end-to-end ecosystem model. *Plos One* **13**.
- Barnes, C., S. Jennings, and J. T. Barry. 2009. Environmental correlates of large-scale spatial variation in the delta C-13 of marine animals. *Estuarine Coastal and Shelf Science* **81**:368-374.
- Beets, J. 1997. Effects of a predatory fish on the recruitment and abundance of Caribbean coral reef fishes. *Marine Ecology Progress Series* **148**:11-21.
- Berlinsky, D., M. Watson, G. Nardi, and T. M. Bradley. 2000. Investigations of selected parameters for growth of larval and juvenile black sea bass *Centropristis striata* L. *Journal of the World Aquaculture Society* **31**:426-435.
- Bradley, C. J., N. J. Wallsgrove, C. A. Choy, J. C. Drazen, E. D. Hetherington, D. K. Hoen, and B. N. Popp. 2015. Trophic position estimates of marine teleosts using amino acid compound specific isotopic analysis. *Limnology and Oceanography-Methods* **13**:476-493.
- Bullock, L. H., and G. B. Smith. 1991. Seabasses (Pisces: Serranidae). *Memoirs of the Hourglass Cruises* **8**:1-243.
- Burghart, S. E., L. Van Woudenberg, C. A. Daniels, S. D. Meyers, E. B. Peebles, and M. Breitbart. 2014. Disparity between planktonic fish egg and larval communities as indicated by DNA barcoding. *Marine Ecology Progress Series* **503**:195-204.
- Burns, K. M., and J. T. Froeschke. 2012. Survival of Red Grouper (*Epinephalus morio*) and red snapper (*Lutjanus campechanus*) caught on J-hooks and circle hooks in the Florida recreational and recreational-for-hire fisheries. *Bulletin of Marine Science* **88**:633-646.

- Burrows, M., J. S. Browning, M. Breitbart, S. A. Murawski, and E. B. Peebles. 2018. DNA barcoding reveals clear delineation between spawning sites for neritic versus oceanic fishes in the Gulf of Mexico. *Fisheries Oceanography*:1-12.
- Casselman, J. M. 1990. Growth and relative size of calcified structures of fish. *Transactions of the American Fisheries Society* **119**:673-688.
- Chang, M.-Y., and A. J. Geffen. 2013. Taxonomic and geographic influences on fish otolith microchemistry. *Fish and Fisheries* **14**:458-492.
- Clarke, A. D., K. H. Telmer, and J. M. Shrimpton. 2015. Movement patterns of fish revealed by otolith microchemistry: a comparison of putative migratory and resident species. *Environmental Biology of Fishes* **98**:1583-1597.
- Coleman, F. C., P. B. Baker, and C. C. Koenig. 2004. A review of Gulf of Mexico marine protected areas: Successes, failures, and lessons learned. *Fisheries* **29**:10-21.
- Coleman, F. C., C. C. Koenig, and L. A. Collins. 1996. Reproductive styles of shallow-water groupers (Pisces: Serranidae) in the eastern Gulf of Mexico and the consequences of fishing spawning aggregations. *Environmental Biology of Fishes* **47**:129-141.
- Coleman, F. C., C. C. Koenig, K. M. Scanlon, S. Heppell, S. Heppell, and M. W. Miller. 2010. Benthic habitat modification through excavation by red grouper, *Epinephelus morio*, in the northeastern Gulf of Mexico. *Open Fish Science Journal* **3**:1-15.
- Coleman, F. C., K. M. Scanlon, and C. C. Koenig. 2011. Groupers on the edge: shelf edge spawning habitat in and around marine reserves of the northeastern Gulf of Mexico. *Professional Geographer* **63**:456-474.
- Colin, P. L. 2012. Aggregation spawning: biological aspects of the early life history. Pages 191-224 in Y. S. DeMitcheson and P. L. Colin, editors. *Reef Fish Spawning Aggregations: Biology, Research and Management*. Springer, Dordrecht.
- Colin, P. L., C. C. Koenig, and W. A. Laroche. 1996. Development from egg to juvenile of the Red Grouper (*Epinephelus morio*) (Pisces: Serranidae) in the laboratory. Pages 399-414 in F. ArreguinSanchez, J. L. Munro, M. C. Balgos, and D. Pauly, editors. *Biology, fisheries and culture of tropical groupers and snappers: Proceedings of an EPOMEX/ICARM International workshop on tropical snappers and groupers*. International Center for Living Aquatic Resources Management, University of Campeche, Mexico.
- Collery, R. F., K. N. Veth, A. M. Dubis, J. Carroll, and B. A. Link. 2014. Rapid, accurate, and non-invasive measurement of Zebrafish axial length and other eye dimensions using SD-OCT allows longitudinal analysis of myopia and emmetropization. *Plos One* **9**.
- Cook, G. S., P. E. Parnell, and L. A. Levin. 2014. Population connectivity shifts at high frequency within an open-coast marine protected area network. *Plos One* **9**.
- Cowen, R. K. 1991. Variation in the planktonic larval duration of the temperate wrasse *Semicossyphus pulcher*. *Marine Ecology Progress Series* **69**:9-15.
- Dalponti, G., R. D. Guariento, and A. Caliman. 2018. Hunting high or low: body size drives trophic position among and within marine predators. *Marine Ecology Progress Series* **597**:39-46.
- Drass, D. M., K. L. Bootes, J. Lyczkowski-Shultz, B. H. Comyns, G. J. Holt, C. M. Riley, and R. P. Phelps. 2000. Larval development of red snapper, *Lutjanus campechanus*, and comparisons with co-occurring snapper species. *Fishery Bulletin* **98**:507-527.
- Du, Q. S., D. Q. Wei, and K. C. Chou. 2003. Correlations of amino acids in proteins. *Peptides* **24**:1863-1869.

- Edwards, K. P., J. A. Hare, and F. E. Werner. 2008. Dispersal of black sea bass (*Centropristis striata*) larvae on the southeast US continental shelf: results of a coupled vertical larval behavior - 3D circulation model. *Fisheries Oceanography* **17**:299-315.
- Eldridge, P. J. 1988. The southeast area monitoring and assessment program (SEAMAP)- A state-federal-university program for collection, management, and dissemination of fishery-independent data and information in the southeastern United States. *Marine Fisheries Review* **50**:29-39.
- Ellis, G. S. 2012. Compound-specific stable isotopic analysis of protein amino acids: Ecological applications in modern and ancient systems. PhD. University of South Florida, Tampa, Florida.
- Ellis, R. D., and J. E. Powers. 2012. Gag Grouper, marine reserves, and density-dependent sex change in the Gulf of Mexico. *Fisheries Research* **115**:89-98.
- Fitzhugh, G. R., C. C. Koenig, F. C. Coleman, C. B. Grimes, and W. Sturges. 2005. Spatial and temporal patterns in fertilization and settlement of young gag (*Mycteroperca microlepis*) along the west Florida shelf. *Bulletin of Marine Science* **77**:377-396.
- Fry, B. 2006. Stable isotope ecology. Springer Science+Business Media, New York, NY.
- Fry, B., and S. C. Wainright. 1991. Diatom sources of C-13 rich carbon in marine food webs. *Marine Ecology Progress Series* **76**:149-157.
- Graham, B. S., P. L. Koch, S. D. Newsome, K. W. McMahon, and D. Aurioles. 2010. Using Isoscapes to Trace the Movements and Foraging Behavior of Top Predators in Oceanic Ecosystems. Pages 299-318 in J. B. West, G. J. Bowen, T. E. Dawson, and K. P. Tu, editors. *Isoscapes: Understanding movement, pattern, and process on earth through isotope mapping*.
- Granneman, J. E. 2018. Evaluation of trace-metal and isotopic records as techniques for tracking lifetime movement patterns in fishes. University of South Florida, Tampa, FL.
- Grasty, S., C. C. Wall, J. W. Gray, J. Brizzolara, and S. A. Murawski. 2019. Temporal persistence of Red Grouper holes and analysis of associated fish assemblages from towed camera data in the Steamboat Lumps marine protected area. *Transactions of the American Fisheries Society*:1-9.
- Guinan, M. E., Jr., K. L. Kapuscinski, and M. A. Teece. 2015. Seasonal diet shifts and trophic position of an invasive cyprinid, the Rudd *Scardinius erythrophthalmus* (Linnaeus, 1758), in the upper Niagara River. *Aquatic Invasions* **10**:217-225.
- Hansson, S., J. E. Hobbie, R. Elmgren, U. Larsson, B. Fry, and S. Johansson. 1997. The stable nitrogen isotope ratio as a marker of food-web interactions and fish migration. *Ecology* **78**:2249-2257.
- Hine, A. C., and S. D. Locker. 2011. The Florida Gulf of Mexico continental shelf—great contrasts and significant transitions. *The Gulf of Mexico: Origin, Waters, and Marine Life*.
- Hjort, J. 1914. Fluctuations in the great fisheries of Northern Europe viewed in the light of biological research. Copenhagen Conseil permanent international pour l'exploration de la mer. *Rapports et Proces-Verbaux des Reunions* **20**:(234)-(234).
- Holl, C. M., T. A. Villareal, C. D. Payne, T. D. Clayton, C. Hart, and J. P. Montoya. 2007. *Trichodesmium* in the western Gulf of Mexico: N-15(2)-fixation and natural abundance stable isotope evidence. *Limnology and Oceanography* **52**:2249-2259.

- Hollenbeck, C. M., D. S. Portnoy, E. Saillant, and J. R. Gold. 2015. Population structure of red snapper (*Lutjanus campechanus*) in US waters of the western Atlantic Ocean and the northeastern Gulf of Mexico. *Fisheries Research* **172**:17-25.
- Hood, P. B., M. F. Godcharles, and R. S. Barco. 1994. Age, growth, reproduction, and the feeding ecology of black-sea bass, *Centropristis striata* (Pisces, Serranidae), in the eastern Gulf of Mexico. *Bulletin of Marine Science* **54**:24-37.
- Houde, E. D. 2009. Emerging from Hjort's shadow. *Journal of Northwest Atlantic Fishery Science* **41**:53-70.
- Huelster, S. 2015. Comparison of isotope-based biomass pathways with groundfish community structure in the eastern Gulf of Mexico. Masters. University of South Florida, Tampa.
- Jackson, A. L., R. Inger, A. C. Parnell, and S. Bearhop. 2011. Comparing isotopic niche widths among and within communities: SIBER - Stable Isotope Bayesian Ellipses in R. *Journal of Animal Ecology* **80**:595-602.
- Johnson, A. G., and L. A. Collins. 1994. Age-size structure of red grouper, (*Epinephelus morio*), from the eastern Gulf of Mexico. *Northeast Gulf Science* **13**:101-106.
- Johnson, M. W., S. P. Powers, C. L. Hightower, and M. Kenworthy. 2010. Age, growth, mortality, and diet composition of Vermilion Snapper from the north-central Gulf of Mexico. *Transactions of the American Fisheries Society* **139**:1136-1149.
- Jones, D., T. S. Switzer, B. Houston, and E. B. Peebles. 2013. Use of otolith microchemistry to improve fisheries-independent indices of recruitment for gag (*Mycteroperca microlepis*): linking estuarine nurseries to nearshore reefs in the eastern Gulf of Mexico. Page 25pp SEDAR33-DW9. SEDAR, North Charleston, SC.
- Kendall, C., S. R. Silva, and V. J. Kelly. 2001. Carbon and nitrogen isotopic compositions of particulate organic matter in four large river systems across the United States. *Hydrological Processes* **15**:1301-1346.
- Kimura, D. K., and J. J. Lyons. 1991. Between-reader bias and variability in the age-determination process. *Fishery Bulletin* **89**:53-60.
- Kurth, B. N., E. Peebles, and C. D. Stallings. 2019. Atlantic Tarpon (*Megalops atlanticus*) exhibit upper estuarine habitat dependence followed by foraging system fidelity after ontogenetic habitat shifts. *Estuarine Coastal and Shelf Science*.
- Leis, J. M., and B. M. Carson-Ewart. 1999. In situ swimming and settlement behaviour of larvae of an Indo-Pacific coral-reef fish, the coral trout *Plectropomus leopardus* (Pisces : Serranidae). *Marine Biology* **134**:51-64.
- Lim, L.-S., and Y. Mukai. 2014. Morphogenesis of sense organs and behavioural changes in larvae of the brown-marbled grouper *Epinephelus fuscoguttatus* (Forsskal). *Marine and Freshwater Behaviour and Physiology* **47**:313-327.
- Locker, S. D., R. A. Armstrong, T. A. Battista, J. J. Rooney, C. Sherman, and D. G. Zawada. 2010. Geomorphology of mesophotic coral ecosystems: current perspectives on morphology, distribution, and mapping strategies. *Coral Reefs* **29**:329-345.
- Lombardi-Carlson, L. 2014. Age and growth description of red grouper (*Epinephelus morio*) from the northeastern Gulf of Mexico: 1978-2013. SEDAR 42, North Charleston, SC.
- Lynnerup, N., H. Kjeldsen, S. Heegaard, C. Jacobsen, and J. Heinemeier. 2008. Radiocarbon Dating of the Human Eye Lens Crystallines Reveal Proteins without Carbon Turnover throughout Life. *Plos One* **3**.

- MacKenzie, K. M., C. N. Trueman, M. R. Palmer, A. Moore, A. T. Ibbotson, W. R. C. Beaumont, and I. C. Davidson. 2012. Stable isotopes reveal age-dependent trophic level and spatial segregation during adult marine feeding in populations of salmon. *Ices Journal of Marine Science* **69**:1637-1645.
- Mahler, B., Y. W. Chen, J. Ford, C. Thiel, G. Wistow, and Z. R. Wu. 2013. Structure and dynamics of the fish eye lens protein, gamma M7-Crystallin. *Biochemistry* **52**:3579-3587.
- Mahmoud, A., and J. Sunarso. 2018. A new graphical method to target carbon dioxide emission reductions by simultaneously aligning fuel switching, energy saving, investment cost, carbon credit, and payback time. *International Journal of Energy Research* **42**:1551-1562.
- Marancik, K. E., D. E. Richardson, J. Lyczkowski-Shultz, R. K. Cowen, and M. Konieczna. 2012. Spatial and temporal distribution of grouper larvae (Serranidae: Epinephelinae: Epinephelini) in the Gulf of Mexico and Straits of Florida. *Fishery Bulletin* **110**:1-20.
- Mayer, D. A., R. H. Weisberg, L. Y. Zheng, and Y. G. Liu. 2017. Winds on the West Florida Shelf: Regional comparisons between observations and model estimates. *Journal of Geophysical Research-Oceans* **122**:834-846.
- McCutchan, J. H., W. M. Lewis, C. Kendall, and C. C. McGrath. 2003. Variation in trophic shift for stable isotope ratios of carbon, nitrogen, and sulfur. *Oikos* **102**:378-390.
- McMahon, K. W., M. L. Fogel, B. J. Johnson, L. A. Houghton, and S. R. Thorrold. 2011. A new method to reconstruct fish diet and movement patterns from delta C-13 values in otolith amino acids. *Canadian Journal of Fisheries and Aquatic Sciences* **68**:1330-1340.
- McMahon, K. W., L. L. Hamady, and S. R. Thorrold. 2013. A review of ecogeochemistry approaches to estimating movements of marine animals. *Limnology and Oceanography* **58**:697-714.
- McMahon, K. W., and M. D. McCarthy. 2016. Embracing variability in amino acid delta N-15 fractionation: mechanisms, implications, and applications for trophic ecology. *Ecosphere* **7**.
- McMahon, K. W., S. R. Thorrold, T. S. Elsdon, and M. D. McCarthy. 2015. Trophic discrimination of nitrogen stable isotopes in amino acids varies with diet quality in a marine fish. *Limnology and Oceanography* **60**:1076-1087.
- McMeans, B. C., T. Kadoya, T. K. Pool, G. W. Holtgrieve, S. Lek, H. Kong, K. Winemiller, V. Elliot, N. Rooney, P. Laffaille, and K. S. McCain. 2019. Consumer trophic positions respond variably to seasonally fluctuating environments. *Ecology*:1-10.
- Meath, B., E. B. Peebles, B. A. Seibel, and H. Judkins. 2019. Stable isotopes in the eye lenses of *Doryteuthis plei* (Blainville 1823): exploring natal origins and migratory patterns in the eastern Gulf of Mexico. *Continental Shelf Research*.
- Moe, M. A. J. 1969. Biology of the Red grouper *Epinephelus morio* from the eastern Gulf of Mexico. Pages 1-95 Florida Department of Natural Resources Marine Research Laboratory Professional Papers Series. Fish and Wildlife Research Institute, St. Petersburg, FL.
- Nicol, J. A. C. 1989. The eyes of fishes. Clarendon, Oxford, England.
- Nielsen, J., R. B. Hedeholm, J. Heinemeier, P. G. Bushnell, J. S. Christiansen, C. B. Ramsey, R. W. Brill, M. Simon, K. F. Steffensen, and J. F. Steffensen. 2016. Eye lens radiocarbon reveals centuries of longevity in the Greenland shark (*Somniosus microcephalus*). *Science* **353**:702-704.

- Oksanen, J., F. G. Blanchet, M. Friendly, R. Kindt, P. Legendre, D. McGlinn, P. R. Minchin, R. B. O'Hara, G. L. Simpson, P. Solymos, M. H. H. Stevens, E. Szoecs, and H. Wagner. 2019. Vegan: community ecology package. R package version 2.5-4.
- Park, J.-M., J.-K. Cho, K.-H. Han, N.-r. Kim, H.-K. Hwang, K.-M. Kim, J.-I. Myeong, and M.-H. Son. 2014. Early life history of the Sevenband Grouper, *Epinephelus septemfasciatus* from Korea. *Development and Reproduction* **18**:13-23.
- Peebles, E. B., and D. J. Hollander. 2020. Combining Isoscapes with Tissue-Specific Isotope Records to Recreate the Geographic Histories of Fish. Pages 203-218 in S. A. Murawski, C. H. Ainsworth, S. Gilbert, D. J. Hollander, C. B. Paris, M. Schlüter, and D. L. Wetzel, editors. *Scenarios and Responses to Future Deep Oil Spills*. Springer, Cham, Switzerland.
- Pepin, P., and R. A. Myers. 1991. Significance of egg and larval size to recruitment variability of temperate marine fish. *Canadian Journal of Fisheries and Aquatic Sciences* **48**:1820-1828.
- Post, D. M. 2002. Using stable isotopes to estimate trophic position: Models, methods, and assumptions. *Ecology* **83**:703-718.
- Powell, A. B., and J. W. Tucker. 1992. Egg and larval development of laboratory-reared Nassau Grouper, *Epinephelus striatus* (Pisces Serranidae). *Bulletin of Marine Science* **50**:171-185.
- Quaek-Davies, K., V. A. Bendall, K. M. MacKenzie, S. Hetherington, J. Newton, and C. N. Trueman. 2018. Teleost and elasmobranch eye lenses as a target for life-history stable isotope analyses. *Peerj* **6**:26.
- Quaek, K. 2017. Stable isotope analysis of fish eye lenses: reconstruction of ontogenetic trends in spatial and trophic ecology of elasmobranchs and deep water teleosts. University of Southampton, Southampton, England.
- R Core Team. 2018. R: A language and environment for statistical computing. R Foundation for Statistical Computing, Vienna, Austria.
- Radabaugh, K. R., D. J. Hollander, and E. B. Peebles. 2013. Seasonal delta C-13 and delta N-15 isoscapes of fish populations along a continental shelf trophic gradient. *Continental Shelf Research* **68**:112-122.
- Radabaugh, K. R., E. M. Malkin, D. J. Hollander, and E. B. Peebles. 2014. Evidence for light-environment control of carbon isotope fractionation by benthic microalgal communities. *Marine Ecology Progress Series* **495**:77-90.
- Radabaugh, K. R., and E. B. Peebles. 2014. Multiple regression models of $\delta^{13}\text{C}$ and $\delta^{15}\text{N}$ for fish populations in the eastern Gulf of Mexico. *Continental Shelf Research* **84**:158-168.
- Robertson, D. R., S. E. Swearer, K. Kaufmann, and E. B. Brothers. 1999. Settlement vs. environmental dynamics in a pelagic-spawning reef fish at Caribbean Panama. *Ecological Monographs* **69**:195-218.
- Rogers, P. J., T. M. Ward, L. J. McLeay, M. Lowry, R. J. Saunders, and D. Williams. 2009. Reproductive biology of blue mackerel, *Scomber australasicus*, off southern and eastern Australia: suitability of the Daily Egg Production Method for stock assessment. *Marine and Freshwater Research* **60**:187-202.
- Salazar, G. 2019. EcolUtils: Utilities for community ecology analysis. R package version 0.1.
- Saul, S. E., J. F. Walter, III, D. J. Die, D. F. Naarc, and B. T. Donahue. 2013. Modeling the spatial distribution of commercially important reef fishes on the West Florida Shelf. *Fisheries Research* **143**:12-20.
- SEDAR. 2018. SEDAR 52: Gulf of Mexico Red Snapper. NOAA, North Charleston, SC.

- Seminoff, J. A., S. R. Benson, K. E. Arthur, T. Eguchi, P. H. Dutton, R. F. Tapilatu, and B. N. Popp. 2012. Stable isotope tracking of endangered sea turtles: validation with satellite telemetry and delta N-15 analysis of amino acids. *Plos One* **7**.
- Shi, Y. R., K. Barton, A. De Maria, J. M. Petrash, A. Shiels, and S. Bassnett. 2009. The stratified syncytium of the vertebrate lens. *Journal of Cell Science* **122**:1607-1615.
- Simpson, S. 2018. Spatial ecology and fisheries interactions of Rajidae in the UK. University of Southampton.
- Stallings, C. D., F. C. Coleman, C. C. Koenig, and D. A. Markiewicz. 2010. Energy allocation in juveniles of a warm-temperate reef fish. *Environmental Biology of Fishes* **88**:389-398.
- Stallings, C. D., J. A. Nelson, K. L. Rozar, C. S. Adams, K. R. Wall, T. S. Switzer, B. L. Winner, and D. J. Hollander. 2015. Effects of preservation methods of muscle tissue from upper-trophic level reef fishes on stable isotope values (delta C-13 and delta N-15). *PeerJ* **3**.
- Stewart, D. N., J. Lango, K. P. Nambiar, M. J. S. Falso, P. G. FitzGerald, D. M. Rocke, B. D. Hammock, and B. A. Buchholz. 2013. Carbon turnover in the water-soluble protein of the adult human lens. *Molecular Vision* **19**:463-475.
- Sturrock, A. M., C. N. Trueman, J. A. Milton, C. P. Waring, M. J. Cooper, and E. Hunter. 2014. Physiological influences can outweigh environmental signals in otolith microchemistry research. *Marine Ecology Progress Series* **500**:245-264.
- Switzer, T. S., T. C. MacDonald, R. H. McMichael, Jr., and S. F. Keenan. 2012. Recruitment of juvenile Gags in the eastern Gulf of Mexico and factors contributing to observed spatial and temporal patterns of estuarine occupancy. *Transactions of the American Fisheries Society* **141**:707-719.
- Trueman, C. N., K. M. MacKenzie, and K. S. Glew. 2017. Stable isotope-based location in a shelf sea setting: accuracy and precision are comparable to light-based location methods. *Methods in Ecology and Evolution* **8**:232-240.
- Tzadik, O. E., D. L. Jones, E. B. Peebles, C. C. Koenig, and C. D. Stallings. 2017a. The effects of spatial scale on assigning nursery habitats in Atlantic Goliath Groupers (*Epinephelus itajara*) using non-lethal analyses of fin rays. *Estuaries and Coasts* **40**:1785-1794.
- Tzadik, O. E., E. B. Peebles, and C. D. Stallings. 2017b. Life-history studies by non-lethal sampling: using microchemical constituents of fin rays as chronological recorders. *Journal of Fish Biology* **90**:611-625.
- Umezawa, Y., A. Tamaki, T. Suzuki, S. Takeuchi, C. Yoshimizu, and I. Tayasu. 2018. Phytoplankton as a principal diet for callinassid shrimp larvae in coastal waters, estimated from laboratory rearing and stable isotope analysis. *Marine Ecology Progress Series* **592**:141-158.
- Vanderklift, M. A., and S. Ponsard. 2003. Sources of variation in consumer-diet delta(15)N enrichment: a meta-analysis. *Oecologia* **136**:169-182.
- Vandersea, M. W., R. W. Litaker, K. E. Marancik, J. A. Hare, H. J. Walsh, S. Lem, M. A. West, D. M. Wyanski, E. H. Labani, and P. A. Tester. 2008. Identification of larval sea basses (*Centropristis* spp.) using ribosomal DNA-specific molecular assays. *Fishery Bulletin* **106**:183-193.
- Vihtelic, T. S. 2008. Teleost lens development and degeneration. *International Review of Cell and Molecular Biology*, Vol 269 **269**:341-373.
- Wall, C. C., B. T. Donahue, D. F. Naar, and D. A. Mann. 2011. Spatial and temporal variability of red grouper holes within Steamboat Lumps Marine Reserve, Gulf of Mexico. *Marine Ecology Progress Series* **431**:243-254.

- Wall, C. C., P. Simard, M. Lindemuth, C. Lembke, D. F. Naar, C. Hu, B. B. Barnes, F. E. Muller-Karger, and D. A. Mann. 2014. Temporal and spatial mapping of red grouper *Epinephelus morio* sound production. *Journal of Fish Biology* **85**:1470-1488.
- Wall, K. R., and C. D. Stallings. 2018. Subtropical epibenthos varies with location, reef type, and grazing intensity. *Journal of Experimental Marine Biology and Ecology* **509**:54-65.
- Wallace, A. A., D. J. Hollander, and E. B. Peebles. 2014. Stable isotopes in fish eye lenses as potential recorders of trophic and geographic history. *Plos One* **9**.
- Weaver, D. C. 1996. Feeding ecology and ecomorphology of three seabasses (Pisces: Serranidae) in the northeastern Gulf of Mexico. University of Florida, Gainesville, FL.
- Weisberg, R. H., L. Zheng, and E. B. Peebles. 2014. Gag grouper larvae pathways on the West Florida Shelf. *Continental Shelf Research* **88**:11-23.
- Wells, R. J. D., J. H. Cowan, and B. Fry. 2008. Feeding ecology of red snapper *Lutjanus campechanus* in the northern Gulf of Mexico. *Marine Ecology Progress Series* **361**:213-225.
- White, D. B., and S. M. Palmer. 2004. Age, growth and reproduction of the Red Snapper, *Lutjanus campechanus*, from the Southeastern U.S. *Bulletin of Marine Science* **75**:335-360.
- Whiteman, J. P., E. A. Elliott Smith, A. C. Besser, and S. D. Newsome. 2019. A Guide to Using Compound-Specific Stable Isotope Analysis to Study the Fates of Molecules in Organisms and Ecosystems. *Diversity* **11**:1-18.
- Winemiller, K. O., and K. A. Rose. 1993. Why do most fish produce so many tiny offspring. *American Naturalist* **142**:585-603.
- Wride, M. A. 2011. Lens fibre cell differentiation and organelle loss: many paths lead to clarity. *Philosophical Transactions of the Royal Society B-Biological Sciences* **366**:1219-1233.
- Zhang, J. Y., A. Fujiwara, and J. Sawara. 2006. Multidimensional timing decisions: a case study in tourism behavior analysis. *Tourism Analysis* **11**:319-329.

Table 3.1. Expected isotopic outcomes (increase, decrease, or no change) of all possible combinations of three effects: geographic distribution of spawning (geographic origin), changes in trophic position (trophic growth), and movement along an isotopic gradient. Consistent effects result in consistent outcomes. Mixed effects result in variable outcomes.

Effect			
Geographic origin	Trophic growth	Movement along gradient	Isotopic Outcome
+	+	+	+
0	+	+	+
+	0	+	+
+	+	0	+
0	0	+	+
0	+	0	+
+	0	0	+
-	-	-	-
-	0	-	-
-	-	0	-
0	-	-	-
-	0	0	-
0	-	0	-
0	0	-	-
0	0	0	0
+	+	-	-, 0, +
+	-	+	-, 0, +
-	+	+	-, 0, +
+	-	-	-, 0, +
-	+	-	-, 0, +
-	-	+	-, 0, +
0	+	-	-, 0, +
0	-	+	-, 0, +
+	-	0	-, 0, +
+	0	-	-, 0, +
-	0	+	-, 0, +
-	+	0	-, 0, +

Table 3.2. Rules of interpretation for all isotopic outcomes based on known isotopic trends in fish tissue and WFS isoscape. In this context, all interpretations are based on Spearman rank correlation between the combined core isotopic values for each species and two additional measurable parameters: eye-lens diameter (ELD) and juvenile capture location. Each correlation addresses straight-line movement over some period along the $\delta^{15}\text{N}$ and $\delta^{13}\text{C}$ gradients, which are orthogonal to one another, on the northern West Florida Shelf.

-
1. $\delta^{15}\text{N}$ correlation with ELD (among individuals within a species)
 - 1A. If $\delta^{15}\text{N}$ negatively correlates with ELD,
then species decreases trophic position or moves against $\delta^{15}\text{N}$ gradient before settlement.
 - 1B. If $\delta^{15}\text{N}$ positively correlates with ELD,
then species increases trophic position or moves along $\delta^{15}\text{N}$ gradient before settlement.
 - 1C. If $\delta^{15}\text{N}$ does not correlate with ELD,
then no trophic growth or movement along $\delta^{15}\text{N}$ gradient occurred before settlement.
 2. $\delta^{15}\text{N}$ correlation with collection latitude (among individuals within a species)
 - 2A. If $\delta^{15}\text{N}$ negatively correlates with juvenile collection latitude,
then individuals spawned farthest south settle farthest north (and vice versa).
 - 2B. If $\delta^{15}\text{N}$ positively correlates with juvenile collection latitude,
then individuals spawned farthest north settle farthest north (and vice versa).
 - 2C. If $\delta^{15}\text{N}$ does not correlate with juvenile collection latitude,
then spawning location does not affect juvenile location in the north-south direction.
 3. $\delta^{13}\text{C}$ correlation with ELD (among individuals within species)
 - 3A. If $\delta^{13}\text{C}$ negatively correlates with ELD,
then species switches from benthic to planktonic basal resource or moves offshore.
 - 3B. If $\delta^{13}\text{C}$ positively correlates with ELD,
then species switches from planktonic to benthic basal resource or moves inshore.
 - 3C. If $\delta^{13}\text{C}$ does not correlate with ELD,
then no change in basal resource use or inshore-offshore movement occurs.
 4. $\delta^{13}\text{C}$ correlation with collection longitude (among individuals within a species)
 - 4A. If $\delta^{13}\text{C}$ negatively correlates with collection longitude,
then individuals spawned farthest offshore settle farthest inshore (and vice versa).
 - 4B. If $\delta^{13}\text{C}$ positively correlates with collection longitude,
then individuals spawned farthest inshore settle farthest inshore (and vice versa).
 - 4C. If $\delta^{13}\text{C}$ does not correlate with juvenile collection longitude,
then spawning location does not affect juvenile location in the inshore-offshore direction.
 5. Simplifying assumptions
 - 5A. If species does not become more herbivorous prior to settlement,
then 1A can be simplified to movement against $\delta^{15}\text{N}$ gradient (southward on WFS).
 - 5B. If species does not increase trophic position prior to settlement,
then 1B can be simplified to movement along the $\delta^{15}\text{N}$ gradient (northward on WFS).
 - 5C. If a species does not switch from benthic to planktonic basal resource prior to settlement,
then 3A can be simplified to movement against $\delta^{13}\text{C}$ gradient (offshore on WFS).
 - 5D. If species does not switch from planktonic to benthic basal resource prior to settlement,
then 3B can be simplified to movement along $\delta^{13}\text{C}$ gradient (inshore on WFS).
-

Table 3.3. Capture information and regression parameters used to convert eye-lens diameters to fish length. For each of the four species number collected, collection length, collection age, total eye-lens diameter (ELD at collection) and size of analyzed eye-lens core (core ELD) are listed. Regression equation used to calculate standard length (SL) from ELD, R², slope p-value (***) is ≤ 0.001) and estimated SL at analysis. Additional information on SL (mm) and age (d) at metamorphosis from post-larval to juvenile stage are provided from literature.

	Black Seabass	Gag	Red Grouper	Red Snapper
Number collected	51	52	51	38
Collection SL (mm)	48-231	94-321	37-256	140-325
Collection age (yr)	0-3	0-2	0-2	1-3
ELD at collection (mm)	1.5-6.1	1.5-6.2	0.9-7.0	3.0-7.5
Core ELD (mm)	0.4-1.1	0.3-0.8	0.4-1.0	0.4-0.8
Regression equation	SL = 35.33*ELD	SL = 56.54*ELD	SL = (5.94*√(ELD)) ²	SL = (6.02*√(ELD)) ²
Estimated SL at analysis (mm)	15-40	18-47	14-36	15-29
Slope p-value	< 0.001	< 0.001	< 0.001	<0.001
R ²	0.98	0.96	0.99	0.99
Metamorphosis SL (mm)	11	17-25	20	21
Metamorphosis age (d)	20-35	29-52	35	30-35
Source (Metamorphosis)	Roberts et al. 1976	Fitzhugh et al. 2005	Colin et al. 1996	Drass et al. 2000 Wells et al. 2008

Table 3.4. Number of samples, minimum, maximum, range, mean, and standard error for both δ¹⁵N and δ¹³C values recorded for eye-lens cores from the four species.

Species	n	Mean ± SE (‰)	Min (‰)	Max (‰)	Range (‰)
Black Seabass (δ ¹⁵ N)	51	8.12 ± 0.20	5.31	10.97	5.65
Gag (δ ¹⁵ N)	52	7.33 ± 0.11	5.59	9.40	3.81
Red Grouper (δ ¹⁵ N)	51	7.05 ± 0.09	5.82	9.07	3.25
Red Snapper (δ ¹⁵ N)	38	7.97 ± 0.24	4.61	11.24	6.62
Black Seabass (δ ¹³ C)	51	-18.49 ± 0.20	-20.82	-14.15	6.67
Gag (δ ¹³ C)	52	-19.02 ± 0.16	-21.00	-14.93	6.07
Red Grouper (δ ¹³ C)	51	-19.26 ± 0.12	-20.65	-15.19	5.47
Red Snapper (δ ¹³ C)	38	-18.96 ± 0.14	-20.44	-16.36	4.07

Table 3.5. Spearman rank correlations between $\delta^{15}\text{N}$ and ELD or collection latitude and between $\delta^{13}\text{C}$ and ELD or collection longitude by species. Significant p -values can be interpreted as follows: * < 0.05, ** < 0.01, *** < 0.001. Isotopic Interpretations refer to Table 3.2.

	$\delta^{15}\text{N}$ vs ELD <i>Rho</i>	$\delta^{15}\text{N}$ vs collection Lat <i>Rho</i>	$\delta^{13}\text{C}$ vs ELD <i>Rho</i>	$\delta^{13}\text{C}$ vs collection Lon <i>Rho</i>	Isotopic Interpretations
Black Seabass	-0.30 *	0.37 **	0.27(n.s.)	-0.37 **	1A, 2B, 3C, 4A
Gag	-0.02 (n.s)	0.30 *	0.48 ***	-0.10 (n.s.)	1C, 2B, 3B, 4C
Red Grouper	0.54 ***	-0.12 (n.s.)	0.30 *	0.15 (n.s.)	1B, 2C, 3B, 4C
Red Snapper	0.25 (n.s.)	0.63 ***	0.06 (n.s.)	-0.31 (n.s.)	1C, 2B, 3C, 4C

Table 3.6. Pairwise SEAc proportion overlap and PERMANOVA comparisons. Proportional overlap between SEAc are not evaluated for significance. Adjusted p-values for pairwise PERMANOVA are presented as * < 0.05, ** < 0.01, *** < 0.001. Global PERMANOVA (F = 8.42, p < 0.001)

SEAc Proportion overlap				
	Black Seabass	Gag	Red Grouper	Red Snapper
Black Seabass				
Gag	0.21			
Red Grouper	0.08	0.49		
Red Snapper	0.48	0.43	0.26	
PERMANOVA Pairwise Comparisons				
	Black Seabass	Gag	Red Grouper	Red Snapper
Black Seabass				
Gag	0.072 **			
Red Grouper	0.149 ***	0.026 (0.06)		
Red Snapper	0.017 (0.22)	0.042 *	0.115 **	

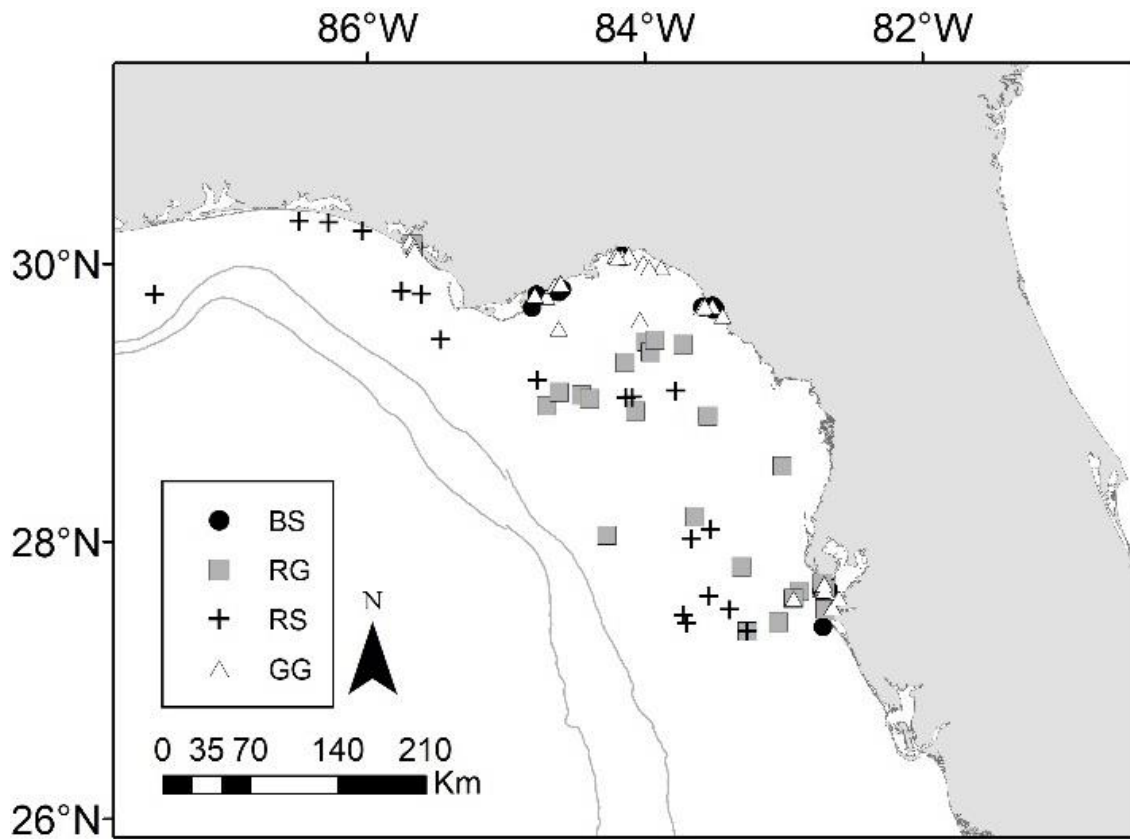


Figure 3.1. Capture locations by species. Bathymetry lines represent 100 m and 200 m depth contours. All specimens were captured between six months and 3 years of age. SL (mm) at capture were Black Seabass (BS): 48-231; Red Grouper (RG): 37-256; Red Snapper (RS): 140-325; and Gag (GG): 94-321.

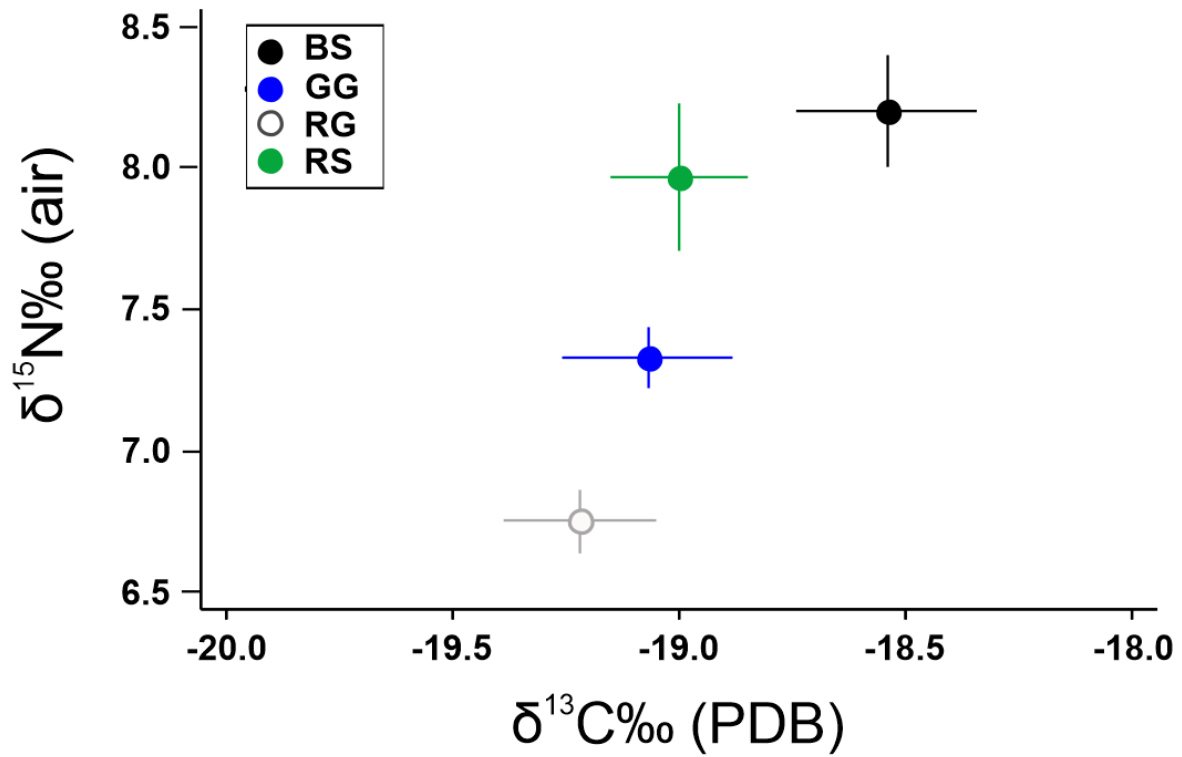


Figure 3.2. Mean (\pm SE) eye-lens core $\delta^{13}\text{C}$ and $\delta^{15}\text{N}$ values by species. Black Seabass (BS), Gag (GG), Red Grouper (RG), and Red Snapper (RS).

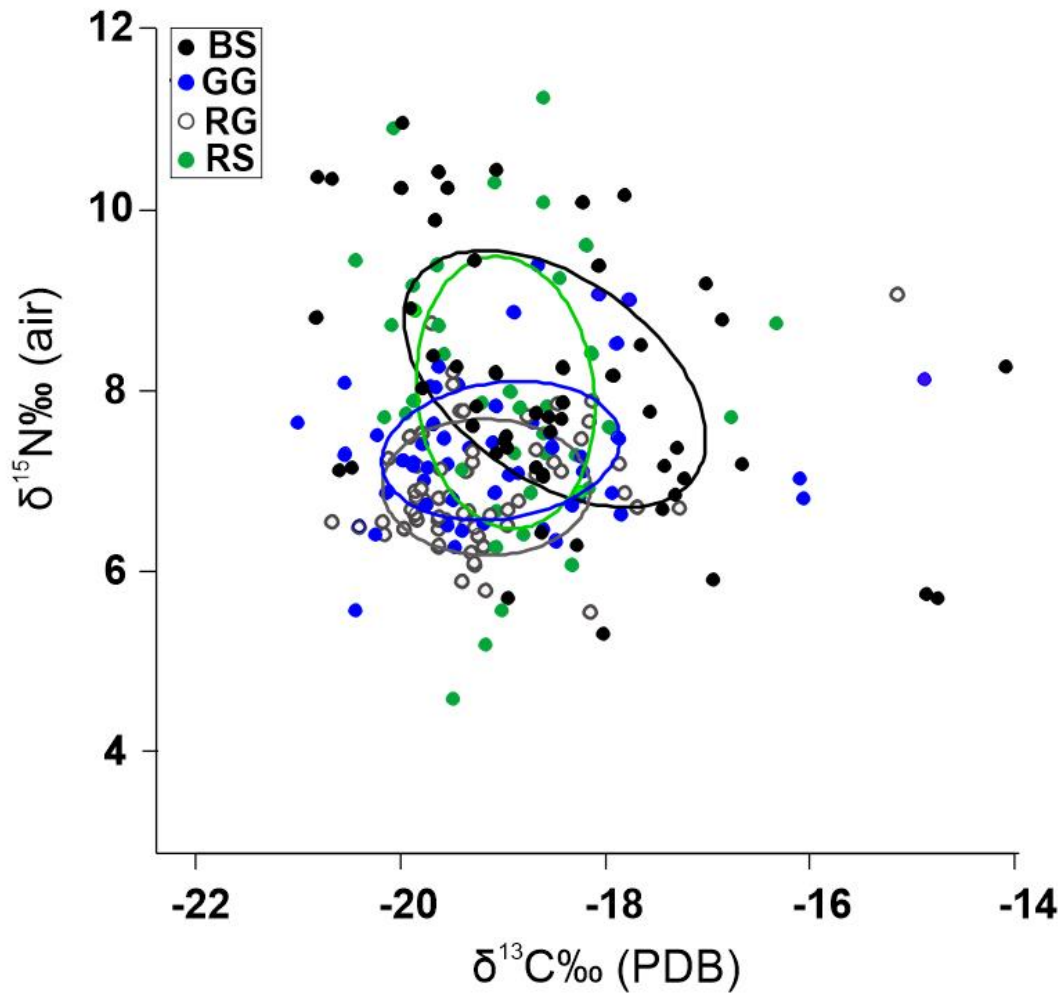


Figure 3.3. Eye-lens core $\delta^{13}\text{C}$ and $\delta^{15}\text{N}$ values by species. Each data point represents the $\delta^{15}\text{N}$ and $\delta^{13}\text{C}$ values for the core eye-lens from an individual fish. Superimposed on the scatterplot are standard ellipses containing 40% of the observations for each species (from SIBER routine in R). Species are Black Seabass (BS), Gag (GG), Red Grouper (RG), and Red Snapper (RS). Notice that scale of both x-axis and y-axis differs from Figure 2.

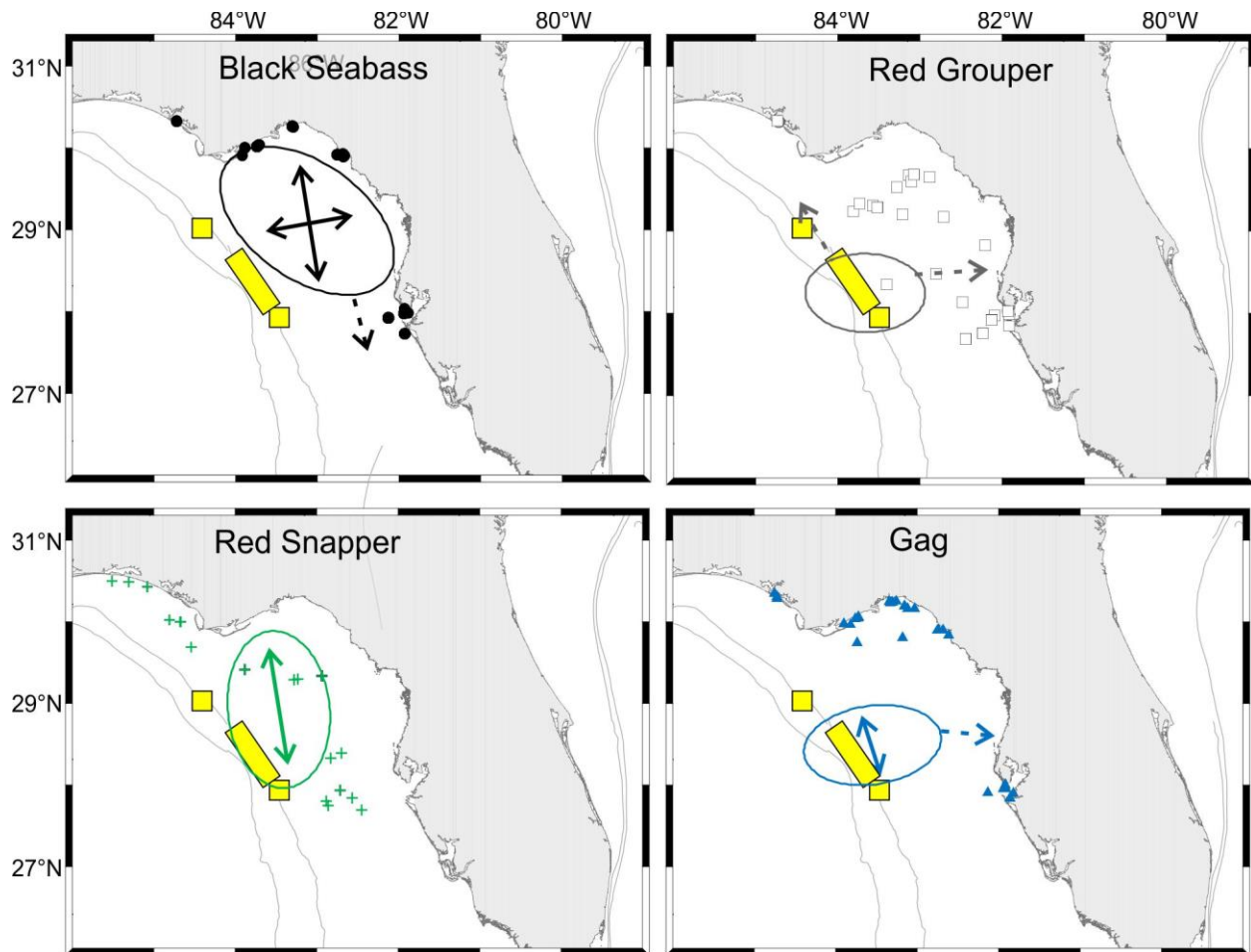


Figure 3.4. Schematic of spawning locations and profiles for each species based on the interpretations in Table 5, with differences in relative spawning locations indicated by Figure 2. Isotopic information is relative rather than geo-referenced. Ovals represent core spawning area with relative locations from Figure 2. Solid arrows represent significant relationships between core isotopic value and juvenile location. Dashed arrows represent relationship between core isotopic values and eye-lens diameter (ELD; movement over the larval/post-larval period). Individual fish icons represent general distribution of juvenile fish collections for each species.

CHAPTER 4: CHARACTERIZING LIFETIME-SCALE MOVEMENT IN MARINE FISHES:
TILEFISH ARE MODELS OF A SEDENTARY LIFE, RED GROUPEL ARE MODELS OF
CRYPTIC MOVEMENT

ABSTRACT

For various organism types, stable isotopes are used to establish trophic relationships and to detect movement. Animal-tissue isotope values typically represent discrete periods in the life of the specimen, whereas the laminar structure of the vertebrate eye lens can provide isotope records for the entire lifetime. We analyzed the $\delta^{13}\text{C}$ and $\delta^{15}\text{N}$ in sequential eye-lens laminae to provide lifetime records of trophic position and movement for two mesopredators in the eastern Gulf of Mexico, Tilefish (*Lopholatilus chamaeleonticeps*) and Red Grouper (*Epinephelus morio*). In Tilefish, which are known to have very high site fidelity, both $\delta^{13}\text{C}$ and $\delta^{15}\text{N}$ increased consistently throughout life ($\Delta^{13}\text{C}$ range: 0.83 – 3.91‰; $\Delta^{15}\text{N}$ range: 2.77 – 7.41‰). In Red Grouper, which tend to move to shallower water while young, $\delta^{15}\text{N}$ increased consistently, but $\delta^{13}\text{C}$ did not ($\Delta^{13}\text{C}$ range: -1.54 – 4.75‰; $\Delta^{15}\text{N}$ range: 0.73 – 6.19‰). In Tilefish, $\delta^{13}\text{C}$ and $\delta^{15}\text{N}$ each had a strong correlation with eye-lens diameter (mean Spearman $r = 0.70$ and 0.80 respectively), and strong correlations between the two isotopes were present in all specimens (mean Spearman $r = 0.86$), reflecting trophic growth and little lifetime movement. In contrast, Red Grouper $\delta^{15}\text{N}$ also correlated strongly with eye-lens diameter (mean Spearman $r = 0.83$), but trends in $\delta^{13}\text{C}$ were irregular among individual and were consistent with movement back and

forth across the local $\delta^{13}\text{C}$ gradient; correlations between $\delta^{15}\text{N}$ and $\delta^{13}\text{C}$ were also weaker (mean Spearman $r = 0.29$). We suggest strong correlations between $\delta^{13}\text{C}$ and $\delta^{15}\text{N}$ within variable isoscapes is indicative of high site fidelity.

INTRODUCTION

Trophic position and basal resource dependence using $\delta^{15}\text{N}$ and $\delta^{13}\text{C}$

Stable isotope data are often used to construct food webs and interpret species movements for ecosystem models and management decisions (Ainsworth et al. 2015; Gruss et al. 2016). The most commonly used stable isotope values for ecological studies are $\delta^{15}\text{N}$ and $\delta^{13}\text{C}$. Analyses in a variety of terrestrial and marine systems has shown $\delta^{15}\text{N}$ to be useful as a proxy for trophic position (Post 2002; Fry 2006). Average increases in $\delta^{15}\text{N}$ across taxa are 3.4‰ per trophic level (Post 2002). In addition, larger individuals tend to have higher values of $\delta^{15}\text{N}$ than smaller ones within the same species. This phenomenon has been demonstrated using individuals of varying sizes from the same species, including Summer Flounder, *Paralichthys dentatus* (Buchheister and Latour 2011), Boreoatlantic Armhook Squid, *Gonatus fabricii* (Golikov et al. 2018) and Yellowfin Tuna, *Thunnus albacares* (Graham et al. 2007). In contrast, $\delta^{13}\text{C}$ is considered a poor indicator of trophic position, with an average trophic fractionation of 0.4-1.0‰ per trophic level (Post 2002) and high variability. However, $\delta^{13}\text{C}$ is known to be a useful indicator of basal-resource dependence. Within many aquatic ecosystems, values of $\delta^{13}\text{C}$ for benthic primary producers are higher than values of $\delta^{13}\text{C}$ for corresponding planktonic producers, with a difference of approximately 5‰ (Keough et al. 1998; Araujo et al. 2007; Ellis et al. 2014; Radabaugh et al. 2014). Thus, rapid temporal changes in the $\delta^{13}\text{C}$ of archival tissue may be interpreted as a shift in the individual's relative dependence on benthos-based vs. plankton-based

food webs. If an archival tissue displays no rapid increases or decreases in either $\delta^{13}\text{C}$ or $\delta^{15}\text{N}$ over the lifetime, but instead shows steady, coordinated increases in both isotopes, this may indicate trophic increase over the lifetime with little change in basal resource.

Fish eye-lenses as an archival tissue: physiology and isotopic conservation

During organismal growth and cell maintenance, new isotopic information is continuously incorporated into each tissue at a unique rate (Sweeting et al. 2005; Buchheister and Latour 2010; Heady and Moore 2013). White muscle, the most commonly used tissue for isotopic investigations, experiences 50% isotopic turnover within a few months in a growing fish (Hesslein et al. 1993; Guelinckx et al. 2007; Mohan et al. 2016). Liver undergoes 50% isotopic turnover within a few weeks (Hesslein et al. 1993; Logan et al. 2006; Sacramento et al. 2016), and blood plasma is faster (Heady and Moore 2013), making each tissue useful for investigation recent events, but not lifetime histories.

Internal eye-lens layers (laminae) experience little or no turnover after creation, and function as conservative recorders of the isotopic histories of individual animals (Lynnerup et al. 2008; Stewart et al. 2013; Peebles and Hollander 2020). The conservative isotopic behavior of vertebrate eye-lenses arises from the synthesis of optical proteins, called crystallins, within the laminae. Once a new lens-fiber cell is grown, the nucleus and other organelles are removed (via attenuated apoptosis) to improve optical clarity (Wride 2011). New protein synthesis within individual lens-fiber cells becomes impossible (Rinyu et al. 2019) and results in preservation of the original organic material within the successively created laminae (Nicol 1989; Lynnerup et al. 2008; Stewart et al. 2013; Nielsen et al. 2016). [See Peebles and Hollander (2020) for a thorough review of fish eye-lens physiology as related to stable isotopes].

The conservation of isotopic values has been demonstrated in fish eye-lenses several times in recent years. Nielsen et al. (2016) used radiocarbon to show extreme longevity in Greenland Sharks. Granneman (2018) conducted an isotopic diet-switch experiment using captive Red Drum (*Sciaenops ocellatus*) and documented associated isotopic shifts within the eye-lens mirroring the isotopic change in the feed. Wallace et al. (2014) Quaeck-Davies et al. (2018) and Curtis et al. (unpubl. data) have all plotted $\delta^{13}\text{C}$ and $\delta^{15}\text{N}$ to show lifetime trends in individual teleosts consistent with a combination of trophic growth and movement over time. Similar trends have been noted in both the eye-lenses (Onthank 2013; Meath et al. 2019) and beaks (Golikov et al. 2018; Queiros et al. 2018) of cephalopods, with increases in trophic position over time underlying possible movement through isotopically variable geographies. However, precise interpretations of movement through eye-lens isotope profiles have not yet been explored.

Stable isotopes and detection of movement

One factor that may add complexity the use of bulk isotopes for trophic position and basal-resource dependence is geographic variation in isotopic baselines. Whereas changes in isotope values over time may result from increasing trophic position or a change in diet, they may also arise from movement to areas with different background values. Previous work (Radabaugh and Peebles 2014) has established that trends in background $\delta^{15}\text{N}$ and $\delta^{13}\text{C}$ on the West Florida Shelf (WFS) are consistent among years, seasons, and species (Radabaugh et al. 2014; Huelster 2015), with higher $\delta^{15}\text{N}$ in the north-central Gulf of Mexico. The lowest values of $\delta^{15}\text{N}$ are on the southern end of the WFS, consistent with greater dependence on elemental nitrogen fixation by diazotrophs in oligotrophic waters (McClelland et al. 2003). Trends in $\delta^{13}\text{C}$ on the WFS are

orthogonal to those of $\delta^{15}\text{N}$ with highest background values in shallow, clear waters where benthic primary producers are more important (Radabaugh et al. 2013). Movement through these two isoscapes ($\delta^{15}\text{N}$ and $\delta^{13}\text{C}$) would tend to decouple temporal trends in $\delta^{13}\text{C}$ and $\delta^{15}\text{N}$ within the eye-lenses of an individual fish.

Tilefish and Red Grouper: demersal predators with contrasting life histories

Tilefish, *Lopholatilus chamaeleonticeps*, and Red Grouper, *Epinephelus morio*, are large, demersal predators common to the continental shelf of the eastern Gulf of Mexico. Both species play an outsized ecological role in the region. Both species dig in soft sediment (Scanlon et al. 2005; Ellis et al. 2017) and associate closely with the holes or depressions they create, including spawning nearby (Able et al. 1982; Coleman et al. 2011; Ellis 2019; Grasty et al. 2019).

However, there are notable distinctions between these two species.

Tilefish is an outer continental shelf species with a range throughout the western Atlantic Ocean from New England to Suriname. Maximum size of females and males is 95 cm fork length (FL) and 112 cm FL respectively, with maximum age in the Gulf of Mexico confirmed by lead-radium dating to 26 years (Turner et al. 1983; Lombardi-Carlson and Andrews 2015). Gulf of Mexico Tilefish may be protogynous hermaphrodites, but unequivocal evidence is lacking, and the species is considered to be gonochoristic throughout its range (Erickson and Grossman 1986; SEDAR 2011). Juvenile Tilefish consume primarily benthic organisms such as crustaceans, mollusks, and echinoderms (Steimle et al. 1999). Adult Tilefish consume primarily crustaceans and demersal fishes (Able et al. 1982; Grimes et al. 1986a).

Tilefish create and maintain vertical burrows in clay sediments (Grossman et al. 1985; Grimes et al. 1986b; Able et al. 1987). In the Gulf of Mexico, this substrate is present at depths

between approximately 225 and 425 m (Nelson and Carpenter 1968; Balsam and Beeson 2003). Juvenile Tilefish reared in the lab have been observed to settle to the bottom and begin to dig in sediment by 1.5 cm SL (Fahay 1983). In the wild, juveniles have been observed sharing burrows of other benthic modifiers such as crabs (Able et al. 1982). The shaft-like burrows are excavated by movement of the fins and body (Able et al. 1982). Observations of adult Tilefish behavior suggest they usually associate directly with burrows but may forage away from them along the sea floor. Able et al. (1982) showed that smaller fish were associated with smaller burrows, suggesting that the fish continue to excavate the same burrow over the lifetime. Exceptionally high site fidelity is a key behavioral characteristic that helps to constrain the interpretation of stable isotope data for this species. Tilefish appear to move very little during life (Able et al. 1982; Grimes 1983; Grimes et al. 1986a; Fisher et al. 2014). Because this species rarely consumes migratory prey, profiles of both $\delta^{13}\text{C}$ and $\delta^{15}\text{N}$ should reflect local conditions at a single location throughout the lifespan.

Red Grouper is also a large, demersal predator. The species inhabits continental shelf waters from North Carolina to southern Brazil (Heemstra and Randall 1993) with the center of abundance being the WFS (Moe 1969; Gruss et al. 2017). Red Grouper is a known protogynous hermaphrodite. Individuals first mature as female (50% maturity by 2.8 y and 29.2 cm FL) and may become male around age 5-7 y (SEDAR 2015). The largest and oldest Red Grouper recorded in the eastern Gulf of Mexico were > 90 cm FL and > 27 years of age (SEDAR 2015). However, with a legal harvest limit of approximately 50 cm FL, individuals > 70 cm FL are rare (SEDAR 2015). Juvenile Red Grouper diets are composed almost exclusively of invertebrates, primarily crabs and stomatopods (Brule and Canche 1993; Weaver 1996). As the fish grow, the

fish becomes more piscivorous with almost 50% of the diet being composed of fish in the adult stage (Weaver 1996).

Red Grouper spawning occurs in small groups spread across the middle to outer continental shelf (Coleman et al. 1996; Gruss et al. 2017), where adults maintain depressions in soft sediment (Coleman et al. 2010; Wall et al. 2011; Gratsy et al. 2019). These depressions are thought to be used as the spawning locations (Wall et al. 2014) and have been shown to persist for over 11 years (Gratsy et al. 2019). Juvenile Red Grouper are found on the inner continental shelf (< 30 m depth) where they use rocky reef habitats (Bullock and Smith 1991). Newly settled individuals are aggressive and territorial toward conspecifics (Colin and Koenig 1996). Individuals younger than two years of age are rare in fisheries surveys, suggesting that the smallest individuals are spread at low density across the WFS (Moe 1969), and are unavailable to most sampling gears due to their use of continuous reef habitat.

Both acoustic and conventional tagging studies indicate most Red Grouper on the middle and outer continental shelf do not move over a one to two year period (Burns and Froeschke 2012; Farmer and Ault 2014). However, recaptures of individuals that did move were in deeper water than original tagging (Moe 1969; Burns 2009; Saul et al. 2012). Based on these data and the relationship between size and capture depth, it is clear that Red Grouper use different habitats throughout the lifespan (Moe 1969; Johnson and Collins 1994; Gruss et al. 2017).

Potential as a model species

The idea of a single species or a small group of species serving as models for life history and autecology has been used in the context of stable isotopes in a variety of settings. For example, estimating the photosynthetic plasticity of CAM plants (Holtum and Winter 2014), describing energy pathways for juvenile insects (Tallamy and Pesek 1996), and investigating

climate-change effects on aestivating fishes in freshwater pools (Ogston et al. 2016) are a few of the areas which have used this approach. Once a particular autecological characteristic has been identified using other methods, the isotopic patterns associated with that characteristic can be used as a reference. Taxa with similar isotopic patterns to the model species can then be considered to have the same characteristic as the model species.

Objectives

Here we use $\delta^{13}\text{C}$ and $\delta^{15}\text{N}$ stable isotopes profiles of Tilefish and Red Grouper eye lenses as models of two distinct life history strategies undertaken by two benthos-modifying predators in the eastern Gulf of Mexico. We compare the isotopic histories of burrow-inhabiting Tilefish, which are known to have lifelong site fidelity with Red Grouper, which seem to move long distances over the lifetime. We suggest that Tilefish $\delta^{13}\text{C}$ and $\delta^{15}\text{N}$ records are tightly coupled throughout life because they reflect only trophic growth (increases in trophic position), whereas those of Red Grouper are decoupled by movement within the orthogonal $\delta^{15}\text{N}$ and $\delta^{13}\text{C}$ trends of the WFS (Radabaugh et al. 2013, Radbaugh and Peebles 2014).

MATERIALS AND METHODS

Material collection and preparation

We obtained 36 adult Tilefish *Lopholatilus chamaeleonticeps* and 30 Red Grouper *Epinephelus morio* from reef-fish monitoring efforts conducted by NOAA Fisheries, Florida Fish and Wildlife Research Institute (Eldridge 1988), and University of South Florida (Murawski et al. 2018). Tilefish were collected from the north-central Gulf of Mexico in water depths from 178 to 375 m. Red Grouper were collected from the WFS in water depths ranging from 10 to 40 m (Figure 1). Fish were measured (cm FL) and dissected at sea. All specimens were beyond the

length at 50% maturity (32.4 mm FL for Tilefish (SEDAR 2011) and 29.2 mm FL for Red Grouper (SEDAR 2015)). Otoliths were collected and cleaned of tissue. Whole eyes were wrapped in aluminum foil, placed in plastic bags, and frozen at -20°C until analysis (Stallings et al. 2015).

Prior to isotope analysis, we dissected and processed eye-lenses according to Wallace et al. (2014). We thawed whole eyes individually and removed the lens from the capsule. We placed each lens on a glass petri dish and measured eye-lens diameter (ELD) under a dissecting stereomicroscope using an ocular micrometer (nearest 0.05 mm). We delaminated each lens using two fine-tipped forceps and recoded ELD after each lamina removal. The lens core (< 1 mm diameter) was the final tissue in the analyzed series. Whereas deionized water was used sparingly for Tilefish eye-lens delamination Red Grouper eye-lenses were submerged in water for delamination. The two methods have been shown to result in comparable isotopic values (Meath et al. 2019). We individually identified each lamina based on the diametric midpoint. Individual lamina material became desiccated in <1 h at 25 °C, and we sealed each one into an individual container until isotopic analysis.

Sagittal otoliths were aged by counting annuli under transmitted light microscopy. Tilefish otoliths were thin-sectioned, attached to a microscope slide, and annuli were counted using the methods outlined by Lombardi et al. (2015). Red Grouper otoliths were aged whole after the methods of Johnson and Collins (1994).

Isotope analysis

We weighed 200-600 µg of eye-lens material representing a single lamina to the nearest µg on a Mettler-Toledo precision microbalance. We used a Carlo-Erba NA2500 Series II

Elemental Analyzer (EA) combustion furnace coupled to a continuous-flow ThermoFinnigan Delta+XL isotope ratio mass spectrometer (IRMS) to measure $^{13}\text{C}/^{12}\text{C}$ and $^{15}\text{N}/^{14}\text{N}$ and C:N in duplicate at the University of South Florida College of Marine Science in St. Petersburg, Florida. The lower limit of quantification was 12 μg for both $\delta^{13}\text{C}$ and $\delta^{15}\text{N}$. Calibration standards were NIST 8573 and NIST 8574 L-glutamic acid standard reference materials. Analytical precision, obtained by replicate measurements of NIST 1577b bovine liver, was $\pm 0.20\text{‰}$ for $\delta^{13}\text{C}$ and $\pm 0.30\text{‰}$ for $\delta^{15}\text{N}$ (maximum standard deviations of $n = 300$ replicates). Results are presented in delta notation (δ , in ‰) relative to international standards Vienna Pee Dee Belemnite (VPDB) and air:

$$\delta X = \left(\frac{R_{\text{sample}}}{R_{\text{standard}}} - 1 \right) \times 1000$$

where X is either carbon or nitrogen.

Eye-lens isotope data analysis

Eye-lenses do not contain known age-marks. Therefore, we used the best-fit regression for each species to relate eye-lens lamina diameter to FL for the species. For Tilefish, we used the linear regression:

$$FL(\text{cm}) = 6.03 \times ELD (\text{mm})$$

($F = 1220$, $R^2 = 0.97$, $p < 0.001$).

For Red Grouper, we used the logarithmic regression:

$$FL (\text{cm}) = e^{(e+0.21 \times ELD)}$$

($F = 5.09.57$, $R^2 = 0.84$, $p < 0.01$).

We used routine PERMANOVA (package *vegan*: Oksanen et al. 2019) to examine whether $\delta^{13}\text{C}$ and $\delta^{15}\text{N}$ within each species differed based on catch location, depth, FL or sex.

Isotope data did not differ based on these parameters, therefore we conducted further analyses under the assumption of a single population for each species. For each species, we examined Spearman rank correlation of species FL to capture latitude and depth as a method of separating general movement of the species from trophic change. We found no correlation between FL and capture latitude or depth in either species, suggesting that each species does not reliably change location or depth as the individuals grow.

We calculated mean and standard error for the $\delta^{13}\text{C}$ and $\delta^{15}\text{N}$ of each species.

Subsequently, we used routines PERMDISPER and PERMANOVA (package vegan: Oksanen et al. 2019) to compare $\delta^{13}\text{C}$ and $\delta^{15}\text{N}$ values from the 468 individual Tilefish eye-lens laminae to and 406 Red Grouper eye-lens laminae. For each species we used non-linear regression in the form

$$\delta X = a + b \times \ln(ELD)$$

a simplified form of the growth equation, to model isotope values as a function of fish size.

Isotope interpretations: movement or trophic increase

We used a series of correlations to segregate the influence of trophic increase and movement on the eye-lens isotope values. First, we listed all possible isotopic outcomes from the two inputs (geographic movement and trophic growth: Table 4.1). Next, we used known isotopic trends to construct interpretations for each $\delta^{13}\text{C}$ or $\delta^{15}\text{N}$ eye-lens profile (Table 4.2). We then used a series of Spearman rank correlations (r_s) to identify the likely trophic and geographic histories of each fish (Tables 4.4 and 4.5).

- 1) We correlated $\delta^{15}\text{N}$ with ELD in each individual eye-lens profile to investigate whether the individual had experienced trophic change or movement along the $\delta^{15}\text{N}$ gradient over the lifetime (Fry 2006; Radabaugh and Peebles 2014).
- 2) We correlated $\delta^{13}\text{C}$ with ELD in each individual eye-lens profile to investigate whether individuals had moved along the $\delta^{13}\text{C}$ or changed basal resource over the lifetime (Fry and Wainright 1991; Radabaugh and Peebles 2014).
- 3) We correlated $\delta^{13}\text{C}$ to $\delta^{15}\text{N}$ within each individual to investigate degree of consistency between the two isotopic values.

Individuals with a strong correlation in all three tests were interpreted as having experienced trophic growth with little to no geographic movement, eliminating one of two possible interpretations for the isotopic results. We acknowledge that this approach is subject to both Type I and Type II error but assumed that repetition of these statistical tests for numerous individuals would result in weight-of-evidence support.

Tilefish simulation: model species approach

We simulated a large Tilefish population using bootstrap analysis (package boot: Canty and Ripley (2017)). We first left out ~20% of the $\delta^{13}\text{C}$ and $\delta^{15}\text{N}$ pairs (seven fish: 92 eye-lens isotope data points) from the full dataset. Using the remaining 376 data points, we randomly selected between 8 and 19 data points (corresponding to the total range of laminae per individual) and calculated r_s between $\delta^{13}\text{C}$ and $\delta^{15}\text{N}$ for these randomly selected values to simulate a population of 1,000 Tilefish. We recorded both r_s and p-value for each of the simulated Tilefish and used the upper 95% of the distribution to represent the simulated Tilefish population. We then compared the r_s and p-values from the seven individuals left out of the

bootstrap analysis to the r_s distributions of the simulated Tilefish population to test classification success.

All fish collections and dissections were sanctioned under research collecting permits and IACUC protocols for the University of South Florida. All data were published in the Gulf of Mexico Research Initiative Information and Data Cooperative (GRIIDC) website (<https://data.gulfresearchinitiative.org/data/R1.x135.120:0012>). All data were analyzed using the R statistical environment (R Core Team 2018).

RESULTS

Tilefish *Lopholatilus chamaeleonticeps* lengths ranged from 48 to 99 cm FL, and ages ranged from 8 to 20 years with four fish unaged (Table S.1). Red Grouper *Epinephelus morio* ranged from 29.2 to 78.1 cm FL, and ages ranged from 2 to 10 years (Table S.1). Multivariate location was significantly different between the isotope values for the two species ($F = 923.56$, $R^2 = 0.49$, $p < 0.001$; Figure 2) as was multivariate dispersion ($F = 14.60$, $p < 0.001$). Tilefish mean (\pm SE) $\delta^{15}\text{N}$ was 12.97 ± 0.07 while Red Grouper mean (\pm SE) $\delta^{15}\text{N}$ was 9.46 ± 0.06 . Tilefish mean (\pm SE) $\delta^{13}\text{C}$ was -17.49 ± 0.04 while Red Grouper mean (\pm SE) $\delta^{13}\text{C}$ was -16.49 ± 0.06 .

Isotopic profiles and lifetime isotopic trends

Isotope profiles represent changes in the eye-lens $\delta^{13}\text{C}$ and $\delta^{15}\text{N}$ throughout each fish's lifetime (early juvenile to date of capture), starting with the smallest lamina (signifying the youngest time-point) and ending with the largest lamina (signifying time of capture). In each Tilefish eye-lens profile, there was an overall increase in $\delta^{13}\text{C}$ and $\delta^{15}\text{N}$ over the lifetime (Figure S.1). The range of early-life $\delta^{13}\text{C}$ values was -20.01‰ to -16.97‰ with a mean (\pm SE) of -18.90

$\pm 0.13\text{‰}$. For $\delta^{15}\text{N}$ the range of early-life values was 7.69‰ to 12.18‰ with a mean (\pm SE) of $10.21 \pm 0.18\text{‰}$. Mean (\pm SE) lifetime change in $\delta^{13}\text{C}$ was $2.50 \pm 0.12\text{‰}$ with a range from 0.83 to 3.91‰. Mean (\pm SE) lifetime change in $\delta^{15}\text{N}$ was $4.67 \pm 0.17\text{‰}$ with a range from 2.77 to 7.41‰ (Figure S.1).

Red Grouper $\delta^{15}\text{N}$ increased as the individuals age; however, many of the $\delta^{13}\text{C}$ profiles did not follow similar profiles. While $\delta^{13}\text{C}$ did increase throughout the lifetime of some individuals, visual inspection indicated that most peaked near 2 mm ELD (Figure S.2). The range of early-life $\delta^{13}\text{C}$ values was -20.15‰ to -15.62‰ with a mean (\pm SE) of $-18.63 \pm 0.18\text{‰}$. For $\delta^{15}\text{N}$ the range of early-life values was 5.57 to 8.48‰ with a mean (\pm SE) value of $7.13 \pm 0.13\text{‰}$. Mean (\pm SE) lifetime change in $\delta^{13}\text{C}$ was $1.93 \pm 0.22\text{‰}$ but ranged from -0.64‰ to 4.75‰. Mean (\pm SE) lifetime change in $\delta^{15}\text{N}$ was $3.60 \pm 0.20\text{‰}$ with a range of 0.73‰ to 6.19‰ (Figure S.2). For both Red Grouper and Tilefish, $\delta^{13}\text{C}$ and $\delta^{15}\text{N}$ isotopes showed positive, logarithmic relationships with ELD. However, fit was poor for $\delta^{13}\text{C}$ in Red Grouper ($R^2 = 0.12$), which may have been due to the early-life peak (Table 3, Figure 3d).

Correlations between isotopes

Tilefish Spearman rank correlation values (r_s) comparing $\delta^{15}\text{N}$ and ELD for all individuals combined was 0.80 ($p < 0.001$) with individual values ranging from 0.62 to 0.99 (Table S.1). Spearman rank correlations values comparing $\delta^{13}\text{C}$ to ELD for all Tilefish combined was $r_s = 0.70$ with individual values ranging from 0.61 to 0.97. A similar pattern was observed in $\delta^{15}\text{N}$ for all Red Grouper combined with r_s values between $\delta^{15}\text{N}$ and ELD of 0.75 ($p < 0.001$), with individuals ranging from $r_s = 0.23$ to $r_s = 1.0$. For all Red Grouper combined, the

correlation between $\delta^{13}\text{C}$ and ELD was 0.29 with a range from $r_s = -0.74$ to $r_s = 0.93$. The correlations were positive and significant for only 10 of 30 individuals (Table S.2).

For all Tilefish eye-lenses combined, $r_s = 0.86$ ($p < 0.001$) between $\delta^{13}\text{C}$ and $\delta^{15}\text{N}$. Values of r_s ranged from 0.56 to 0.99 (Table S.1). Both isotope values increased consistently, and all appeared to have similar slopes when examined visually (Figure S.3). Red Grouper correlations between $\delta^{13}\text{C}$ and $\delta^{15}\text{N}$ were substantially more variable among individuals. Overall r_s values for all individuals combined was -0.007 ($p = 0.87$) with a range from -0.39 ($p = 0.17$) to 0.86 ($p < 0.05$) (Table S.2). Profiles of $\delta^{15}\text{N}$ vs. $\delta^{13}\text{C}$ for each individual were highly variable in both slope and direction (Figure S.4).

Interpreting isotopic profiles as trophic growth and movement

Using the interpretation rules conceptualized in Tables 1 and 2, we listed our interpretations of the ecological history of each individual Tilefish and Red Grouper (Tables S.1 and S.2). We inferred that 35 of 36 Tilefish increased trophic position over the lifetime while remaining in the same location and feeding within the same basal resource regime. Only the smallest Tilefish was suspected of change in basal resource dependence. We inferred that five Red Grouper increased trophic position while remaining stationary and continuing to feed on the same basal resource. All other individuals were interpreted as moving substantial distances across the isotopic gradients and/or changing basal resources over the lifetime.

Tilefish simulation: model species approach

By simulating a population of 1,000 “Tilefish” using the $\delta^{13}\text{C}/\delta^{15}\text{N}$ point data, we created a robust population representing many possible relationships between $\delta^{13}\text{C}$ and $\delta^{15}\text{N}$

Tilefish eye-lenses (Figure 4). The upper 95% of the distribution was $r_s > 0.59$ (< 0.01). Comparing r_s values for the seven reserved fish to this distribution, we found that all reserved fish fit within the distribution, indicating a 100% classification success rate. Comparing the r_s values for collected Red Grouper to the simulated population, we found that the five individuals previously classified as stationary could not be distinguished from the Tilefish population. The remainder were outside the bounds of the r_s values for the simulated population.

DISCUSSION

We developed a novel approach for interpreting trophic increase and movement using eye-lens isotope profiles, adding power to a valuable archival record within fish tissues. We then used these isotopic interpretations to demonstrate difference in the trophic and movement histories of Tilefish *Lopholatilus chamaeleonticeps* and Red Grouper *Epinephelus morio* over the lifetime, two species with similar adult behavior in the eastern Gulf of Mexico (Coleman and Williams 2002). The strong correlations between isotopes and ELD and between $\delta^{13}\text{C}$ and $\delta^{15}\text{N}$ within an individual Tilefish eye lens, indicated that these fish remain stationary while increasing their trophic position with growth. Whereas most Red Grouper increased in trophic position over the lifetime, most individuals showed no correlation between $\delta^{13}\text{C}$ and ELD or between $\delta^{13}\text{C}$ and $\delta^{15}\text{N}$, suggesting basal resource changes via diet shifts and/or movement across isotopic gradients. These eye-lens isotope interpretations are consistent with decades of biological data in both species. We suggest using strong correlation between $\delta^{13}\text{C}$ and $\delta^{15}\text{N}$ as an indicator of high site fidelity and consistent basal resource dependence in species with little historical data. Species for which correlation is weak between the isotopes should be further investigated for movement or changes in basal resource dependence.

Development of an interpretation matrix

In order to enhance the value of eye-lens stable isotope data (Wallace et al. 2014; Meath et al. 2019; Simpson et al. 2019), we developed an interpretation approach using the trend in isotopic values with trophic position and geography. We segregated the potential effects of trophic change and movement on fish eye-lens isotope values and recombined them to simulate all possible isotopic outcomes (Table 4.1). We then continued the thought experiment to include all possible correlations between isotope values and fish size. We chose Spearman rank correlation because of the less stringent assumptions (Sokal and Rohlf 1994). When $\delta^{15}\text{N}$ and $\delta^{13}\text{C}$ are tested against ELD (proxy for individual size), a significant correlation could be interpreted as a change in trophic position (Fry 2006) or movement to an area with different isotope baseline values (Radabaugh and Peebles 2014; Lorrain et al. 2015). These multiple interpretations are difficult to segregate without additional biological or chemical information. Therefore, we used the correlation between $\delta^{15}\text{N}$ and $\delta^{13}\text{C}$ within the individual to segregate movement from trophic interpretations. A significant positive correlation between $\delta^{13}\text{C}$ and $\delta^{15}\text{N}$ indicates that the fish remained stationary while increasing in trophic position due to the orthogonal nature of the isoscapes within the WFS system (Fry et al. 2003; Radabaugh and Peebles 2014). By growing and eating within a confined region, both isotopes increase consistently (Buchheister and Latour 2011; Acosta-Pachon et al. 2015; Vane et al. 2018). A non-significant correlation or a negative correlation can only result from movement or a sustained diet shift breaking the correlation between $\delta^{15}\text{N}$ and $\delta^{13}\text{C}$ with trophic increase. By creating generalizable interpretation rules and using easily accessible statistical techniques, this approach can be applied to additional species, especially those with limited biological data.

Geographic differences and trends in $\delta^{15}\text{N}$

Mean values and overall distributions of both isotopes differed between Red Grouper and Tilefish over the lifetime (Figure 2). Differences in observed isotopic values between species follow the isotopic trends in $\delta^{13}\text{C}$ and $\delta^{15}\text{N}$ isoscape for the eastern Gulf of Mexico (Radabaugh and Peebles 2014), reflecting the areas in which each species is typically found. Red Grouper occur in patchy reef habitats of the WFS (Moe 1969; Coleman et al. 2010), usually in waters less than 100 m depth (SEDAR 2015). All Red Grouper in this study collected in 10 to 40 m (Figure 4.1), which was reflected in the wide range of eye-lens $\delta^{13}\text{C}$ values and lower values of $\delta^{15}\text{N}$. Tilefish in the Gulf of Mexico inhabit a narrow geographic range with a steep depth gradient (Steimle et al. 1999; Pierdomenico et al. 2015). All Tilefish in this study were collected in 178 to 375 m depth with a wide east – west distribution (Figure 4.1). Within the WFS isoscape, this area is represented by high values of background $\delta^{15}\text{N}$ and low $\delta^{13}\text{C}$ reflecting the planktonic dependence of all fish in these deep water habitats (Radabaugh and Peebles 2014) .

Eye-lens $\delta^{15}\text{N}$ values increased with length in both species (Figures 4.7 and 4.8). Spearman rank correlations corroborated this result in all 36 Tilefish and 27 of 30 Red Grouper (Tables 4.4 and 4.5). We observed the lowest $\delta^{15}\text{N}$ values during the earliest phases of exogenous feeding in both species, consistent with all previous eye-lens work (Wallace et al. 2014; Quaeck 2017; Simpson 2018; Meath et al. 2019). Values of $\delta^{15}\text{N}$ in each species fit well to a logarithmic function of ELD (Table 4.3, Figure 4.3), with isotope values increasing at a faster rate during early life, similar to trends seen in fish body length (Juanes 2016). Hussey et al. (2014) demonstrated mathematically that as trophic position increases, differences between $\delta^{15}\text{N}$ values of predators and prey become smaller. The curvilinear trend in $\delta^{15}\text{N}$ profiles for both species in our study suggest that this trend may occur within an individual as it grows. Highest

rates of $\delta^{15}\text{N}$ increase occurred when individuals were small and feeding at a low trophic position. Change in $\delta^{15}\text{N}$ slowed considerably in both species toward the outer edge of the eye-lens, suggesting that most individuals were likely continuing to increase in trophic position, but fractionation was decreasing with increasing trophic position.

Red Grouper move throughout the lifetime

Three Red Grouper (10%) showed no significant correlation between $\delta^{15}\text{N}$ and ELD, suggesting that either some individuals do not increase in trophic position or move in a direction that negates the increase in $\delta^{15}\text{N}$ expected through trophic growth (southward on the WFS). Whereas it is possible that a fish could continue growing while consuming sub-optimal resources, growth would slow and the fish's condition would be low (Peebles 2002). However, all Red Grouper with this pattern were above mean length at age (SEDAR 2015). A more likely explanation is that each of these individuals moved against the $\delta^{15}\text{N}$ gradient. Whereas tagging studies have shown that substantial movement is uncommon for adult Red Grouper over a one to two-year time period (Burns and Froeschke 2012), several individual Red Grouper have been demonstrated to move 50 km and more southward, a large enough distance to negate $\delta^{15}\text{N}$ increase from trophic growth over the same period (Burns 2009).

Red Grouper $\delta^{13}\text{C}$ was not well modeled using a logarithmic relationship to ELD (Table 4.3, Figure 4.3). In addition, $\delta^{13}\text{C}$ did not correlate significantly with ELD in most individuals. Many of the non-significant relationships were due to peaks in $\delta^{13}\text{C}$ in early life, potentially revealing ontogenetic changes in basal resource dependence (Keough et al. 1998; Araujo et al. 2007; Ellis et al. 2014). Red Grouper is considered a generalist predator due to its eclectic diet. Recent work indicates that generalist predators may be termed “generalist” due to substantial

dietary differences among individuals (Cobain et al. 2019). In addition, recent modeling has suggested that species-specific ontogenetic diet shifts may have substantial effects on overall ecosystem structure (Reum et al. 2019). Therefore, individuals within a “generalist” predator species, such as Red Grouper, may serve a wide variety of functions within the ecosystem throughout the lifetime.

Although no data exist on the diets of wild Red Grouper larvae, the species has been successfully reared in the lab using wild-caught copepods as prey (Powell and Tucker 1992; Colin et al. 1996; Nunn et al. 2012). Juvenile Red Grouper diet composition consists primarily of benthic invertebrates while adults incorporates a high percentage of fish as prey (Brule and Canche 1993; Weaver 1996), which may themselves utilize both benthic and planktonic trophic pathways (Vander Zanden and Vadeboncoeur 2002). Reconstructing these three phases, one might expect to see low values of $\delta^{13}\text{C}$ in early life, representing zooplankton (Burkhardt et al. 1999), a peak in $\delta^{13}\text{C}$ during the juvenile period representing a primarily benthic diet (Fry and Wainright 1991), and a subsequent decrease in $\delta^{13}\text{C}$ as adults incorporate fish prey (Davis et al. 2015). The lack of correlation between $\delta^{13}\text{C}$ and $\delta^{15}\text{N}$ within the eye-lens profiles of most Red Grouper adds to the hypothesis of basal resource changes, which may be the result of ontogenetic movement (Burns 2009; Radabaugh and Peebles 2014; Huelster 2015), diet changes (Weaver 1996), or both. If these changes can be investigated and mapped isotopically throughout the lifetime, changes in the overall ecosystem can be modeled.

Tilefish move little across isotopic gradients and are models of a sedentary life

Non-linear regression of aggregated Tilefish $\delta^{13}\text{C}$ data indicated curvilinear increase with ELD (Table 3, Figure 3), paralleling the increase in $\delta^{15}\text{N}$ for the species. Baseline $\delta^{13}\text{C}$ decreases

as depth increases away from the shoreline in the eastern Gulf of Mexico (Radabaugh and Peebles 2014). Inshore movement during the lifetime may cause an increase in $\delta^{13}\text{C}$ but would be expected to create a depth gradient in fish length, with larger fish living in shallower water. We found no correlation between Tilefish length and capture depth. In addition, no previous studies have found that Tilefish move into shallower water as they age (Grossman et al. 1985; SEDAR 2011). A more parsimonious explanation exists in trophic growth along with high site fidelity [sensu Wallace et al. (2014), Buchheister and Latour (2011)] wherein $\delta^{13}\text{C}$ and $\delta^{15}\text{N}$ both increase as the fish advance to higher trophic positions during ontogeny. One advantage of ontogenetic progression to higher trophic positions is reduced vulnerability to basal-resource instability because higher trophic position individuals are capable of incorporating a variety of resources within the diet (MacKenzie et al. 2012; Burghart et al. 2013; Dalponti et al. 2018).

Tight coupling between $\delta^{13}\text{C}$ and $\delta^{15}\text{N}$ (Table 4.4, Figure 4.2) increases the likelihood of this interpretation. If individual Tilefish had been moving in relation to either the $\delta^{13}\text{C}$ or $\delta^{15}\text{N}$ gradient for the region, correlations between the two isotopes would be low. The species is known to dig deep burrows in soft sediments, beginning soon after settlement and increasing with increasing fish size (Grimes et al. 1986a; Able et al. 1987; Scanlon et al. 2003). Snyder et al. (2019) found persistent polycyclic aromatic hydrocarbons in Tilefish tissues up to seven years after the Deepwater Horizon oil spill, suggesting that Tilefish prolong their exposure to such chemicals via a consistent association with the benthos over the lifetime. Stomach content studies indicate that Tilefish derive sustenance from the benthos throughout the lifetime (Able et al. 1982; Grimes et al. 1986b; Steimle et al. 1999). Therefore, it seems likely that stable isotopes in the Tilefish eye-lenses are reflecting a sedentary lifestyle, with a consistent trophic growth over the lifetime.

We were able to simulate the $\delta^{13}\text{C}$: $\delta^{15}\text{N}$ trend in Tilefish by using 1,000 by random draws from the overall dataset. Over 95% of the simulated isotope profiles resulted in Spearman rank correlation coefficients for $\delta^{13}\text{C}$: $\delta^{15}\text{N}$ above 0.56 ($p < 0.05$). Spearman rank correlations for $\delta^{13}\text{C}$: $\delta^{15}\text{N}$ values in all members of a reserved Tilefish test set fit within this simulated population, indicating that this simulated distribution is a suitable proxy for members of the Tilefish population. This high degree of coupling between $\delta^{13}\text{C}$ and $\delta^{15}\text{N}$ suggests that Tilefish move little once they settle to the bottom, remaining in virtually the same location, feeding within the same energy pathway.

For future researchers investigating the trophic and movement histories of fish via eye-lens isotopes, we suggest using a series of Spearman rank correlations as we demonstrated with Red Grouper. First, the population should be investigated for known ontogenetic movement in the direction of the isotopic gradient. Next, relationships between $\delta^{15}\text{N}$ and ELD as well as $\delta^{13}\text{C}$ and ELD may be investigated to infer whether the individual has undergone trophic position changes or movement along the isotopic gradient. If trophic growth can be confirmed, Spearman rank correlations between $\delta^{15}\text{N}$ and $\delta^{13}\text{C}$ may be used as an approach for investigating movement within an individual over the lifetime. If the individual fits within the bounds described by the simulated Tilefish population ($r_s \geq 0.59$), then that fish can be suspected of both high site fidelity and consistent use of a single energetic pathway throughout the lifetime. If, on the other hand, the $\delta^{15}\text{N}$ vs $\delta^{13}\text{C}$ Spearman correlation falls below this value, then the individual should be investigated further for ontogenetic habitat or diet shifts. These differing scenarios can be investigated using gut content analysis using both visual and genetic prey identification, compound specific stable isotope analyses of the eye-lenses (Wallace 2019), tagging studies, or a combination of analysis types.

LITERATURE CITED

- Able, K. W., C. B. Grimes, R. A. Cooper, and J. R. Uzmann. 1982. Burrow construction and behavior of tilefish, *Lopholatilus chamaeleonticeps*, in Hudson submarine canyon. *Environmental Biology of Fishes* **7**: 199-205.
- Able, K. W., D. C. Twichell, C. B. Grimes, and R. S. Jones. 1987. Tilefishes of the genus *Caulolatilus* construct burrows in the sea floor. *Bulletin of Marine Science* **40**: 1-10.
- Acosta-Pachon, T. A., S. Ortega-Garcia, and B. Graham. 2015. Stable carbon and nitrogen isotope values of dorsal spine age rings indicate temporal variation in the diet of striped marlin (*Kajikia audax*) in waters around Cabo San Lucas, Mexico. *Rapid Communications in Mass Spectrometry* **29**: 1676-1686.
- Ainsworth, C. H., M. J. Schirripa, and H. N. M. Luna. 2015. An ATLANTIS ecosystem model for the Gulf of Mexico supporting integrated ecosystem assessment, p. 161. *In* U. D. o. Commerce [ed.].
- Araujo, M. S., D. I. Bolnick, G. Machado, A. A. Giaretta, and S. F. dos Reis. 2007. Using delta C-13 stable isotopes to quantify individual-level diet variation. *Oecologia* **152**: 643-654.
- Balsam, W. L., and J. P. Beeson. 2003. Sea-floor sediment distribution in the Gulf of Mexico. *Deep-Sea Research Part I-Oceanographic Research Papers* **50**: 1421-1444.
- Brule, T., and L. G. R. Canche. 1993. Food habits of juvenile red groupers, *Epinephelus morio* (Valenciennes, 1828) from Campeche bank, Yucatan, Mexico. *Bulletin of Marine Science* **52**: 772-779.
- Buchheister, A., and R. J. Latour. 2010. Turnover and fractionation of carbon and nitrogen stable isotopes in tissues of a migratory coastal predator, summer flounder (*Paralichthys dentatus*). *Canadian Journal of Fisheries and Aquatic Sciences* **67**: 445-461.
- . 2011. Trophic ecology of Summer Flounder in lower Chesapeake Bay inferred from stomach content and stable isotope analyses. *Transactions of the American Fisheries Society* **140**: 1240-1254.
- Bullock, L. H., and G. B. Smith. 1991. Seabasses (Pisces: Serranidae). *Memoirs of the Hourglass Cruises* **8**: 1-243.
- Burghart, S. E., D. L. Jones, and E. B. Peebles. 2013. Variation in estuarine consumer communities along an assembled eutrophication gradient: Implications for trophic instability. *Estuaries and Coasts* **36**: 951-965.
- Burkhardt, S., U. Riebesell, and I. Zondervan. 1999. Stable carbon isotope fractionation by marine phytoplankton in response to daylength, growth rate, and CO₂ availability. *Mar. Ecol. Prog. Ser.* **184**: 31-41.
- Burns, K. 2009. Evaluation of the efficacy of the minimum size rule in the Red Grouper and Red Snapper fisheries with respect to J and circle hook mortality and barotrauma and the consequences for survival and movement. University of South Florida.
- Burns, K. M., and J. T. Froeschke. 2012. Survival of Red Grouper (*Epinephalus morio*) and red snapper (*Lutjanus campechanus*) caught on J-hooks and circle hooks in the Florida recreational and recreational-for-hire fisheries. *Bulletin of Marine Science* **88**: 633-646.
- Canty, A., and B. Ripley. 2017. *Boot: Bootstrap R (S-Plus) Functions*.
- Cobain, M. R. D., W. Steward, C. N. Trueman, and A. Jensen. 2019. Individual trophic specialization in juvenile European seabass: implications for the management of a commercially important species. *Ices Journal of Marine Science* 10.1093/icesjms/fsz045.

- Coleman, F. C., C. C. Koenig, and L. A. Collins. 1996. Reproductive styles of shallow-water groupers (Pisces: Serranidae) in the eastern Gulf of Mexico and the consequences of fishing spawning aggregations. *Environmental Biology of Fishes* **47**: 129-141.
- Coleman, F. C., C. C. Koenig, K. M. Scanlon, S. Heppell, S. Heppell, and M. W. Miller. 2010. Benthic habitat modification through excavation by red grouper, *Epinephelus morio*, in the northeastern Gulf of Mexico. *Open Fish Science Journal* **3**: 1-15.
- Coleman, F. C., K. M. Scanlon, and C. C. Koenig. 2011. Groupers on the edge: shelf edge spawning habitat in and around marine reserves of the northeastern Gulf of Mexico. *Professional Geographer* **63**: 456-474.
- Coleman, F. C., and S. L. Williams. 2002. Overexploiting marine ecosystem engineers: potential consequences for biodiversity. *Trends in Ecology & Evolution* **17**: 40-44.
- Colin, P. L., and C. Koenig. 1996. Spines in larval Red Grouper, *Epinephelus morio*: development and function. *Gulf and Caribbean Research Institute* # 44.
- Colin, P. L., C. C. Koenig, and W. A. Laroche. 1996. Development from egg to juvenile of the Red Grouper (*Epinephelus morio*) (Pisces: Serranidae) in the laboratory, p. 399-414. *In* F. ArreguinSanchez, J. L. Munro, M. C. Balgos and D. Pauly [eds.], *Biology, fisheries and culture of tropical groupers and snappers: Proceedings of an EPOMEX/ICARM International workshop on tropical snappers and groupers*. International Center for Living Aquatic Resources Management.
- Dalponti, G., R. D. Guariento, and A. Caliman. 2018. Hunting high or low: body size drives trophic position among and within marine predators. *Mar. Ecol. Prog. Ser.* **597**: 39-46.
- Davis, J. P., K. A. Pitt, B. Fry, and R. M. Connolly. 2015. Stable isotopes as tracers of residency for fish on inshore coral reefs. *Estuarine Coastal and Shelf Science* **167**: 368-376.
- Eldridge, P. J. 1988. The southeast area monitoring and assessment program (SEAMAP)- A state-federal-university program for collection, management, and dissemination of fishery-independent data and information in the southeastern United States. *Marine Fisheries Review* **50**: 29-39.
- Ellis, G. S., G. Herbert, and D. J. Hollander. 2014. Reconstructing carbon sources in a dynamic estuarine ecosystem using oyster amino acid delta C-13 values from shell and tissue. *Journal of Shellfish Research* **33**: 217-225.
- Ellis, R. 2019. Red Grouper (*Epinephelus morio*) shape faunal communities via multiple ecological pathways. *Diversity* **11**, 89.
- Ellis, R. D., F. C. Coleman, and C. C. Koenig. 2017. Effects of habitat manipulation by red grouper, *Epinephelus morio*, on faunal communities associated with excavations in Florida Bay. *Bulletin of Marine Science* **93**: 961-983.
- Erickson, D. L., and G. D. Grossman. 1986. Reproductive demography of Tilefish from the South Atlantic Bight with a test for the presence of protogynous hermaphroditism. *Transactions of the American Fisheries Society* **115**: 279-285.
- Fahay, M. P. 1983. Guide to the early stages of marine fishes occurring in the western north Atlantic Ocean, Cape Hatteras to the southern Scotian Shelf. *Journal of Northwest Atlantic Fishery Science* **4**: 493.
- Farmer, N. A., and J. S. Ault. 2014. Modeling coral reef fish home range movements in Dry Tortugas, Florida. *The Scientific World Journal* **2014**: 629791-629791.
- Fisher, J. A. D., K. T. Frank, B. Petrie, and W. C. Leggett. 2014. Life on the edge: environmental determinants of tilefish (*Lopholatilus chamaeleonticeps*) abundance since its virtual extinction in 1882. *Ices Journal of Marine Science* **71**: 2371-2378.

- Fry, B. 2006. Stable isotope ecology. Springer Science+Business Media.
- Fry, B., D. M. Baltz, M. C. Benfield, J. W. Fleeger, A. Gace, H. L. Haas, and Z. J. Quinones-Rivera. 2003. Stable isotope indicators of movement and residency for brown shrimp (*Farfantepenaeus aztecus*) in coastal Louisiana marshscapes. *Estuaries* **26**: 82-97.
- Fry, B., and S. C. Wainright. 1991. Diatom sources of C-13 rich carbon in marine food webs. *Mar. Ecol. Prog. Ser.* **76**: 149-157.
- Golikov, A. V., F. R. Ceia, R. M. Sabirov, Z. I. Zaripova, M. E. Blicher, D. V. Zakharov, and J. C. Xavier. 2018. Ontogenetic changes in stable isotope ($\delta^{13}\text{C}$ and $\delta^{15}\text{N}$) values in squid *Gonatus fabricii* (Cephalopoda) reveal its important ecological role in the Arctic. *Mar. Ecol. Prog. Ser.* **606**: 65-78.
- Graham, B. S., D. Grubbs, K. Holland, and B. N. Popp. 2007. A rapid ontogenetic shift in the diet of juvenile Yellowfin Tuna from Hawaii. *Mar. Biol.* **150**: 647-658.
- Granneman, J. E. 2018. Evaluation of trace-metal and isotopic records as techniques for tracking lifetime movement patterns in fishes. University of South Florida.
- Grasty, S., C. C. Wall, J. W. Gray, J. Brizzolara, and S. A. Murawski. 2019. Temporal persistence of Red Grouper holes and analysis of associated fish assemblages from towed camera data in the Steamboat Lumps marine protected area. *Transactions of the American Fisheries Society* 10.1002/tafs.10154: 1-9.
- Grasty, S., C. C. Wall, J. W. Gray, J. Brizzolara, and S. A. Murawski. 2019. Temporal Persistence of Red Grouper Holes and Analysis of Associated Fish Assemblages from Towed Camera Data in the Steamboat Lumps Marine Protected Area. *Transactions of the American Fisheries Society* 10.1002/tafs.10154: 1-9.
- Grimes, C. B. 1983. A technique for tagging deepwater fish. *Fishery Bulletin* **81**: 663-666.
- Grimes, C. B., K. W. Able, and R. S. Jones. 1986a. Tilefish, *Lopholatilus chamaeleonticeps*, habitat, behavior and community structure in md-Atlantic and southern New England waters. *Environmental Biology of Fishes* **15**: 273-292.
- . 1986b. Tilefish, *Lopholatilus chamaeleonticeps*, habitat, behavior and community structure in mid-Atlantic and Southern New England waters. *Environmental Biology of Fishes* **15**: 273-292.
- Grossman, G. D., M. J. Harris, and J. E. Hightower. 1985. The relationship between tilefish, *Lopholatilus chamaeleonticeps*, abundance and sediment composition off Georgia. *Fishery Bulletin* **83**: 443-447.
- Gruss, A., M. J. Schirripa, D. Chagaris, L. Velez, Y. J. Shin, P. Verley, R. Oliveros-Ramos, and C. H. Ainsworth. 2016. Estimating natural mortality rates and simulating fishing scenarios for Gulf of Mexico red grouper (*Epinephelus morio*) using the ecosystem model OSMOSE-WFS. *J. Mar. Syst.* **154**: 264-279.
- Gruss, A., J. T. Thorson, S. R. Sagarese, E. A. Babcock, M. Karnauskas, J. F. Walter, III, and M. Drexler. 2017. Ontogenetic spatial distributions of red grouper (*Epinephelus mono*) and gag grouper (*Mycteroperca microlepis*) in the US Gulf of Mexico. *Fisheries Research* **193**: 129-142.
- Guelinckx, J., J. Maes, P. Van Den Driessche, B. Geysen, F. Dehairs, and F. Ollevier. 2007. Changes in delta C-13 and delta N-15 in different tissues of juvenile Sand Goby *Pomatoschistus minutus*: a laboratory diet-switch experiment. *Mar. Ecol. Prog. Ser.* **341**: 205-215.
- Heady, W. N., and J. W. Moore. 2013. Tissue turnover and stable isotope clocks to quantify resource shifts in anadromous rainbow trout. *Oecologia* **172**: 21-34.

- Heemstra, P. C., and J. E. Randall. 1993. Groupers of the world (family Serranidae, subfamily Epinephelinae). An annotated and illustrated catalogue of the grouper, rockcod, hind, coral grouper and lyretail species known to date. FAO.
- Hesslein, R. H., K. A. Hallard, and P. Ramlal. 1993. Replacement of sulfur, carbon, and nitrogen in tissue of growing broad whitefish (*Coregonus nasus*) in response to a change in diet traced by delta-S-34, delta-C-13, and delta-N-15. *Canadian Journal of Fisheries and Aquatic Sciences* **50**: 2071-2076.
- Holtum, J. A. M., and K. Winter. 2014. Limited photosynthetic plasticity in the leaf-succulent CAM plant *Agave angustifolia* grown at different temperatures. *Funct. Plant Biol.* **41**: 843-849.
- Huelster, S. 2015. Comparison of isotope-based biomass pathways with groundfish community structure in the eastern Gulf of Mexico. Masters. University of South Florida.
- Hussey, N. E., M. A. MacNeil, B. C. McMeans and others 2014. Rescaling the trophic structure of marine food webs. *Ecol. Lett.* **17**: 239-250.
- Johnson, A. G., and L. A. Collins. 1994. Age-size structure of red grouper, (*Epinephelus morio*), from the eastern Gulf of Mexico. *Northeast Gulf Science* **13**: 101-106.
- Juanes, F. 2016. A length-based approach to predator-prey relationships in marine predators. *Canadian Journal of Fisheries and Aquatic Sciences* **73**: 677-684.
- Keough, J. R., C. A. Hagley, E. Ruzycski, and M. Sierszen. 1998. delta C-13 composition of primary producers and role of detritus in a freshwater coastal ecosystem. *Limnology and Oceanography* **43**: 734-740.
- Logan, J., H. Haas, L. Deegan, and E. Gaines. 2006. Turnover rates of nitrogen stable isotopes in the salt marsh mummichog, *Fundulus heteroclitus*, following a laboratory diet switch. *Oecologia* **147**: 391-395.
- Lombardi-Carlson, L. A., and A. H. Andrews. 2015. Age estimation and lead-radium dating of golden tilefish, *Lopholatilus chamaeleonticeps*. *Environmental Biology of Fishes* **98**: 1787-1801.
- Lorrain, A., B. S. Graham, B. N. Popp and others 2015. Nitrogen isotopic baselines and implications for estimating foraging habitat and trophic position of yellowfin tuna in the Indian and Pacific Oceans. *Deep-Sea Research Part II-Topical Studies in Oceanography* **113**: 188-198.
- Lynnerup, N., H. Kjeldsen, S. Heegaard, C. Jacobsen, and J. Heinemeier. 2008. Radiocarbon Dating of the Human Eye Lens Crystallines Reveal Proteins without Carbon Turnover throughout Life. *Plos One* **3**.
- MacKenzie, K. M., C. N. Trueman, M. R. Palmer, A. Moore, A. T. Ibbotson, W. R. C. Beaumont, and I. C. Davidson. 2012. Stable isotopes reveal age-dependent trophic level and spatial segregation during adult marine feeding in populations of salmon. *Ices Journal of Marine Science* **69**: 1637-1645.
- Meath, B., E. B. Peebles, B. A. Seibel, and H. Judkins. 2019. Stable isotopes in the eye lenses of *Doryteuthis plei* (Blainville 1823): exploring natal origins and migratory patterns in the eastern Gulf of Mexico. *Continental Shelf Research* doi.org/10.1016/j.csr.2018.12.013.
- Moe, M. A. J. 1969. Biology of the Red grouper *Epinephelus morio* from the eastern Gulf of Mexico, p. 1-95. Florida Department of Natural Resources Marine Research Laboratory Professional Papers Series. Fish and Wildlife Research Institute.

- Mohan, J. A., S. D. Smith, T. L. Connelly, E. T. Attwood, J. W. McClelland, S. Z. Herzka, and B. D. Walther. 2016. Tissue-specific isotope turnover and discrimination factors are affected by diet quality and lipid content in an omnivorous consumer. *Journal of Experimental Marine Biology and Ecology* **479**: 35-45.
- Murawski, S. A., E. B. Peebles, A. Gracia, J. W. Tunnell, and M. Armenteros. 2018. Comparative abundance, species composition, and demographics of continental shelf fish assemblages throughout the Gulf of Mexico. *Marine and Coastal Fisheries* **10**: 325-346.
- Nelson, W. R., and J. S. Carpenter. 1968. Bottom longline explorations in the Gulf of Mexico. *Commercial Fisheries Review* **30**: 57-62.
- Nicol, J. A. C. 1989. *The eyes of fishes*. Clarendon.
- Nielsen, J., R. B. Hedeholm, J. Heinemeier and others 2016. Eye lens radiocarbon reveals centuries of longevity in the Greenland shark (*Somniosus microcephalus*). *Science* **353**: 702-704.
- Nunn, A. D., L. H. Tewson, and I. G. Cowx. 2012. The foraging ecology of larval and juvenile fishes. *Reviews in Fish Biology and Fisheries* **22**: 377-408.
- Ogston, G., S. J. Beatty, D. L. Morgan, B. J. Pusey, and A. J. Lymbery. 2016. Living on burrowed time: Aestivating fishes in south-western Australia face extinction due to climate change. *Biological Conservation* **195**: 235-244.
- Onthank, K. L. 2013. Exploring the life histories of cephalopods using stable isotope analysis of an archival tissue. University of Washington.
- Peebles, E. B. 2002. Temporal resolution of biological and physical influences on bay anchovy *Anchoa mitchilli* egg abundance near a river-plume frontal zone. *Mar. Ecol. Prog. Ser.* **237**: 257-269.
- Peebles, E. B., and D. J. Hollander. 2020. Combining Isoscapes with Tissue-Specific Isotope Records to Recreate the Geographic Histories of Fish, p. 203-218. *In* S. A. Murawski et al. [eds.], *Scenarios and Responses to Future Deep Oil Spills*. Springer, Cham.
- Pierdomenico, M., V. G. Guida, L. Macelloni, F. L. Chiocci, P. A. Rona, M. I. Scranton, V. Asper, and A. Diercks. 2015. Sedimentary facies, geomorphic features and habitat distribution at the Hudson Canyon head from AUV multibeam data. *Deep-Sea Research Part II-Topical Studies in Oceanography* **121**: 112-125.
- Post, D. M. 2002. Using stable isotopes to estimate trophic position: Models, methods, and assumptions. *Ecology* **83**: 703-718.
- Powell, A. B., and J. W. Tucker. 1992. Egg and larval development of laboratory-reared Nassau Grouper, *Epinephelus striatus* (Pisces Serranidae). *Bulletin of Marine Science* **50**: 171-185.
- Quaek-Davies, K., V. A. Bendall, K. M. MacKenzie, S. Hetherington, J. Newton, and C. N. Trueman. 2018. Teleost and elasmobranch eye lenses as a target for life-history stable isotope analyses. *PeerJ* **6**: 26.
- Quaek, K. 2017. Stable isotope analysis of fish eye lenses: reconstruction of ontogenetic trends in spatial and trophic ecology of elasmobranchs and deep water teleosts. University of Southampton.
- Queiros, J. P., Y. Cherel, F. R. Ceia, A. Hilario, J. Roberts, and J. C. Xavier. 2018. Ontogenic changes in habitat and trophic ecology in the Antarctic squid *Kondakovia longimana* derived from isotopic analysis on beaks. *Polar Biol.* **41**: 2409-2421.
- R Core Team. 2018. R: A language and environment for statistical computing. R Foundation for Statistical Computing.

- Radabaugh, K. R., E. M. Malkin, D. J. Hollander, and E. B. Peebles. 2014. Evidence for light-environment control of carbon isotope fractionation by benthic microalgal communities. *Mar. Ecol. Prog. Ser.* **495**: 77-90.
- Radabaugh, K. R., and E. B. Peebles. 2014. Multiple regression models of $\delta^{13}\text{C}$ and $\delta^{15}\text{N}$ for fish populations in the eastern Gulf of Mexico. *Continental Shelf Research* **84**: 158-168.
- Reum, J. C. P., J. L. Blanchard, K. K. Holsman, K. Aydin, and A. E. Punt. 2019. Species-specific ontogenetic diet shifts attenuate trophic cascades and lengthen food chains in exploited ecosystems. *Oikos* doi.org/10.1111/oik.05630.
- Rinyu, L., R. Janovics, M. Molnar, Z. Kisvarday, and A. Kemeny-Beke. 2019. Radiocarbon map of a bomb-peak labeled human eye. *Radiocarbon* 10.1017/RDC.2019.78.
- Sacramento, P. A., G. I. Manetta, and E. Benedito. 2016. Diet-tissue discrimination factors ($\Delta\text{C-13}$ and $\Delta\text{N-15}$) and turnover rate in somatic tissues of a neotropical detritivorous fish on C-3 and C-4 diets. *Journal of Fish Biology* **89**: 213-219.
- Saul, S., D. Die, E. N. Brooks, and K. Burns. 2012. An individual-based model of ontogenetic migration in reef fish using a biased random walk. *Transactions of the American Fisheries Society* **141**: 1439-1452.
- Scanlon, K. M., F. C. Coleman, and C. C. Koenig. 2005. Pockmarks on the outer shelf in the northern Gulf of Mexico: Gas-release features or habitat modifications by fish? *Benthic Habitats and the Effects of Fishing* **41**: 301-312.
- Scanlon, K. M., C. C. Koenig, F. C. Coleman, and M. Miller. 2003. Importance of geology to fisheries management: Examples from the northeastern Gulf of Mexico, p. 95-99. *In* D. R. Stanley and A. Scarborough [eds.], *Fisheries, Reefs, and Offshore Development*. American Fisheries Society Symposium.
- SEDAR. 2011. SEDAR 22-Gulf of Mexico Tilefish, p. 467.
- . 2015. SEDAR 42 Stock Assessment Report - Gulf of Mexico Red Grouper.
- Simpson, S. 2018. Spatial ecology and fisheries interactions of Rajidae in the UK. University of Southampton.
- Simpson, S., D. Sims, and C. N. Trueman. 2019. Ontogenetic trends in resource partitioning and trophic geography of sympatric skates (Rajidae) inferred from stable isotope composition across eye lenses. *Mar. Ecol. Prog. Ser.* **624**: 103-116.
- Snyder, S. M., E. L. Pulster, and S. Murawski. 2019. Associations Between Chronic Exposure to Polycyclic Aromatic Hydrocarbons and Health Indices in Gulf of Mexico Tilefish (*Lopholatilus chamaeleonticeps*) Post Deepwater Horizon. *Environ. Toxicol. Chem.* **38**: 2659-2671.
- Sokal, R. R., and F. J. Rohlf. 1994. *Biometry: The principles and practices of statistics in biological research* third (3rd) edition.
- Stallings, C. D., J. A. Nelson, K. L. Rozar, C.S. Adams, K. R. Wall, T. S. Switzer, B. L. Winner, D. J. Hollander. 2015. Effects of preservation methods of muscle tissue from upper-trophic level reef fishes on stable isotope values ($\Delta\text{C-13}$ and $\Delta\text{N-15}$). *PeerJ* **3**: e874; DOI 10.7717/peerj.874.
- Steimle, F. W., C. A. Zetlin, P. L. Berrien, D. L. Johnson, and C. Sukwoo. 1999. Essential fish habitat source document: Tilefish, *Lopholatilus chamaeleonticeps*, life history and habitat characteristics. NOAA Technical Memorandum. National Marine Fisheries Service.
- Stewart, D. N., J. Lango, K. P. Nambiar, M. J. S. Falso, P. G. FitzGerald, D. M. Rocke, B. D. Hammock, and B. A. Buchholz. 2013. Carbon turnover in the water-soluble protein of the adult human lens. *Molecular Vision* **19**: 463-475.

- Sweeting, C. J., S. Jennings, and N. V. C. Polunin. 2005. Variance in isotopic signatures as a descriptor of tissue turnover and degree of omnivory. *Functional Ecology* **19**: 777-784.
- Tallamy, D. W., and J. D. Pesek. 1996. Carbon isotopic signatures of elytra reflect larval diet in Luperine rootworms (Coleoptera: Chrysomelidae). *Environ. Entomol.* **25**: 1167-1172.
- Turner, S. C., C. B. Grimes, and K. W. Able. 1983. Growth, mortality, and age size structure of the fisheries for tilefish, *Lopholatilus chamaeleonticeps*, in the middle Atlantic-southern New England region. *Fishery Bulletin* **81**: 751-763.
- Vander Zanden, M. J., and Y. Vadeboncoeur. 2002. Fishes as integrators of benthic and pelagic food webs in lakes. *Ecology* **83**: 2152-2161.
- Vane, K., N. J. Wallsgrove, W. Ekau, and B. N. Popp. 2018. Reconstructing lifetime nitrogen baselines and trophic position of *Cynoscion acoupa* from delta N-15 values of amino acids in otoliths. *Mar. Ecol. Prog. Ser.* **597**: 1-11.
- Wall, C. C., B. T. Donahue, D. F. Naar, and D. A. Mann. 2011. Spatial and temporal variability of red grouper holes within Steamboat Lumps Marine Reserve, Gulf of Mexico. *Mar. Ecol. Prog. Ser.* **431**: 243-254.
- Wall, C. C., P. Simard, M. Lindemuth and others 2014. Temporal and spatial mapping of red grouper *Epinephelus morio* sound production. *Journal of Fish Biology* **85**: 1470-1488.
- Wallace, A. A., D. J. Hollander, and E. B. Peebles. 2014. Stable isotopes in fish eye lenses as potential recorders of trophic and geographic history. *Plos One* **9**.
- Weaver, D. C. 1996. Feeding ecology and ecomorphology of three seabasses (Pisces: Serranidae) in the northeastern Gulf of Mexico. University of Florida.
- Wride, M. A. 2011. Lens fibre cell differentiation and organelle loss: many paths lead to clarity. *Philosophical Transactions of the Royal Society B-Biological Sciences* **366**: 1219-1233.

Table 4.1. General interpretations of bulk isotopic trends within fish eye-lenses. Bulk isotopes incorporate influences from both trophic position and location within an isoscape. Isotopic outcome is the value or trend observed in the eye-lens record. Effects are various influences on the isotopic outcome. Isotopic outcomes: (+, -, 0) positive, negative or non-significant trends in eye-lens isotope profile within an individual. Trophic change or movement along gradient: (+, -, 0) are isotopic inputs increasing, decreasing, or not changing over time. Consistent changes in trophic position and movement result in consistent outcomes. Mixed effects result in mixed outcomes.

Effect			
Trophic position	Movement along gradient		Isotopic Outcome
+	+	→	+
0	+	→	+
+	0	→	+
-	-	→	-
0	-	→	-
-	0	→	-
0	0	→	0
+	-	→	+, 0, -
-	+	→	+, 0, -

Table 4.2. General interpretations for all correlation outcomes within the eye-lens isotopic profiles of individual fishes as well as capture location as a function of length for the species. $\delta^{15}\text{N}$ and $\delta^{13}\text{C}$ are the order of $\delta^{15}\text{N}$ or $\delta^{13}\text{C}$ values over the lifetime. ELD is eye-lens diameter as measured by ocular micrometer at the diameter midpoint of the layer for which the isotopes were analyzed. In the context of this publication, correlation refers to Spearman rank correlation applied to the entire lifetime eye-lens isotopic record for an individual fish (or species if indicated). Interpretations can only be made at the level of analysis.

-
1. $\delta^{15}\text{N}$ correlation with ELD (within individuals)
 - 1A. If $\delta^{15}\text{N}$ negatively correlates with ELD,
 - then individual reduced trophic position or moved against $\delta^{15}\text{N}$ gradient.
 - 1B. If $\delta^{15}\text{N}$ positively correlates with ELD,
 - then individual increased trophic position or moved along $\delta^{15}\text{N}$ gradient.
 - 1C. If $\delta^{15}\text{N}$ does not significantly correlate with ELD,
 - then trophic position or movement along $\delta^{15}\text{N}$ gradient during life were inconsistent.
 2. $\delta^{13}\text{C}$ correlation with ELD (within individuals)
 - 2A. If $\delta^{13}\text{C}$ negatively correlates with ELD,
 - Then individual reduced trophic position or moved against $\delta^{13}\text{C}$ gradient.
 - 2B. If $\delta^{13}\text{C}$ positively correlates with ELD,
 - then individual increased trophic position or moved along $\delta^{13}\text{C}$ gradient.
 - 2C. If $\delta^{13}\text{C}$ does not significantly correlate with ELD,
 - then trophic position, basal resource, or movement during life were not consistent.
 3. Capture length (FL) correlation with relative capture location (among individuals within species)
 - 3A. If capture length correlates (positively or negatively) with relative capture position,
 - then the species tends to have directional movement during life.
 - 3B. If capture length does not correlate with relative capture position,
 - then the species tends to be stationary or moves inconsistently.
 4. $\delta^{13}\text{C}$ correlation with $\delta^{15}\text{N}$ (within individuals)
 - 4A. If $\delta^{13}\text{C}$ negatively correlates with $\delta^{15}\text{N}$,
 - then the individual (or its prey) moved against one isotopic gradient and along the other.
 - 4B. If $\delta^{13}\text{C}$ positively correlates with $\delta^{15}\text{N}$,
 - then the individual remained largely stationary while increasing trophic position.
 - 4C. If $\delta^{13}\text{C}$ does not correlate with $\delta^{15}\text{N}$,
 - then the individual (or its prey) likely moved inconsistently during the lifetime.
-

Table 4.3. Statistics for non-linear least-squares regression for isotopic values ($\delta^{15}\text{N}$ and $\delta^{13}\text{C}$) as a function of eye lens diameter (ELD) in both Tilefish and Red Grouper. All regressions took the form of: isotopic value ($\delta^{15}\text{N}$ or $\delta^{13}\text{C}$) = $a + b \cdot \ln(\text{ELD})$. Parameters are presented \pm standard error.

Regressed with Eye-lens diameter	<i>n</i>	a (\pm SE)	b (\pm SE)	F	p	R ²
Tilefish $\delta^{15}\text{N}$	468	11.02 \pm 0.07	1.54 \pm 0.05	1069	\leq 0.001	0.70
Tilefish $\delta^{13}\text{C}$	468	-18.59 \pm 0.05	0.86 \pm 0.04	496	\leq 0.001	0.52
Red Grouper $\delta^{15}\text{N}$	406	8.12 \pm 0.07	1.28 \pm 0.06	526	\leq 0.001	0.57
Red Grouper $\delta^{13}\text{C}$	406	-17.27 \pm 0.11	0.68 \pm 0.09	56	\leq 0.001	0.12

Table 4.4. Individual Tilefish information ordered by capture fork length (FL). Eye-lens diameter (ELD), Number of eye-lens laminae (ELL), Spearman rank correlations $\delta^{15}\text{N}$ vs ELD and $\delta^{13}\text{C}$ vs $\delta^{15}\text{N}$ are listed along with interpretations corresponding to Table 4.2. Significance is indicated as follows: n.s.: $p > 0.05$, * $p \leq 0.05$, ** $p \leq 0.01$, *** $p \leq 0.001$. Individual capture length did not correlate with relative capture position (i.e., interpretation 3B in Table 4.2).

FL (cm)	Sex	Age (y)	ELD	ELL	$\delta^{15}\text{N}$ vs ELD <i>Rho</i>	$\delta^{13}\text{C}$ vs ELD <i>Rho</i>	$\delta^{13}\text{C}$ vs $\delta^{15}\text{N}$ <i>Rho</i>	Isotopic Interpretation
48	F	10	10.2	10	0.95 ***	0.61 (n.s.)	0.56 (n.s.)	1B, 2C, 3B, 4C
49	F	9	10.2	12	0.97 ***	0.97 ***	0.99 ***	1B, 2B, 3B, 4B
50	F	11	11.6	13	0.97 ***	0.93 ***	0.94 ***	1B, 2B, 3B, 4B
51	F	15	12.5	12	0.68 *	0.92 ***	0.87 ***	1B, 2B, 3B, 4B
52	F	9	11.3	12	0.98 ***	0.97 ***	0.96 ***	1B, 2B, 3B, 4B
55	F	10	11.5	12	0.92 ***	0.92 ***	0.93 ***	1B, 2B, 3B, 4B
56	F	13	11.3	18	0.89 ***	0.90 ***	0.94 ***	1B, 2B, 3B, 4B
61	F	13	13.5	12	0.97 ***	0.95 ***	0.91 ***	1B, 2B, 3B, 4B
62	F	9	11.2	16	0.81 **	0.84 ***	0.57 *	1B, 2B, 3B, 4B
62	F	11	10.1	8	0.98 ***	0.79 *	0.76 *	1B, 2B, 3B, 4B
63	U	12	10.8	13	0.69 *	0.84 ***	0.88 ***	1B, 2B, 3B, 4B
64	M	8	11.2	15	0.91 ***	0.9 ***	0.89 ***	1B, 2B, 3B, 4B
66	F	12	11.5	12	0.97 ***	0.99 ***	0.95 ***	1B, 2B, 3B, 4B
68	M	13	10.5	9	0.98 ***	0.87 **	0.88 **	1B, 2B, 3B, 4B
69	F	17	12.4	19	0.84 ***	0.92 ***	0.87 ***	1B, 2B, 3B, 4B
70	U	NA	11.7	12	0.97 ***	0.73 **	0.76 **	1B, 2B, 3B, 4B
70	U	20	12.5	10	0.95 ***	0.73 *	0.68 *	1B, 2B, 3B, 4B
71	M	11	11.2	13	0.87 ***	0.95 ***	0.96 **	1B, 2B, 3B, 4B
72	U	NA	11.5	14	0.91 ***	0.79 **	0.65 *	1B, 2B, 3B, 4B
72	M	12	10.8	11	0.87 ***	0.78 **	0.85 **	1B, 2B, 3B, 4B
73	U	16	12.8	13	0.62 *	0.97 ***	0.65 *	1B, 2B, 3B, 4B
74	U	11	12.2	14	0.93 ***	0.97 ***	0.95 ***	1B, 2B, 3B, 4B
75	M	10	11.7	14	0.90 ***	0.60 *	0.77 **	1B, 2B, 3B, 4B
76	M	9	11.7	9	0.97 ***	0.93 ***	0.98 ***	1B, 2B, 3B, 4B
77	U	12	12.4	16	0.92 ***	0.82 ***	0.81 ***	1B, 2B, 3B, 4B
78	U	14	11.9	8	0.91 **	0.93 **	0.97 ***	1B, 2B, 3B, 4B
79	F	NA	12.1	15	0.93 ***	0.94 ***	0.91 ***	1B, 2B, 3B, 4B
81	M	10	11.9	12	0.99 ***	0.97 ***	0.97 ***	1B, 2B, 3B, 4B
83	F	13	13.3	17	0.97 ***	0.98 ***	0.98 ***	1B, 2B, 3B, 4B
85	M	12	11.8	14	0.89 ***	0.84 ***	0.87 ***	1B, 2B, 3B, 4B
89	F	12	11.9	13	0.93 ***	0.82 **	0.74 **	1B, 2B, 3B, 4B
90	F	NA	12.5	16	0.92 ***	0.89 ***	0.76 ***	1B, 2B, 3B, 4B
92	M	13	12.8	14	0.98 ***	0.81 ***	0.78 **	1B, 2B, 3B, 4B
92	M	NA	13.1	15	0.95 ***	0.97 ***	0.95 ***	1B, 2B, 3B, 4B
93	M	NA	13.1	16	0.95 ***	0.90 ***	0.95 ***	1B, 2B, 3B, 4B
99	M	14	12.4	11	0.79 ***	0.95 ***	0.83 **	1B, 2B, 3B, 4B

Table 4.5. Individual Red Grouper information ordered by capture fork length (FL). Eye-lens diameter (ELD), Number of eye-lens laminae (ELL), Spearman rank correlations $\delta^{15}\text{N}$ vs ELD and $\delta^{13}\text{C}$ vs $\delta^{15}\text{N}$ are listed along with interpretations corresponding to Table 2. Significance is indicated as follows: n.s.: $p > 0.05$, * $p \leq 0.05$, ** $p \leq 0.01$, *** $p \leq 0.001$. Individual capture length did not correlate with relative capture position (i.e., interpretation 2B in Table 4.2).

FL (cm)	Age	ELD	ELL	$\delta^{15}\text{N}$ vs ELD <i>Rho</i>	$\delta^{13}\text{C}$ vs ELD <i>Rho</i>	$\delta^{13}\text{C}$ vs $\delta^{15}\text{N}$ <i>Rho</i>	Isotopic Interpretation
29.2	2	5.3	9	0.70 *	0.11 (n.s.)	-0.25 (n.s.)	1B, 2C, 3B, 4C
29.4	2	6.2	15	0.80 ***	0.43 (n.s.)	0.38 (n.s.)	1B, 2C, 3B, 4C
30.0	2	4.9	7	1.00 ***	0.03 (n.s.)	0.04 (n.s.)	1B, 2C, 3B, 4C
30.1	2	6.5	11	0.98 ***	0.83 **	0.82 **	1B, 2B, 3B, 4B
30.4	2	5.3	9	0.73 *	0.55 (n.s.)	0.4 (n.s.)	1B, 2C, 3B, 4C
30.9	2	7.2	11	0.46 (n.s.)	0.75 *	0.27 (n.s.)	1C, 2B, 3B, 4C
31.8	2	6.5	9	0.95 ***	0.30 (n.s.)	0.22 (n.s.)	1B, 2C, 3B, 4C
32.0	2	7.0	8	0.98 ***	0.71 (n.s.)	0.67 (n.s.)	1B, 2C, 3B, 4C
32.4	2	7.0	8	0.93 **	0.19 (n.s.)	-0.07 (n.s.)	1B, 2C, 3B, 4C
32.6	3	5.0	9	0.88 **	0.93 ***	0.87 **	1B, 2B, 3B, 4B
32.7	2	5.6	13	0.60 *	0.20 (n.s.)	-0.39 (n.s.)	1B, 2C, 3B, 4C
32.9	2	7.1	9	1.00 ***	-0.11 (n.s.)	-0.12(n.s.)	1B, 2C, 3B, 4C
32.9	2	6.8	10	0.92 ***	-0.11 (n.s.)	0.04 (n.s.)	1B, 2C, 3B, 4C
33.1	2	6.0	11	0.86 **	0.16 (n.s.)	-0.02 (n.s.)	1B, 2C, 3B, 4C
33.4	3	6.0	9	0.85 **	0.70 *	0.40 (n.s.)	1B, 2B, 3B, 4C
33.6	2	8.2	16	0.99 ***	0.41 (n.s.)	0.43 (n.s.)	1B, 2C, 3B, 4C
33.9	2	6.3	15	0.40 (n.s.)	-0.06 (n.s.)	-0.29 (n.s.)	1C, 2C, 3B, 4C
34.1	2	7.5	17	0.78 ***	0.38 (n.s.)	-0.02 (n.s.)	1B, 2C, 3B, 4C
34.5	2	6.1	9	0.78 *	0.62 (n.s.)	0.02 (n.s.)	1B, 2C, 3B, 4C
34.9	2	7.2	14	0.71 **	0.81 ***	0.53 *	1B, 2B, 3B, 4B
36.8	4	9.0	18	0.93***	-0.22 (n.s.)	-0.35 (n.s.)	1B, 2C, 3B, 4C
49.1	5	9.5	20	0.97 ***	-0.50 *	-0.55 *	1B, 2A, 3B, 4A
49.6	5	9.0	21	0.97 ***	-0.74 ***	-0.75 ***	1B, 2A, 3B, 4A
50.5	3	9.2	19	0.98 ***	0.49 *	0.51 *	1B, 2B, 3B, 4B
51.8	10	9.0	20	0.94 ***	-0.14 (n.s.)	-0.17 (n.s.)	1B, 2C, 3B, 4C
52.7	6	9.8	23	0.95 ***	0.00 (n.s.)	-0.05 (n.s.)	1B, 2C, 3B, 4C
54.1	5	9.5	20	0.23 (n.s.)	0.21 (n.s.)	-0.52 *	1C, 2C, 3B, 4A
57.0	6	9.8	22	0.98 ***	0.09 (n.s.)	0.11 (n.s.)	1B, 2C, 3B, 4C
72.7	4	11.5	17	0.98 ***	-0.03 (n.s.)	-0.05 (n.s.)	1B, 2C, 3B, 4C
78.2	NA	9.8	17	0.94 **	0.61 *	0.64 **	1B, 2B, 3B, 4B

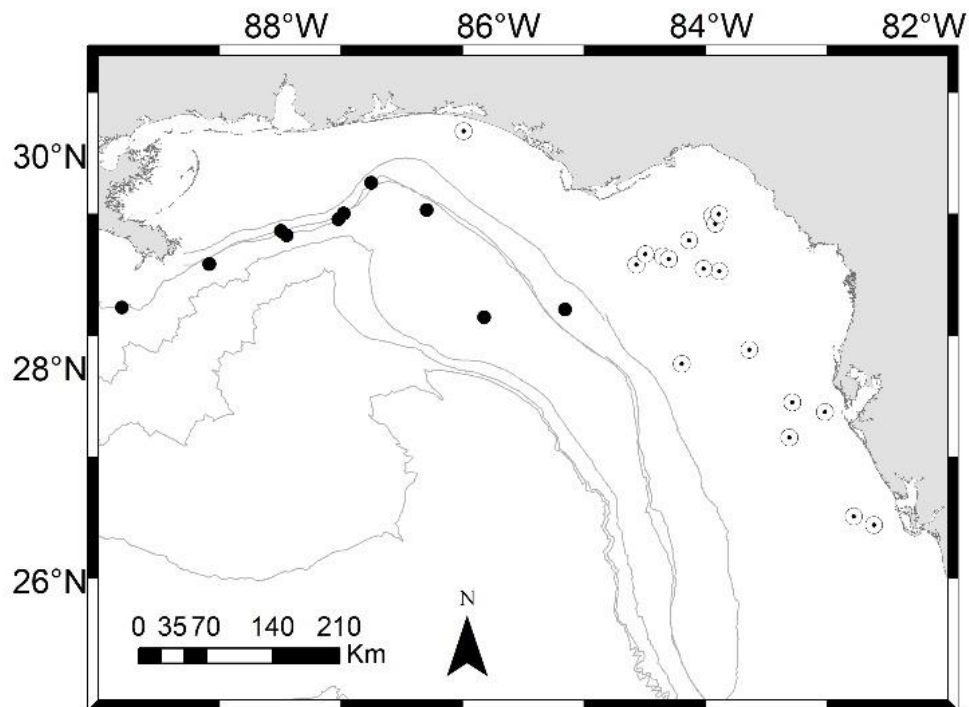


Figure 4.1. Collection locations for all individuals within the Gulf of Mexico. Red Grouper collection locations are white circles. Tilefish collection locations are black circles. More than one fish was collected at several of the mapped locations. Bathymetry markings are 100, 200, 1000, 2000, and 3000 m.

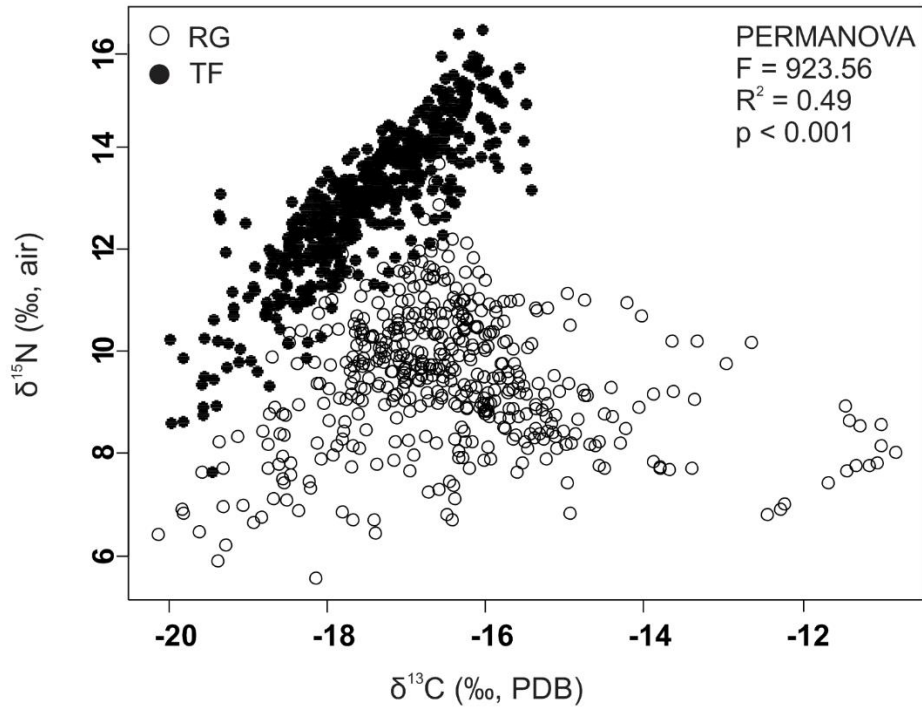


Figure 4.2. Isotopic distribution for all Red Grouper and Tilefish eye-lens layers. PERMANOVA results comparing the combined difference in $\delta^{15}\text{N}$ and $\delta^{13}\text{C}$ by species are listed. Red Grouper are white circles. Tilefish are black circles.

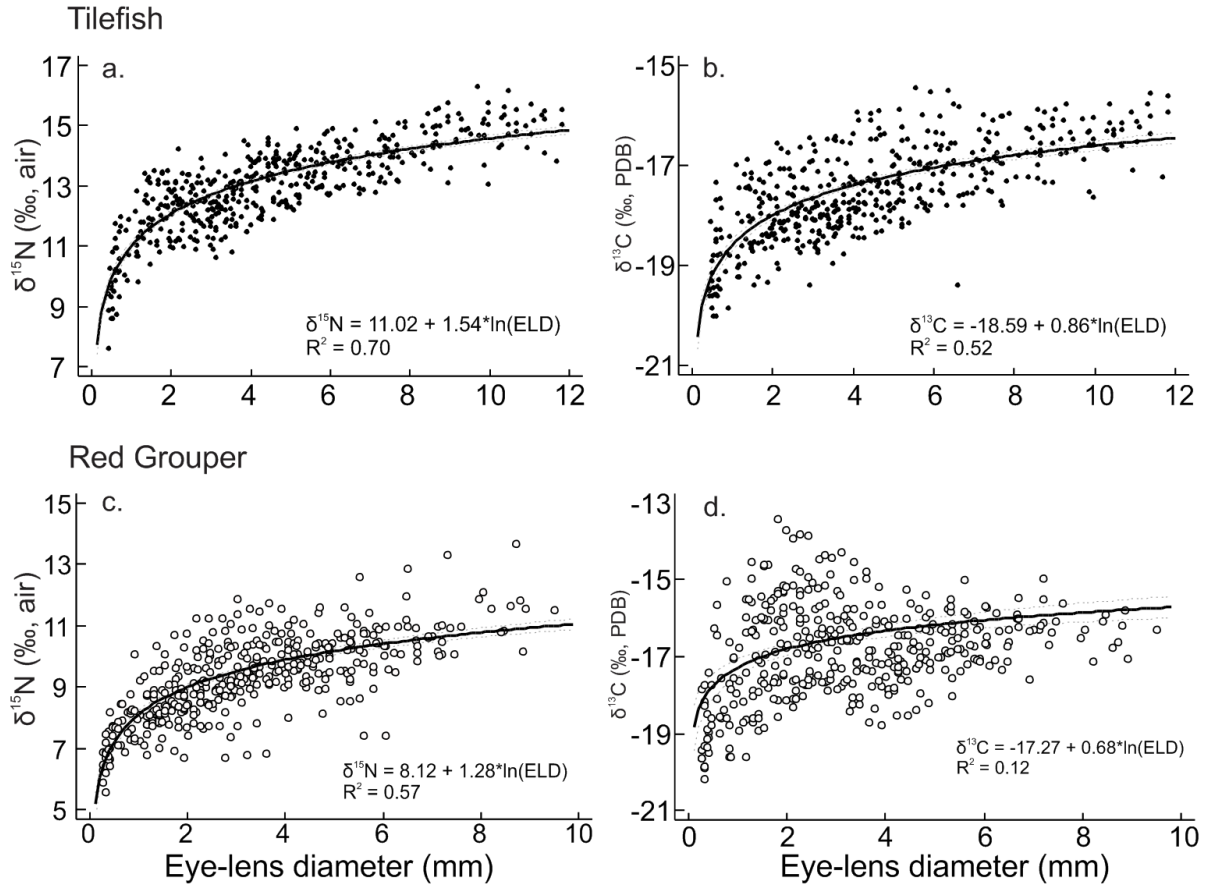


Figure 4.3. Non-linear regression of isotopic values $\delta^{15}\text{N}$ and $\delta^{13}\text{C}$ as a function of eye-lens diameter (ELD) for both Tilefish and Red Grouper. Equations and R^2 values are listed for each.

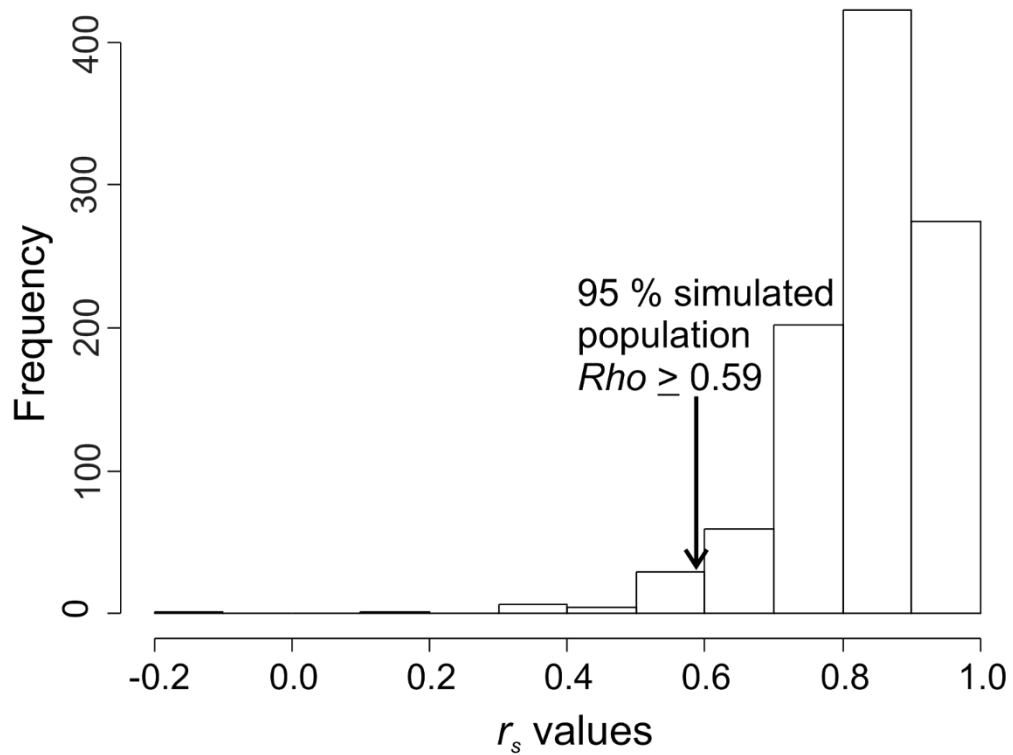


Figure 4.4. Spearman rank correlations (Rho) representing correlation between $\delta^{15}\text{N}$ and $\delta^{13}\text{C}$ for simulated population of 1,000 Tilefish. 95% of all simulated fish resulted in a correlation > 0.59

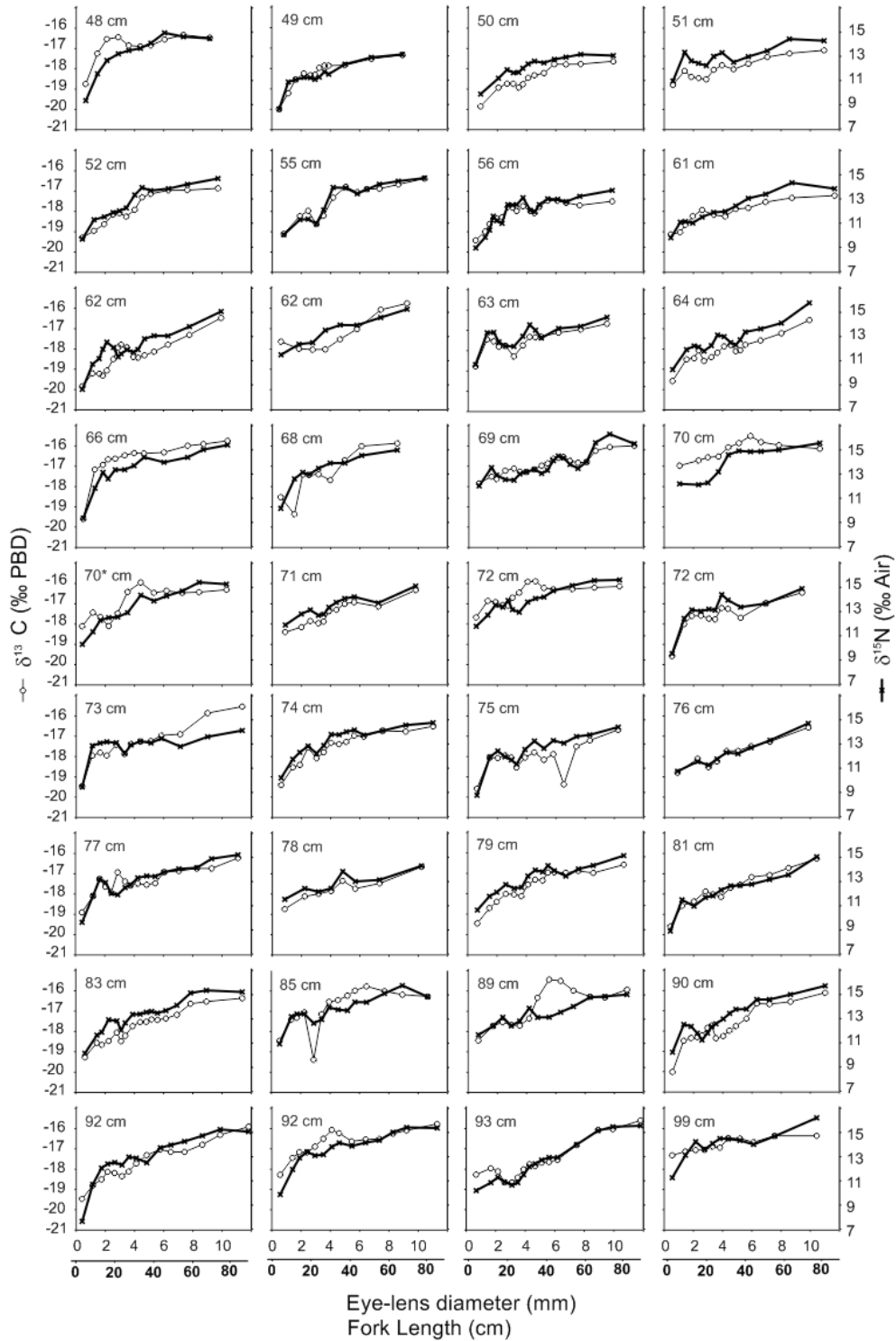


Figure 4.5. Lifetime profiles of $\delta^{13}\text{C}$ and $\delta^{15}\text{N}$ in Tilefish eye-lenses ordered by fork length at capture. Primary x-axis is eye-lens diameter. Secondary x-axis is approximate fork length calculated from linear regression between fork length and eye-lens diameter.

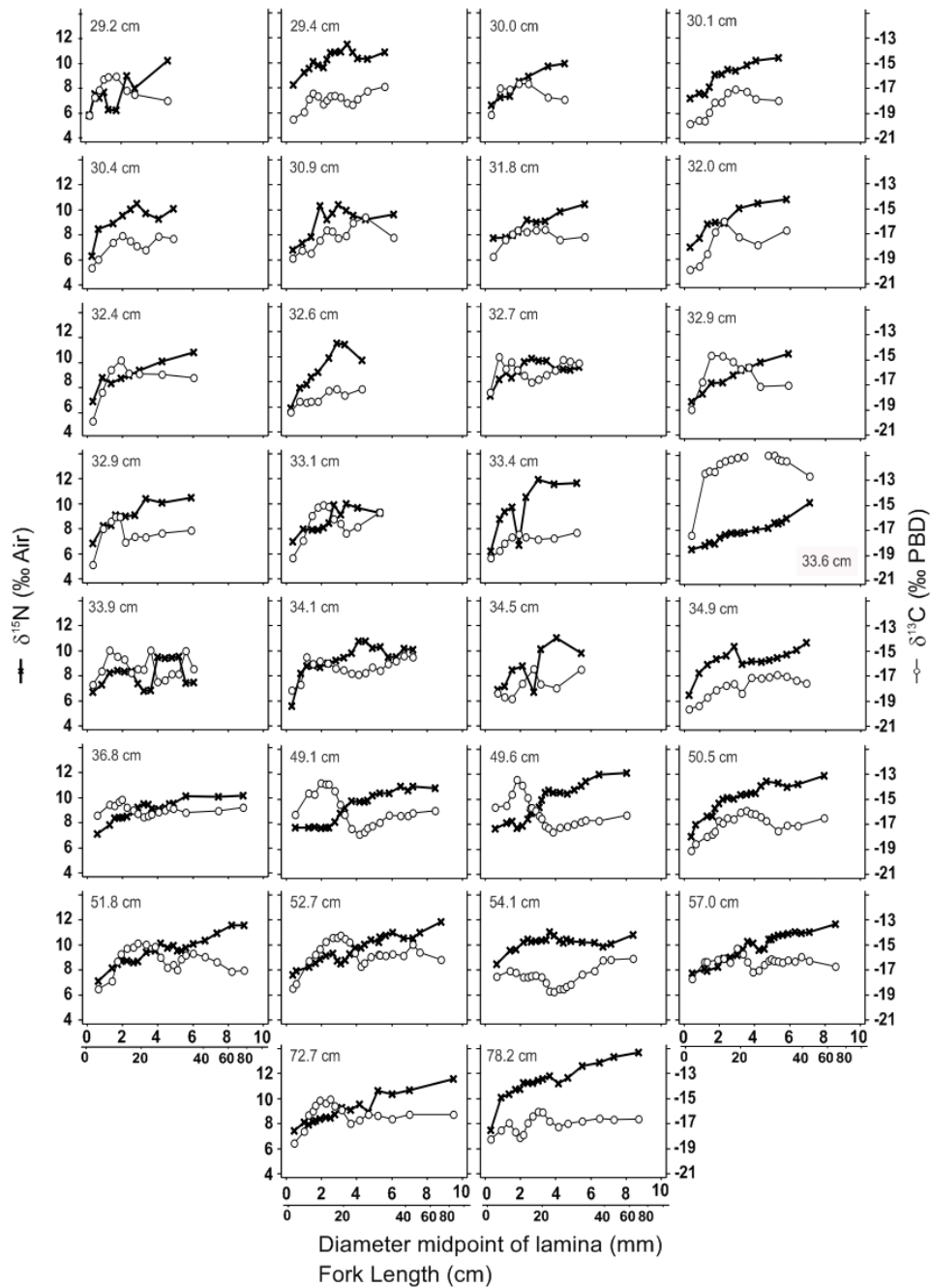


Figure 4.6. Lifetime profiles of $\delta^{13}\text{C}$ and $\delta^{15}\text{N}$ in Red Grouper eye-lenses ordered by fork length at capture. Primary x-axis is eye-lens diameter. Secondary x-axis is approximate fork length calculated from linear regression between fork length and eye-lens diameter.

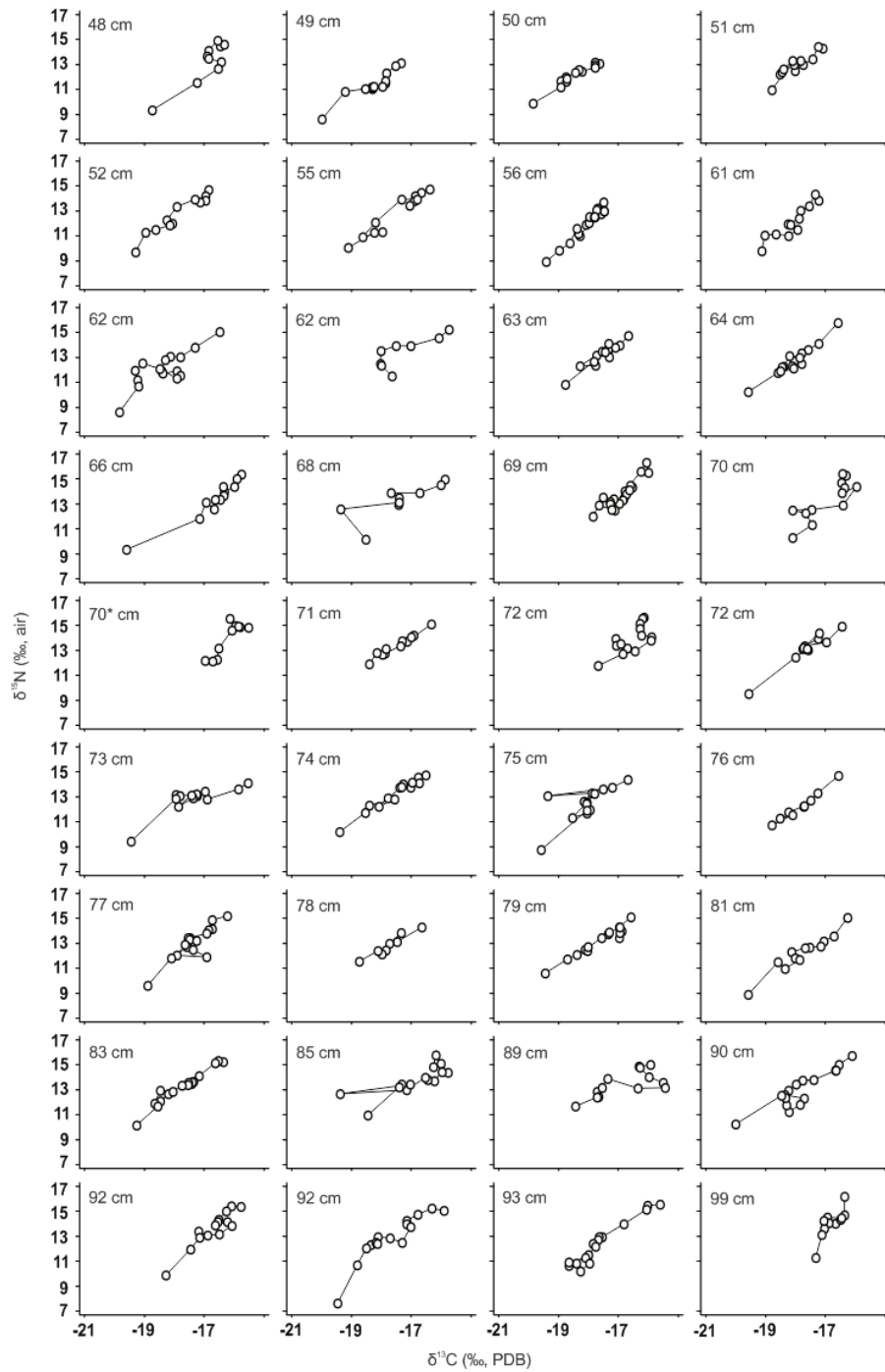


Figure 4.7. Tilefish lifetime correlations between $\delta^{15}\text{N}$ and $\delta^{13}\text{C}$. Individuals are ordered by fork length. Individual eye-lens layers are signified by dots. Lines indicate profiles over time. Innermost eye-lens layer is always at the bottom (usually left) of the graph. Outermost eye-lens layer is always at the top (usually right) of the graph.

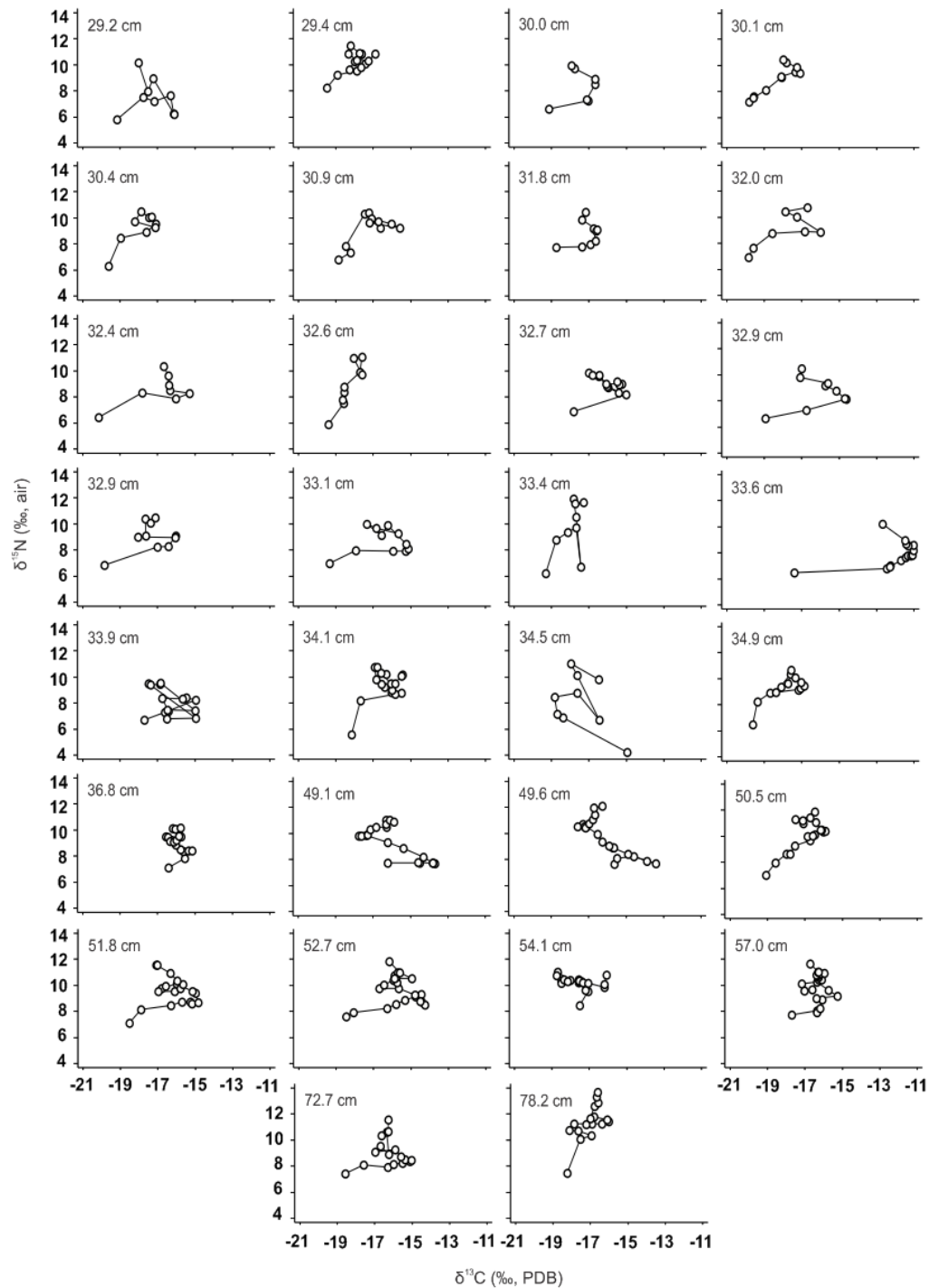


Figure 4.8. Red Grouper lifetime correlations between $\delta^{15}\text{N}$ and $\delta^{13}\text{C}$. Individuals are ordered by fork length. Individual eye-lens layers are signified by dots. Lines indicate profiles over time. Innermost eye-lens layer is always at the bottom (usually left) of the graph.

CHAPTER 5: ONTOGENETIC MOVEMENT AND DIET SHIFTS IN JUVENILE RED GROUPEL

ABSTRACT

Eye-lenses are valuable as an archival tissue to track the movements and diets of fish over their lifetime. We analyzed the bulk $\delta^{13}\text{C}$ and $\delta^{15}\text{N}$ in the sequential eye-lens laminae of 55 juvenile and 38 adult Red Grouper (*Epinephelus morio*) from continental shelf waters of Campeche, Mexico and Florida, USA. We used published rules to interpret isotopic patterns within the eye lens. We complimented these data with stomach contents and catch locations from an additional 521 Red Grouper. We found that postlarval locations and movements were consistent among juvenile and adult Red Grouper from the eastern Gulf of Mexico. Postlarval locations for fish from Mexico and southeastern Florida were easily distinguished by their $\delta^{15}\text{N}$ values. We found a unique shape to the $\delta^{13}\text{C}$ profiles of eastern Gulf of Mexico Red Grouper whereby values increased sharply and subsequently decreased sharply by the end of the first year of life, suggesting cross-shelf movement or radical diet shifts. Stomach-contents indicated that Red Grouper are dependent on small shrimps (68% of diet) and crabs (20% of diet) early in life but eat more squids and fishes as they approach maturity. It appears likely that the shape of the $\delta^{13}\text{C}$ profile reflects these diet shifts accompanied by cross-shelf movement in young Red Grouper in the eastern Gulf of Mexico. Eye lens isotope profiles have the potential to corroborate existing movement and diet information or be used to identify species for which more study is warranted.

INTRODUCTION

Movement and diet histories of targeted species are important for ecosystem modeling and fisheries stock assessments. However, the data are often sparse due to sampling difficulty and expense. Bulk stable isotopes in body tissues, such as muscle, have provided information regarding trophic position (Choy et al. 2015), basal-resource dependence (Grippe et al. 2011), and movement (Acosta-Pachon et al. 2015) in fish and other marine organisms with high economic value. Due to tissue turnover, most stable isotope records provide information covering only a few months of the organism's life. Unlike most tissues, eye lens proteins are not reworked once formed (Lynnerup et al. 2008). Instead, new layers of protein are added to the outer edge of the lens as the organism grows (Dahm et al. 2007). Once dissected, the isotopes of fish eye lenses provide a historical perspective unavailable in other tissues (Wallace et al. 2014, Quaeck-Davies et al. 2018, Simpson et al. 2019). These isotope profiles can enhance traditional fisheries datasets by providing high resolution movement and diet information regarding life history stages often unavailable to traditional fisheries gears.

Fish eye lenses as archival tissue

Vertebrate eye-lenses grow sequentially during life (Shi et al. 2009). Cells at the outer edge of the eye lens exchange atoms with the body via the humors. In captive Red Drum (*Sciaenops ocellatus*), isotopic values from a new diet were 90% incorporated into the outer eye lens 54 days after the diet was changed (Granneman 2018). Once lens fiber cells are out of direct contact with the capsule, they undergo attenuated apoptosis, in which the organism removes all organelles and ceases protein synthesis (Stewart et al. 2013, Peebles and Hollander 2020). Lack of turnover within the lens has been demonstrated in vertebrates including humans (Lynnerup et al. 2008, Kjeldsen et al. 2010) and Greenland Sharks (*Somniosus microcephalus*) (Nielsen et al.

2016) using radiocarbon dating. The sequential $\delta^{13}\text{C}$ and $\delta^{15}\text{N}$ records within the lens provide a method for tracking the ontogenetic diet shifts and movements of individuals over the lifespan. This has been demonstrated in several species of squid (Parry 2008, Hunsicker et al. 2010, Golikov et al. 2018, Queiros et al. 2018, Meath et al. 2019), elasmobranchs (Quaek-Davies et al. 2018, Simpson et al. 2019), and bony fishes (Wallace et al. 2014, Tzadik et al. 2017, Quaek-Davies et al. 2018).

Interpretation of $\delta^{13}\text{C}$ and $\delta^{15}\text{N}$ profiles in fish eye lenses

The geographic interpretation of animal tissue isotope values requires a spatially variable isotopic background (isoscape). On the West Florida Shelf (WFS) in the eastern Gulf of Mexico, bulk-tissue derived $\delta^{13}\text{C}$ and $\delta^{15}\text{N}$ isoscapes exist that are stable on seasonal (Radabaugh et al. 2014) and inter-annual timescales (Huelster 2015). Recent work suggests that $\delta^{15}\text{N}$ is regionally consistent with highest values in the north central Gulf near the mouth of the Mississippi River and lowest in the eastern Gulf of Mexico near the Florida Keys (Peebles and Hollander 2020). These pattern of $\delta^{15}\text{N}$ values is consistent with municipal run-off and animal husbandry from the Mississippi River valley (Kendall et al. 2001, O'Connor et al. 2016), and little terrestrial nitrogen input near the Florida Keys, leaving diazotrophs such as *Trichodesmium* spp, to introduce much of the nitrogen to the biosphere via the incorporation of atmospheric N_2 (Carpenter et al. 1997, McClelland et al. 2003).

Values of $\delta^{13}\text{C}$ decrease with increasing depth, in a westward direction from peninsular Florida (Radabaugh and Peebles 2014). Phytoplankton, the dominant primary producer in outer continental shelf waters, undergo high rates of isotopic fractionation during photosynthesis, resulting in low values of $\delta^{13}\text{C}$ (Fry and Wainright 1991, Keough et al. 1998, Burkhardt et al.

1999). In shallow, clear waters, benthic microalgae, macroalgae and seagrasses make up a large proportion of primary producers (Keough et al. 1998, Grippo et al. 2011, McMahon et al. 2016), and contain high values of $\delta^{13}\text{C}$ (Fry and Wainright 1991, Radabaugh et al. 2014). Isotopic trends in primary producers are transmitted to higher trophic levels with $\delta^{13}\text{C}$ values in muscle tissue from a single species of fish varying by $\sim 4\%$ across depth (Radabaugh et al. 2013, Radabaugh and Peebles 2014).

Red Grouper life history

Red Grouper (*Epinephelus morio*) is a reef-fish species common to the eastern Gulf of Mexico, with a center of abundance near the central WFS (Lombardi-Carlson et al. 2008, Carruthers et al. 2015, Gruss et al. 2017). Between 2.3 and 5.6 million pounds of Red Grouper were landed annually by the commercial sector between 2004 and 2018 (NOAA Fisheries 2019). Between 1.9 and 8.7 million pounds were landed annually by the recreational sector over the same period (personal communication to JV, National Marine Fisheries Service, Fisheries Statistics Division, September 4, 2019), making the species one of the most heavily exploited reef fish in the Gulf of Mexico.

Little information is available for larval and juvenile Red Grouper, a critical life history stage for accurate stock assessment. Fishery independent monitoring programs rarely capture individuals smaller than ~ 300 mm total length (TL) (SEDAR 2015). Moe (1969) suggested that small juveniles are rarely observed because they inhabit continuous reef habitats, avoiding traps and trawls. A visual fish monitoring effort of central WFS reefs records juvenile Red Grouper (< 200 mm SL) in continuous natural reef and artificial reef habitats, areas inaccessible to most capture gears (Stallings, unpublished data).

The species is a protogynous hermaphrodite with 50% maturity for females occurring at 2.8 years and 242 mm standard length (SL). Sexual transition to male begins as early as three years, but often occurs later, with 50% males in the population occurring around 12.6 years and 725 mm SL (SEDAR 2015). Adult Red Grouper excavate sandy sediments to reveal limestone outcrops, for use as a home territory and spawning area (Coleman et al. 2010, Wall et al. 2011, Grasty et al. 2019). Tagged Red Grouper are largely recaptured within 1 km of their original location (Coleman et al. 2011, Burns and Froeschke 2012), suggesting that their movement is quite restricted.

Red Grouper diet changes as the fish grows. Juvenile Red Grouper diets are composed of benthic invertebrates (Weaver 1996, Brule et al. 1999). The one available study from the WFS indicated the small juveniles (100–200 mm SL) fed on various types of shrimps, while larger juveniles incorporated crabs, and adults added fish (Weaver 1996). This geographically limited study was conducted over 20 years ago and was based on fewer than 200 total individuals.

A number of recent studies have paired stomach-content analysis with muscle stable-isotope values to better integrate the diets of various fish species on timescales of days and months (e.g., Curtis et al. 2017, Matley et al. 2018, Burbank et al. 2019). To date, no studies have combined eye-lens isotope data with large-scale stomach content and catch location data. By integrating these datasets, we aim to produce the most complete lifetime-scale records of movement and diet to date for a heavily exploited predatory reef fish species.

Objectives

Here we present eye-lens isotope profiles alongside stomach-content and catch depth data from a wide size range of Red Grouper. The isotope data largely corroborates known biological

information and fills gaps in knowledge of the species. By combining these data, we show that most Red Grouper on the WFS are spawned near the shelf-edge, migrate long distances during the first year of life, and switch diet multiple times. By using a relatively well-studied species, we show that eye-lens isotope profiles can enhance the specificity of existing demographic and diet data or be used to identify additional species for which closer scrutiny of these data is warranted.

MATERIALS AND METHODS

Fish collection and eye lens preparation

We collected 85 Red Grouper for eye-lens isotope analysis from the West Florida Shelf (WFS) through a variety of mechanisms including fish traps and trawls (FWC-FWRI & NOAA Fisheries), scientific longline (Murawski et al. 2018), and by a scientist (JV) accompanying recreational anglers (all sub-legal fish were collected under NOAA LOA with J. Vecchio). Stomach-content data were obtained from FWC-FWRI Fisheries Independent Monitoring Program (FIM) Stomach Content Laboratory (collection locations Figure 5.1B). FIM personnel collected stomachs from Red Grouper using unbaited gears, primarily balloon trawls and otter trawls (Eldridge 1988). Field crews recorded capture latitude, longitude, and depth for all fish used isotope and diet studies.

We froze fish for eye-lens isotope analysis whole at -20°C soon after capture. We measured each fish for standard length (SL), fork length (FL), and total length (TL). We removed otoliths and cleaned them of tissue. We aged all otoliths whole under transmitted light using a dissecting microscope in the FWRI otolith laboratory (Carroll, personal communication).

We dissected and processed eye-lens samples according to Wallace et al. (2014) with the exception that all delamination was conducted while the lens was submerged in water (Stewart et al. 2013), which results in identical isotope values (Meath et al. 2019). Briefly, we thawed whole eyes, made a corneal incision, and removed the lens epithelium/capsule. We placed each lens under a dissecting stereomicroscope, where we separated laminae with two fine-tipped forceps. The lens core (~0.5 mm diameter) was the final analyzed tissue. We used an ocular micrometer to measure the diameter at the equator to the nearest 0.05 mm. We defined laminar midpoint as the lens diameter after lamina removal plus half the thickness of the removed lamina and identified each lamina by its unique laminar midpoint or eye-lens diameter (ELD). We placed each lamina in a drying oven at 50°C overnight to ensure complete desiccation.

Isotope analysis

We added a dry weight of 150-600 µg of material from an individual eye-lens lamina to a tin capsule and weighed each sample to the nearest µg on a Mettler-Toledo precision microbalance. We measured isotopes $^{13}\text{C}/^{12}\text{C}$ and $^{15}\text{N}/^{14}\text{N}$ along with C:N in duplicate using a Carlo-Erba NA2500 Series II Elemental Analyzer (EA) combustion furnace coupled to a continuous-flow ThermoFinnigan Delta+XL isotope ratio mass spectrometer (IRMS) at the University of South Florida College of Marine Science in St. Petersburg, Florida. The limit of quantification was 12 µg for both $\delta^{13}\text{C}$ and $\delta^{15}\text{N}$. Calibration standards were NIST 8573 and NIST 8574 L-glutamic acid standard reference materials. Analytical precision, obtained by replicate measurements of NIST 1577b bovine liver, was $\pm 0.13\text{‰}$ for $\delta^{13}\text{C}$ and $\pm 0.17\text{‰}$ for $\delta^{15}\text{N}$ (mean standard deviations of $n = 530$ replicates conducted over an 11-month period).

Results are presented in delta notation (δ , in ‰) relative to international standards Vienna Pee Dee Belemnite (VPDB) and air:

$$\delta X = \left(\frac{R_{sample}}{R_{standard}} - 1 \right) \times 1000$$

where X is ^{13}C or ^{15}N and R is the corresponding ratio $^{13}\text{C}/^{12}\text{C}$ or $^{15}\text{N}/^{14}\text{N}$.

Eye-lens isotope data analysis

We divided fish into the categories of juveniles (0–2 y, < 242 mm SL) and adults (2⁺ y; \geq 242 mm SL) (Figure 5.1A). Individuals not meeting both criteria to be considered adult were classified as juveniles.

Eye-lens core isotope data analysis

The eye-lens core represents the period during life from first feeding (~72 h after hatch) to age/length at the core edge. We used the isotopic data from the core to represent location during the late larval (postlarval) period (see Vecchio and Peebles 2019). We used the regression equation $SL = (5.94 * \sqrt{ELD})^2$ to calculate the standard length at which the core was completed. Based on the SL: ELD regression equation, cores represented the entire larval duration plus a short period (days-weeks) of the early juvenile stage.

We calculated mean (\pm SE), minimum, and maximum eye-lens core values for both $\delta^{15}\text{N}$ and $\delta^{13}\text{C}$ within each group. We used package Vegan (Oksanen et al. 2019) to calculate beta dispersion and PERMANOVA for eye-lens core values of each group. We conducted Spearman rank correlations (r_s) between eye-lens core isotopic values ($\delta^{15}\text{N}$ and $\delta^{13}\text{C}$) and the independent variables core ELD and capture location (latitude and longitude). To interpret the results of these correlations, we used the Table 3.2 interpretation rules (Vecchio and Peebles 2019). Briefly, a

significant correlation between core isotopic value and ELD indicated a change in trophic position during the larval period or a move to an area with a different isotopic baseline. A significant correlation between core isotopic value and capture location (latitude, longitude) indicated a relationship between spawning location and the locations of juveniles or adults. No correlation indicated no change or inconsistent change during the larval period.

Lifetime eye-lens profiles

We used the regression equation $SL = e^{(4.21 + 0.20 * ELD)}$ to relate SL to ELD across the lifespan (discussed in Chapter 4). The lifetime-scale equation accounts for the logarithmic relationship between ELD and fish length in later life. We calculated lifetime $\Delta\delta^{15}N$ and $\Delta\delta^{13}C$ as the final value of $\delta^{15}N$ or $\delta^{13}C$ minus the initial value. We performed a series of Spearman rank correlations comparing sequential $\delta^{15}N$ and $\delta^{13}C$ values to ELD or to one another over the lifetime. We then used the lifetime-scale interpretation rules (Table 4.2) to sedentary from moving individuals. To reliably calculate Spearman rank correlation values, a minimum of 8 to 10 samples is necessary, and p-values for correlation coefficients are heavily influenced by sample number (Sokal and Rohlf 1994). This presented a problem when evaluating eye-lens profiles of juvenile Red Grouper with small numbers of eye-lens laminae. Therefore, we used Spearman $r > |0.5|$ as the definition of substantial correlation between isotopic values and ELD.

Carbon bump: $\delta^{13}C$ maximum during the first year of life

We observed that most individuals with consistently increasing $\delta^{15}N$, but no correlation between $\delta^{15}N$ and $\delta^{13}C$, appeared to have profiles in which $\delta^{13}C$ reached a maximum during the first year of life with a subsequent decrease in $\delta^{13}C$ values. We called this feature in the $\delta^{13}C$

profile “carbon bump.” We used a 1:1 relationship between $\delta^{13}\text{C}$ and $\delta^{15}\text{N}$ to represent a maximum expected rate of increase for $\delta^{13}\text{C}$ with no diet change or movement. Despite the theoretical 1:3 relationship between increases in $\delta^{13}\text{C}$ and $\delta^{15}\text{N}$ with increasing trophic position (Fry 2006), field studies have indicated a relationship between 1:1 and 1:2 in eye-lens profiles for stationary individuals (Table 4.1), and trophic discrimination factors have suggested similar values (Eddy 2019, Patterson et al. 2020).

To locate and measure a carbon bump within an individual $\delta^{13}\text{C}$ profile, we:

1. identified fish for which $\delta^{15}\text{N}$ resulted in > 0.5 correlation with ELD and $\delta^{13}\text{C}$ did not.
2. located the first segment of these eye-lens in which $\delta^{13}\text{C}$ continuously increased faster than $\delta^{15}\text{N}$ ($\delta^{13}\text{C}_{\text{initial}}$) in an individual fish (each “segment” often extended through several laminae)
3. located the first segment in which $\delta^{13}\text{C}$ continuously decreased faster than $\delta^{15}\text{N}$ in that fish ($\delta^{13}\text{C}_{\text{top}}$). We identified this as the transition from increasing to decreasing $\delta^{13}\text{C}$.
4. located the ELD of transition as the ELD of this $\delta^{13}\text{C}_{\text{top}}$ value.
5. calculated the height of transition as $\delta^{13}\text{C}_{\text{top}} - \delta^{13}\text{C}_{\text{initial}}$

We then calculated mean (\pm SE) ELD and height of transition for each group.

Stomach-content collection, prey identification, and data analysis

Researchers immediately removed stomachs from each Red Grouper, placed them in cheesecloth bags, and submerged them in 10% formalin for at least 48 h. Stomachs were then rinsed in fresh water and stored in 50% isopropanol until processing. Fresh water was used to flush contents into a gridded petri dish and contents were identified to the lowest possible taxonomic level using both dissecting and compound microscopes. Each prey was enumerated

based upon identifiable structures and was measured volumetrically (see Hall-Scharf et al. (2016) for full description of identification methods).

We used 50 mm SL size-classes to group the stomach-content data. We grouped data from all fish ≤ 100 mm SL together and data from all fish ≥ 401 mm SL together due to sample sizes. We calculated volume and percent volume for each prey type within each Red Grouper size-class. We aggregated prey taxa by family for analysis. If original identification was not below the family level, then we left prey items at the taxonomic level of identification. We calculated percent volume of each prey category by size-class. For graphical purposes, we further grouped the data into a few primary categories. We divided decapods into shrimps, crabs, and lobsters. We classified fish prey as pelagic or demersal based on their typical location in the water column. We classified all groups of prey that comprised less than one percent of total volume as “other.”

All statistical analyses were completed in R statistical computing environment (R Core Team 2018). All data are published in the Gulf of Mexico Research Initiative Information and Data Cooperative (GRIIDC) website (<https://data.gulfresearchinitiative.org/data/R1.x135.120:0012>).

RESULTS

Analyzed Red Grouper

Lengths, ages, ELDs, and numbers of eye-lens laminae were broadly similar in all adult fish (Table 5.1). Collection locations spanned the north-south extent of the WFS in fish analyzed for both eye-lens isotopes and for stomach contents (Figure 5.1A and B). In both cases, the

smallest fish were primarily captured closest to shore, while no fish larger than 175 mm SL were captured in less than 7 m of water.

Eye-lens core isotopes

Core ELD for 93 Red Grouper ranged from 0.20 to 0.65 mm. Using regression (1) relating standard length (SL) to ELD, we calculated that the fish were 14-46 mm SL at the time of core completion, representing the postlarval and very early (first days) post-settlement periods (Table 5.2).

Multivariate homogeneity of group dispersion (using routine betadisper in R) found no difference in dispersion between WFS juveniles and adults ($F = 1.10$, $p = 0.30$). PERMANOVA indicated a difference between the core isotopic values of these fish ($F = 3.34$, $p < 0.05$). However, the range of values in both isotopes was quite similar (Figure 5.2A). Means for adults was slightly higher in the $\delta^{13}\text{C}$ dimension and slightly lower in the $\delta^{15}\text{N}$ dimension (Table 5.2, Figure 5.2B).

Due to low sample sizes, no statistical analyses were conducted on the additional two geographic groups (Mexico and SEFL). Visual analysis of these two groups indicated that core isotopic values for SEFL fish differed from Mexico fish, primarily in the $\delta^{15}\text{N}$ direction (Table 5.2, Figure 5.2). Although eye-lens core values for all individuals caught outside the WFS fell within the range of values observed on the WFS, these values clustered closely together within their respective $\delta^{15}\text{N}$ ranges at the extreme edges of $\delta^{15}\text{N}$ range for the WFS. Eye-lens core isotopic values for fish captured in Mexico also clustered in the $\delta^{13}\text{C}$ direction (Figure 5.2A).

Based on rules of interpretation for the eye-lens cores (Table 3.2), Spearman rank correlation indicated little difference in the isotopically derived movements of the postlarvae for

WFS juveniles and adults. In both groups, $\delta^{15}\text{N}$ had strong and moderate correlation (respectively) with ELD, indicating fish increased trophic position or moved north with increasing length during the postlarval period. In contrast, $\delta^{15}\text{N}$ did not correlate significantly with collection latitude in either group, suggesting juvenile and adult location are not related to larval location in the north-south direction (Table 5.3). In both juveniles and adults, $\delta^{13}\text{C}$ moderately correlated with ELD, indicating fish in both groups moved inshore or changed from planktonic to benthic basal-resource dependence during early life. Although juveniles had no significant correlation between eye-lens core $\delta^{13}\text{C}$ and collection longitude, a moderate negative correlation in adults suggests fish captured farthest inshore originated from farthest offshore (Table 5.3).

Lifetime eye-lens profiles: juveniles

Lifetime change in $\delta^{15}\text{N}$ was positive for all WFS juveniles except for three. Of 53 WFS juveniles, 45 (85%) had ≥ 0.5 positive correlation between $\delta^{15}\text{N}$ and ELD, increasing trophic position over the lifetime. All fish longer than 110 mm SL resulted in positive Spearman rank correlation values between $\delta^{15}\text{N}$ and ELD (Table 5.4).

Lifetime change in $\delta^{13}\text{C}$ for WFS juveniles was positive in all but one very small individual. However, correlation between $\delta^{13}\text{C}$ and ELD as well as between $\delta^{13}\text{C}$ and $\delta^{15}\text{N}$ were highly variable (Table 5.4). Visual inspection of individual $\delta^{13}\text{C}$ profiles as a function of ELD indicated many had steep increases in $\delta^{13}\text{C}$ between the core and ~ 2 mm EDL, with subsequent decreases. This observation is noted using blue or red dots in each individual profile (Figure 5.3). Note that fish for which total ELD < 2 mm do not have the descending $\delta^{13}\text{C}$ values (Figure 5.3).

Taken together, these data indicate that the majority of juvenile Red Grouper increased in trophic position while having inconsistent basal-resource dependence and moving throughout life. However, up to 11 juvenile Red Grouper (21% of sampled fish) spent their entire lives increasing $\delta^{15}\text{N}$ (increasing trophic position) while also increasing $\delta^{13}\text{C}$, indicating consistent basal-resource dependence throughout life (Figure 5.3).

Lifetime eye-lens profiles: WFS adults

WFS adult Red Grouper also increased in both $\delta^{13}\text{C}$ and $\delta^{15}\text{N}$ over the lifetime. Of the 30 individuals sampled, 25 (83%) had Spearman rank correlation between $\delta^{15}\text{N}$ and ELD of $r_s \geq 0.5$ over the lifetime (Table 5.5). This can be seen visually in individual profiles of $\delta^{15}\text{N}$:ELD (Figure 5.4).

Fewer WFS adults had significant correlations between $\delta^{13}\text{C}$ and ELD. Ten individuals (33%) had $r_s \geq 0.5$ between $\delta^{13}\text{C}$ and ELD (Table 5.5) and eight (26%) had $r_s \geq 0.5$ between $\delta^{15}\text{N}$ and $\delta^{13}\text{C}$. Again, visual analysis shows that many WFS adults had consistent regions for which $\delta^{13}\text{C}$ increased faster than $\delta^{15}\text{N}$, followed by a decrease (Figure 5.4).

Five individuals increased their trophic position while continuing to depend on the same basal resource. An additional three individuals had inconsistent trophic positions or moved sufficiently to mask trophic increase or consistent basal resource dependence. However, most WFS adults ($n = 21$) experienced trophic-position increase over the lifetime while switching basal-resource dependence or moving inconsistently within the isoscape.

Lifetime eye-lens profiles: non-WFS Red Grouper

In the five adult Red Grouper collected from Mexico, $\delta^{15}\text{N}$ and $\delta^{13}\text{C}$ increased over the lifetime. All Mexico fish had significant positive correlation between $\delta^{15}\text{N}$ and ELD. However,

only three of five had significant positive correlation between $\delta^{13}\text{C}$ and ELD and two had significant correlation between $\delta^{15}\text{N}$ and $\delta^{13}\text{C}$ (Table 5.5). Interpretations of these trends indicate that all five individuals increased trophic position throughout life. Two of five also maintained consistent basal-resource dependence. However, three switched between basal resources, potentially moving substantial distances over the lifetime (Table 5.5, Figure 5.5).

SEFL Red Grouper increased in both $\delta^{13}\text{C}$ and $\delta^{15}\text{N}$ over the lifetime. Correlation between $\delta^{15}\text{N}$ and ELD were significant and positive in all three. However, in one of three, correlation between $\delta^{13}\text{C}$ and ELD as well as between $\delta^{15}\text{N}$ and $\delta^{13}\text{C}$ were low (Table 5.5). Interpretations for these three individuals (Table 4.2) indicated that all increased trophic position over their lifetimes while two maintained single basal-resource dependence. The third fish experienced a trophic position increase but changed basal-resource dependence through life (Table 5.5, Figure 5.5).

Carbon bump

The carbon bump occurred in 33 of 55 (60%) WFS juvenile Red Grouper (Figure 5.3) and 20 of 30 (66%) WFS adult Red Grouper (Figure 5.4). Only one individual from Mexico and one from SEFL displayed a similar $\delta^{13}\text{C}$ profile (Figure 5.5).

We found no correlation between capture latitude or SL and existence of a carbon bump in the eye-lens profile of WFS juvenile or WFS adult Red Grouper. In WFS juvenile Red Grouper, the average ELD of $\delta^{13}\text{C}$ transition was 1.88 ± 0.04 mm (Table 5.6). The mean height was $3.23 \pm 0.18\text{‰}$, (Table 5.6, Figure 5.6A). In WFS adults, the average ELD of transition was 2.28 ± 0.13 mm. The mean height of transition was $3.03 \pm 0.33\text{‰}$, (Table 5.6, Figure 5.6B). The single individual from Mexico with a carbon bump displayed one of the most extreme examples,

with a height of 6.36‰, but with a similar location in the eye-lens to those from the WFS (ELD = 1.38 mm) (Figure 5.5). The single individual to display the trait from SEFL had a somewhat different pattern. $\delta^{13}\text{C}$ increased quickly 3.97‰ in early in life (ELD = 0.8 mm) but remained essentially steady until much later in the juvenile period, when the isotopic decline occurred (Figure 5.5).

Basal resource dependence

WFS juvenile and adult Red Grouper appeared to have similar basal-resource dependence. Both spent approximately 75% of the lifespan depending on mixed basal resources (Table 5.7, Figure 5.7). Latitude of capture did not correlate with proportion of the lifespan that depended on mixed basal resources in either juveniles or adults (juvenile $r_s = -0.18$, $p = 0.11$; adult $r_s = -0.08$, $p = 0.66$). In both WFS juvenile and adult fish, some individuals depended on a variety of basal resources over the lifetime while others depended on mixed basal resources throughout (Figures 5.3 and 5.4). Many WFS adults and juveniles began their lives depending on planktonic basal resources, but quickly transitioned to mixed resource used around the time of settlement (Figures 5.3 and 5.4).

We observed a similar distribution of resource use in Mexican fish (Table 5.7, Figure 5.7), with four of five individuals beginning life depending on planktonic resources and quickly transitioning to mixed resource dependence. Stable-isotope values for one of five fish indicated benthic resource dependence during the juvenile period (Figure 5.5). SEFL Red Grouper spent less time dependent on planktonic resources and more time dependent on benthic basal resources (Table 5.7, Figure 5.7). Two of three individuals spent the latter half of their lifetimes dependent on strictly benthic basal resources (Figure 5.5)

Stomach contents

The stomach contents from 521 Red Grouper collected on the WFS (Figure 5.1B) revealed multiple diet shifts over the lifetime. Red Grouper between 37- and 150-mm SL preyed heavily on decapod shrimps, which comprised 62–72% of dietary volume. The primary families of shrimp consumed by Red Grouper less than 100 mm SL were Penaeidae and Caridae (26 and 37% respectively), with crabs from the family Galatheidae comprising an additional 23% of volume. Individuals between 100- and 150-mm SL also consumed diets heavy in penaeid shrimps (69%), with crabs from the family Majidae comprising an additional 18% by volume. Although not comprising a large volume, several species of grass shrimp were recorded in the stomachs of Red Grouper in the length range of 100-150 mm SL, including *Hippolyte zostericola* and *Palaemonetes pugio*, both of which inhabit very shallow, estuarine waters.

By 150 mm SL, Red Grouper were less heavily dependent on shrimps, and began feeding on various families of crabs and other types of invertebrates. While penaeid shrimps still comprised 20% by volume for Red Grouper in the length range of 150–200 mm SL, the most consumed category of prey was crabs with various families (primarily Portunidae and Majidae), comprising 44% of the diet. At this length, fish comprised approximately 16% of the diet. Red Grouper between 200- and 300-mm SL had the most eclectic diets, consuming prey from 20 families of shrimps and crabs along with small volumes of cnidarians, gastropods, annelid worms, and even tunicates and several families of fish. Between 200- and 350-mm SL, fish and invertebrates each comprised about half of the diet.

By 250 mm SL, squids from the family Loliginidae began contributing substantially to the diet (15% by volume) and continued to be an important diet component until about 350 mm SL. By 300 mm SL, squids were the primary invertebrate consumed (25% by volume), with

crabs still making up about 17% of the diet and over 52% of the diet being composed of fish, primarily demersal fishes. Red Grouper larger than 350 mm SL consumed higher proportions of fishes (63–78%), with most of the identifiable prey being demersal fishes. Red Grouper continued to consume shrimps (up to 3%) and lobsters (up to 18%) but the most consumed non-fish prey was crabs (8–37%) (Table 5.8 and Figure 5.8).

DISCUSSION

We characterized the lifetime geographic and diet histories of Red Grouper using a combination of eye-lens stable isotope, catch locations, and stomach-contents. We found that Red Grouper natal origins on the WFS were relatively consistent between juveniles and adults, suggesting a stable spawning area year-to-year within the time constraints of the study. Red Grouper from outside WFS (Mexico and SEFL) had distinctly different core $\delta^{15}\text{N}$ values from one another, which is consistent with known or inferred isotopic trends for their respective regions. We found that virtually all Red Grouper, regardless of age or location, increased in $\delta^{15}\text{N}$ during life, indicating increasing trophic position with body growth. We also found that an increase and subsequent decrease in $\delta^{13}\text{C}$ (i.e., carbon bump) occurred in the majority of WFS Red Grouper, suggesting two distinct shifts in basal-resource dependence through movement during the first year of life. The apex of the carbon bump approximately coincided with a brief period during which Red Grouper are found in shallow water. We found that Red Grouper captured in Mexico and SEFL displayed consistent basal-resource dependence (through $\delta^{13}\text{C}$ eye-lens profiles). This may be due to shorter distances moved during the first year or smaller differences in $\delta^{13}\text{C}$ for the region. The techniques developed here are applicable to numerous other marine fisheries species in the southeastern United States and beyond.

WFS Spawning locations and postlarval habits

Average WFS Red Grouper $\delta^{13}\text{C}$ and $\delta^{15}\text{N}$ eye-lens core values near -19‰ and 7‰ respectively suggest a trophic position of approximately 3 and planktonic basal-resource dependence when compared to the isotopes measured for primary producers on the WFS (Radabaugh et al. 2013). Red Grouper use broadcast spawning to produce millions of buoyant eggs (Lowerre-Barbieri et al. 2014). Although no diet data exist for wild Red Grouper larvae, the species has been successfully reared in the lab using wild-collected zooplankton (Colin et al. 1996). A closely related species, Nassau Grouper (*Epinephelus striatus*), has been found to feed primarily on calanoid copepods and decapod larvae during the larval period (Grover et al. 1998). Copepods are omnivorous, feeding on a combination of phytoplankton and heterotrophic protists, and have been calculated to feed at a trophic position of 2.1-2.7 (Bode et al. 2015, Umezawa et al. 2018). Feeding on these resources would put the larval grouper near trophic position 3-3.5 with plankton-based basal-resource dependence (Popp et al. 1998, Burkhardt et al. 1999, Grippo et al. 2011, Radabaugh et al. 2014), corroborating the isotopic findings.

Assuming all larval Red Grouper feed on the same types of prey and at the same trophic position, the isotopic values in eye-lens cores may be interpreted as geographic location. With a wide range of both $\delta^{13}\text{C}$ and $\delta^{15}\text{N}$ core values ($\sim 3\text{‰}$ in $\delta^{15}\text{N}$ and $\sim 5\text{‰}$ in $\delta^{13}\text{C}$) and little difference between observed core isotope values between juveniles and adults, these results suggest that Red Grouper maintain a consistent central spawning region year-to-year on the WFS. Within one marine protected area on the WFS, Red Grouper “holes” known to be used as spawning locations (Coleman et al. 1996) have been observed to be maintained by members of the species for at least ten years (Grasty et al. 2019). These known spawning sites are centered around 70 m depth. Observed core isotope values suggest that postlarvae may remain nearby.

In eye-lens cores of WFS juveniles and adults, $\delta^{13}\text{C}$ and $\delta^{15}\text{N}$ correlated positively with core ELD, indicating a rapid diet change that included more benthic-associated prey (Fry and Wainright 1991) along with a small but perceptible increase in trophic position over the weeks of the postlarval and settlement periods, represented by cores of increasing size (Pinnegar and Polunin 1999). However, when we investigated both $\delta^{13}\text{C}$ and $\delta^{15}\text{N}$ for correlation with collection location, the isotopic values had no relationship in either adults or juveniles, suggesting that Red Grouper maintain a continuous spawning area on the WFS that varies little over time (Radabaugh and Peebles 2014).

WFS lifetime isotopic profiles: trophic growth, diet, shifts, and basal-resource dependence

Most WFS Red Grouper had at least 50% correlation between $\delta^{15}\text{N}$ and ELD across the lifetime. These results suggest that Red Grouper experience an increase in trophic position during life. The consistency of the increase over time suggests the fish did not migrate along the $\delta^{15}\text{N}$ gradient. A similar pattern been shown using muscle $\delta^{15}\text{N}$ from variously sized individuals from the same species (Graham et al. 2007, Sweeting et al. 2007, Buchheister and Latour 2011) as well as the eye lenses of several species of fish (Wallace et al. 2014, Quaeck-Davies et al. 2018, Kurth et al. 2019, Simpson et al. 2019).

Lifetime profiles for $\delta^{13}\text{C}$ were quite different from $\delta^{15}\text{N}$ profiles in most WFS Red Grouper. The majority of WFS juvenile and adult eye-lenses had low correlation between $\delta^{13}\text{C}$ and ELD, in contrast with 36 Tilefish (*Lopholatilus chamaeleonticeps*) from a similar region (Chapter 4). Tilefish represent a model of high lifetime site fidelity and consistent lifetime diet (Chapter 4). Therefore, we suspect that diets and/or locations of Red Grouper changed throughout the lifetime across depth.

Of the approximately 600 individuals collected for the current work, we found that larger Red Grouper tended to be located in deeper water than smaller individuals, with individuals between 75- and 150-mm SL being the only size-class captured in water shallower than 10 m. Some Red Grouper stomachs from fish < 150 mm SL contained prey known to occur only in seagrass beds, which grow in a maximum of 2 m of water on the WFS. Historic survey data support the interpretation of lifetime movement crossing the depth gradient of the WFS. Catch records for both fishery-independent and fishery-dependent surveys indicate that small Red Grouper are usually encountered in shallower water than large fish on the WFS (Moe 1969, Lombardi-Carlson et al. 2008, Gruss et al. 2017). When examining movement of tagged individuals, Burns (2009) found that while most Red Grouper remained within 1 km of original capture location, longer times at-large (> 2 y) correlated with higher probability of long-distance movement. She also found that Red Grouper movements > 1 km were uniformly toward deeper water.

These data suggest that Red Grouper follow similar patterns of movement to those verified for Gag (*Mycteroperca microlepis*), on a somewhat different timescale. Postlarvae move to shallow-water habitats to become juveniles and adults return to deeper water as they mature (Weisberg et al. 2014, Carruthers et al. 2015). However, differences are notable between the species. While Gag are encountered routinely in polyhaline seagrass beds throughout their first year of life, few Red Grouper are captured in these areas over a much more limited time-period (Figure 5.1A, SEADAR 2015). Young Red Grouper are more often observed by divers hidden in small crevices of natural and artificial reefs on the WFS (Stallings, unpublished data, (Moe 1969)). This strategy of remaining hidden under ledges may partially account for the inaccessibility of the small size-classes by standard fisheries sampling gears. In addition, the

shape and location of the carbon bump, indicates that Red Grouper spend only short period in shallow water, subsequently moving to deeper water within a few months.

A bump in the $\delta^{13}\text{C}$ profiles of WFS Red Grouper

When we investigated WFS juveniles and adults $\delta^{13}\text{C}$ eye-lens profiles more closely, we noticed a carbon bump (rapid increase and subsequent decrease in $\delta^{13}\text{C}$) in the majority of fish. We also observed that the smallest Red Grouper displayed only an increase in $\delta^{13}\text{C}$, with no subsequent decrease. These fish had maximum ELDs smaller than the diameter at which $\delta^{13}\text{C}$ values began declining in larger fish. We found the average peak in the carbon bump to be at approximately 2 mm ELD, which is consistent with a SL of approximately 100 mm SL and an age of less than one year. We found that, according to the SL:ELD regression, resolution of eye-lens profiles was highest in the first year due to faster growth during this period (Casselmann 1990, Pankhurst and Eagar 1996, Beullens et al. 1997).

Initial $\delta^{13}\text{C}$ values corresponded with a diet composed of zooplankton. However, as Red Grouper settled into benthic habitats, they appear to rely more heavily on benthic prey. The smallest individuals (37-100 mm SL) in our stomach-content analysis fed almost exclusively on various families of small shrimps. These small shrimp taxa are omnivorous benthic feeders (Winkler et al. 2007, Sierszen et al. 2011). While this places the growing Red Grouper near the same trophic position as during the postlarval stage, a diet composed primarily of benthic organisms could result in $\delta^{13}\text{C}$ increasing quickly.

A rapid switch from feeding in the plankton to feeding from the benthos is common among reef-associated species. Other grouper species have been shown to have similar post-settlement diets. For example, Nassau Grouper have been found to feed primarily on

gammaridean amphipods, isopods and mysid shrimps (Grover et al. 1998), and Gag rely heavily on epibenthic prey (Mullaney and Gale 1996). Isotopic values may represent not only prey but also depth (through the dominant basal resource for the region). In the example of Gag, muscle $\delta^{13}\text{C}$ in fish 100-200 mm SL (found in shallow seagrass beds) were similar to values observed near the apex of the Red Grouper $\delta^{13}\text{C}$ profiles. Together catch records, isotope records, and stomach content records suggest that most WFS Red Grouper are spawned in deep water, transit the WFS to shallower nursery areas, and begin returning toward deeper water over the first year of life. Over the first year of life, the species also transitions food sources several times, taking advantage of the availability of larger prey as gape-size increases.

It is possible that some Red Grouper on the WFS do not make cross-shelf migrations but remain stationary through life. Approximately one-third of WFS Red Grouper did not show a carbon bump in their $\delta^{13}\text{C}$ profile. These individuals had high correlations between $\delta^{13}\text{C}$ and $\delta^{15}\text{N}$, much like Tilefish (Chapter 4), suggesting little movement and no basal-resource dependence transitions throughout the juvenile period. A large tagging study of over 30,000 fish on the WFS encountered a few fish < 200 mm SL in water deeper than 30 m, and several fish > 400 mm SL in water shallower than 10 m (FWRI-FDM, personal communication). If an individual finds adequate resources, there is no need to move.

Non-WFS spawning locations

Stable isotopic values in the eye-lens cores of SEFL and Mexico Red Grouper fell within the range of WFS values, but differed substantially from one another, primarily in the $\delta^{15}\text{N}$ direction. This difference reflects the isotopic backgrounds for the two regions. Red Grouper from Mexico had $\delta^{13}\text{C}$ and $\delta^{15}\text{N}$ eye-lens core values that were tightly grouped despite being

collected across a large geographic area. This may indicate a restricted spawning area in the region, or may be a symptom of a low-variability isoscape (Peebles and Hollander 2020).

The $\delta^{15}\text{N}$ values off the southeast coast of Florida are expected to be lower than other regions in this study due to the dominance of diazotrophs in the marine primary productivity for the area (McClelland et al. 2003). In addition, $\delta^{13}\text{C}$ would be expected to be high due the exceptionally clear water, allowing for benthic primary productivity throughout continental shelf waters (Palandro et al. 2004, Lidz et al. 2008). In a small stable isotope study examining fish tissue from Biscayne National Park, the authors showed relatively low values of $\delta^{15}\text{N}$ and high values of $\delta^{13}\text{C}$ throughout their study area in relation to values observed on the WFS (Curtis et al. 2017). In addition, the $\delta^{15}\text{N}$ and $\delta^{13}\text{C}$ core values for two mesopredator species (Curtis 2016) were quite similar to our results for Red Grouper, suggesting all three species begin life at similar trophic positions and similar depths in this region. These results also highlight the need to develop a high-resolution isoscape for coastal waters of the southeastern United States.

Non-WFS lifetime isotopic profiles: trophic growth and basal-resource dependence

With a less variable $\delta^{13}\text{C}$ isotopic backgrounds than the WFS, we observe consistent $\delta^{13}\text{C}$ over the lifetime rather than a frequent shifting of $\delta^{13}\text{C}$ in the eye-lens record. Of the eight Red Grouper investigated from outside the WFS, the carbon bump occurred in only two $\delta^{13}\text{C}$ profiles. It seems striking that Red Grouper in these other regions do not show similar $\delta^{13}\text{C}$ patterns to Red Grouper captured on the WFS. Broadly similar diets have been reported for juveniles captured on Campeche Bank and WFS (Brule and Canche 1993, Weaver 1996). Although no diet information is available for Red Grouper captured off the southeast coast of the United States, Red Grouper from Brazilian reefs displayed similar reliance on crustaceans early in life while

incorporating fish into their diets later in life (Freitas et al. 2017). It appears reasonable to assume that juvenile Red Grouper using the clear water reefs of the Florida reef tract would also have broadly similar ontogenetic diet trends. Differences in diet do not seem to be driving differences in $\delta^{13}\text{C}$ among regions.

Differences in the $\delta^{13}\text{C}$ profiles between the WFS and the other regions may highlight differences in ontogenetic movements among the populations. It is possible that Red Grouper from the Florida reef tract and Campeche Bank move shorter distances during the first year of life than those from the WFS. Suitable habitats for each life-stage may be more confined and/or more contiguous on these areas than on the WFS. WFS reefs are highly fractured and scattered across large expanses of unconsolidated sediments (Hine and Locker 2011); whereas, the Florida reef tract and the Alacran reef on the Campeche Bank are composed of more contiguous hard substrates (Kormmcker et al. 1959, Ogden et al. 1994). The Red Grouper population on the WFS may have evolved to take advantage of heterogeneous habitat availability with variability in food resources across large spatial scales. While this adaptation may not have been necessary outside the region.

Conclusions and future directions

We used eye-lens stable isotope analysis paired with stomach-content analysis and catch data to reconstruct the diets, basal-resource dependence, and potential movements of Red Grouper throughout the lifespan, particularly in the first one to two years. We found that isotopic values of postlarval Red Grouper on the WFS varied broadly, which is consistent with a spawning area covering much of the WFS, as described in the literature. We also found that mean and distribution of eye-lens core isotope values were quite similar between WFS juveniles and adults, indicating dominant areas may shift subtly, but do not change radically year-over-

year. While Red Grouper captured outside the WFS displayed eye-lens core isotope values similar to those found on the WFS, they were clustered at opposite ends of the $\delta^{15}\text{N}$ spectrum, which is consistent with the isotopic background for those regions.

Juvenile and adult Red Grouper from the WFS and Mexico spent a comparable percentage of their life depending on each of the three available basal-resource classes (benthic, mixed, planktonic), whereas fish captured on the east coast of Florida depended most heavily on benthic basal resources. Finally, we found that over two-thirds of WFS Red Grouper displayed a large increase and subsequent decrease in $\delta^{13}\text{C}$ (carbon bump) during the first year of life. These clear isotopic shifts with ontogeny paralleled catch depth records, with a limited time use of very shallow water during the first year of life. The concurrence of these data types suggests cross-shelf movement of the fish during the first year while taking advantage of additional types of prey. In contrast, only a small fraction of fish from outside the WFS displayed a similar pattern in $\delta^{13}\text{C}$. This may be due to the larger distances traveled by WFS Red Grouper, higher variability of the WFS isoscape, or a combination of factors. In short, the interpretations of eye-lens stable isotopes corroborate and clarify Red Grouper habitat needs and diets observed through traditional data types. This powerful tool has the potential to streamline and simplify studies of numerous species going forward.

LITERATURE CITED

- Acosta-Pachon, T. A., S. Ortega-Garcia, and B. Graham. 2015. Stable carbon and nitrogen isotope values of dorsal spine age rings indicate temporal variation in the diet of striped marlin (*Kajikia audax*) in waters around Cabo San Lucas, Mexico. *Rapid Communications in Mass Spectrometry* **29**:1676-1686.
- Beullens, K., E. H. Eding, F. Ollevier, J. Komen, and C. J. J. Richter. 1997. Sex differentiation, changes in length, weight and eye size before and after metamorphosis of European eel (*Anguilla anguilla* L) maintained in captivity. *Aquaculture* **153**:151-162.

- Bode, M., W. Hagen, A. Schukat, L. Teuber, D. Fonseca-Batista, F. Dehairs, and H. Auel. 2015. Feeding strategies of tropical and subtropical calanoid copepods throughout the eastern Atlantic Ocean - Latitudinal and bathymetric aspects. *Progress in Oceanography* **138**:268-282.
- Brule, T., and L. G. R. Canche. 1993. Food habits of juvenile red groupers, *Epinephelus morio* (Valenciennes, 1828) from Campeche bank, Yucatan, Mexico. *Bulletin of Marine Science* **52**:772-779.
- Brule, T., C. Deniel, T. Colas-Marrufo, and M. Sanchez-Crespo. 1999. Red Grouper reproduction in the southern Gulf of Mexico. *Transactions of the American Fisheries Society* **128**:385-402.
- Buchheister, A., and R. J. Latour. 2011. Trophic ecology of Summer Flounder in lower Chesapeake Bay inferred from stomach content and stable isotope analyses. *Transactions of the American Fisheries Society* **140**:1240-1254.
- Burbank, M., M. Finch, D. A. R. Andrew R. Drake, and M. Power. 2019. Diet and isotopic niche of Eastern Sand Darter (*Ammocrypta pellucida*) near the northern edge of its range: a test of niche specificity. *Canadian Journal of Zoology*.
- Burkhardt, S., U. Riebesell, and I. Zondervan. 1999. Stable carbon isotope fractionation by marine phytoplankton in response to daylength, growth rate, and CO₂ availability. *Marine Ecology Progress Series* **184**:31-41.
- Burns, K. 2009. Evaluation of the efficacy of the minimum size rule in the Red Grouper and Red Snapper fisheries with respect to J and circle hook mortality and barotrauma and the consequences for survival and movement. University of South Florida, Tampa.
- Burns, K. M., and J. T. Froeschke. 2012. Survival of Red Grouper (*Epinephalus morio*) and red snapper (*Lutjanus campechanus*) caught on J-hooks and circle hooks in the Florida recreational and recreational-for-hire fisheries. *Bulletin of Marine Science* **88**:633-646.
- Carpenter, E. J., H. R. Harvey, B. Fry, and D. G. Capone. 1997. Biogeochemical tracers of the marine cyanobacterium Trichodesmium. *Deep-Sea Research Part I-Oceanographic Research Papers* **44**:27-38.
- Carruthers, T. R., J. F. Walter, M. K. McAllister, and M. D. Bryan. 2015. Modelling age-dependent movement: an application to Red and Gag Groupers in the Gulf of Mexico. *Canadian Journal of Fisheries and Aquatic Sciences* **72**:1159-1176.
- Casselman, J. M. 1990. Growth and relative size of calcified structures of fish. *Transactions of the American Fisheries Society* **119**:673-688.
- Choy, C. A., B. N. Popp, C. C. S. Hannides, and J. C. Drazen. 2015. Trophic structure and food resources of epipelagic and mesopelagic fishes in the North Pacific Subtropical Gyre ecosystem inferred from nitrogen isotopic compositions. *Limnology and Oceanography* **60**:1156-1171.
- Coleman, F. C., C. C. Koenig, and L. A. Collins. 1996. Reproductive styles of shallow-water groupers (Pisces: Serranidae) in the eastern Gulf of Mexico and the consequences of fishing spawning aggregations. *Environmental Biology of Fishes* **47**:129-141.
- Coleman, F. C., C. C. Koenig, K. M. Scanlon, S. Heppell, S. Heppell, and M. W. Miller. 2010. Benthic habitat modification through excavation by red grouper, *Epinephelus morio*, in the northeastern Gulf of Mexico. *Open Fish Science Journal* **3**:1-15.
- Coleman, F. C., K. M. Scanlon, and C. C. Koenig. 2011. Groupers on the edge: shelf edge spawning habitat in and around marine reserves of the northeastern Gulf of Mexico. *Professional Geographer* **63**:456-474.

- Colin, P. L., C. C. Koenig, and W. A. Laroche. 1996. Development from egg to juvenile of the Red Grouper (*Epinephelus morio*) (Pisces: Serranidae) in the laboratory. Pages 399-414 in F. ArreguinSanchez, J. L. Munro, M. C. Balgos, and D. Pauly, editors. Biology, fisheries and culture of tropical groupers and snappers: Proceedings of an EPOMEX/ICARM International workshop on tropical snappers and groupers. International Center for Living Aquatic Resources Management, University of Campeche, Mexico.
- Curtis, J. S. 2016. Resource use overlap in a native grouper and invasive lionfish. University of South Florida, Tampa, FL.
- Curtis, J. S., K. R. Wall, M. A. Albins, and C. D. Stallings. 2017. Diet shifts in a native mesopredator across a range of invasive lionfish biomass. *Marine Ecology Progress Series* **573**:215-228.
- Dahm, R., H. B. Schonhaler, A. S. Soehn, J. Van Marle, and G. Vrensen. 2007. Development and adult morphology of the eye lens in the zebrafish. *Experimental Eye Research* **85**:74-89.
- Eddy, C. 2019. Trophic discrimination factors for invasive lionfish (*Pterois volitans* and *P. miles*) in Bermuda. *Biological Invasions*.
- Eldridge, P. J. 1988. The southeast area monitoring and assessment program (SEAMAP)- A state-federal-university program for collection, management, and dissemination of fishery-independent data and information in the southeastern United States. *Marine Fisheries Review* **50**:29-39.
- Freitas, M. O., V. Abilhoa, H. L. Spach, C. V. Minte-Vera, R. B. Francini, L. Kaufman, and R. L. Moura. 2017. Feeding ecology of two sympatric species of large-sized groupers (Perciformes: Epinephelidae) on Southwestern Atlantic coralline reefs. *Neotropical Ichthyology* **15**.
- Fry, B. 2006. Stable isotope ecology. Springer Science+Business Media, New York, NY.
- Fry, B., and S. C. Wainright. 1991. Diatom sources of C-13 rich carbon in marine food webs. *Marine Ecology Progress Series* **76**:149-157.
- Golikov, A. V., F. R. Ceia, R. M. Sabirov, Z. I. Zaripova, M. E. Blicher, D. V. Zakharov, and J. C. Xavier. 2018. Ontogenetic changes in stable isotope ($\delta^{13}\text{C}$ and $\delta^{15}\text{N}$) values in squid *Gonatus fabricii* (Cephalopoda) reveal its important ecological role in the Arctic. *Marine Ecology Progress Series* **606**:65-78.
- Graham, B. S., D. Grubbs, K. Holland, and B. N. Popp. 2007. A rapid ontogenetic shift in the diet of juvenile Yellowfin Tuna from Hawaii. *Marine Biology* **150**:647-658.
- Granneman, J. E. 2018. Evaluation of trace-metal and isotopic records as techniques for tracking lifetime movement patterns in fishes. University of South Florida, Tampa, FL.
- Grasty, S., C. C. Wall, J. W. Gray, J. Brizzolara, and S. A. Murawski. 2019. Temporal persistence of Red Grouper holes and analysis of associated fish assemblages from towed camera data in the Steamboat Lumps marine protected area. *Transactions of the American Fisheries Society*:1-9.
- Grippo, M. A., J. W. Fleeger, S. F. Dubois, and R. Condrey. 2011. Spatial variation in basal resources supporting benthic food webs revealed for the inner continental shelf. *Limnology and Oceanography* **56**:841-856.
- Grover, J. J., D. B. Eggleston, and J. M. Shenker. 1998. Transition from pelagic to demersal phase in early-juvenile Nassau grouper, *Epinephelus striatus*, pigmentation, squamation, and ontogeny of diet. *Bulletin of Marine Science* **62**:97-113.

- Gruss, A., J. T. Thorson, S. R. Sagarese, E. A. Babcock, M. Karnauskas, J. F. Walter, III, and M. Drexler. 2017. Ontogenetic spatial distributions of red grouper (*Epinephelus morio*) and gag grouper (*Mycteroperca microlepis*) in the US Gulf of Mexico. *Fisheries Research* **193**:129-142.
- Hall-Scharf, B. J., T. S. Switzer, and C. D. Stallings. 2016. Ontogenetic and Long-Term Diet Shifts of a Generalist Juvenile Predatory Fish in an Urban Estuary Undergoing Dramatic Changes in Habitat Availability. *Transactions of the American Fisheries Society* **145**:502-520.
- Hine, A. C., and S. D. Locker. 2011. The Florida Gulf of Mexico continental shelf—great contrasts and significant transitions. *The Gulf of Mexico: Origin, Waters, and Marine Life*.
- Huelster, S. 2015. Comparison of isotope-based biomass pathways with groundfish community structure in the eastern Gulf of Mexico. Masters. University of South Florida, Tampa.
- Hunsicker, M. E., T. E. Essington, K. Y. Aydin, and B. Ishida. 2010. Predatory role of the commander squid *Beryteuthis magister* in the eastern Bering Sea: insights from stable isotopes and food habits. *Marine Ecology Progress Series* **415**:91-108.
- Kendall, C., S. R. Silva, and V. J. Kelly. 2001. Carbon and nitrogen isotopic compositions of particulate organic matter in four large river systems across the United States. *Hydrological Processes* **15**:1301-1346.
- Keough, J. R., C. A. Hagley, E. Ruzzycki, and M. Sierszen. 1998. delta C-13 composition of primary producers and role of detritus in a freshwater coastal ecosystem. *Limnology and Oceanography* **43**:734-740.
- Kjeldsen, H., J. Heinemeier, S. Heegaard, C. Jacobsen, and N. Lynnerup. 2010. Dating the time of birth: A radiocarbon calibration curve for human eye-lens crystallines. *Nuclear Instruments & Methods in Physics Research Section B-Beam Interactions with Materials and Atoms* **268**:1303-1306.
- Kormicker, L. S., F. Bonet, R. Cann, and C. Hoskin. 1959. Alacran Reef, Campeche Bank, Mexico. *Institute of marine science* **6**:1-22.
- Kurth, B. N., E. Peebles, and C. D. Stallings. 2019. Atlantic Tarpon (*Megalops atlanticus*) exhibit upper estuarine habitat dependence followed by foraging system fidelity after ontogenetic habitat shifts. *Estuarine Coastal and Shelf Science*.
- Lidz, B. H., J. C. Brock, and D. B. Nagle. 2008. Utility of shallow-water ATRIS images in defining biogeologic processes and self-similarity in skeletal Scleractinia, Florida reefs. *Journal of Coastal Research* **24**:1320-1338.
- Lombardi-Carlson, L. A., M. A. Graee, and D. E. D. A. Fuentes. 2008. Comparison of Red grouper populations from Campeche Bank, Mexico and West Florida Shelf, United States. *Southeastern Naturalist* **7**:651-664.
- Lowerre-Barbieri, S., L. Crabtree, T. S. Switzer, and R. H. McMichael Jr. 2014. Maturity, sexual transition, and spawning seasonality in the protogynous red grouper on the West Florida Shelf. Page 21 pp SEDAR 42. SEDAR42-DW-7, North Charleston, SC.
- Lynnerup, N., H. Kjeldsen, S. Heegaard, C. Jacobsen, and J. Heinemeier. 2008. Radiocarbon Dating of the Human Eye Lens Crystallines Reveal Proteins without Carbon Turnover throughout Life. *Plos One* **3**.
- Matley, J. K., G. E. Maes, F. Devloo-Delva, R. Huerlimann, G. Chua, A. J. Tobin, A. T. Fisk, C. A. Simpfendorfer, and M. R. Heupel. 2018. Integrating complementary methods to improve diet analysis in fishery-targeted species. *Ecology and Evolution*:1-13.

- McClelland, J. W., C. M. Holl, and J. P. Montoya. 2003. Relating low delta N-15 values of zooplankton to N-2-fixation in the tropical North Atlantic: insights provided by stable isotope ratios of amino acids. *Deep-Sea Research Part I-Oceanographic Research Papers* **50**:849-861.
- McMahon, K. W., S. R. Thorrold, L. A. Houghton, and M. L. Berumen. 2016. Tracing carbon flow through coral reef food webs using a compound-specific stable isotope approach. *Oecologia* **180**:809-821.
- Meath, B., E. B. Peebles, B. A. Seibel, and H. Judkins. 2019. Stable isotopes in the eye lenses of *Doryteuthis plei* (Blainville 1823): exploring natal origins and migratory patterns in the eastern Gulf of Mexico. *Continental Shelf Research*.
- Moe, M. A. J. 1969. Biology of the Red grouper *Epinephelus morio* from the eastern Gulf of Mexico. Pages 1-95 Florida Department of Natural Resources Marine Research Laboratory Professional Papers Series. Fish and Wildlife Research Institute, St. Petersburg, FL.
- Mullaney, M. D., and L. D. Gale. 1996. Ecomorphological relationships in ontogeny: Anatomy and diet in gag, *Mycteroperca microlepis* (Pisces: Serranidae). *Copeia*:167-180.
- Murawski, S. A., E. B. Peebles, A. Gracia, J. W. Tunnell, and M. Armenteros. 2018. Comparative abundance, species composition, and demographics of continental shelf fish assemblages throughout the Gulf of Mexico. *Marine and Coastal Fisheries* **10**:325-346.
- Nawrocki, B., S. F. Colborne, D. J. Yurkowski, and A. T. Fisk. 2016. Foraging ecology of Bowfin (*Amia calva*), in the Lake Huron-Erie Corridor of the Laurentian Great Lakes: Individual specialists in generalist populations. *Journal of Great Lakes Research* **42**:1452-1460.
- Nielsen, J., R. B. Hedeholm, J. Heinemeier, P. G. Bushnell, J. S. Christiansen, C. B. Ramsey, R. W. Brill, M. Simon, K. F. Steffensen, and J. F. Steffensen. 2016. Eye lens radiocarbon reveals centuries of longevity in the Greenland shark (*Somniosus microcephalus*). *Science* **353**:702-704.
- NOAA Fisheries. 2019. Gulf of Mexico Historical Commercial Landings and Annual Catch Limit Monitoring.
- O'Connor, B. S., F. E. Muller-Karger, R. W. Nero, C. M. Hu, and E. B. Peebles. 2016. The role of Mississippi River discharge in offshore phytoplankton blooming in the northeastern Gulf of Mexico during August 2010. *Remote Sensing of Environment* **173**:133-144.
- Ogden, J. C., J. W. Porter, N. P. Smith, A. M. Szmant, W. C. Jaap, and D. Forcucci. 1994. A long-term interdisciplinary study of the Florida-keys seascape. *Bulletin of Marine Science* **54**:1059-1071.
- Oksanen, J., F. G. Blanchet, M. Friendly, R. Kindt, P. Legendre, D. McGinn, P. R. Minchin, R. B. O'Hara, G. L. Simpson, P. Solymos, M. H. H. Stevens, E. Szoecs, and H. Wagner. 2019. Vegan: community ecology package. R package version 2.5-4.
- Palandro, D., C. Hu, S. Andrefouet, and F. E. Muller-Karger. 2004. Synoptic water clarity assessment in the Florida Keys using diffuse attenuation coefficient estimated from Landsat imagery. *Hydrobiologia* **530**:489-493.
- Pankhurst, P. M., and R. Eagar. 1996. Changes in visual morphology through life history stages of the New Zealand snapper, *Pagrus auratus*. *New Zealand Journal of Marine and Freshwater Research* **30**:79-90.
- Parry, M. 2008. Trophic variation with length in two ommastrephid squids, *Ommastrephes bartramii* and *Sthenoteuthis oualaniensis*. *Marine Biology* **153**:249-256.

- Patterson, W. F., J. Chanton, D. Hollander, E. A. Goddard, B. Barnett, and J. H. Tarnecki. 2020. The Utility of Stable and Radioisotopes in Fish Tissues as Biogeochemical Tracers of Marine Oil Spill Food Web Effects. *in* M. S. e. a. (eds), editor. Scenarios and Responses to Future Deep Oil Spills.
- Peebles, E. B., and D. J. Hollander. 2020. Combining Isoscapes with Tissue-Specific Isotope Records to Recreate the Geographic Histories of Fish. Pages 203-218 *in* S. A. Murawski, C. H. Ainsworth, S. Gilbert, D. J. Hollander, C. B. Paris, M. Schlüter, and D. L. Wetzel, editors. Scenarios and Responses to Future Deep Oil Spills. Springer, Cham, Switzerland.
- Pinnegar, J. K., and N. V. C. Polunin. 1999. Differential fractionation of delta C-13 and delta N-15 among fish tissues: implications for the study of trophic interactions. *Functional Ecology* **13**:225-231.
- Popp, B. N., E. A. Laws, R. R. Bidigare, J. E. Dore, K. L. Hanson, and S. G. Wakeham. 1998. Effect of phytoplankton cell geometry on carbon isotopic fractionation. *Geochimica Et Cosmochimica Acta* **62**:69-77.
- Quaeck-Davies, K., V. A. Bendall, K. M. MacKenzie, S. Hetherington, J. Newton, and C. N. Trueman. 2018. Teleost and elasmobranch eye lenses as a target for life-history stable isotope analyses. *Peerj* **6**:26.
- Queiros, J. P., Y. Chereil, F. R. Ceia, A. Hilario, J. Roberts, and J. C. Xavier. 2018. Ontogenic changes in habitat and trophic ecology in the Antarctic squid *Kondakovia longimana* derived from isotopic analysis on beaks. *Polar Biology* **41**:2409-2421.
- R Core Team. 2018. R: A language and environment for statistical computing. R Foundation for Statistical Computing, Vienna, Austria.
- Radabaugh, K. R., D. J. Hollander, and E. B. Peebles. 2013. Seasonal delta C-13 and delta N-15 isoscapes of fish populations along a continental shelf trophic gradient. *Continental Shelf Research* **68**:112-122.
- Radabaugh, K. R., E. M. Malkin, D. J. Hollander, and E. B. Peebles. 2014. Evidence for light-environment control of carbon isotope fractionation by benthic microalgal communities. *Marine Ecology Progress Series* **495**:77-90.
- Radabaugh, K. R., and E. B. Peebles. 2014. Multiple regression models of $\delta^{13}\text{C}$ and $\delta^{15}\text{N}$ for fish populations in the eastern Gulf of Mexico. *Continental Shelf Research* **84**:158-168.
- SEDAR. 2015. SEDAR 42 Stock Assessment Report - Gulf of Mexico Red Grouper. 42.
- Shi, Y. R., K. Barton, A. De Maria, J. M. Petrash, A. Shiels, and S. Bassnett. 2009. The stratified syncytium of the vertebrate lens. *Journal of Cell Science* **122**:1607-1615.
- Sierszen, M. E., J. R. Kelly, T. D. Corry, J. V. Scharold, and P. M. Yurista. 2011. Benthic and pelagic contributions to Mysis nutrition across Lake Superior. *Canadian Journal of Fisheries and Aquatic Sciences* **68**:1051-1063.
- Simpson, S., D. Sims, and C. N. Trueman. 2019. Ontogenetic trends in resource partitioning and trophic geography of sympatric skates (Rajidae) inferred from stable isotope composition across eye lenses. *Marine Ecology Progress Series* **624**:103-116.
- Sokal, R. R., and F. J. Rohlf. 1994. *Biometry: The principles and practices of statistics in biological research* third (3rd) edition.
- Stewart, D. N., J. Lango, K. P. Nambiar, M. J. S. Falso, P. G. FitzGerald, D. M. Rocke, B. D. Hammock, and B. A. Buchholz. 2013. Carbon turnover in the water-soluble protein of the adult human lens. *Molecular Vision* **19**:463-475.

- Sweeting, C. J., J. Barry, C. Barnes, N. V. C. Polunin, and S. Jennings. 2007. Effects of body size and environment on diet-tissue delta N-15 fractionation in fishes. *Journal of Experimental Marine Biology and Ecology* **340**:1-10.
- Tzadik, O. E., J. S. Curtis, J. E. Granneman, B. N. Kurth, T. J. Pusack, A. A. Wallace, D. J. Hollander, E. B. Peebles, and C. D. Stallings. 2017. Chemical archives in fishes beyond otoliths: A review on the use of other body parts as chronological recorders of microchemical constituents for expanding interpretations of environmental, ecological, and life-history changes. *Limnology and Oceanography-Methods* **15**:238-263.
- Umezawa, Y., A. Tamaki, T. Suzuki, S. Takeuchi, C. Yoshimizu, and I. Tayasu. 2018. Phytoplankton as a principal diet for callinassid shrimp larvae in coastal waters, estimated from laboratory rearing and stable isotope analysis. *Marine Ecology Progress Series* **592**:141-158.
- Wall, C. C., B. T. Donahue, D. F. Naar, and D. A. Mann. 2011. Spatial and temporal variability of red grouper holes within Steamboat Lumps Marine Reserve, Gulf of Mexico. *Marine Ecology Progress Series* **431**:243-254.
- Wallace, A. A., D. J. Hollander, and E. B. Peebles. 2014. Stable isotopes in fish eye lenses as potential recorders of trophic and geographic history. *Plos One* **9**.
- Weaver, D. C. 1996. Feeding ecology and ecomorphology of three seabasses (Pisces: Serranidae) in the northeastern Gulf of Mexico. University of Florida, Gainesville, FL.
- Weisberg, R. H., L. Zheng, and E. B. Peebles. 2014. Gag grouper larvae pathways on the West Florida Shelf. *Continental Shelf Research* **88**:11-23.
- Winkler, G., C. Martineau, J. J. Dodson, W. F. Vincent, and L. E. Johnson. 2007. Trophic dynamics of two sympatric mysid species in an estuarine transition zone. *Marine Ecology Progress Series* **332**:171-187.

Table 5.1. Basic biological parameters for all Red Grouper with eye-lenses analyzed. Fish were collected from the West Florida Shelf (WFS), Campeche Bank (Mexico), and the north Atlantic Ocean off the coast of southeast Florida (SE-FL). Numbers of individuals collected (*n*), standard length at collection (SL), age in years, Eye-lens diameter (ELD), and total number of analyzed eye-lens layers (ELL) are each listed. Geographic areas are identified on Figure 5.1.

	<i>n</i>	SL (mm)	Age (y)	ELD (mm)	ELL (#)
WFS juvenile	55	37 - 241	0-2	0.90 – 7.00	2 – 16
WFS adult	30	242 - 667	2-10	6.10 – 11.50	7 – 22
Mexico	5	354 - 530	3-5	7.50 – 9.25	20 – 26
SE-FL	3	431 - 557	3-5	8.40 – 9.75	14 – 18

Table 5.2. Isotopic values of Red Grouper eye-lens cores (inner-most eye-lens layer) collected from the West Florida Shelf (WFS), Campeche Bank (Mexico), and the north Atlantic Ocean off the coast of southeast Florida (SE-FL). Size of the analyzed eye-lens core and the calculated SL at analysis (based on regression (1)), Mean \pm SE, minimum and maximum values are listed for both $\delta^{15}\text{N}$ and $\delta^{13}\text{C}$.

	Core ELD (mm)	Analysis SL (mm)	core $\delta^{15}\text{N}$			core $\delta^{13}\text{C}$		
			mean \pm SE	min	max	mean \pm SE	min	max
WFS juvenile	0.40 – 1.10	14 - 39	7.13 \pm 0.09	5.82	9.07	-19.07 \pm 0.13	-20.65	-15.19
WFS adult	0.50 – 1.30	18 - 46	7.00 \pm 0.13	5.57	8.49	-18.56 \pm 0.22	-20.15	-14.95
Mexico	0.80 – 1.00	28 - 35	8.22 \pm 0.13	7.72	8.45	-18.74 \pm 0.26	-19.84	-17.82
SE-FL	0.60 – 1.00	21 - 35	6.43 \pm 0.29	5.91	6.96	-17.93 \pm 0.96	-19.34	-16.09

Table 5.3. Spearman rank correlations between stable isotope values ($\delta^{15}\text{N}$ or $\delta^{13}\text{C}$) and eye-lens diameter (ELD) or collection location (Collection Lat & Collection Lon) in Red Grouper eye-lens. Isotopic interpretations based on decision table presented in Chapter 2. Significance values are as follows: n.s. $p > 0.05$, * $p \leq 0.05$, ** $p \leq 0.01$, *** $p \leq 0.001$

	$\delta^{15}\text{N}$ vs ELD <i>Rho</i>	$\delta^{15}\text{N}$ vs collection Lat <i>Rho</i>	$\delta^{13}\text{C}$ vs ELD <i>Rho</i>	$\delta^{13}\text{C}$ vs collection Lon <i>Rho</i>	Isotopic Interpretations
WFS Juveniles	0.52 ***	-0.26 (n.s.)	0.41**	-0.24 (n.s.)	1B, 2C, 3B, 4C
WFS Adults	0.72 ***	-0.16 (n.s.)	0.44 **	-0.49 **	1B, 2C, 3B, 4A

Table 5.4. Biological, statistical, and interpretation information for individual juvenile Red Grouper ordered by capture standard length (SL). Eye -lens diameter (ELD), number of eye-lens laminae (ELL), lifetime changes in $\delta^{13}\text{C}$ and $\delta^{15}\text{N}$. Spearman rank correlations ($\delta^{15}\text{N}:\text{ELD}$, $\delta^{13}\text{C}:\text{ELD}$, $\delta^{13}\text{C}:\delta^{15}\text{N}$) are listed along with interpretations from Table 4.2 Significance is indicated as follows: n.s. $p > 0.05$, * $p \leq 0.05$, ** $p \leq 0.01$, *** $p \leq 0.001$. Individual capture length did not correlate with relative capture latitude or capture depth (i.e. interpretation 3B in Table 4.2).

SL (mm)	Age (y)	ELD (mm)	ELL	Lifetime $\delta^{15}\text{N}$ change	Lifetime $\delta^{13}\text{C}$ change	d15N v ELD <i>Rho</i>	d13C v ELD <i>Rho</i>	d15N v d13C v <i>Rho</i>	Isotopic interpretation
37	0	0.9	2	-0.39	3.07	-1.00 #	1.00 #	-1.00 #	* * * *
83	0	3.0	4	-0.23	4.11	-0.40 #	0.20 #	-0.80 #	* * * *
92	0	2.0	4	0.45	2.25	0.40 #	0.80 #	-0.20 #	* * * *
97	0	3.1	4	0.28	2.89	0.50 #	1.00 #	0.50 #	* * * *
102	0	2.4	3	-0.71	4.64	-0.50 #	1.00 #	-0.50 #	* * * *
120	0	4.5	9	2.35	1.67	0.98 ***	0.41 (n.s.)	0.37 (n.s.)	1B 2C 3B 4C
121	0	4.0	8	2.34	0.97	0.93 ***	0.17 (n.s.)	0.29 (n.s.)	1B 2C 3B 4C
134	0	4.2	9	1.46	2.28	0.83 *	0.70 *	0.55 (n.s.)	1B 2B 3B 4B
142	1	5.4	8	2.96	1.87	1.00 ***	0.74 *	0.74 *	1B 2B 3B 4B
147	1	5.5	13	2.30	1.66	0.91 ***	0.27 (n.s.)	-0.01 (n.s.)	1B 2C 3B 4C
158	1	5.1	9	3.79	2.01	1.00 ***	0.33 (n.s.)	0.33 (n.s.)	1B 2C 3B 4C
160	1	5.9	9	3.00	3.41	0.88 ***	0.24 (n.s.)	0.44 (n.s.)	1B 2C 3B 4C
165	1	5.4	5	3.05	3.33	0.89 *	0.49 (n.s.)	0.49 (n.s.)	1B 2C 3B 4C
166	1	6.2	16	1.97	0.93	0.96 ***	-0.42 (n.s.)	-0.49 (n.s.)	1B 2C 3B 4C
166	1	4.2	5	2.04	2.16	1.00 *	0.10 (n.s.)	0.10 (n.s.)	1B 2C 3B 4C
167	0	4.5	5	2.09	2.76	1.00 *	1.00 *	1.00 *	1B 2B 3B 4B
170	1	4.5	7	2.80	2.97	0.93 *	0.50 (n.s.)	0.46 (n.s.)	1B 2C 3B 4C
171	1	6.0	13	1.96	1.06	0.86 ***	-0.32 (n.s.)	-0.58 *	1B 2C 3B 4A
175	1	4.5	7	1.70	2.21	0.86 *	0.71 (n.s.)	0.36 (n.s.)	1B 2B 3B 4C
176	2	4.5	8	1.70	2.98	0.90 ***	0.43 (n.s.)	0.24 (n.s.)	1B 2C 3B 4C
177	1	4.2	5	3.07	2.36	0.94 *	0.43 (n.s.)	0.49 (n.s.)	1B 2C 3B 4C
177	1	4.7	6	4.15	2.12	0.96 ***	0.43 (n.s.)	0.36 (n.s.)	1B 2C 3B 4C
177	1	4.5	8	3.65	2.14	1.00 ***	0.05 (n.s.)	0.05 (n.s.)	1B 2C 3B 4C
178	1	3.7	5	1.02	-2.21	0.37 (n.s.)	-0.89 *	-0.14 (n.s.)	1C 2A 3B 4C
178	1	4.6	8	2.11	1.31	0.96 ***	-0.21 (n.s.)	-0.14 (n.s.)	1B 2C 3B 4C
179	1	4.4	7	1.94	3.11	0.43 (n.s.)	0.50 (n.s.)	-0.21 (n.s.)	1C 2C 3B 4C
180	1	4.6	9	3.68	0.44	0.98 ***	0.00 (n.s.)	-0.03 (n.s.)	1B 2C 3B 4C
182	1	4.9	9	2.97	2.67	0.98 ***	-0.02 (n.s.)	0.00 (n.s.)	1B 2C 3B 4C
182	1	4.8	5	2.81	2.38	1.00 ***	0.09 (n.s.)	0.09 (n.s.)	1B 2C 3B 4C
183	1	4.1	5	2.98	2.22	0.71 (n.s.)	0.66 (n.s.)	0.89 *	1B 2B 3B 4B
187	1	6.1	9	1.64	2.60	0.88 ***	0.48 (n.s.)	0.64 (n.s.)	1B 2C 3B 4B
187	1	5.6	6	3.34	2.84	0.96 ***	0.39 (n.s.)	0.46 (n.s.)	1B 2C 3B 4C
190	1	6.8	11	2.96	0.59	0.94 ***	0.66 *	0.48 (n.s.)	1B 2B 3B 4C
190	1	4.6	8	2.45	2.63	1.00 ***	0.00 (n.s.)	0.00 (n.s.)	1B 2C 3B 4C
191	1	4.7	7	3.59	2.23	0.86 *	0.36 (n.s.)	0.64 (n.s.)	1B 2C 3B 4B
195	1	5.0	5	3.19	2.79	0.66 (n.s.)	0.49 (n.s.)	-0.03 (n.s.)	1B 2C 3B 4C
197	1	7.0	12	2.18	2.91	0.95 ***	0.38 (n.s.)	0.35 (n.s.)	1B 2C 3B 4C
201	1	6.6	11	1.84	3.17	0.97 ***	0.59 (n.s.)	0.54 (n.s.)	1B 2B 3B 4B
204	2	5.7	7	3.00	3.47	0.82 *	0.86 *	0.54 (n.s.)	1B 2B 3B 4B
206	1	5.0	7	3.56	1.97	0.89 *	0.86 *	0.61 (n.s.)	1B 2B 3B 4B
206	1	5.5	9	2.75	1.54	1.00 ***	-0.03 (n.s.)	-0.03 (n.s.)	1B 2C 3B 4C
207	2	5.2	9	4.29	2.93	0.92 ***	0.98 ***	0.97 ***	1B 2B 3B 4B
216	2	6.8	11	2.19	2.35	0.93 ***	0.00 (n.s.)	-0.23 (n.s.)	1B 2C 3B 4C
219	1	6.5	9	0.21	0.44	0.48 (n.s.)	0.75 (n.s.)	0.17 (n.s.)	1C 2B 3B 4C
219	2	6.3	8	3.71	3.11	1.00 ***	0.31 (n.s.)	0.31 (n.s.)	1B 2C 3B 4C
221	2	5.8	7	1.57	2.65	0.57 (n.s.)	0.21 (n.s.)	-0.02 (n.s.)	1B 2C 3B 4C
225	2	5.7	6	2.03	2.50	0.68 (n.s.)	0.71 (n.s.)	0.57 (n.s.)	1B 2B 3B 4B
226	1	6.5	9	3.06	1.12	0.65 (n.s.)	-0.32 (n.s.)	-0.37 (n.s.)	1B 2C 3B 4C
229	2	6.4	7	2.60	1.79	0.93 ***	0.17 (n.s.)	0.00 (n.s.)	1B 2C 3B 4C
233	1	6.7	16	4.13	3.90	0.65 *	0.11 (n.s.)	-0.34 (n.s.)	1B 2C 3B 4C
233	2	7.0	9	1.49	3.06	0.93 ***	0.78 *	0.87 ***	1B 2B 3B 4B
234	1	6.1	8	0.98	2.17	0.36 (n.s.)	0.26 (n.s.)	0.40 (n.s.)	1C 2C 3B 4C
235	1	5.8	6	4.02	1.54	1.00 ***	0.49 (n.s.)	0.49 (n.s.)	1B 2C 3B 4C
239	2	5.5	9	3.51	2.70	0.93 ***	0.28 (n.s.)	0.05 (n.s.)	1B 2C 3B 4C
240	1	6.4	11	4.68	1.94	0.88 ***	0.44 (n.s.)	0.25 (n.s.)	1B 2C 3B 4C

Table 5.5 Biological, statistical, and interpretation information for individual adult Red Grouper ordered by capture standard length (SL). Capture location [Florida southeast coast (SEFL), or Campeche Bank (Mexico), West Florida Shelf (WFS)] are listed. Eye-lens diameter (ELD), number of eye-lens laminae (ELL), Spearman rank correlations ($\delta^{15}\text{N}:\text{ELD}$, $\delta^{13}\text{C}:\text{ELD}$, $\delta^{13}\text{C}:\delta^{15}\text{N}$) are listed along with interpretations from Table 3.2. Significance is indicated as follows: n.s. $p > 0.05$, * $p \leq 0.05$, ** $p \leq 0.01$, *** $p \leq 0.001$. Individual capture length did not correlate with relative capture position (i.e. interpretation 3B in Table 3.2).

Catch Area	SL (mm)	Age (y)	ELD	ELL	Lifetime	Lifetime	d15N vs ELD		d13C v ELD		d13C v d15N		Isotopic interpretations			
					$\delta^{15}\text{N}$ change	$\delta^{13}\text{C}$ change	Rho	Significance	Rho	Significance	Rho	Significance	1B	2C	3B	4C
SE-FL	431	4	9.5	15	3.21	4.08	0.81	***	0.03	(n.s.)	0.43	(n.s.)	1B	2C	3B	4C
SE-FL	483	3	10.0	14	4.78	4.13	0.96	***	0.69	*	0.82	***	1B	2B	3B	4B
SE-FL	557	5	10.7	18	3.86	6.62	0.99	***	0.98	***	0.96	***	1B	2B	3B	4B
Mexico	355	3	8.2	20	2.29	1.28	0.74	***	0.52	***	0.20	(n.s.)	1B	2B	3B	4C
Mexico	381	3	9.0	21	2.50	2.45	0.66	***	0.93	***	0.56	**	1B	2B	3B	4B
Mexico	442	5	9.4	21	3.49	3.11	0.86	***	-0.13	(n.s.)	-0.26	(n.s.)	1B	2C	3B	4C
Mexico	512	5	9.8	23	2.78	2.38	0.93	***	0.56	*	0.61	***	1B	2B	3B	4B
Mexico	530	NA	10.0	26	3.03	2.13	0.81	***	0.29	(n.s.)	0.33	(n.s.)	1B	2C	3B	4C
WFS	241	2	5.3	9	4.35	1.14	0.70	*	0.12	(n.s.)	-0.25	(n.s.)	1B	2C	3B	4C
WFS	243	2	6.2	15	2.65	2.60	0.80	***	0.44	(n.s.)	0.39	(n.s.)	1B	2C	3B	4C
WFS	248	2	4.9	7	3.33	1.20	1.00	***	0.04	(n.s.)	0.04	(n.s.)	1B	2C	3B	4C
WFS	249	2	6.5	11	3.27	1.83	0.98	***	0.83	***	0.82	***	1B	2B	3B	4B
WFS	254	2	5.3	8	3.77	2.31	0.73	*	0.55	(n.s.)	0.40	(n.s.)	1B	2B	3B	4C
WFS	256	2	7.2	11	2.83	1.65	0.46	(n.s.)	0.75	*	0.27	(n.s.)	1C	2B	3B	4C
WFS	263	2	6.5	9	2.72	1.58	0.95	***	0.30	(n.s.)	0.22	(n.s.)	1B	2C	3B	4C
WFS	265	2	7.0	8	3.83	3.16	0.98	***	0.71	(n.s.)	0.67	(n.s.)	1B	2B	3B	4B
WFS	268	2	7.0	8	3.94	3.47	0.93	***	0.19	(n.s.)	-0.07	(n.s.)	1B	2C	3B	4C
WFS	270	3	5.0	9	3.83	1.81	0.88	***	0.93	*	0.87	***	1B	2B	3B	4B
WFS	271	2	5.6	13	2.29	2.33	0.60	*	0.20	(n.s.)	-0.39	(n.s.)	1B	2C	3B	4C
WFS	273	2	6.8	10	3.79	1.94	0.92	***	-0.12	(n.s.)	0.04	(n.s.)	1B	2C	3B	4C
WFS	273	2	7.1	9	3.64	2.74	1.00	***	-0.12	(n.s.)	-0.12	(n.s.)	1B	2C	3B	4C
WFS	275	2	6.0	11	2.30	3.68	0.86	***	0.16	(n.s.)	-0.03	(n.s.)	1B	2C	3B	4C
WFS	278	3	6.0	9	5.41	2.00	0.85	*	0.70	*	0.40	(n.s.)	1B	2B	3B	4C
WFS	279	2	8.2	16	3.73	4.75	0.99	***	0.42	(n.s.)	0.43	(n.s.)	1B	2C	3B	4C
WFS	282	2	6.3	15	0.73	1.24	0.40	(n.s.)	-0.06	(n.s.)	-0.29	(n.s.)	1C	2C	3B	4C
WFS	283	2	7.5	17	4.51	2.67	0.78	***	0.38	(n.s.)	-0.02	(n.s.)	1B	2C	3B	4C
WFS	287	2	6.1	9	2.91	1.89	0.69	(n.s.)	0.62	(n.s.)	0.02	(n.s.)	1B	2B	3B	4C
WFS	290	2	7.2	14	4.16	2.06	0.71	*	0.81	***	0.54	*	1B	2B	3B	4B
WFS	306	4	9.0	18	3.05	0.63	0.93	***	-0.23	(n.s.)	-0.35	(n.s.)	1B	2C	3B	4C
WFS	414	5	9.5	20	3.15	0.33	0.97	***	-0.50	*	-0.55	*	1B	2A	3B	4A
WFS	418	5	9.0	21	4.47	-0.65	0.97	***	-0.74	***	-0.75	***	1B	2A	3B	4A
WFS	425	3	9.2	19	4.87	2.60	0.98	***	0.49	*	0.52	*	1B	2C	3B	4B
WFS	437	10	9.0	20	4.44	1.49	0.94	***	-0.14	(n.s.)	-0.17	(n.s.)	1B	2C	3B	4C
WFS	444	6	9.8	22	4.26	2.31	0.95	***	0.00	(n.s.)	-0.05	(n.s.)	1B	2C	3B	4C
WFS	457	5	9.5	20	2.33	1.46	0.23	(n.s.)	0.21	(n.s.)	-0.52	*	1C	2C	3B	4A
WFS	482	6	9.8	22	3.93	0.98	0.98	***	0.09	(n.s.)	0.11	(n.s.)	1B	2C	3B	4C
WFS	618	4	11.5	17	4.11	2.30	0.98	***	-0.03	(n.s.)	-0.05	(n.s.)	1B	2C	3B	4C
WFS	667	NA	9.8	17	6.19	1.64	0.93	***	0.61	*	0.64	**	1B	2B	3B	4B

Table 5.6. Height and diametric location within the eye-lens of first transition from quickly increasing $\delta^{13}\text{C}$ to quickly decreasing $\delta^{13}\text{C}$ in eye-lens profiles (Carbon Bump). Fish are grouped by maturity and capture location [West Florida Shelf (WFS juvenile or WFS adult), Campeche Bank (Mexico), and the north Atlantic Ocean off the coast of southeast Florida (SE-FL)] n = number of fish for which the feature occurred in the eye-lens profile for that group.

	n	Mean ELD (\pm SE; mm)	Min ELD (mm)	Max ELD (mm)	Mean height (\pm SE; ‰)	Min height (‰)	Max height (‰)
WFS juvenile	33	1.88 \pm 0.04	0.76	3.16	3.23 \pm 0.18	0.86	4.91
WFS adult	20	2.28 \pm 0.13	0.76	5.10	3.03 \pm 0.33	0.63	6.39
Mexico	1	-	-	1.38	-	-	6.36
SE-FL	1	-	-	0.80	-	-	3.97

Table 5.7. Mean (\pm SE), min, and max proportion of the lifespan utilizing each available basal resource. Fish are grouped by size and capture location [West Florida Shelf (WFS juvenile or WFS adult), Campeche Bank (Mexico), and the north Atlantic Ocean off the coast of southeast Florida (SE-FL)]. Planktonic basal resource is represented by $\delta^{13}\text{C}$ values $\leq -18\text{‰}$, benthic basal resource is represented by $\delta^{13}\text{C} \geq -15\text{‰}$, mixed benthic and pelagic basal resources is represented by $-18\text{‰} < \delta^{13}\text{C} < -15\text{‰}$.

		n	mean (\pm SE)	min	max
WFS juvenile	planktonic	55	0.20 \pm 0.02	0.00	0.63
WFS juvenile	mixed	-	0.75 \pm 0.02	0.09	1.00
WFS juvenile	benthic	-	0.05 \pm 0.02	0.00	0.80
WFS adult	planktonic	30	0.18 \pm 0.03	0.00	0.66
WFS adult	mixed	-	0.75 \pm 0.04	0.09	1.00
WFS adult	benthic	-	0.06 \pm 0.03	0.00	0.91
SE-FL	planktonic	3	0.03 \pm 0.01	0.00	0.05
SE-FL	mixed	-	0.39 \pm 0.28	0.08	0.95
SE-FL	benthic	-	0.58 \pm 0.29	0.00	0.92
Mexico	planktonic	5	0.10 \pm 0.03	0.00	0.18
Mexico	mixed	-	0.82 \pm 0.07	0.55	1.00
Mexico	benthic	-	0.08 \pm 0.08	0.00	0.38

Table 5.8. Percent by volume of diets consumed by 521 Red Grouper collected from the WFS 2007-2015. All Red Grouper were collected, and stomachs analyzed by the Fisheries Independent Monitoring program at the Florida Fish and Wildlife Conservation Commission. Size categories are listed in SL. Vertical line represents approximate size at 50% maturity. All prey items were identified to the lowest taxonomic level possible. Prey were aggregated to family for analysis as listed here. Prey were aggregated to higher taxonomic levels for graphical representation (Figure 5.8). Any grouping (family or higher) that comprised less than 1% of total prey for the dataset was classified as “other” for graphical representation.

Family or higher taxon	Grouping (Figure 5.8)	0-100 (n = 10)	101-150 (n = 41)	151-200 (n = 92)	201-250 (n = 154)	251-300 (n = 132)	301-350 (n = 51)	351-400 (n = 19)	401+ (n = 22)
Algae	other	-	-	-	0.35	0.06	*	-	*
Seagrass	other	-	-	-	-	-	-	-	-
Cnidaria	other	-	-	-	0.06	-	-	-	-
Decapoda	unId Decapoda	0.85	2.56	4.66	1.14	3.37	1.05	0.27	0.40
Alpheoidea	shrimps	-	1.38	6.28	1.13	0.66	-	0.31	-
Caridae	shrimps	37.48	0.99	0.84	0.85	0.31	0.12	*	-
Processidae	shrimps	-	*	-	-	-	-	-	-
Penaeidae	shrimps	26.77	68.85	19.72	2.28	1.21	0.81	-	-
Penaeoidea	shrimps	-	-	1.40	0.95	0.15	-	-	-
Sicyoniidae	shrimps	-	-	1.49	1.06	1.05	0.32	-	-
Stomatopoda	shrimps	-	0.83	1.50	1.73	1.56	0.91	2.26	0.67
Porcellanidae	crabs	-	0.14	0.84	0.05	-	-	-	-
Anomura	crabs	-	-	0.18	0.34	0.04	-	-	5.55
Paguroidea	crabs	-	-	4.12	0.67	0.16	-	-	-
Galatheidae	crabs	22.69	0.00	1.40	0.04	-	-	-	-
Portunidae	crabs	-	2.50	9.90	10.85	0.49	-	1.68	-
Pilumnoidea	crabs	-	-	-	0.17	0.00	-	0.00	-
Pinnotheridae	crabs	-	-	0.11	-	-	-	-	-
Brachyura	crabs	0.27	-	0.91	3.48	2.46	0.74	0.27	12.46
Calappidae	crabs	-	-	-	4.22	-	6.66	3.03	6.78
Leucosiidae	crabs	-	-	2.81	0.49	0.36	0.07	0.34	-
Goneplacidae	crabs	-	0.59	1.45	0.03	0.51	-	-	-

Table 5.8. (Continued)

Family or higher taxon	Grouping (Figure 5.8)	0-100	101-150	151-200	201-250	251-300	301-350	351-400	401+
Parthenopidae	crabs	-	-	-	1.72	-	0.70	-	0.62
Majoidea	crabs	-	18.46	13.98	12.52	16.39	5.21	2.96	7.58
Xanthoidea	crabs	5.35	-	8.12	9.54	3.79	4.16	-	-
Scyllaridae	lobsters	-	-	0.84	0.14	0.08	0.04	18.18	-
Amphipoda	other	0.15	-	-	*	-	-	0.02	-
Isopoda	other	-	-	0.04	-	0.07	-	-	-
Mysida	other	1.09	-	-	*	-	-	-	-
Arthropoda	other	-	-	*	0.10	*	-	-	-
Ostracoda	other	-	-	*	-	-	-	-	-
Axiidea	other	-	0.88	0.09	-	0.55	0.14	-	-
Crustacea	other	-	-	0.29	0.08	0.06	0.35	0.34	-
Copepoda	other	-	-	*	*	0.00	-	-	-
Mollusca	other	-	*	-	-	0.18	-	1.35	-
Gastropoda	other	-	-	2.53	0.15	0.07	-	-	-
Bivalvia	other	-	-	0.03	-	0.07	-	-	*
Loliginidae	squid	-	-	0.01	0.32	15.43	24.53	6.06	-
Cephalopoda	other	-	0.37	0.05	0.05	*	0.04	-	-
Annelida	other	-	0.08	0.17	0.16	0.20	0.07	0.40	0.10
Holothuroidea	other	-	-	-	0.15	-	-	-	-
Ophiuroidea	other	-	-	-	-	-	*	-	-
Tunicata	other	-	-	-	0.10	-	-	-	-
Actinopterygii	unID fish	5.35	1.90	16.22	17.02	14.20	12.27	62.55	3.34
Clupeidae	pelagic fish	-	-	-	5.94	6.15	-	-	41.95
Carangidae	pelagic fish	-	-	-	-	-	1.75	-	-
Anguilliformes	demersal fish	-	-	-	0.98	-	-	-	-
Apogonidae	demersal fish	-	-	-	-	-	-	-	3.70
Balistidae	demersal fish	-	-	-	-	0.15	-	-	-
Batrachoididae	demersal fish	-	-	-	4.42	-	-	-	-
Blenniidae	demersal fish	-	-	-	-	-	0.11	-	-
Diodontidae	demersal fish	-	-	-	-	*	-	-	-

Table 5.8 (Continued)

Family or higher taxon	Grouping (Figure 5.8)	0-100	101-150	151-200	201-250	251-300	301-350	351-400	401+
Haemulidae	demersal fish	-	-	-	0.05	3.27	3.15	-	-
Labridae	demersal fish	-	-	-	3.44	8.91	-	-	0.20
Lutjanidae	demersal fish	-	-	-	-	1.45	-	-	-
Muraenidae	demersal fish	-	-	-	-	-	-	-	14.81
Monacanthidae	demersal fish	-	-	-	0.15	-	0.18	-	-
Opistognathidae	demersal fish	-	-	-	0.74	-	-	-	-
Pomacentridae	demersal fish	-	-	-	-	6.18	8.06	-	-
Scaridae	demersal fish	-	-	-	11.29	-	-	-	-
Sciaenidae	demersal fish	-	-	-	-	-	-	-	-
Serranidae	demersal fish	-	-	-	0.98	7.82	28.59	-	-
Sparidae	demersal fish	-	-	-	0.01	2.55	-	-	0.30
Syngnathidae	demersal fish	-	-	-	0.05	-	-	-	-
Synodontidae	demersal fish	-	-	-	-	-	-	-	1.23

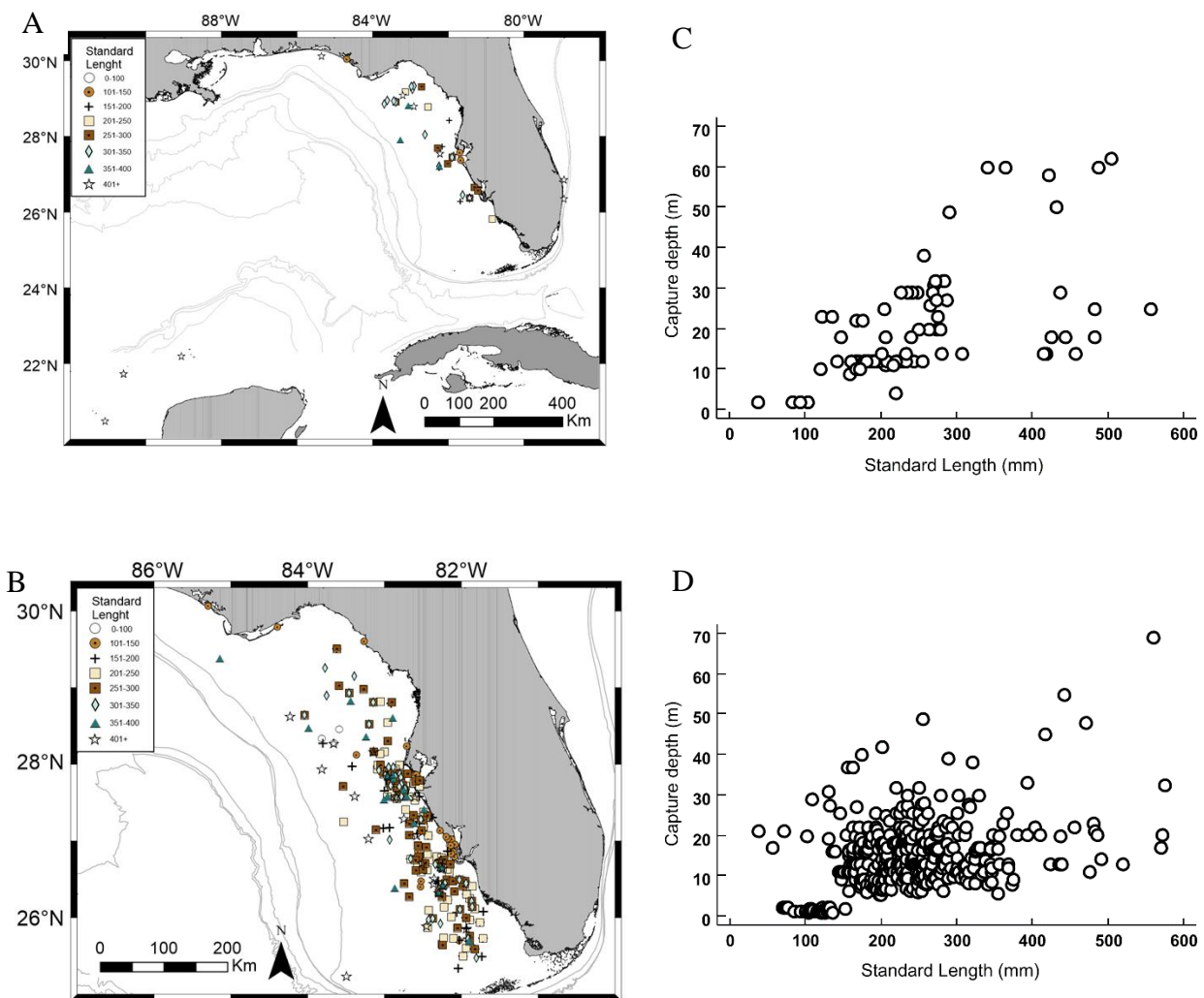


Figure 5.1. Collection locations and collection depths for all Red Grouper organized by standard length (SL) at capture. Bathymetry lines represent 100 m depth intervals. A. Collection locations for Red Grouper collected for stable isotope analysis 2015-2017. B. Collection locations for Red Grouper collected for stomach content analysis 2007-2015. C. Capture depth (m) as a function of standard length (mm) for Red Grouper collected for stable isotopes analysis. D. Capture depth (m) as a function of standard length (mm) for Red Grouper collected for stomach content analysis.

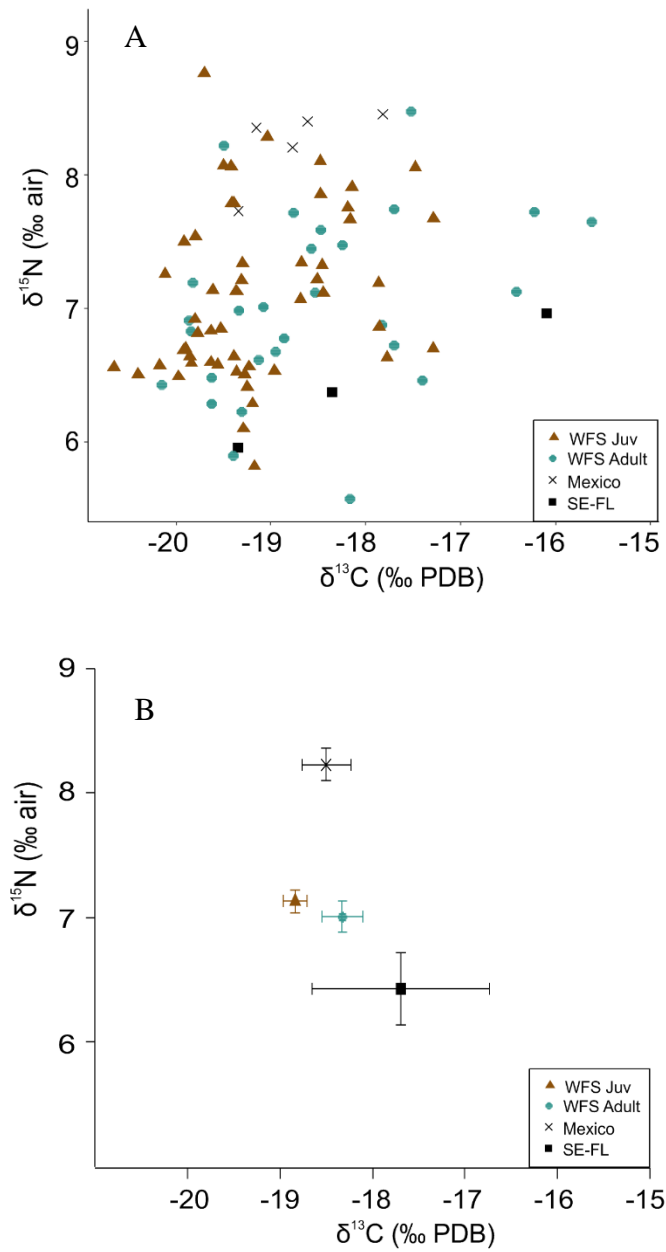


Figure 5.2. Eye-lens core isotopic values for all Red Grouper analyzed. Points are coded by catch location and maturity [West Florida Shelf (WFS juvenile or WFS adult), Campeche Bank (Mexico), and the north Atlantic Ocean off the coast of southeast Florida (SE-FL)]. A. Individual eye-lens core isotopic values. B mean (\pm SE) by location/maturity group.

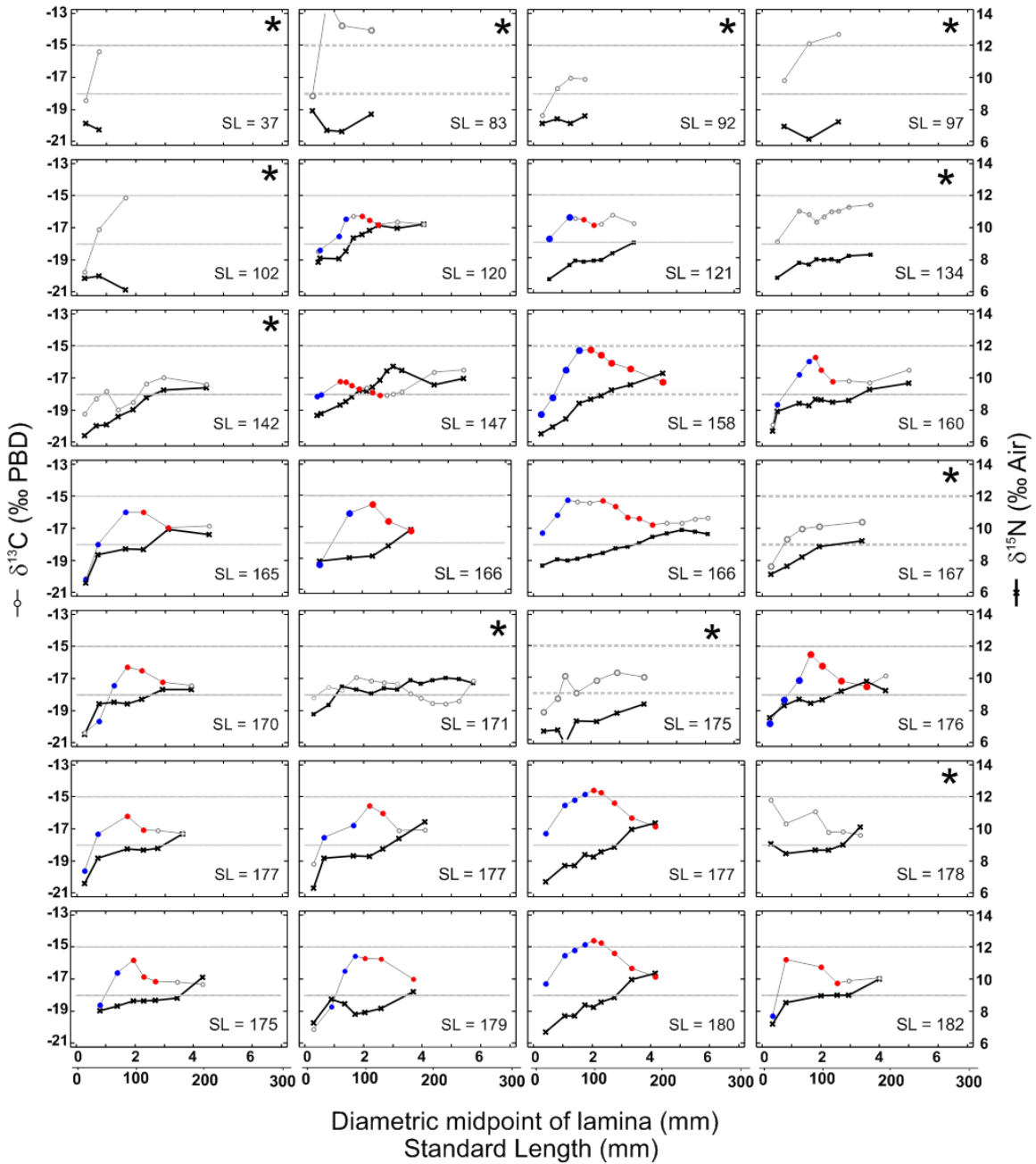


Figure 5.3. Profiles of $\delta^{13}\text{C}$ and $\delta^{15}\text{N}$ as a function of eye-lens diameter for individual juvenile Red Grouper from the West Florida Shelf (WFS) ordered by standard length (SL). First x-axis is eye-lens diameter. Second x-axis is approximate standard length as computed using regression (2). Blue dots denote areas of the eye-lens for which $\delta^{13}\text{C}$ increases faster than $\delta^{15}\text{N}$ and red dots denote areas of the eye-lens for which $\delta^{13}\text{C}$ decreases faster than $\delta^{15}\text{N}$ in fish for which $\delta^{15}\text{N}:\text{ELD } r_s > 0.5$ and $\delta^{13}\text{C}:\text{ELD } r_s < 0.5$. Fish for which $\delta^{15}\text{N}:\text{ELD } r_s < 0.5$ or $\delta^{13}\text{C}:\text{ELD } r_s > 0.5$ are noted with *. No sections of these $\delta^{13}\text{C}$ profiles highlighted. Individual standard length is noted. In the case of SL ties, fish are presented in identical order to Table 5.4.

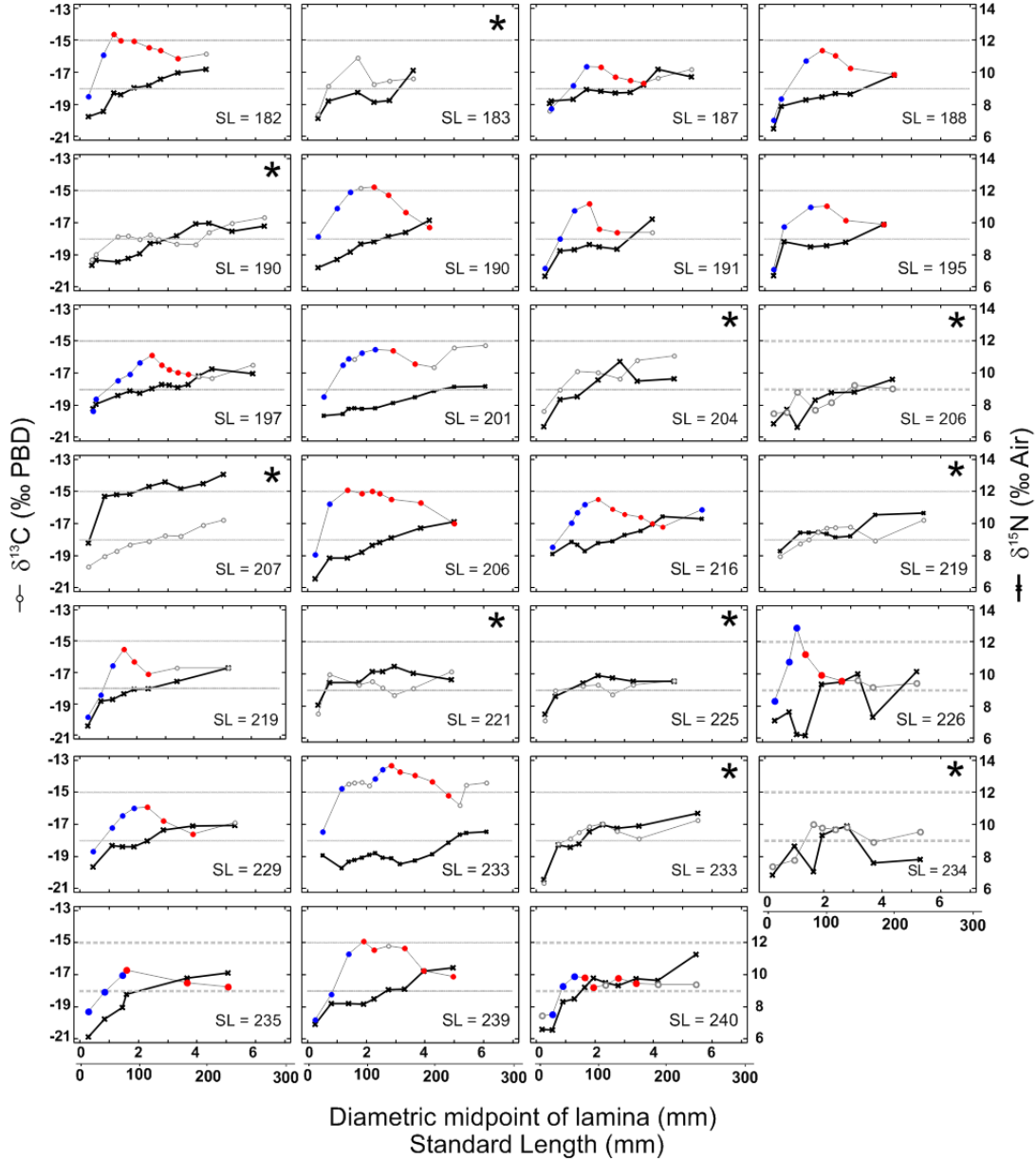


Figure 5.3 (cont.). Profiles of $\delta^{13}\text{C}$ and $\delta^{15}\text{N}$ as a function of eye-lens diameter for individual juvenile Red Grouper from the West Florida Shelf (WFS) ordered by standard length (SL). First x-axis is eye-lens diameter. Second x-axis is approximate standard length as computed using regression (2). Blue dots denote areas of the eye-lens for which $\delta^{13}\text{C}$ increases faster than $\delta^{15}\text{N}$ and red dots denote areas of the eye-lens for which $\delta^{13}\text{C}$ decreases faster than $\delta^{15}\text{N}$ in fish for which $\delta^{15}\text{N}:\text{ELD } r_s > 0.5$ and $\delta^{13}\text{C}:\text{ELD } r_s < 0.5$. Fish for which $\delta^{15}\text{N}:\text{ELD } r_s < 0.5$ or $\delta^{13}\text{C}:\text{ELD } r_s > 0.5$ are noted with *. No sections of these $\delta^{13}\text{C}$ profiles highlighted. Individual standard length is noted. In the case of SL ties, fish are presented in identical order to Table 4.

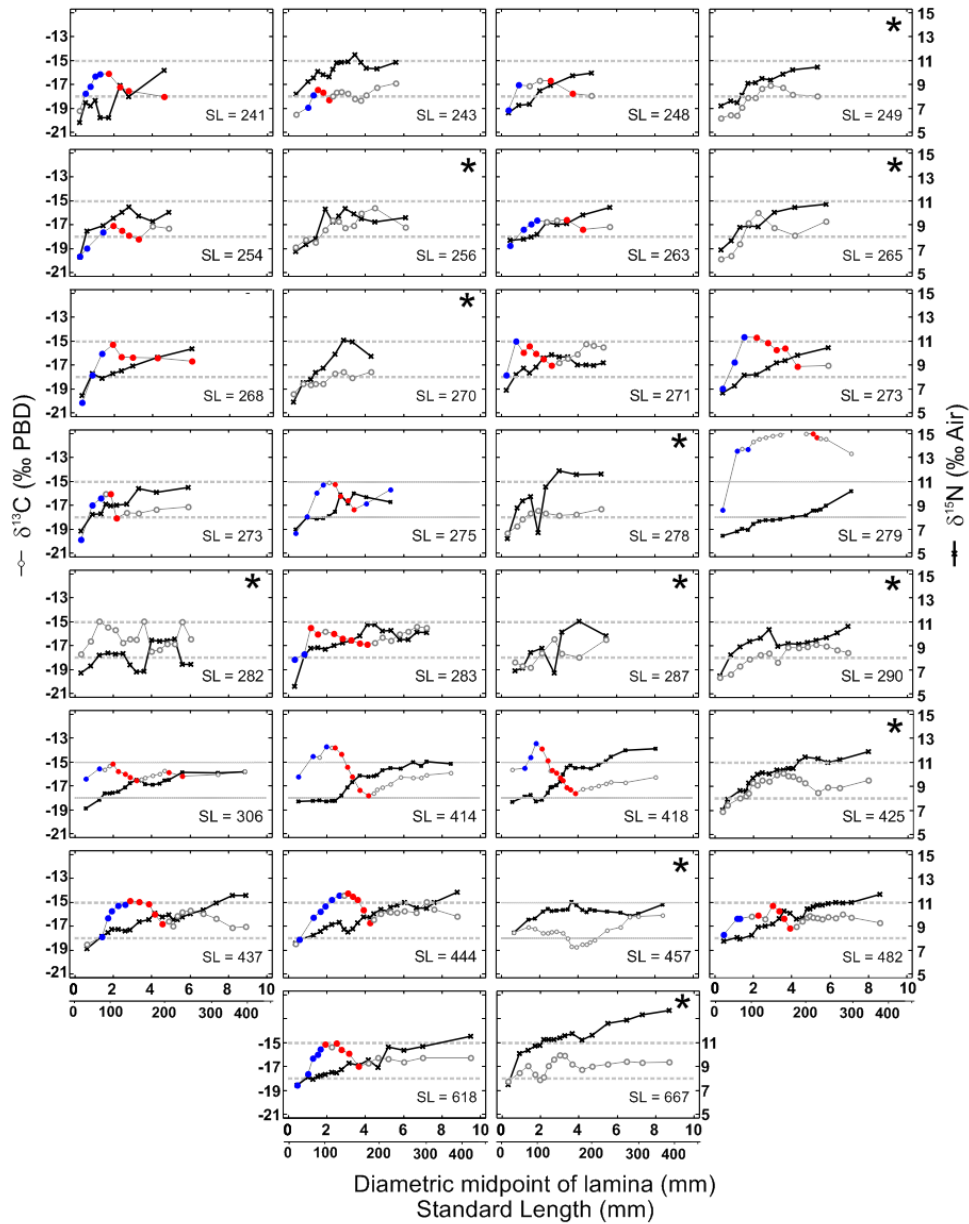


Figure 5.4. Profiles of $\delta^{13}\text{C}$ and $\delta^{15}\text{N}$ as a function of eye-lens diameter for individual adult Red Grouper from the West Florida Shelf (WFS) ordered by standard length (SL). First x-axis is eye-lens diameter. Second x-axis is approximate standard length as computed using regression (2). Blue dots denote areas of the eye-lens for which $\delta^{13}\text{C}$ increases faster than $\delta^{15}\text{N}$ and red dots denote areas of the eye-lens for which $\delta^{13}\text{C}$ decreases faster than $\delta^{15}\text{N}$ in fish for which $\delta^{15}\text{N}:\text{ELD } r_s > 0.5$ and $\delta^{13}\text{C}:\text{ELD } r_s < 0.5$. Fish for which $\delta^{15}\text{N}:\text{ELD } r_s < 0.5$ or $\delta^{13}\text{C}:\text{ELD } r_s > 0.5$ are noted with *. No sections of these $\delta^{13}\text{C}$ profiles highlighted. Individual standard length is noted. In the case of SL ties, fish are presented in identical order to Table 5.5.

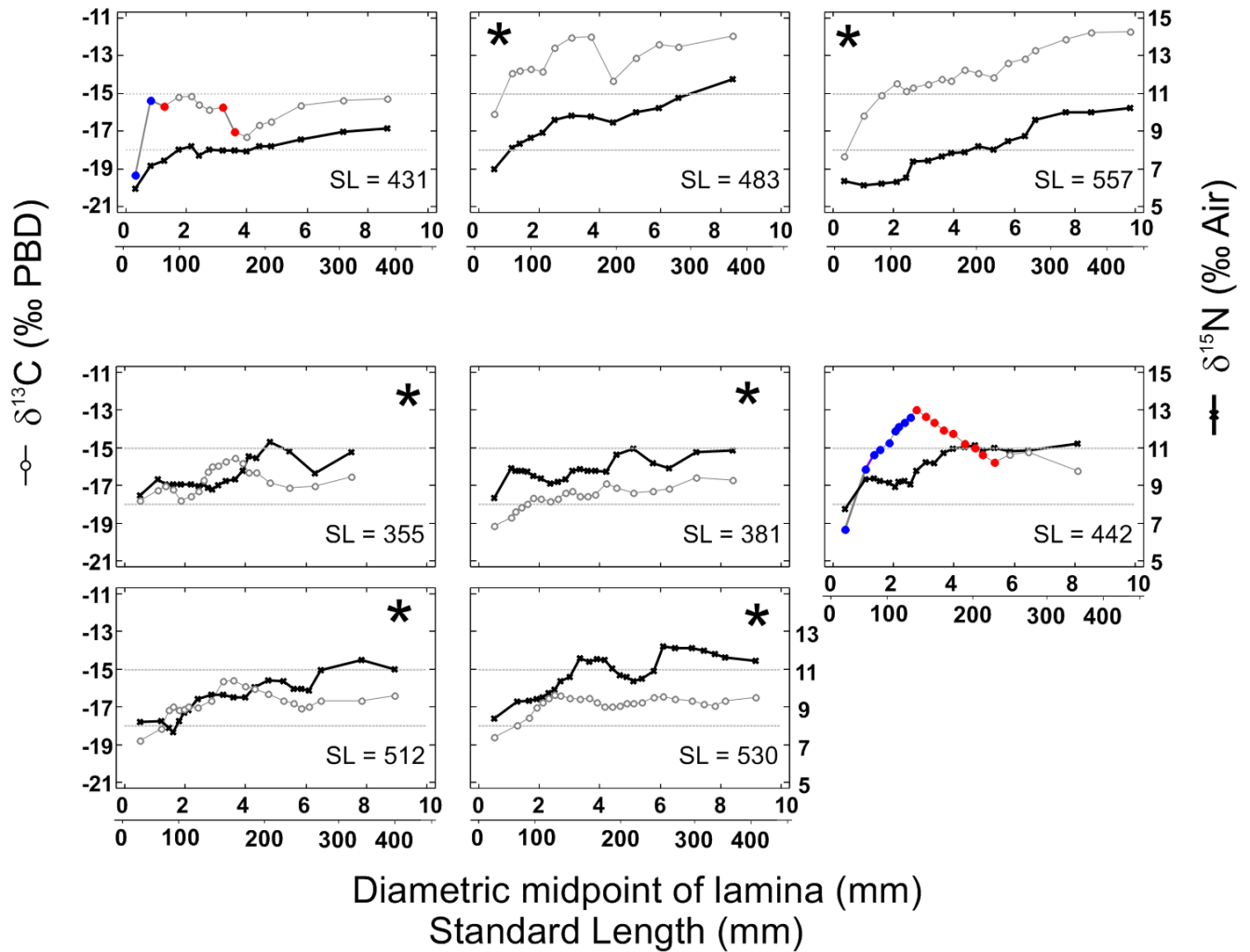


Figure 5.5. Profiles of $\delta^{13}\text{C}$ and $\delta^{15}\text{N}$ as a function of eye-lens diameter for individual adult Red Grouper. Top row of panels indicate fish captured off the southeast coast of Florida (SE-FL). Remaining panels are fish captured on the Campeche Bank (Mexico). First x-axis is eye-lens diameter. Second x-axis is approximate standard length as computed using regression (2). Blue dots denote areas of the eye-lens for which $\delta^{13}\text{C}$ increases faster than $\delta^{15}\text{N}$ and red dots denote areas of the eye-lens for which $\delta^{13}\text{C}$ decreases faster than $\delta^{15}\text{N}$ in fish for which $\delta^{15}\text{N}:\text{ELD } r_s > 0.5$ and $\delta^{13}\text{C}:\text{ELD } r_s < 0.5$. Fish for which $\delta^{15}\text{N}:\text{ELD } r_s < 0.5$ or $\delta^{13}\text{C}:\text{ELD } r_s > 0.5$ are noted with *. No sections of these $\delta^{13}\text{C}$ profiles highlighted. Individual standard length is noted. In the case of SL ties, fish are presented in identical order to Table 5.5.

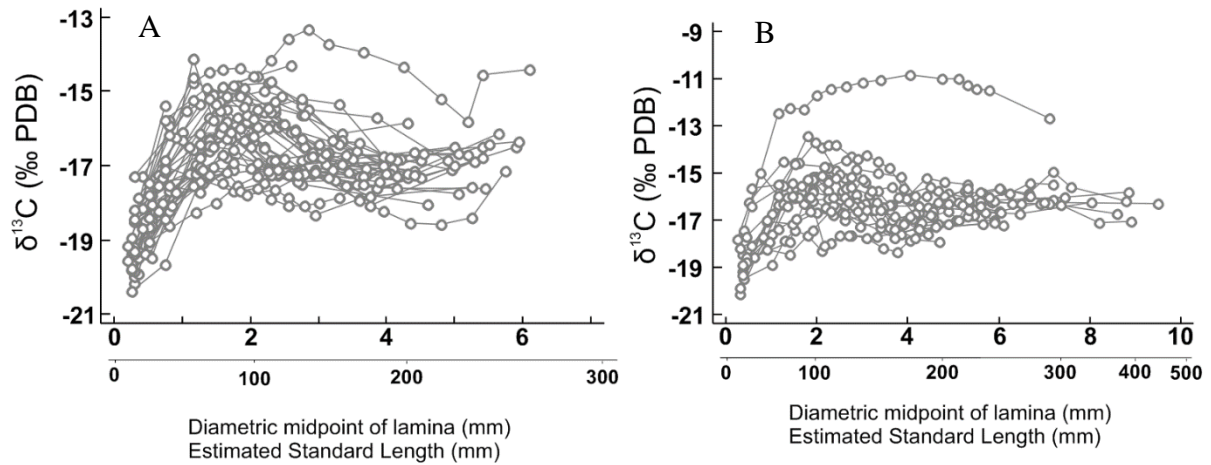


Figure 5.6. Profiles of $\delta^{13}\text{C}$ as a function of eye-lens diameter for all West Florida Shelf (WFS) Red Grouper identified as having a “carbon bump.” Primary x-axis is eye-lens diameter. Secondary x-axis is approximate standard length based on regression (2). A. WFS Juveniles B. WFS Adults. Note different scales in both x- and y-axes between panels A and B.

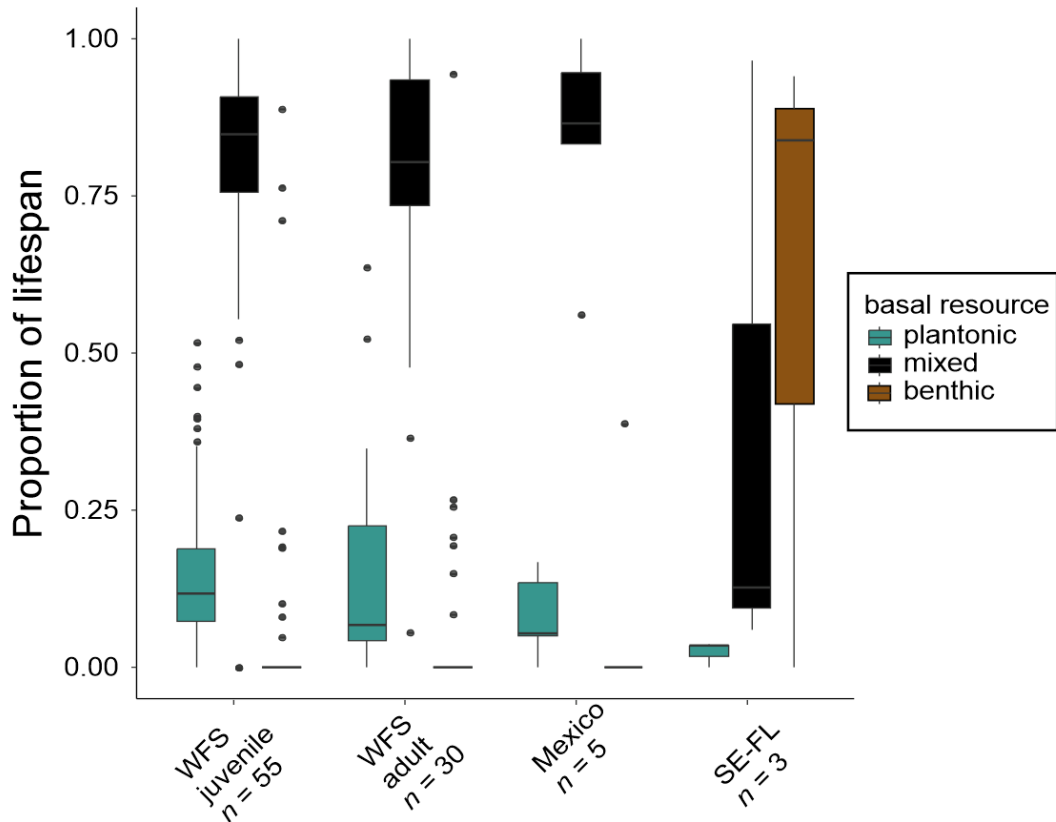


Figure 5.7. Proportion of total lifespan utilizing each available basal resource. Fish are grouped by location/maturity [West Florida Shelf (WFS juvenile or WFS adult), Campeche Bank (Mexico), and the north Atlantic Ocean off the coast of southeast Florida (SE-FL)]. Planktonic basal resource: $\delta^{13}\text{C} \leq -18\text{‰}$, benthic basal resource: $\delta^{13}\text{C} \geq -15\text{‰}$, mixed basal resource: $-18\text{‰} < \delta^{13}\text{C} < -15\text{‰}$

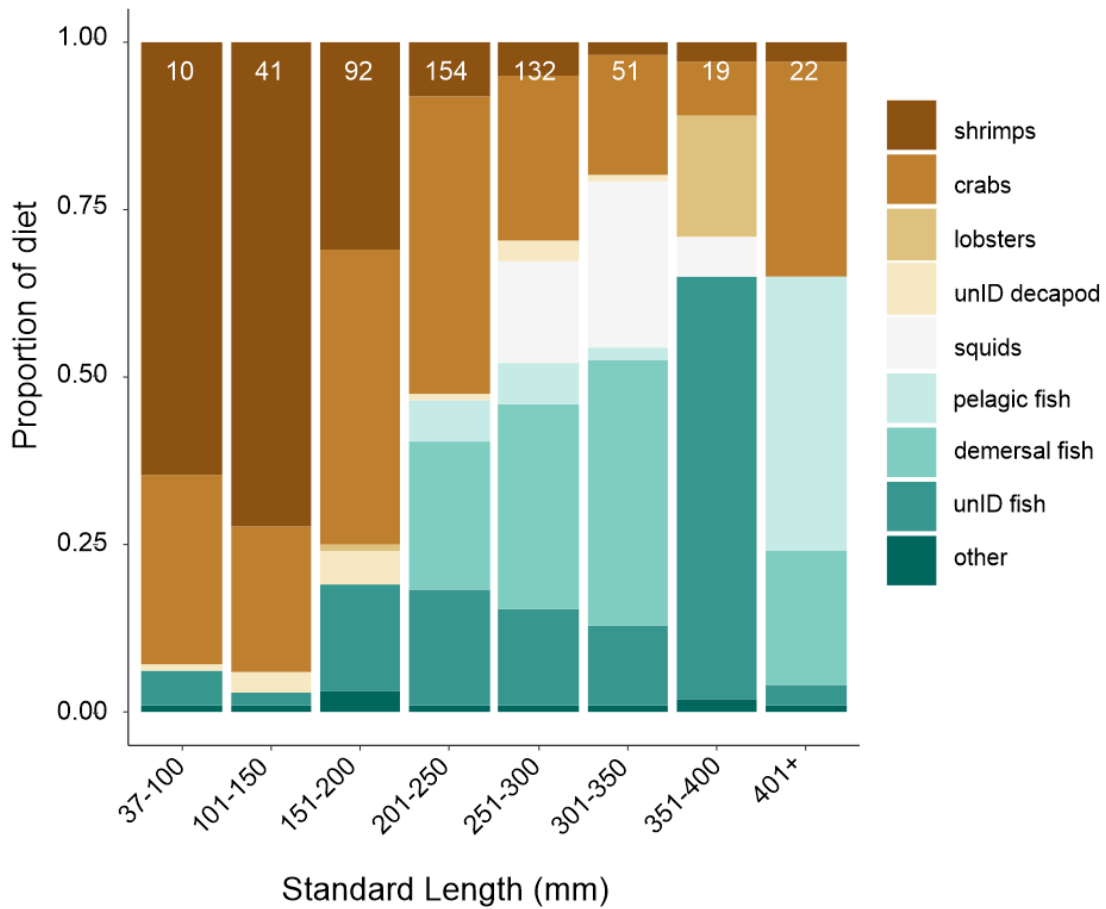


Figure 5.8. Proportion by volume of diets consumed by 521 Red Grouper collected from the WFS 2007-2015. All Red Grouper were collected, and stomachs analyzed by the Fisheries Independent Monitoring program at the Florida Fish and Wildlife Conservation Commission. Size categories are listed in standard length (SL). All prey items were identified to the lowest taxonomic level possible. Prey were aggregated to general categories for analysis (see Table 5.8 for families within each group). Any grouping (family or higher) that comprised less than 1% of total prey for the entire dataset was classified as “other” for graphical representation. Numbers at the tops of columns are total number of individuals included in that size class.

CHAPTER 6: SUMMARY AND CONCLUSIONS

Ecosystem modeling and fisheries stock assessments require large datasets consisting of life history parameters, diets, and the habitat needs of target species. I developed four novel interpretations for $\delta^{13}\text{C}$ and $\delta^{15}\text{N}$ in fish tissues, each of which is potentially useful in providing data to the stock assessment process. First, I showed that a consistent difference (constant partitioning offset) exists between the $\delta^{15}\text{N}$ of muscle and liver within the same fish in a laboratory setting. I showed that the isotopic partitioning offset in wild fish can be compared to this constant value to infer movement across an isoscape. Within the West Florida Shelf (WFS) context, similar species resulted in variable outcomes, suggesting differential habitat use and diets among species. I suggest that this method can be used as a screening technique for detecting movement or diet shifts in wild fish populations on short (weeks to months) timescales. Next, I showed that relative geolocation and evaluation of postlarval movement is possible using the historical approach of stable isotope values in fish eye-lens cores. This method can be used to understand habitat needs and movements in the earliest phases of life, which are difficult to sample in many fish species. Third, I showed that eye-lenses can be used to investigate the trophic and movement histories of individual marine fishes over the lifetime. By contrasting the eye-lens isotopic histories of two important benthic-modifying species, I showed that two species which play a similar ecological role as adults can have disparate trophic histories. Finally, I utilized the tools devised earlier to present a lifetime depiction of the trophic and movement histories of a single species from several sub-regions and two maturity classes. Throughout this work, I showed that isotopic tools can be used to monitor the stability of trophic and movement

histories over time and that isotopic data can be combined with traditional fisheries data such as stomach contents to increase knowledge of target species. Each method developed here is directly applicable to fisheries data in the Gulf of Mexico, and each has the potential to be adapted to systems around the world.

CHAPTER SUMMARIES

Chapter two: Isotopic differences between muscle and liver in captive and wild fishes

Tissue $\delta^{15}\text{N}$ values have been used to indicate trophic position for a wide variety of organisms. However, several authors have noted that differences exist between the values in various body tissues such as muscle and liver (Gaston and Suthers 2004; Chen et al. 2012; Schmidt et al. 2016). Differential turnover rates (Elsdon et al. 2010; Heady and Moore 2013) and differences in the organismal uses (Bunnell et al. 2007; Barreto-Curiel et al. 2018) of these tissues can explain some of the observed difference between $\delta^{15}\text{N}$ in the liver and muscle of a single individual. Stable isotope values in muscle tissue are often controlled by growth in fish (Varela et al. 2012; Davis et al. 2015; Mohan et al. 2016) while stable isotope values in liver are controlled by metabolism (Matley et al. 2013). In addition, the turnover in fish muscle tissue (and its proxy $\delta^{15}\text{N}$ value) occurs on a timescale of approximately one to two months (Guelinckx et al. 2007; Colborne and Robinson 2013), while the turnover in liver tissue occurs on a timescale of days to weeks (Matley et al. 2013). It is also known that the difference between available resources and the need for a nutrient can drive the fractionation within a tissue or organism. For example, fractionation in $\delta^{13}\text{C}$ in photosynthetic diatoms has been shown to be highly correlated with light availability (Radabaugh et al. 2014). Following this logic, it would make sense to suspect that a high-energy tissue such as liver would be more selective of nitrogen

atom incorporation than a longer-term storage tissue such as muscle, where high energy investment into isotopic discrimination may be wasted.

The objectives of this study were two-fold. The first goal was to determine whether a consistent difference (constant partitioning offset: CPO_{M-L}) existed between the liver and muscle $\delta^{15}N$ values for a variety of marine teleosts fed a consistent diet over time. To accomplish this goal, I used a literature review of captive, diet-switch studies examining marine teleosts. The second goal was to identify local reef-fish species for which liver and muscle tissue $\delta^{15}N$ fell within the range of CPO_{M-L} . To do this, I compared the CPO_{M-L} value to $\delta^{15}N$ differences calculated between muscle and liver of wild-caught reef-associated fishes captured from neritic waters surrounding Florida, USA.

For the literature review, I selected studies that used captive, diet-switch techniques of marine teleosts. All studies followed individual fish for a minimum of three months post diet-switch. I used the published end values for muscle and for liver of fish in control groups in each study. I found that across a variety of independent parameters: species, temperature, region, and others, a relatively tight relationship existed between values of $\delta^{15}N_{\text{muscle}}$ and $\delta^{15}N_{\text{liver}}$ ($\Delta\delta^{15}N_{M-L}$), with average (\pm SE) for $\Delta\delta^{15}N_{M-L}$ being $1.67 \pm 0.14\%$. I dubbed this parameter the constant partitioning offset (CPO_{M-L}).

I then compared this average difference to the differences I calculated ($\Delta\delta^{15}N_{M-L}$) for 575 individuals from eight wild reef-fish species collected in the eastern Gulf of Mexico (West Florida Shelf: WFS) and southeast Florida (SEFL). Among species, I found differences in the mean value of $\Delta\delta^{15}N_{M-L}$. Mean values could not be distinguished from CPO_{M-L} in five species, White Grunt, lionfishes, Golden Tilefish, Red Snapper, and Black Seabass. However, values of

$\Delta\delta^{15}\text{N}_{\text{M-L}}$ were significantly lower than $\text{CPO}_{\text{M-L}}$ in three species, Gray Snapper, Graysby, and Red Grouper.

I investigated differences in both sex and season for a few of the species. I investigated whether male and female White Grunt showed differences in their $\Delta\delta^{15}\text{N}_{\text{M-L}}$ values during the spawning season. I found that reproductive females differed significantly from $\text{CPO}_{\text{M-L}}$, but males and immature fish did not. I also investigated differences in season for both Red Grouper and Black Seabass. Although $\Delta\delta^{15}\text{N}_{\text{M-L}}$ was significantly lower than $\text{CPO}_{\text{M-L}}$ in both species for all seasons, differences existed among seasons, with spring having the lowest value of $\Delta\delta^{15}\text{N}_{\text{M-L}}$ in Red Grouper and winter having the lowest value of $\Delta\delta^{15}\text{N}_{\text{M-L}}$ in Black Seabass.

Due to the high consistency of $\Delta\delta^{15}\text{N}_{\text{M-L}}$ values observed in controlled, diet-switch studies of marine teleosts, I suggest that the value is robust and applicable worldwide. I further suggest that deviations from $\text{CPO}_{\text{M-L}}$ in wild fish populations may be attributable to movement of either the fish itself or the prey. If true, differences in $\Delta\delta^{15}\text{N}_{\text{M-L}}$ could be used as a screening tool to assess movement in a variety of marine teleost predator and prey species around the globe. However, this claim requires additional investigation. Physiological stressors such as starvation (Colborne and Robinson 2013; Varela et al. 2015; Barreto-Curiel et al. 2017) or reproduction (Martin et al. 1993) may affect bulk isotopic values in various body tissues. Therefore, further investigations using compound specific isotope analysis should be used to probe the physiological mechanisms for the observed difference between the $\delta^{15}\text{N}$ values in liver and muscle tissues. In addition, highly migratory species such as tunas, migratory baitfish and others must be investigated to verify patterns in bulk isotopes as well as individual amino acids.

While questions remain contrasting the role of movement and the role of physiology, the observation of a consistent value for $\Delta\delta^{15}\text{N}_{\text{M-L}}$ is quite useful. Fish for which $\Delta\delta^{15}\text{N}_{\text{M-L}}$ conforms

to CPO_{M-L} can be assumed to be in good condition and eating a consistent diet. Fish for which $\Delta\delta^{15}N_{M-L}$ differs from this value should be further investigated for the reason for the difference, whether it be physiological or movement-related.

Chapter three: Using eye-lens cores to assess postlarval locations

Traditionally, the study of fish larvae has been conducted using direct-capture techniques such as plankton net tows (Eldridge 1988; Schobernd et al. 2018). However, a few factors make this approach both cumbersome and potentially misleading. Once larvae are collected in the field, they must be identified microscopically. The process is time-consuming and many larvae within the same family are difficult to visually distinguish (Schobernd et al. 2018). In addition, larvae spend a minimum of one month in the water column (Cowen 1991; Powell and Tucker 1992; Drass et al. 2000). Finding and identifying larvae in the water column does not aid in locating spawning sites (Burghart et al. 2014) or give any indication of differential survival to later life stages (Takasuka et al. 2004; Tolley et al. 2012).

Scholars in both the US and UK have shown that stable isotopes ($\delta^{13}C$ and $\delta^{15}N$) in eye-lenses can be used to indicate patterns of movement and diets over the lifetime of fish (Wallace et al. 2014; Quaeck-Davies et al. 2018). The earliest records within each eye-lens are created with the first instance of nutrient uptake. In sharks and rays, the nutrition from the maternal investment of yolk can be observed (Simpson et al. 2019). However, in subtropical teleost fish, yolk sac feeding only lasts a few days (Colin et al. 1996), rendering the initiation of first feeding (~72 h) the first available isotopic record within the eye-lens (Kurth et al. 2019). The material of the outer cell layers of a lamina account for the highest percentage of the total mass. Due to analytical constraints, the minimum mass of 100 μg from an eye-lens core incorporates ~ 1 month of growth. Therefore, the isotopic values of the eye-lens core are most representative of

the latter half of the larval period (postlarval period). I used the $\delta^{13}\text{C}$ and $\delta^{15}\text{N}$ in eye-lens cores of four reef-fish species as a historical record to document larval diets and locations for individuals that survived to the juvenile period. The first objective of this study was to create universally effective rules of interpretation for correlations between $\delta^{13}\text{C}$ or $\delta^{15}\text{N}$ and external factors such as fish size at isotopic incorporation or location at capture. These rules can be applied to numerous additional species both on and off the WFS. The second objective was to isotopically identify difference in habitat use of four species found in broadly similar regions of the northern WFS.

To accomplish these goals, I collected juveniles from four species of reef fish on the northern WFS, Black Seabass (*Centropristis striata*), Gag (*Mycteroperca microlepis*), Red Grouper (*Epinephelus morio*), and Red Snapper (*Lutjanus campechanus*). I delaminated the eye-lenses of these fish until cores 0.5 – 1.0 mm remained. If tissue mass was insufficient to be processed by Isotope Ratio Mass Spectrometer (IRMS), I combined the cores from both eye lenses of the same fish. Each eye-lens core was packaged in tin capsules and analyzed for bulk $\delta^{13}\text{C}$ and bulk $\delta^{15}\text{N}$ using IRMS. I conducted Spearman rank correlations (r_s) between the isotopic value in the core and external parameters such as eye-lens diameter (a proxy for fish length/age at core-completion) and capture location (a proxy for juvenile location). I created a series of interpretation rules to describe the movement patterns of the individual larvae at the time of eye-lens core formation. I assumed that all larvae were at a similar trophic position, leaving location as the dominate driver of differences in the observed isotopic values. I also used a Bayesian statistical routine (SIBER; Jackson et al. 2011) to characterize the isotopic breadth and relative geographic location of larvae in each of the four species.

I found that Black Seabass was the most distributed species during the postlarval period with the largest central geographic area, as well as the species situated closest to shore during the larval period. According to correlations between the eye-lens core diameter and isotopic value, some Black Seabass seemed to move southward during the larval period. Historically, Black Seabass in the Gulf of Mexico are known to be centered in the Big Bend region of Florida, with adults and juveniles spread throughout the region (Bullock and Smith 1991; Hood et al. 1994; Weaver 1996). No specialized spawning areas are known to exist, lending credence to the idea of distributed spawning and larval locations throughout the northeastern WFS. Although Black Seabass are documented as far south as Tampa Bay, catch seems to be seasonal, and it is unknown whether spawning occurs this far south (Bullock and Smith 1991). A general drift southward by some larvae could assist in explaining the seasonal nature of Black Seabass catches in the southern extent of the range.

According to isotopic records in eye-lens cores, Red Grouper had the smallest central larval geographic region, situated farthest to the southwest of the four species. While pits dug by adult Red Grouper have been documented across the WFS, high concentrations have been found in the Steamboat Lumps Marine Protected Area (Coleman and Koenig 2010; Wall et al. 2011; Grasty et al. 2019). These known biological patterns corroborate the central isotopic values. While isotopic data did not indicate significant correlation with juvenile capture location, correlation between larval size and isotopic value suggested movement both north and inshore during the latter half of the larval period. The assumed distributed spawning agrees with the lack of correlation between juvenile capture locations and isotopic value.

Gag postlarval distribution was similar to Red Grouper, but the central area was farther north. The Madison-Swanson Marine Protected Area (just north of Steamboat Lumps) was

created, in part, in an effort to preserve Gag spawning populations (Coleman et al. 2011; Gruss et al. 2017), corroborating the isotopic data. There was a significant correlation between $\delta^{13}\text{C}$ and juvenile location in the inshore-offshore direction, an indication of inshore movement over the postlarval period. Inshore movement is well documented in larval Gag (Weisberg et al. 2016), with juveniles spending their first year in oligohaline portions of estuaries that empty into the Gulf of Mexico.

Red Snapper isotopically overlapped with all three other species. While significant correlation existed between $\delta^{15}\text{N}$ and juvenile location in the north-south direction, no correlation was found between either isotope ($\delta^{15}\text{N}$ or $\delta^{13}\text{C}$) and larval size, suggesting that larvae were not moving in a single direction with size. Little is known about the life history patterns of Red Snapper on the WFS. However, individuals of all sizes are found on relatively deep reefs in comparison to the other three species (SEDAR 2018). Isotopic data from eye-lens cores increase the evidence of multi-generational Red Snapper re-establishment on the WFS.

Each of the isotopic results presented above is consistent with known or inferred life history characteristics from decades of study in each of the four study species. They demonstrate the utility of isotopic values in eye-lens cores as indicators of location during the postlarval period. This technique is applicable to a wide variety of species including valuable fisheries species on the WFS or other coastal systems with well-known isoscapes. These techniques could also be applied to migratory fishes such as tunas and billfish, or even deep-sea fishes. The technique can be paired with a variety of new and traditional fisheries techniques as well. By pairing this technique with fish egg DNA barcoding (Burghart et al. 2014; Burrows et al. 2018) a complete picture of the egg and larval period can be developed for a species. This could reduce cost and manpower necessary for larval fish study and increase the understanding of essential

fish habitat for a variety of important species (Steimle et al. 1999; Lindeman et al. 2000; Drohan et al. 2007). In addition, eye-lens cores can be harvested and compared between members of a population over a several year period to investigate changes in central geography over time, or other changes that may occur with changes in climate or physiochemical environment.

Chapter four: Contrasting isotopic profiles in two benthic-modifying fish species

While eye-lens core isotopes can be used to study the geography of larvae, the entire eye-lens can be used to investigate the trophic and movement histories of individual fish. These data can be a useful addition single-species management plans and could be of use as ecosystem modeling becomes more integrated into the fisheries management process. I compared the lifetime isotopic records from adult Tilefish (*Lopholatilus chamaeleonticeps*) with those from adult Red Grouper. These two species were chosen because of their similar ecological roles during the adult phase. Both are demersal species found on the WFS and both are generally considered to be sedentary (Coleman and Koenig 2010). Both dig depressions in soft sediment and are assumed to reside near the depressions they created (Able et al. 1982; Ellis et al. 2017). However, historical evidence suggests some movement of juvenile Red Grouper across the WFS (SEDAR 2015), whereas Tilefish are not known to change location with length (SEDAR 2011). The primary objectives of this study were to discover whether differences in the lifetime eye-lens isotope profiles of Tilefish and Red Grouper were similar and whether inferences could be made about diet changes or movement over the lifetime using these data.

To address these questions, I conducted bulk isotope analysis of $\delta^{13}\text{C}$ and $\delta^{15}\text{N}$ within the eye-lenses of adult Tilefish and Red Grouper. Once collected, I delaminated each eye-lens into several successive laminae, with the innermost eye-lens lamina representing the postlarval stage

and the outermost lamina representing the most recent few months of life. I created rules for interpreting these data based on correlation between the isotopic value ($\delta^{13}\text{C}$ or $\delta^{15}\text{N}$) and the eye-lens diameter or correlation between the two isotopic values. I interpreted high correlation values in all three tests to indicate that fish were depending on the same basal resource throughout life and moving little across the landscape over the lifetime. Low correlation in one or more of the tests indicated some movement or change in basal-resource dependence over time.

I found that all individual Tilefish had tight correlations in all three tests. Both $\delta^{13}\text{C}$ and $\delta^{15}\text{N}$ correlated closely with eye-lens diameter, and both correlated closely with one another. We, therefore, suggest that Tilefish can be used as a model of lifetime isotopic consistency. If another species had correlation values as high as Tilefish, then that species could be considered highly sedentary with a consistent basal-resource dependence over the lifetime.

Results for Red Grouper correlations between isotopes and eye-lens diameters were quite different. While $\delta^{15}\text{N}$ correlated closely with eye-lens diameter throughout life, $\delta^{13}\text{C}$ correlations were weak in most fish. In turn, $\delta^{13}\text{C}$ did not correlate closely with $\delta^{15}\text{N}$. Historic stomach content records of Red Grouper suggest that the species goes through several shifts in diet before reaching maturity (Weaver 1996), potentially explaining large fluctuations in the lifetime $\delta^{13}\text{C}$ record. Despite similarities in Tilefish and Red Grouper as adults, they seem to have quite different routes of arriving at the evident stability observed within adults from both species.

In future studies using eye-lens stable isotopes, the interpretation rules developed here can be applied to a wide range of fish species on the WFS as well as fish species inhabiting other areas with established isoscapes. For example, the movement histories of Gag are thought to be well-established. However, the use of isotopic eye-lens profiles may elucidate movements or diet changes that have not been observed to date. Many other important species on the WFS such as

other groupers, grunts, and even some snappers, have little-known life history. The use of eye-lens isotopic profiles may aid in understanding of these species. In addition, eye-lens profiles of known seasonal and lifetime migrators such as tunas and mackerels (family: Scombridae) could be used as additional model species for comparison of species with unknown trophic or movement histories. Regardless of species, eye-lens isotope profiles can provide information regarding diet and movement over the entire lifetime and has the potential to streamline life history studies for use in ecosystem modeling, and eventually, fisheries stock assessments around the globe.

Chapter five: Red Grouper lifetime isotopes and the carbon bump

In this chapter, I utilized the tools developed in chapters three and four combined with traditional fisheries data to create a clearer depiction of the Red Grouper life history. By comparing the eye-lens core $\delta^{13}\text{C}$ and $\delta^{15}\text{N}$ values between maturity-classes, I showed that Red Grouper larval distribution is relatively consistent across time on the WFS. By comparing the eye-lens core isotopic values among capture areas, I showed that isotopic values differed among the three regions studied [WFS, Campeche Bank (Mexico), and southeast Florida (SEFL)]. These results suggest that Red Grouper spawned in one area, such as the Campeche bank of Mexico do not move to another area, such as the WFS, with growth. Although population genetics has shown a high degree of mixing among these populations (Zatcoff et al. 2004), tagging data suggests little long-distance movement (Burns 2009).

In this study, the largest eye-lens core isotopic differences were between fish from Mexico and those from SEFL, with fish from Mexico having much higher values of $\delta^{15}\text{N}$ than SEFL fish. This result aligns with the known isotopic trends for the region. Background $\delta^{15}\text{N}$

values on Campeche Bank are quite high (Peebles and Hollander 2020) while values for the Florida Reef Tract are probably much lower (Curtis 2016).

In chapter five I showed that most Red Grouper $\delta^{15}\text{N}$ profiles over the whole eye lens were positively correlated with ELD, suggesting increasing trophic position with growth, as occurs in other predatory species (Buchheister and Latour 2010). However, I showed that $\delta^{13}\text{C}$ peaked during the first year of life, suggesting movement or diet switching as a mechanism for undulations in the $\delta^{13}\text{C}$ profile over the lifetime.

Over 65% of both juvenile and adult Red Grouper from the WFS showed a similar pattern of values in the $\delta^{13}\text{C}$ over the lifetime, with a steep increase in $\delta^{13}\text{C}$ early in life, followed by a short-term decrease before leveling over the remainder of the lifetime. Due to its high prevalence, I dubbed this feature of the $\delta^{13}\text{C}$ profile “carbon bump” and quantified both height and location in each fish. I found that the mean ELD for the apex of the carbon bump was approximately 2 mm, corresponding to a standard length of approximately 100 mm. I found that the mean height of the carbon bump was approximately 3‰ above the initial $\delta^{13}\text{C}$ values from the eye-lens core.

I found that the feature was quite rare in both Mexico and SEFL. Of five adult Red Grouper from Mexico, only one showed the feature. The remainder showed increasing, linear $\delta^{13}\text{C}$ profiles with strong correlation between $\delta^{13}\text{C}$ and $\delta^{15}\text{N}$. Of three adult Red Grouper from SEFL, one fit the definition for having a carbon bump, but the $\delta^{13}\text{C}$ eye-lens profile was visibly quite different from the WFS fish with a carbon bump. The remaining fish from SEFL also showed increasing, linear trends in $\delta^{13}\text{C}$ with high correlation between $\delta^{13}\text{C}$ and $\delta^{15}\text{N}$.

I compared basal-resource dependence among the regions and maturity classes. I found that fish on the WFS and Campeche Bank, Mexico spent approximately 75% of their lifetime

dependent on a mixture of both planktonic and benthic basal resources. However, the earliest life stages were dependent on planktonic basal resource, and several individual fish became dependent on benthic resources at the apex of the carbon bump. The distribution of lifetime basal resource dependence was starkly different in the Red Grouper collected in SEFL. Only the earliest life history stage was dependent upon planktonic basal resource, the remainder of the lifespan were dependent upon mixed for benthic resources, with an average of 58% and a high of 92% of the lifetime represented by benthic resource dependence. This difference seems reasonable if Red Grouper captured in SEFL spend their entire lifetime within this clear-water, coral-reef ecosystem.

I found that the isotopic results corroborated existing fisheries data. Through stomach-content analysis, I found that small Red Grouper from the WFS (in similar size ranges to the height of the carbon bump) consumed large proportion of shrimps and crabs. These prey are benthic feeders themselves, relying on a benthic food web. Larger Red Grouper relied more heavily on fish prey, which are more likely to combine both benthic and planktonic resources. While I did not have access to larval Red Grouper stomachs, previous studies have shown that Red Grouper rely on zooplankton, especially copepods, during the postlarval period (Colin et al. 1996), which themselves rely on a phytoplankton as their primary food sources (Umezawa et al. 2018), indicating a planktonic basal-resource dependence during this life stage.

I used capture location and capture depth data for over 600 individuals (between the isotope and stomach content datasets) to investigate depth distributions for Red Grouper on the WFS. I found that the smallest individuals were captured in a wide range of depths (2 – 40 m), with most individuals <150 mm SL captured in < 3 m water depth and were captured over only a few months period from August to October. Fish over 150 mm SL were rarely observed in water

shallower than 10 meters, suggesting cross-shelf movement with ontogeny. Catch records of Red Grouper dating back to the earliest published works indicate a similar trend (Moe 1969; Burns 2009; SEDAR 2015).

Future researchers can use similar techniques of combining eye-lens bulk isotope data with other fisheries datasets to investigate lifetime changes in diet and movement. In fact, with increased certainty in the interpretation of isotopic data produced by corroboration with catch and stomach-content records, it is possible that eye-lens isotope records may eventually replace traditional techniques when incorporating traditionally under-studied species into ecosystem models.

CONCLUSIONS AND FUTURE DIRECTIONS

I showed that stable isotopes can be used as natural tags to investigate movement and diet over both short (weeks to months) and long (lifetime) time scales. The difference between the $\delta^{15}\text{N}$ values in muscle and liver of an individual fish can indicate movement along the $\delta^{15}\text{N}$ gradient in either the fish itself or its prey. The eye-lens core values of both $\delta^{13}\text{C}$ and $\delta^{15}\text{N}$ can distinguish among spawning locations in species with broadly similar spatial patterns and may be a useful tool for investigating postlarval movements of various species. Lifetime profiles of both $\delta^{13}\text{C}$ and $\delta^{15}\text{N}$ can indicate whether movement or diet changes have occurred over the lifetime of individual fish. Some species, such as Tilefish, remain essentially stationary, relying on consistent food sources throughout the lifetime. Others, such as Red Grouper, may move or switch prey types several times during life. Finally, these data can be combined with a variety of other data types such as stomach content and capture location to present a comprehensive account of the movement and diet patterns within a species or suite of species. Each of these

tools may be applied to the study of teleosts or other marine animals worldwide, provided a stable and known isotopic background for the region. In fact, these isotopic tools may be useful in several difficult-to-study groups such as deep-sea fishes, marine mammals, or turtles.

While the interpretation of bulk $\delta^{13}\text{C}$ and $\delta^{15}\text{N}$ isotopes is an accessible tool with widespread application, a few additional pieces of information may improve utility and help segregate inputs that are not currently possible. First, compound-specific isotope analysis can segregate the isotopic values in amino acids that fractionate within the body from those that are incorporated wholesale (McMahon et al. 2015; Ohkouchi et al. 2017). Using this technique, researchers are able to segregate amino acids that represent location from those that represent trophic position, increasing confidence in geographic interpretations (Graham et al. 2010). However, the method remains time-consuming and expensive, with hours of wet-chemistry required to segregate the amino acids prior to analysis (Ohkouchi et al. 2017).

Incorporating $\delta^{34}\text{S}$ or $\delta^{18}\text{O}$ into analyses may also improve geographic and trophic certainty. By creating an isoscape of $\delta^{34}\text{S}$, researchers have a third geographic axis on which to overlay their observations (Rossman et al. 2016). In addition, $\delta^{34}\text{S}$ is not appreciably fractionated with trophic position, so this isotope may be easier to interpret for geographic location than either $\delta^{13}\text{C}$ or $\delta^{15}\text{N}$ (Dance et al. 2018). Finally, $\delta^{34}\text{S}$ can be used as an additional indicator of benthic dependence, potentially segregating the confounding influences of movement and diet shifts inherent in $\delta^{13}\text{C}$ interpretation. The values of $\delta^{18}\text{O}$ within tissues are dependent upon salinity and temperature fluctuations (Darnaude et al. 2014). While salinity within the open ocean should remain essentially constant, temperature fluctuates much more in shallow water than in deep water, giving a depth signal along with a range of temperatures in which the fish was living. Regardless of which isotope is chosen, adding additional isotopes has the potential to

provide a fourth axis for geographic and dietary interpretation (Dance et al. 2018; Skinner et al. 2019).

Finally, clarifying the timing and connection between eye-lens isotope incorporation and growth parameters will improve researchers' ability to relate changes in isotopes to changes in diet or other ontogenetic shifts. To date, a single study has investigated the timing of isotopic incorporation within the eye-lens of captive fish (Granneman 2018). The study found that isotopic incorporation begins approximately 16 d post diet change. However, all fish within the study were less than one year old. At this life stage, fish are continuing to grow quickly, increasing eye-lens diameter at a comparable rate (Casselman 1990). Investigating the isotopic incorporation time required for both smaller and larger individuals could help constrain some of the assumptions made here. Investigations into eye-lens isotope incorporation of fast-growing fish in contrast to slow-growing fish of the same age could provide additional information about the relationship between body growth, eye-lens growth, and isotopic fractionation prior to incorporation into the eye lens. Additional studies relating eye-lens diameter, lamina number, or some other parameter to age would also aid in pinpointing isotopic interpretations to an even more specific time-period.

The interpretation of bulk $\delta^{13}\text{C}$ and $\delta^{15}\text{N}$ isotopes within the muscle, liver, and eye-lenses of teleost fishes are important tools for both short-term and long-term investigation of movement and diet. In all cases explored here, isotopic interpretations corroborated life history, diet, and movement information known from decades of study. These tools are applicable in a wide variety of species and locations, if background isoscapes exist for the region. Eye-lens isotope profiles may help expand information about difficult-to-study species such as marine mammals, turtles, and deep-sea fishes. Results of these analyses can be combined with traditional fisheries

data such as capture location, conventional tagging data, and stomach content data to present both short-term and long-term accounts of movement and diet. Precision may be increased by the addition of compound-specific isotope analysis and additional isotopes, but the use of bulk $\delta^{13}\text{C}$ and $\delta^{15}\text{N}$ seems sufficient to increase understanding of a wide variety of species at this time.

LITERATURE CITED

- Able, K. W., C. B. Grimes, R. A. Cooper, and J. R. Uzmann. 1982. Burrow construction and behavior of tilefish, *Lopholatilus chamaeleonticeps*, in Hudson submarine canyon. *Environmental Biology of Fishes* **7**: 199-205.
- Barreto-Curiel, F., U. Focken, L. R. D'Abramo, J. A. Cuaron, and M. T. Viana. 2018. Use of isotopic enrichment to assess the relationship among dietary protein levels, growth and nitrogen retention in juvenile *Totoaba macdonaldi*. *Aquaculture* **495**: 794-802.
- Barreto-Curiel, F., U. Focken, L. R. D'Abramo, and M. T. Viana. 2017. Metabolism of *Seriola lalandi* during starvation as revealed by fatty acid analysis and compound-specific analysis of stable isotopes within amino acids. *Plos One* **12**: 17.
- Buchheister, A., and R. J. Latour. 2010. Turnover and fractionation of carbon and nitrogen stable isotopes in tissues of a migratory coastal predator, summer flounder (*Paralichthys dentatus*). *Canadian Journal of Fisheries and Aquatic Sciences* **67**: 445-461.
- Bullock, L. H., and G. B. Smith. 1991. Seabasses (Pisces: Serranidae). *Memoirs of the Hourglass Cruises* **8**: 1-243.
- Bunnell, D. B., S. E. Thomas, and R. A. Stein. 2007. Prey resources before spawning influence gonadal investment of female, but not male, white crappie. *Journal of Fish Biology* **70**: 1838-1854.
- Burghart, S. E., L. Van Woudenberg, C. A. Daniels, S. D. Meyers, E. B. Peebles, and M. Breitbart. 2014. Disparity between planktonic fish egg and larval communities as indicated by DNA barcoding. *Marine Ecology Progress Series* **503**: 195-204.
- Burns, K. 2009. Evaluation of the efficacy of the minimum size rule in the Red Grouper and Red Snapper fisheries with respect to J and circle hook mortality and barotrauma and the consequences for survival and movement. University of South Florida.
- Burrows, M., J. S. Browning, M. Breitbart, S. A. Murawski, and E. B. Peebles. 2018. DNA barcoding reveals clear delineation between spawning sites for neritic versus oceanic fishes in the Gulf of Mexico. *Fisheries Oceanography*: 1-12.
- Casselman, J. M. 1990. Growth and relative size of calcified structures of fish. *Transactions of the American Fisheries Society* **119**: 673-688.
- Chen, G., H. Zhou, D. Ji, and B. Gu. 2012. Stable isotope enrichment in muscle, liver, and whole fish tissues of brown-marbled groupers (*Epinephelus fuscoguttatus*). *Ecological Processes* **1**: 1-5.
- Colborne, S. F., and B. W. Robinson. 2013. Effect of nutritional condition on variation in delta C-13 and delta N-15 stable isotope values in Pumpkinseed sunfish (*Lepomis gibbosus*) fed different diets. *Environmental Biology of Fishes* **96**: 543-554.

- Coleman, F. C., and C. C. Koenig. 2010. The Effects of fishing, climate change, and other anthropogenic disturbances on Red Grouper and other reef fishes in the Gulf of Mexico. *Integrative and Comparative Biology* **50**: 201-212.
- Coleman, F. C., K. M. Scanlon, and C. C. Koenig. 2011. Groupers on the edge: shelf edge spawning habitat in and around marine reserves of the northeastern Gulf of Mexico. *Professional Geographer* **63**: 456-474.
- Colin, P. L., C. C. Koenig, and W. A. Laroche. 1996. Development from egg to juvenile of the Red Grouper (*Epinephelus morio*) (Pisces: Serranidae) in the laboratory, p. 399-414. *In* F. ArreguinSanchez, J. L. Munro, M. C. Balgos and D. Pauly [eds.], *Biology, fisheries and culture of tropical groupers and snappers: Proceedings of an EPOMEX/ICARM International workshop on tropical snappers and groupers*. International Center for Living Aquatic Resources Management.
- Cowen, R. K. 1991. Variation in the planktonic larval duration of the temperate wrasse *Semicossyphus pulcher*. *Marine Ecology Progress Series* **69**: 9-15.
- Curtis, J. S. 2016. Resource use overlap in a native grouper and invasive lionfish. University of South Florida.
- Dance, K. M., J. R. Rooker, J. B. Shipley, M. A. Dance, and R. J. D. Wells. 2018. Feeding ecology of fishes associated with artificial reefs in the northwest Gulf of Mexico. *Plos One* **13**.
- Darnaude, A. M., A. Sturrock, C. N. Trueman, D. Mouillot, S. E. Campana, E. Hunter, and Eimf. 2014. Listening in on the past: What can otolith delta O-18 values really tell us about the environmental history of fishes? *Plos One* **9**.
- Davis, J. P., K. A. Pitt, B. Fry, and R. M. Connolly. 2015. Stable isotopes as tracers of residency for fish on inshore coral reefs. *Estuarine Coastal and Shelf Science* **167**: 368-376.
- Drass, D. M., K. L. Bootes, J. Lyczkowski-Shultz, B. H. Comyns, G. J. Holt, C. M. Riley, and R. P. Phelps. 2000. Larval development of red snapper, *Lutjanus campechanus*, and comparisons with co-occurring snapper species. *Fishery Bulletin* **98**: 507-527.
- Drohan, A. F., J. P. Manderson, and D. B. Packer. 2007. Essential fish habitat source document: Black Sea Bass, *Centropristis striata*, lifeHistory and habitat characteristics. Second Edition, p. 78. National Oceanic and Atmospheric Administration.
- Eldridge, P. J. 1988. The southeast area monitoring and assessment program (SEAMAP)- A state-federal-university program for collection, management, and dissemination of fishery-independent data and information in the southeastern United States. *Marine Fisheries Review* **50**: 29-39.
- Ellis, R. D., F. C. Coleman, and C. C. Koenig. 2017. Effects of habitat manipulation by red grouper, *Epinephelus morio*, on faunal communities associated with excavations in Florida Bay. *Bulletin of Marine Science* **93**: 961-983.
- Elsdon, T. S., S. Ayvazian, K. W. McMahon, and S. R. Thorrold. 2010. Experimental evaluation of stable isotope fractionation in fish muscle and otoliths. *Marine Ecology Progress Series* **408**: 195-205.
- Gaston, T. F., and I. M. Suthers. 2004. Spatial variation in delta C-13 and delta N-15 of liver, muscle and bone in a rocky reef planktivorous fish: the relative contribution of sewage. *Journal of Experimental Marine Biology and Ecology* **304**: 17-33.
- Graham, B. S., P. L. Koch, S. D. Newsome, K. W. McMahon, and D. Aurioles. 2010. Using Isoscapes to Trace the Movements and Foraging Behavior of Top Predators in Oceanic Ecosystems, p. 299-318. *In* J. B. West, G. J. Bowen, T. E. Dawson and K. P. Tu [eds.],

- Isoscapes: Understanding movement, pattern, and process on earth through isotope mapping.
- Granneman, J. E. 2018. Evaluation of trace-metal and isotopic records as techniques for tracking lifetime movement patterns in fishes. University of South Florida.
- Grasty, S., C. C. Wall, J. W. Gray, J. Brizzolara, and S. A. Murawski. 2019. Temporal persistence of Red Grouper holes and analysis of associated fish assemblages from towed camera data in the Steamboat Lumps marine protected area. *Transactions of the American Fisheries Society*: 1-9.
- Gruss, A., J. T. Thorson, S. R. Sagarese, E. A. Babcock, M. Karnauskas, J. F. Walter, III, and M. Drexler. 2017. Ontogenetic spatial distributions of red grouper (*Epinephelus morio*) and gag grouper (*Mycteroperca microlepis*) in the US Gulf of Mexico. *Fisheries Research* **193**: 129-142.
- Guelinckx, J., J. Maes, P. Van Den Driessche, B. Geysen, F. Dehairs, and F. Ollevier. 2007. Changes in delta C-13 and delta N-15 in different tissues of juvenile Sand Goby *Pomatoschistus minutus*: a laboratory diet-switch experiment. *Marine Ecology Progress Series* **341**: 205-215.
- Heady, W. N., and J. W. Moore. 2013. Tissue turnover and stable isotope clocks to quantify resource shifts in anadromous rainbow trout. *Oecologia* **172**: 21-34.
- Hood, P. B., M. F. Godcharles, and R. S. Barco. 1994. Age, growth, reproduction, and the feeding ecology of black-sea bass, *Centropristis striata* (Pisces, Serranidae), in the eastern Gulf of Mexico. *Bulletin of Marine Science* **54**: 24-37.
- Jackson, A. L., R. Inger, A. C. Parnell, and S. Bearhop. 2011. Comparing isotopic niche widths among and within communities: SIBER - Stable Isotope Bayesian Ellipses in R. *Journal of Animal Ecology* **80**: 595-602.
- Kurth, B. N., E. Peebles, and C. D. Stallings. 2019. Atlantic Tarpon (*Megalops atlanticus*) exhibit upper estuarine habitat dependence followed by foraging system fidelity after ontogenetic habitat shifts. *Estuarine Coastal and Shelf Science*.
- Lindeman, K. C., R. Pugliese, G. T. Waugh, and J. S. Ault. 2000. Developmental patterns within a multispecies reef fishery: Management applications for essential fish habitats and protected areas. *Bulletin of Marine Science* **66**: 929-956.
- Martin, N. B., D. F. Houlihan, C. Talbot, and R. M. Palmer. 1993. Protein-metabolism during sexual maturation in female Atlantic salmon (*Salmo salar* L). *Fish Physiology and Biochemistry* **12**: 131-141.
- Matley, J. K., A. T. Fisk, and T. A. Dick. 2013. The foraging ecology of Arctic cod (*Boreogadus saida*) during open water (July-August) in Allen Bay, Arctic Canada. *Marine Biology* **160**: 2993-3004.
- McMahon, K. W., S. R. Thorrold, T. S. Elsdon, and M. D. McCarthy. 2015. Trophic discrimination of nitrogen stable isotopes in amino acids varies with diet quality in a marine fish. *Limnology and Oceanography* **60**: 1076-1087.
- Moe, M. A. J. 1969. Biology of the Red grouper *Epinephelus morio* from the eastern Gulf of Mexico, p. 1-95. Florida Department of Natural Resources Marine Research Laboratory Professional Papers Series. Fish and Wildlife Research Institute.
- Mohan, J. A., S. D. Smith, T. L. Connelly, E. T. Attwood, J. W. McClelland, S. Z. Herzka, and B. D. Walther. 2016. Tissue-specific isotope turnover and discrimination factors are affected by diet quality and lipid content in an omnivorous consumer. *Journal of Experimental Marine Biology and Ecology* **479**: 35-45.

- Ohkouchi, N., Y. Chikaraishi, H. G. Close, B. Fry, T. Larsen, D. J. Madigan, M. D. McCarthy, K. W. McMahon, T. Nagata, Y. I. Naito, N. O. Ogawa, B. N. Popp, S. Steffan, Y. Takano, I. Tayasu, A. S. J. Wyatt, Y. T. Yamaguchi, and Y. Yokoyama. 2017. Advances in the application of amino acid nitrogen isotopic analysis in ecological and biogeochemical studies. *Organic Geochemistry* **113**: 150-174.
- Peebles, E. B., and D. J. Hollander. 2020. Combining Isoscapes with Tissue-Specific Isotope Records to Recreate the Geographic Histories of Fish, p. 203-218. *In* S. A. Murawski et al. [eds.], *Scenarios and Responses to Future Deep Oil Spills*. Springer, Cham.
- Powell, A. B., and J. W. Tucker. 1992. Egg and larval development of laboratory-reared Nassau Grouper, *Epinephelus striatus* (Pisces Serranidae). *Bulletin of Marine Science* **50**: 171-185.
- Quaek-Davies, K., V. A. Bendall, K. M. MacKenzie, S. Hetherington, J. Newton, and C. N. Trueman. 2018. Teleost and elasmobranch eye lenses as a target for life-history stable isotope analyses. *PeerJ* **6**: 26.
- Radabaugh, K. R., E. M. Malkin, D. J. Hollander, and E. B. Peebles. 2014. Evidence for light-environment control of carbon isotope fractionation by benthic microalgal communities. *Marine Ecology Progress Series* **495**: 77-90.
- Rossmann, S., P. H. Ostrom, F. Gordon, and E. F. Zipkin. 2016. Beyond carbon and nitrogen: guidelines for estimating three-dimensional isotopic niche space. *Ecology and Evolution* **6**: 2405-2413.
- Schmidt, S. N., L. C. Lund-Hansen, and E. Kristensen. 2016. Diet-shift driven delta C-13 and delta N-15 changes in liver and muscle tissues of juvenile clownfish *Amphiprion frenatus*: A laboratory experiment. *Journal of Experimental Marine Biology and Ecology* **475**: 137-143.
- Schobernd, C. M., M. C. McManus, J. Lyczkowski-Shultz, N. M. Bacheler, and D. M. Drass. 2018. Extrusion of fish larvae from SEAMAP plankton sampling nets: a comparison between 0.333-mm and 0.202-mm mesh nets. *Fishery Bulletin* **116**: 240-255.
- SEDAR. 2011. SEDAR 22-Gulf of Mexico Tilefish, p. 467.
- . 2015. SEDAR 42 Stock Assessment Report - Gulf of Mexico Red Grouper.
- . 2018. SEDAR 52: Gulf of Mexico Red Snapper, p. 434. SEDAR. NOAA.
- Simpson, S., D. Sims, and C. N. Trueman. 2019. Ontogenetic trends in resource partitioning and trophic geography of sympatric skates (Rajidae) inferred from stable isotope composition across eye lenses. *Marine Ecology Progress Series* **624**: 103-116.
- Skinner, C., A. C. Mill, S. P. Newman, J. Newton, M. R. D. Cobain, and N. V. C. Polunin. 2019. Novel tri-isotope ellipsoid approach reveals dietary variation in sympatric predators. *Ecology and Evolution*: 1-11.
- Steimle, F. W., C. A. Zetlin, P. L. Berrien, D. L. Johnson, and C. Sukwoo. 1999. Essential fish habitat source document: Tilefish, *Lopholatilus chamaeleonticeps*, life history and habitat characteristics. NOAA Technical Memorandum. National Marine Fisheries Service.
- Takasuka, A., Y. Oozeki, R. Kimura, H. Kubota, and I. Aoki. 2004. Growth-selective predation hypothesis revisited for larval anchovy in offshore waters: cannibalism by juveniles versus predation by skipjack tunas. *Marine Ecology Progress Series* **278**: 297-302.
- Tolley, S. G., B. M. Brosious, J. T. Evans, J. L. Nelson, L. H. Haynes, L. K. Smith, S. E. Burghart, and E. B. Peebles. 2012. Freshwater inflow effects on larval fish and crab settlement onto oyster reefs. *Journal of Shellfish Research* **31**: 895-908.

- Umezawa, Y., A. Tamaki, T. Suzuki, S. Takeuchi, C. Yoshimizu, and I. Tayasu. 2018. Phytoplankton as a principal diet for callinassid shrimp larvae in coastal waters, estimated from laboratory rearing and stable isotope analysis. *Marine Ecology Progress Series* **592**: 141-158.
- Varela, J. L., F. de la Gandara, A. Ortega, and A. Medina. 2012. C-13 and N-15 analysis in muscle and liver of wild and reared young-of-the-year (YOY) Atlantic bluefin tuna. *Aquaculture* **354**: 17-21.
- Varela, J. L., A. Ortega, F. de la Gandara, and A. Medina. 2015. Effects of starvation on N-15 and C-13 in Atlantic bonito, *Sarda sarda* (Bloch, 1793). *Aquaculture Research* **46**: 2043-2047.
- Wall, C. C., B. T. Donahue, D. F. Naar, and D. A. Mann. 2011. Spatial and temporal variability of red grouper holes within Steamboat Lumps Marine Reserve, Gulf of Mexico. *Marine Ecology Progress Series* **431**: 243-254.
- Wallace, A. A., D. J. Hollander, and E. B. Peebles. 2014. Stable isotopes in fish eye lenses as potential recorders of trophic and geographic history. *Plos One* **9**.
- Weaver, D. C. 1996. Feeding ecology and ecomorphology of three seabasses (Pisces: Serranidae) in the northeastern Gulf of Mexico. University of Florida.
- Weisberg, R. H., L. Y. Zheng, Y. G. Liu, S. Murawski, C. M. Hu, and J. Paul. 2016. Did Deepwater Horizon hydrocarbons transit to the west Florida continental shelf? *Deep-Sea Research Part II-Topical Studies in Oceanography* **129**: 259-272.
- Zatcoff, M. S., A. O. Ball, and G. R. Sedberry. 2004. Population genetic analysis of red grouper, *Epinephelus morio*, and scamp, *Mycteroperca phenax*, from the southeastern US Atlantic and Gulf of Mexico. *Marine Biology* **144**: 769-777.

APPENDIX A. PERMISSION TO RETAIN FISH AND IOCUC APROVAL



UNITED STATES DEPARTMENT OF COMMERCE
National Oceanic and Atmospheric Administration
NATIONAL MARINE FISHERIES SERVICE
Southern Region Office
255 13th Street South
St. Petersburg, Florida 33701-7605
t: 727.321.5000
f: 727.321.5000

F/SER24:SB

Ms. Julie Vecchio
College of Marine Science
University of South Florida
830 1st Street Southeast
St. Petersburg, Florida 33701

NOV 02 2015

Dear Ms. Vecchio:

This letter of acknowledgment (LOA) recognizes the activities outlined in your October 27, 2015, e-mail as scientific research in accordance with the definitions and guidance at 50 CFR 600.10 and 600.745(a). As such, the proposed activities are not subject to fishing regulations at 50 CFR 622 or Essential Fish Habitat requirements at 50 CFR 600.805 *et seq.*, developed in accordance with the Magnuson-Stevens Fishery Conservation and Management Act. Exemptions or exclusions for any other applicable laws and regulations are not included in this LOA, and should be obtained through appropriate regulating agencies.

NOAA Fisheries understands you will be collecting approximately 100 red grouper that are 300 millimeters total length or less. These fish will be captured using standard recreational rod-and-reel fishing gear in coastal Florida waters, and sacrificed to collect biological tissues. This LOA is effective through December 31, 2018. Copies of this LOA and the scientific research plan should be onboard the vessels included on the enclosure.

Should you have any additional questions, please contact Dr. Steve Branstetter at 727-824-5305 or steve.branstetter@noaa.gov.

Sincerely,

Roy E. Crabtree, Ph.D.
Regional Administrator

Enclosure




Figure AA.1. Letter of agreement granting explicit permission for researchers to collect and retain Red Grouper below minimum legal size.

RESEARCH INTEGRITY AND COMPLIANCE
INSTITUTIONAL ANIMAL CARE & USE COMMITTEE

MEMORANDUM

TO: Ernst Peebles,

FROM: 
Farah Moulvi, MSPH, IACUC Coordinator
Institutional Animal Care & Use Committee
Research Integrity & Compliance

DATE: 1/3/2017

PROJECT TITLE: Post-mortem fish tissue collection

FUNDING SOURCE: USF department, institute, center, etc.

IACUC PROTOCOL #: T IS00003324

PROTOCOL STATUS: **APPROVED**

The Institutional Animal Care and Use Committee (IACUC) reviewed your application requesting the use of animals in research for the above-entitled study. The IACUC **APPROVED** your request to use the following animals in your **protocol for a one-year period beginning 12/27/2016**:

Species: Lutjanidae, Serranidae, Istiophoridae, Malacanthidae, Scombridae, Tetraodontidae, Lamnidae, Squalidae, Centrophoridae, Carcharhinidae, Haemulidae, Sparidae, Triakidae, Ophichthidae, Synodontidae, Phycidae, Ophidiidae, Muraenidae, Sphyrnidae, Carangidae

Tissues: Eyes, otoliths, muscle, internal organs, bone, blood, scales, fin rays, fin spines

Please take note of the following:

- IACUC approval is granted for a one-year period at the end of which, an annual renewal form must be submitted for years two (2) and three (3) of the protocol through the eIACUC system. After three years all continuing studies must be completely re-described in a new electronic application and submitted to IACUC for review.

- All modifications to the IACUC-Approved Protocol must be approved by the IACUC prior to initiating the modification. Modifications can be submitted to the IACUC for review and approval as an Amendment or Procedural Change through the eIACUC system. These changes must be within the scope of the original research hypothesis, involve the original species and justified in writing. Any change in the IACUC-approved protocol that does not meet the latter definition is considered a major protocol change and requires the

Figure AA2. University of South Florida Institutional Animal Care and Use Committee (IACUC) approval for post-mortem fish tissue dissection. Letter was renewed annually 2016-2020.

Collection	Species name: _____		Specimen #: _____	JV #: _____
Lens Diameter (μm)	Lamina Midpoint (μm)	Lamina Number (from center)	Vial ID	Notes

Figure AB.2. Eye-lens peeling datasheet. This sheet includes information on the eye-lens diameter, lamina midpoint, lamina number, and vial identification for all samples peeled from the eye lens of a single fish. This datasheet is used in conjunction with instructions located in Appendix C.

APPENDIX C. SAMPLE PREPARATION PROTOCOLS

Each of these numbered protocols can be printed and used by a technician or student to complete the steps required to get samples from the fish to completing sample preparation for the Isotope Ratio Mass Spectrometer.

Protocol 1. Extract samples from whole fish and dry/pulverize liver or muscle samples

Materials

- Aluminum foil
- Otolith vials
- Write-in-the-rain paper
- Pencil
- Sharpie
- Zip top or Whirlpak bags
-

Extracting samples

1. Prepare materials ahead of time by:
 - Writing # for sample on outside of vial
 - Writing # for sample on outside of Zip top or Whirlpak bag
 - Writing Collection number, species, specimen #, & # on small write-in-the-rain paper tag
 - Cutting 3-inch square piece of aluminum foil & writing # & either L or M on the upper left corner in sharpie
2. Remove fish carcass from cooler, ice, or freezer.
3. Record Collection Number & Species at the top of the Specimen datasheet
4. For each specimen measure and record SL, FL, TL, Total weight
5. Assign each specimen a #.
6. Each specimen from the same reference receives a sequential number starting at 1
7. Slit belly of fish if intact
8. Check sex of fish
9. Record sex of the fish if known. Record “U” if unknown or unchecked
10. Remove whole liver if possible
11. Weigh liver & record
12. Remove remainder of guts
13. Record gutted weight of fish
14. Cut 2 cm x 2 cm piece from liver. Place on aluminum foil labeled “L” for that sample. Fold foil
15. Cut 2 cm x 2 cm piece of muscle from upper left shoulder. Remove skin. Place on aluminum foil labeled “M” for that sample. Fold foil
16. Remove otoliths. Rinse in DI water and place in otolith vial for that sample. Place otolith vial in tray with other otoliths.

17. If fish is small, sever the head and place the whole head in the zip top bag. If fish is large, remove both eyes whole and place eyes in zip top bag.
18. Place folded aluminum foil with liver and muscle into bag with eyes/head.
19. Check each box for samples taken (Otoliths, eyes, liver, muscle)
20. Place whole package into freezer with like samples. Make sure outer bag is labeled.

Drying liver/muscle samples

21. Remove samples from freezer
22. Open aluminum foil to make sure # is written on the inside
23. Place opened foil packet into drying oven
24. Dry in drying oven for 48 hours
25. Once dry, place sample in “Wig-l-bug” to homogenize sample
26. Once ground, place sample into small, numbered plastic vial.
27. Clean Wig-L-Bug between each use using air from compressor.

Protocol 2. Fish Eye Lens Peeling Protocol: Water Method

Materials

- Dissecting microscope with micrometer
- Scalpel
- Fine-tipped forceps (2 pairs)
- Glass petri dish
- Clear tape
- Small container DI water (2)
- Kim wipes
- Small squares aluminum foil (around 20)
- Gloves
- Small vials
- Marking pens
- Datasheets
- 2 beakers (one filled with DI water. The other empty)

Methods

1. Use a small ruler to check the microscope's micrometer. Make sure that 10 marks on the micrometer = 1 mm on the ruler. You will be using this to measure the lens diameter. For most scopes, power 10 should be the correct setting
2. Thaw just one sample at a time. Thawing is fast, peeling is slow
3. Once sample is thawed, use scalpel to gently cut a slit in the eye tissue overlying the lens
4. Gently grasp the lens with forceps & cut the ligament and muscle holding the eye lens in place
5. Place the lens on the glass petri dish
6. There will still be a small envelope of tissue surrounding the lens with a small amount of fluid behind it. Gently peel this envelope of tissue off the lens
7. Add enough water to the petri dish to cover the lens.
8. Examine the lens under the microscope. Look for the striations running from one pole to the other.
9. Position the lens so that you can peel layers off parallel to the striations.
10. After positioning the lens, but before peeling any layers, use the stage micrometer to measure the diameter of the lens & record.
11. Begin peeling by holding the lens in place with one pair of forceps & gently digging the other pair into the outer layer of lens. This should result in a large section of the outer layer peeling away. Place all lens peeled away onto one piece of aluminum foil.
12. Continue peeling until you have peeled away the entire outer layer and the eye lens is relatively smooth again.
13. Remove the lens from the dish & dump the water into the empty beaker. You may also need to use a Kim wipe to get the sticky eye lens material off the petri dish
14. Add water to cover the lens from the beaker of clean DI water
15. Measure the diameter of the lens. Record on datasheet
16. Begin peeling another layer parallel to the striations. Continue until the lens is relatively smooth again.
17. Measure again.
18. Repeat steps 7-17 until diameter of lens is approximately 0.5-0.7 mm. This is the core.

19. If you need to run eye lens layers in duplicate, you will need to peel the second eye as well (see steps 21-26 below). There will not be enough material to get two samples from this inner core layer.

20. Place each layer into a labeled vial. Most should be dry by this time. If not, leave the lid off the vial until the layer is dry.

Peeling second lens from the same fish

21. Repeat steps 1-18 on the second eye.

22. As before, record diameter on datasheet.

23. If diameters of second lens are within 0.1 mm of first and there are the same number of layers, then the material from both eyes can be combined into the same vial for the entire lens.

24. If diameters of second lens are not the same as the first, or the numbers of layers are not the same, layers cannot be combined into the same vial.

25. More common: outer layers are not the same diameter or number of layers, but inner 2-3 are. These inner layers may be combined. These are the ones for which extra material is generally needed for sufficient mass.

26. Discard all material that does not get use (in a single vial for that layer number)

Drying eye lens layers

27. Leave lids open on plastic vials

28. Place vials into vial holder

29. Place vial holder into drying oven at least overnight. Check on vials in morning.

30. If eye lens layers are dry, close lids on all vials

Filling out the eye lens peeling datasheet

Collection Number: _____ Species ID: _____ Specimen #: _____ JV #: _____

Lens Diameter (mm)	Lamina Midpoint (mm)	Lamina Number (from center)	Vial ID	Notes
3.5				
	2.95	7	1100	
2.4				
	2.2	6	1101	
2.0				
	1.8	5	1102	
1.6				
	1.4	4	1103	
1.2				
	1.0	3	1104	
0.8				
	0.65	2	1105	
0.5				
	0.25	1	1106	

1. Begin by filling out the information at the top of the page (Collection number, species ID, Specimen #, JV#)
2. Each time a lens diameter is measured, write that diameter (in mm) in the left-hand column (**Red text**)
3. When you place that layer into a vial, fill out the vial ID (**Blue Text**)
4. Once you have finished peeling the entire lens, record the layer number. Begin with #1 being the most inner layer and increase numbers until you get to the outer layer (**Green Text**)
5. Calculate the lamina midpoint as the mean of the diameters above and below that line. (**Purple Text**)
6. For the final “Lamina midpoint” record half the value of the last diameter
7. If peeling a second eye lens from the same fish, draw a line on the datasheet. Complete Lens Diameter & Lamina Number. Indicate whether additional material from this eye went into the vials with the other eye.
8. Discard all material that does not go into the single vial for that layer.

Protocol 3. Eye lens or Liver/Muscle Material Prep for IRMS

Materials

- Microbalance
- Small tin containers
- Nitrile gloves
- Fish tissue (eye-lens, liver, or muscle)
- Forceps (2 pairs curved tip)
- Small material spoon
- Kim Wipes
- Plastic 12x8 grid tray with letters & numbers
- Standards materials (NIST 1577B, NIST 8573, NIST 8574 or check listed material)

Methods

1. Get out an IRMS datasheet from the tray above the balance
2. Read the instructions on the top of the sheet. Follow all instructions for masses of standards to use.
3. Get out plastic grid tray and tin containers from the drawer next to the microbalance
4. Wipe down the balance, the counter in front of the balance, and all tools to be used with a Kim Wipe
5. Fold an empty capsule and then roll between two fingers until approximately round
6. Place this empty capsule into the first grid cell (A1) in the grid tray
7. Repeat step 5. Place this empty capsule into the second cell (A2) in the grid tray.
8. Place an empty tin capsule on the microbalance and hit the large center button on the balance. This will tare the balance with the tin capsule on it. Once the balance has finished taring, the door will open automatically.
9. Remove the tin capsule from the balance.
10. Find standard **NIST 8573**. Weigh out anywhere between 150 and 1000 ug into the capsule.
11. Place capsule back onto balance. Record mass on datasheet.
12. Wipe down microbalance, counter, and all tools with Kim Wipe
13. Take capsule out, roll into a ball, and place into well A3.
14. Repeat steps 8-12. Place into well A4
15. Repeat steps 8-12 using standard **NIST 8574** twice and follow directions on sheet. These should go in cells A5 & A6
16. Repeat steps 8-12 using **NIST 1577B** (Bovine Liver) twice.
17. Each of these six standards should be in the range 150-1000 ug of material. They should be as evenly spaced as possible. Order does not matter. (Ex: 300 ug, 150 ug, 457 ug, 822 ug, 604 ug, 995 ug).
18. I usually do all standards at once. Cell C1 gets a **NIST 1577B** (Bovine Liver) which should weigh anywhere between 150 and 1000 ug.
19. Cells D10-E1 also get all 3 standards. Masses should be between 150 and 1000 ug, but distribution is not necessary.
20. Once all standards have been weighed, you can start weighing your material.
21. Again, wipe down the balance, counter, and tools with a Kim Wipe to make sure residues from standards are cleaned away

Preparing Eye lenses for IRMS

22. As before, tare an empty tin capsule
23. Take the capsule out and add **100-600 ug** of material to the capsule. If the eye lens pieces are large, a smaller piece can be broken off to place into the capsule.
*Note: 100 ug is an **absolute minimum**. If 100 ug of material is not available, try to get material back into vial and make a note of which vial number the material came from. A second eye will need to be peeled or the layer not used.
24. Record vial number on datasheet under **ID1**. Record mass in mg on datasheet under **Weight (mg)**
25. Close capsule into ball as before. Drop capsule into correct slot in tray. Double check. Triple check.
26. If enough material remains in the vial, make a second capsule from that same layer. If possible, all samples should be run in duplicate.
27. If not enough material remains in the vial for a second capsule from the same layer, make a note on the datasheet that this will be a single sample.
28. If using a core, whether single or double, record this in the notes as well.
29. Attempts should be made to randomize the samples being weighed so that they are not all sequential at all times. I tend to do this by starting on an outside layer. I then find the corresponding core and alternate lenses from both directions on the same fish. However, randomization can happen in any manner.
30. Each tray can hold 36 unknown samples along with the 13 standards. This means that if duplicates are made for each lens, a tray can hold up to 18 total eye lens layers.

Preparing Liver/Muscle for IRMS

31. Prepare tray using steps 1-21
32. As before, tare an empty capsule
33. Take vial of dried and ground liver or muscle. Use tool to stir contents to make sure it is well mixed
34. Take capsule out of balance. Add **500-750 ug** of liver or muscle material to capsule
35. Repeat steps 30-32 for a second capsule from the same liver/muscle vial
36. Attempts should be made to randomize the samples being weighed so that they are not all sequential at all times.
37. Each tray can hold 36 unknown samples along with the 13 standards. This means that tray can hold up to 18 total liver/muscle samples. If both liver and muscle are present for each fish, samples from 9 individuals can be processed in a tray.

APPENDIX D. PRELIMINARY ISOTOPE TESTS USING FISH EYE LENSES

AD.1. Effect of thawing and refreezing on the integrity of eye-lens isotope samples

A freezer holding eye-lens samples was left ajar for approximately three days prior to discovery. This resulted in all samples thawing to approximately 10°C for several hours. I asked the question, what is the effect of long-term thawing on the isotopic composition of the eye-lens laminae?

To answer this question, I selected three fish for which the isotope data was available for a single eye lens, but the other eye was intact in the compromised freezer. I peeled the second eye and produced the IRMS data using normal protocols. I then visually compared the isotope profiles from the two eyes of the same individual.

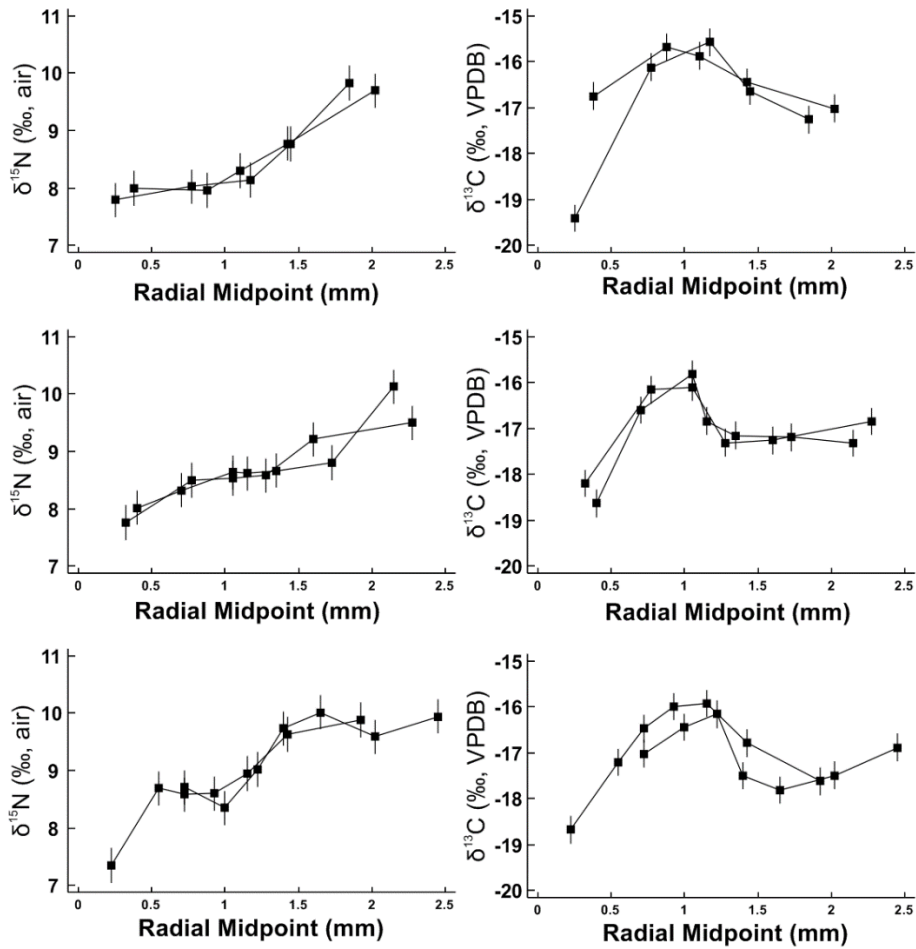


Figure AD.1. Isotope profiles from left and right eyes of the same individual. Each pair of left and right panels corresponds to the $\delta^{15}\text{N}$ and $\delta^{13}\text{C}$ profiles for a single individual. Error bars on each point is marked as 0.3‰, the average error for the IRMS run producing these data.

I found the $\delta^{15}\text{N}$ and $\delta^{13}\text{C}$ profiles to be within the expected variability and error according to the imperfections of manually peeling eye-lenses (Figure AD.1). These results led us to continue using the sampled that had been allowed to thaw.

AD.2. Minimum sample mass for reliable stable isotope measurements

Previous researchers had investigated the maximum eye-lens mass for reliable isotopic measurements. However, the minimum mass required had not been carefully considered previously. I asked the question: what is the minimum mass of eye-lens material that will produce consistent, reliable results using the Carlo-Erba NA2500 Series II Elemental Analyzer (EA) combustion furnace coupled to a continuous-flow ThermoFinnigan Delta+XL isotope ratio mass spectrometer (IRMS) at the University of South Florida College of Marine Science in St. Petersburg, Florida? I used repeated samples from the same eye lens to measure the amplitude of the N₂ (mass 28) peak.

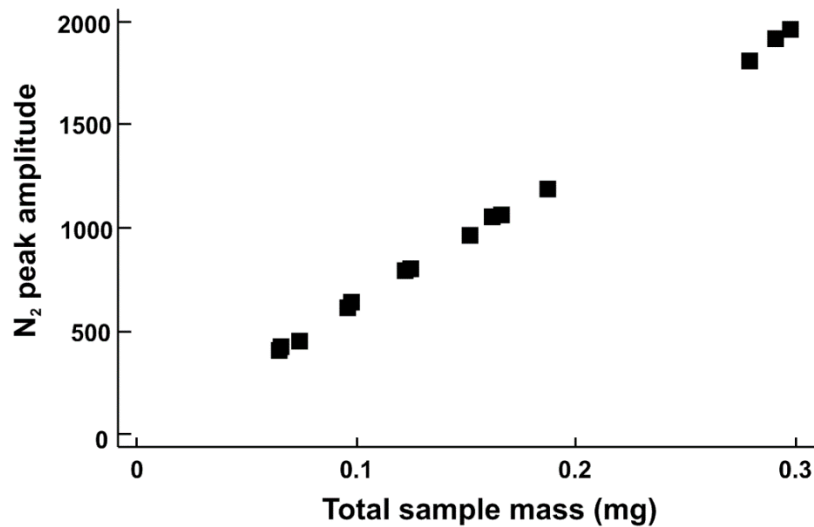


Figure AD2. Plot of N₂ (mass 28) amplitude peak vs total sample mass for eye lens samples.

Peak amplitudes less than 500 can be considered unreliable.

Using a combination of previous knowledge (E. Goddard) and the literature, I found that amplitudes less than approximately 500 become unreliable and prone to high rates of error.

Using the linear relationship between mass and amplitude, I set a minimum acceptable mass of 100 µg for each sample to be analyzed and used for analysis.